The University Of Sheffield.

The University of Sheffield Faculty of Medicine, Dentistry and Health
School of Clinical Dentistry

Can salivary EVs be used as diagnostic biomarkers in oral squamous cell carcinoma?

Karima Elfitory Ahmied Alkasah

A thesis submitted in partial fulfilment of the requirements for the degree of Doctor of Philosophy

September 2022

Acknowledgements

First and foremost, I would like to express my sincere gratitude to my supervisor, Stuart Hunt, for his endless support, encouragement, and guidance during my Master and PhD studies. I have learnt so much from his extensive knowledge and dedication that I cannot thank him enough. I feel extremely lucky to be your student.

I want to thank to Dr Lynne Bingle, my second supervisor, for her invaluable contributions and suggestions along the way. I consider myself fortunate to have had a supervisor that genuinely cared about my work. I must also express my gratitude to Dr Sabine Jurge, Katy D'Apice, Dr Robert Bolt and Mr Iain Varley for helping me collect saliva from patients.

A big thank you to all the technical staff who helped me along these last four years; Brenka, Jason, and Matt, Chris Hill from the EM facility, Sarah Elliott from the Medical School. Special thanks to my colleagues in the Hunt group; Anita, Wenyi, Cathy, and Helal for their assistance whenever I needed it, and to the other fabulous people on the third floor; Esra, Mariam, Asma, Basma, Naeima, Fatma. My lovely friends Rawan and Hyfa, I must acknowledge you here for your endless help, support, and kind words. Our friendship is one of the best things that I achieved during my study abroad.

I must express my gratitude to the University of Sirt and the Ministry of Education-Libya for funding for my doctoral degree.

My husband (Mohammed Abozahow), my children (Shahad, Bashier, Sakar, Shahien, Yousef) no words would suffice to express my deep gratitude to you for supporting me through my studies. Without your assistance, this would not have been achievable.

To my parents, although I spent these years away from you, it was to fulfil your aspirations and inspirations so that you may be totally proud of your daughter. I owe everything to you.

Presentations

Oral presentations:

Optimised enrichment of salivary extracellular vesicles for biomarker studies. The University of Sheffield' School of Clinical Dentistry PGR day, Sheffield, 2020.

Prizes

- Award MDH PGR Society Digital Poster Competition 2020. Isolation of salivary extracellular vesicles for biomarker studies.
- Award MDH PGR Society "60 second presentation 2020". Salivary extracellular vesicles can be as diagnostic biomarkers in head and neck cancer.
- First place, Poster Competition for the faculty of Medicine, Dentistry, and Health' PGR day, Virtual, 2021.
- First place, "Gone in 60 seconds competition" Video presentation for the faculty of Medicine, Dentistry, and Health' PGR day, Virtual, 2021.

Poster presentations

- Isolation of salivary extracellular vesicles for biomarker studies. *UKEV* Forum 2019, the Francis Crick Institute, London.
- Isolation of salivary extracellular vesicles for biomarker studies. The University of Sheffield' School of clinical Dentistry PGR day, Virtual, 2020
- Optimised enrichment of salivary extracellular vesicles for biomarker studies. *UKEV* 2021, online.

Abstract

Background: Oral squamous cell carcinoma (OSCC) is the most frequent cancer of the head and neck and is a major cause of worldwide morbidity and mortality. Saliva is recognised as a non-invasive source of biomarkers that can be used for the detection of oral diseases such as oral cancer. One specific source is salivary extracellular vesicles (EVs). MicroRNA (miRNA) are small non-coding RNA that regulate cellular processes in tumorigenesis and their detection in OSCC-derived EVs represents a source of biomarkers that could be utilised in a diagnostic test. However, saliva is challenging to work with (due to viscosity) and isolation of salivary EVs would need to be higher throughput for a diagnostic test to be realised.

Hypothesis: The miRNA cargo of salivary EV can be used as a biomarker signature to develop a diagnostic test for OSCC.

Methods: Salivary EV isolation was compared for three techniques; serial centrifugation, size exclusion chromatography and Dynabead immunocapture. Characterization of EVs was carried out by Transmission electron microscopy (TEM), Nanoparticle Tracking Analysis (NTA), Exoview and western blotting. EVs were purified from the saliva of OSCC patients and healthy controls by Dynabead immunocapture. Small RNA sequencing was conducted on a discovery cohort (OSCC n=5 and healthy controls n=3) to identify the EV miRNA cargo and differential expression analysis was used to identify up- or down-regulated miRNA. Validation of NGS was done by qRT-PCR on a cohort of n = 14 cancer patients and n = 7 healthy controls.

Results: Dynabead immunocapture was found to be the most appropriate method for isolation of salivary EVs and gave the best yield of intact EVs when processing ≥ 2 ml fresh saliva. Salivary EVs were positive for CD9, CD63, CD81 and TSG101 by western blotting. Small RNA sequencing identified 17 miRNA were up-regulated in OSCC patient EVs compared to healthy controls. qRT-PCR analysis of four of the up-regulated miRNA (miR-21-5p, miR-29a-3p, miR-92a-3p and miR-181a-5p) revealed no significant difference between OSCC samples and healthy controls.

Conclusion: The miRNA cargo of salivary EV is a promising biomarker signature for OSCC diagnosis. However, further work is required to accurately quantify individual miRNA in the absence of suitable endogenous controls.

List of Contents

List of Tables

List of Figures

Abbreviations

AKT	Protein kinase B
AMI	Myocardial Infarction
CAFs	Cancer-associated fibroblasts
CD	Tetraspanins
CDE	Clatherin- independent pathways
CDKN2A	Cyclin-dependent kinase inhibitor 2a
cDNA	Complemtray Deoxyribonucleic acid
CME	Clathrin-mediated endocytosis
CSF	Crebro-spinal fluids
CXCL	Chemokine Ligand
DC	Differential centrifuge
DNA	DNA Deoxyribonucleic acid
dNTP	Deoxynucleotide triphosphate
ECM	Extracellular matrix
ECs	Endothelial cells
EFEMP1	Fibulin-like extracellular matrix protein 1
EGF	Epidermal growth factor
EGFR	Epidermal growth factor receptor
EPC	Endothelial progenitor cells
EPHB2	Ephrin type B receptor 2
ESCRT	Endosomal sorting complexes required for transport
EVs	Extracellular vesicles
ExRNAs	Exosomes RNA
FGF	Fibroblast growth factors
FNDC1	Fibronectin type III domain-containing protein 1
gDNA	Genomic DNA
GPI	Glycosylphosphatidylinositol
GrB	Granzyme B
GW4869	Neutral sphingomyelinase (N-SMase)
H/R	Hyperoxia/reperfusion
HEK293 cell line	Human embryonic kidney 293
HIF-1α	Hypoxia-induced factor-1α
hnRNPA2B1	Heterogeneous ribonuclear protein
HNSCC	Head and neck squamous cell carcinoma
HOTAIR	HOX transcript antisense RNA
HPV	Human papillomavirus
HSC70	Heat-shock proteins
HUVECs	Human umbilical vein endothelial cells

IBD	Inflammatory bowel disease
IBP5/IBP7	Insulin-like growth factor binding proteins 5/7
IFN- β	Interferon beta
IL	Interleukin 1 α/β
ILVs	Intraluminal vesicles
ISEV	International Society for Extracellular Vesicles
MHC class	Major histocompatibility complex
MiRNA	Small single-stranded non-coding RNA molecule
MISEV2018	Minimal information for studies of extracellular vesicles 2018
MMP	Matrix metalloproteases
mRNA	Messenger ribonucleic acid
MV	Microvesicle
MVBs	Multivesicular bodies
MVP	Major vault protein
ncRNA	Non-coding RNA
NECs	Normal endothelial cells
NK	Natural killer cells
NKG2D	Natural Killer Group 2D
nMase-2	Neutral sphingomyelinase-2
NOS	Endothelial nitric oxide synthase
NOTCH1	Notch homolog 1
NTA	Nano-particles analysis
OLP	Oral lichen planus
OSCC	Squamous cell carcinoma
PBS	Phosphate buffered saline
PCR	Polymerase chain reaction
PD	Parkinson's disease
PDCD4	Programmed cell death 4
PDGFD	Platelet derived growth factor D
PFGF	Plasmid DNA encoding fibroblast growth factor-2
PFKFB3	6-phosphofructo-2-kinase/fructose-2,6-biphosphatase
PI3K	Phosphatidylinositol-3-kinase
PSMA7	Proteasome subunit alpha type 7
PTEN	The phosphatase and tensin homologue
PTEN	Phosphatase and tensin homologue
qPCR	Quantitative polymerase chain reaction
RAB	Ras-associated binding protein RAB proteins
Rb	Retinoblastoma
RISC	RNA-induced silencing complex
RNA	Ribonucleic acid
rRNA	Ribosomal ribonucleic acids

SDS	Sodium dodecyl sulfate
SEC	Size exclusion chromatography
SERPINE1	Serpin peptidase inhibitor type 1
SEVs	Salivary Extracellular vesicles
SLE	Sjögren-Larsson Syndrome
SNARE	Soluble N ethylmaleimide-sensitive attachment protein receptor
SS	Sjogren's syndrome
STAT3	Signal transducer and activator of transcription 3
STC2	Stanniocalcin 2
TBST	Tris-buffered saline supplemented with 0.1% (v/v) Tween-20
TEM	Transmission electron microscopic
TGF-β	Transforming growth factor beta
TME	Tumor microenvironment
TNF-α	Tumour necrosis factor alpha
TP53	Tumor protein
TPS	Tissue polypeptide antigen
tRNA	Transfer RNA
TSG101	Tumor susceptibility gene 101
UB	UB Unbound
UC	Ultracentrifugation
UF	Ultrafiltration
UPA	Urokinase plasminogen activator
VPF	Vascular permeability factor
VRNA	Vault RNA
WB	Western blot
YBX-1	Y-Box Binding Protein 1
α-amylase	Alpha amylase
α-synOligs	α-Synuclein

Chapter one

1. Introduction

1.1 Head and Neck cancer

Head and neck cancer (HNC) was the world's seventh most common cancer in 2018 (Bray et al., 2018). About 12,238 new cases were diagnosed and 4,077 people died from the disease in the UK in 2018 (Cancer Research UK, 2018). It encompasses diverse and aggressive groups of malignancies (Bray et al., 2018; Ferlay et al., 2019; Ferlay et al., 2020). HNC occurs at different anatomical sites, including the oral cavity, oropharynx, hypopharynx, nasopharynx, and larynx (Ferlay et al., 2010) (Figure 1.1). Since the early 1990s, the incidence of HNC in the United Kingdom has grown by 33% (Cancer Research UK, 2020). Globally, HNC accounts for around 2% of cancer-related mortalities every year (Economopoulou and Psyrri, 2017).

1.1.1 Epidemiology and risk factors of oral cancer

Oral cancer is a frequent kind of HNC with a global incidence of 400,000 per year (Cai et al., 2019). More than 90% of all HNC cases are classified as oral cancer, which affects the oral cavity (Perdomo et al., 2016). It comprises tumours of the lips, tongue, floor of the mouth, cheeks, sinuses, hard and soft palate, and throat (Johnson et al., 2020). It is commonly referred to as oral squamous cell carcinoma (OSCC) because squamous cells account for 90% of malignancies in the oral cavity (Montero and Patel, 2015). OSCC is most common among men in their fifties and sixties, with tobacco, alcohol, and betel quid use all being associated with an elevated risk (Petti, 2009) (Figure 1.1). The human papillomavirus (HPV), which also causes cervical cancer, has been related to an increased risk of oropharyngeal squamous cell carcinoma (OPSCC)(Thomsen and Kjær, 2019) and is the subject of a vaccination program in the United Kingdom (Waller and Wardle, 2008). Despite a range of well-developed therapies such as surgery, radiation, and chemotherapy, OSCC has a low overall survival rate (about 50-60%) due to late diagnosis for most patients (Blatt et al., 2017).

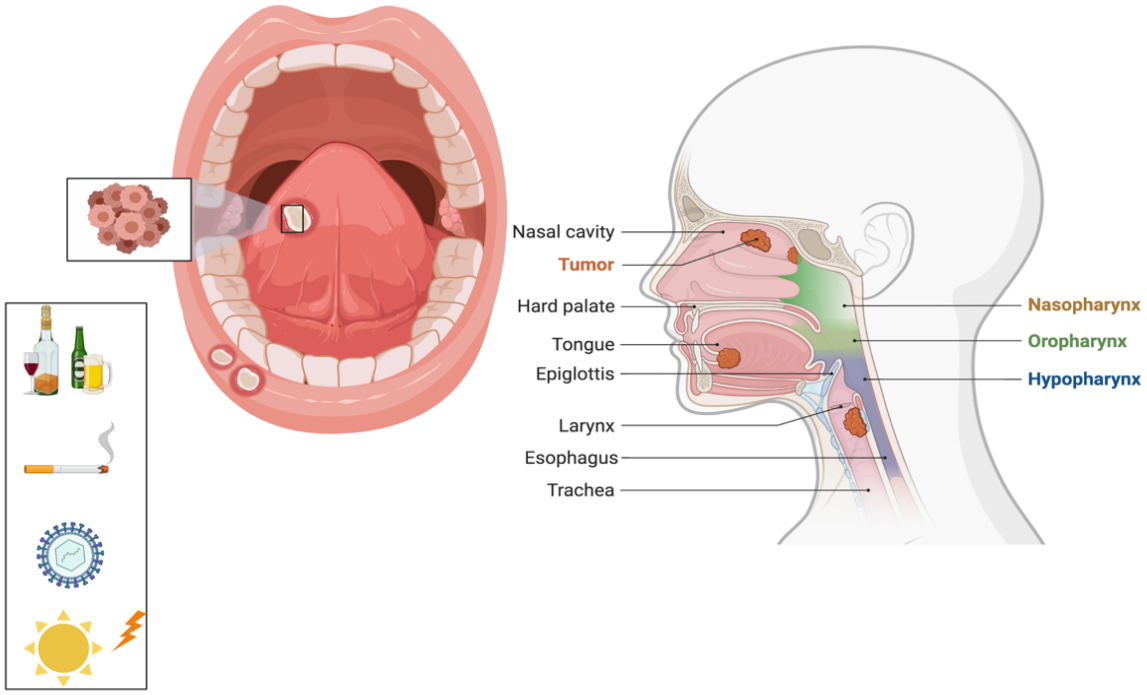

Figure 1. 1 Anatomical locations and risk factors of head and neck cancers. The diagram depicts common locations of head and neck cancers, which include the lips, hard palate, floor of mouth, tongue, retromolar trigone, nasopharynx, oropharynx, soft palate, and posterior pharyngeal wall, as well as the nasopharynx, oropharynx. In addition, the graphic depicts the HNSCC risk factors, adapted from Johnson et al.(2020).

1.1.2 Development of oral squamous cells carcinoma (OSCC)

Development of OSCC is regarded as a multistep process requiring the accumulation of multiple genetic alterations. When normal oral mucosal keratinocytes are constantly subjected to carcinogenic risk factors, genetic instability occurs (Fukuda et al., 2012; Rivera, 2015), including mutations of TP53, Notch homolog 1 (NOTCH1), cyclin-dependent kinase inhibitor 2a (CDKN2A), epidermal growth factor receptor (EGFR), Cyclin D1, signal transducer and activator of transcription 3 (STAT3), retinoblastoma (Rb), and Wnt/-catenin pathway components, among others (Curry et al., 2014) (Figure 1.2). Oral carcinogenesis is most likely initiated by the transformation of a small number of normal keratinocytes (Rivera, 2015). This transformation can be expressed via cytogenetic changes and epi-genetic processes that modify the progression of the cell cycle, DNA repair mechanisms, cell differentiation and apoptosis, which may be caused by random mutation, by exposure to a variety of biological factors, carcinogens or errors in the DNA repair process (Feller et al., 2013), resulting in susceptible to malignant neoplastic alterations (Feller et al., 2013). As a result, selection

forces on the oral mucosa microenvironment may work on the diverse clonal population, permitting development of those cells with advantages in adaptation, proliferation and survival over their normal counterparts (Rivera, 2015).

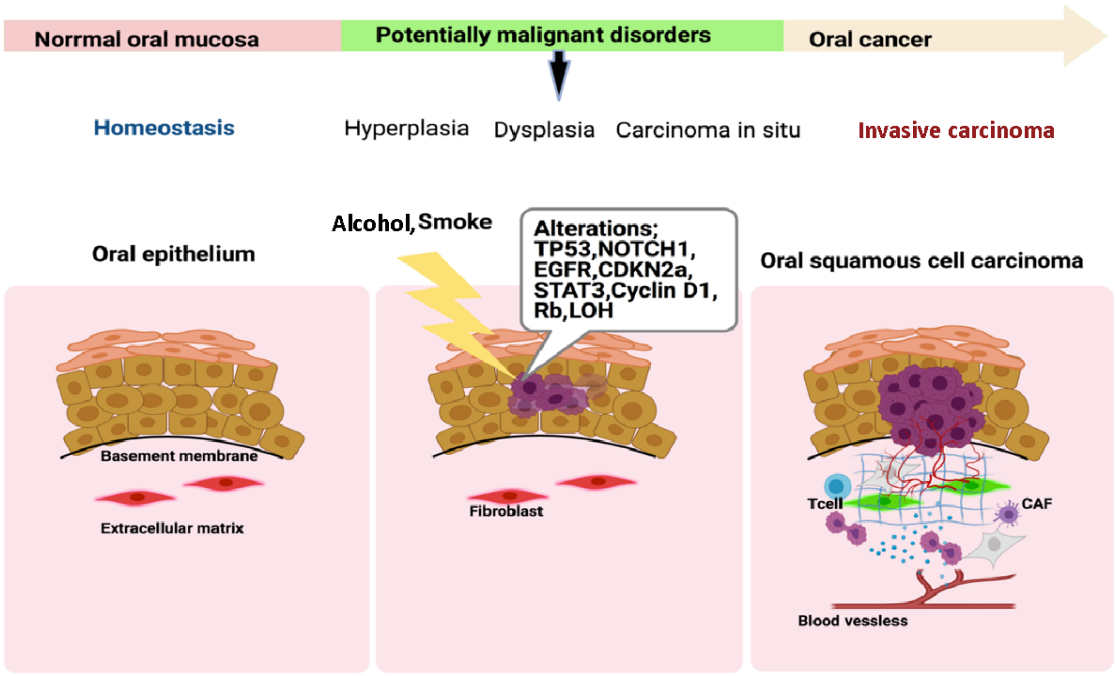

Figure 1. 2 OSCC progression. The diagram depicts changes in oral keratinocytes and the development of OSCC. Bio-Render was utilized to create this modified diagram from (Rivera, 2015).

1.1.3 Features of oral squamous cell carcinoma

Oral cancer can manifest itself in a variety of ways, just like any other tumour, and can occur in any region of the mouth, tongue, or lips. Oral cancer might manifest itself as a painless mouth ulcer that does not heal, or as a tumour with uneven edges that are stiff to the touch (Morfit, 1956). A white or red spot in the mouth might potentially be cancerous. These areas result in the formation of a premalignant lesion or dysplasia, which is classified as a developmental defect or an epithelial growth and differentiation aberration. They might be the earliest sign of an approaching malignancy; the most prevalent oral premalignant lesions are leucoplakia and erythroplakia. Leucoplakia is a disorder characterised by the formation of one or more white patches inside the mouth and differs from other causes of white spots, such as thrush or lichen planus, in that it can progress to oral cancer (Reibel, 2003). Erythroplakia is a red patch or cluster of red spots that appears on the mucous membrane lining the mouth for no known reason (Reibel, 2003). OSCC has many reactive

epithelial alterations such as hyperplasia, hyperkeratosis, and acanthosis that can be seen under the microscope. Increase in nuclear size, hyperchromatism, pleomorphism, aberrant mitotic figures, or enhanced mitosis are various combinations and degrees of atypia seen in epithelial dysplasia. When changes occur in the basal or parabasal keratinocytes, they are referred to as mild dysplasia; when changes occur in the intermediate layer they are referred to as moderate dysplasia and when abnormalities extend to the surface layer they are referred to as severe dysplasia. When there is total atypia (from the base to the surface), the phrase carcinoma *in situ* is used (Figure 1.3). (Neville et al., 2009).

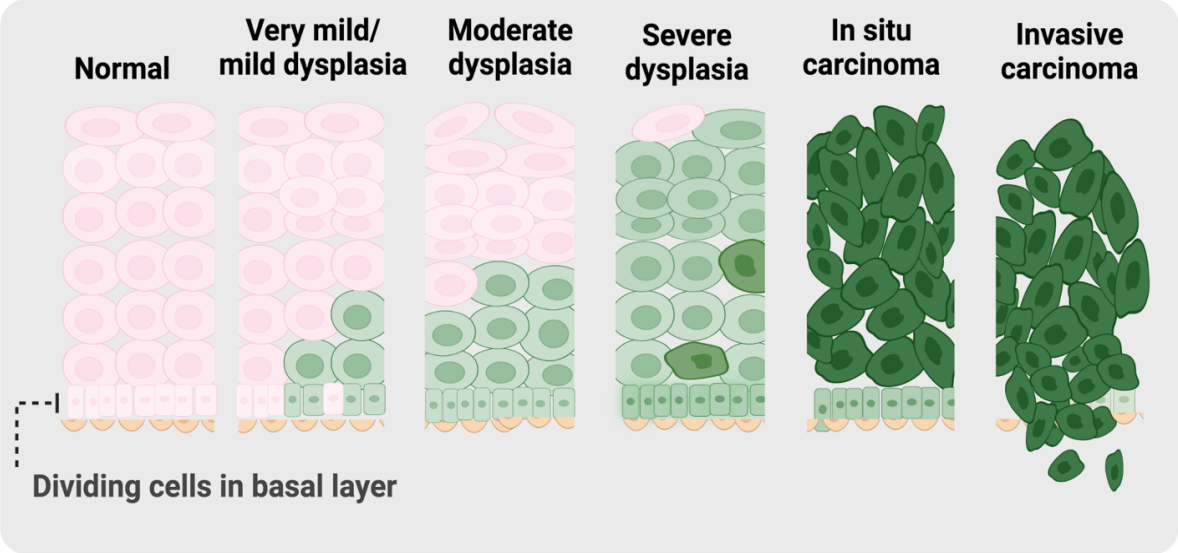

Figure 1. 3 Oral carcinogenesis. The diagram depicts normal oral mucosa, which consist of stratified epithelium and a basal cell layer that connects epithelial cells to connective vascular tissue. Furthermore, the diagram demonstrates that cells at the lowest layers undergo morphological changes in shape and size, which can extend throughout the full thickness of the epithelium. Biorender was used to create this image, which is adapted from (Reyes et al., 2020).

1.1.4 Tumour microenvironment in oral squamous cell carcinoma

The tumour microenvironment (TME) is the environment around a tumour, including the surrounding cancer-associated fibroblasts, macrophages, neutrophils, regulatory T cells, pericytes, natural killer cells and blood vessels, all of these cells embedded in altered the extracellular matrix (ECM) and signalling molecules, all of which can differ according to the type, stage, and location of the cancer (Alfarouk et al., 2011; Joyce and Fearon, 2015). The tumour and surrounding microenvironment are closely related and they interact constantly (Figure 1.4).

Recently, cancer research has focused on the TME as a complex and dynamic entity of cells that promotes the development of tumours by activating cell growth/migration and invasion (Wang et al., 2014b). The oral mucosa is composed of many types of cells. Each one plays a distinctive role that is essential to the function of the entire organ, which can be corrupted during carcinogenesis (Collins and Dawes, 1987). There are many reasons why cancer cells recruit healthy cells and these reasons change as cancer progresses (Wang et al., 2014a). Some examples are discussed below.

1.1.4.1 Oral epithelium

Oral epithelium is a stratified squamous epithelium that consists in various layers: basal, spinous, granular and corneal layers for the keratinized area; basal, spinous, intermediate and superficial layers in the non-keratinized areas. Which direct contact with an underlying, dense connective tissue (lamina propria) containing minor salivary glands, structural fiber, blood vessels, fibroblasts along with other cell types (Collins et al., 1987). Normal oral epithelial cells are which oral cancer will arise, the majority of them have too short a life span (14-24 days) to accumulate the necessary genetic changes to develop into a tumour (Squier et al., 2001). An epithelial layer is constantly being replaced with cells dividing and becoming progressively more differentiated as they rise up the epithelial layers and acting as a source of vital agents for the rapidly proliferating cancer cells (Icard et al., 2014), which is characterised by the uncontrolled proliferation of cells, migration and eventual invasion through the epithelial basement membrane. In addition, the progression of cancer largely depends on the interactions between cancer cells and the tumour microenvironment (TME).

1.1.4.2 Immune cells

The spread of OSCC is associated with immune cell infiltration, for instance, lymphocytes, macrophages, neutrophils, and natural killer (NK) cells, which cause inflammation (Choi et al., 2017). T lymphocytes are found in the microenvironment's edges and in lymph nodes (Pereira et al., 2015). A study considered the importance of the total number of tumour-infiltrating lymphocytes as a diagnostic indicator for head and neck squamous cell carcinoma (HNSCC) patients, including both CD8+ cytotoxic T cells and CD4+

helper T cells, which were examined and connected with clinicopathologic aspects of HNSCC patients (Peltanova et al., 2019). Furthermore, CD4+ helper T cells play a role in helping CD8+ T lymphocytes and enhance the anticancer impact. However, due to their immunosuppressive properties and the ability to impede the activities of cytotoxic CD8+ T cells, they are also efficient in facilitating tumour growth (Ostroumov et al., 2018). In 2008, Bose et al. found that patients with OSCC had lower levels of the T-cell cytotoxic molecules perforin and granzyme B than the control group, which correlates with lower T-cell killing of tumour cells (Bose et al., 2008).

In HNSCC, macrophage infiltration is a key contributor to inflammation and it is linked to a poor prognosis. Tumour associated macrophages (TAMs) are classified as proinflammatory (M1) or immune suppressive (M2) cells (Kumar et al., 2019). They may produce a wide range of molecules, including growth factors, cytokines, proteases, and chemokines, to aid in angiogenesis, metastasis, and invasion, as well as immunosuppression (Kumar et al., 2019). For example, in comparison to healthy controls, M2 macrophages expressing TGF-β and IL-10 were shown to be more prevalent in OSCC (Mori et al., 2011; Peltanova et al., 2019). They also secreted growth factors including VEGF, PDGF, TGF-β, which can increase angiogenesis in squamous cell carcinomas of the oesophagus, according to other research (Marcus et al., 2004).

Natural killer (NK) cells are essential in cancer cell identification and killing (Choi et al., 2017). The presence of NK cells in HNSCC patients was linked to a better prognosis (Agarwal et al., 2016; Wagner et al., 2016). However, it was also demonstrated that there were considerably fewer demethylated copies of NKp46 found in the controls blood of those with head and neck cancer than in control blood, which indicated that there were fewer NK cells overall in those cases (Accomando et al., 2012).

Tumour-associated neutrophils (TANs) are characterised by elevated production of angiogenesis and invasion-promoting proteins VEGF, MMP-9 and CXCR4, as well as the absence of IFN- γ (Jablonska et al., 2010). Neutrophil infiltration was also linked to a higher tumour stage, recurrence, and lymph node metastases (Wang et al., 2014a). Trellakis et al., (2011) looked at how neutrophils interact with oral cancer cells. They discovered that oral cancer-conditioned media decreased neutrophil apoptosis, enhanced neutrophil chemotaxis, and stimulated neutrophil MMP-9 and CCL4 production (Trellakis et al., 2011).

1.1.4.3 Fibroblasts

Fibroblasts are the most predominant cell type in the TME, and they produce the majority of extracellular components, such as extracellular matrix (ECM) and soluble factors (Choi et al., 2017). A switch from quiescent fibroblasts to cancer-associated fibroblasts (CAFs) is driven by the epithelial cells producing protein factors such as transforming growth factor beta (TGF-β), tumour necrosis factor alpha (TNF-α) and interleukin (IL)-1 α/β (Choi et al., 2017). A higher number of CAFs inside the main tumour has been linked to a poorer prognosis in HNSCC patients, and the interaction of CAFs with cancer cells has been proposed as the major mechanism promoting tumour growth. They are extremely effective at promoting carcinogenesis, tumour development, and metastasis (Knops et al., 2020).

Recent research discovered several proteins that were secreted differently in CAF-conditioned media than in normal fibroblasts, which include EGF-containing platelet-derived growth factor D (PDGFD), fibulin-like extracellular matrix protein 1 (EFEMP1), and insulin-like growth factor binding proteins 5/7 (IBP5/IBP7), which might be necessary to maintain the cancer stem cell phenotype in HNSCC (Álvarez-Teijeiro et al., 2018). Furthermore, as compared to normal fibroblasts, HNSCC-derived CAFs exhibit higher amounts of TGF- β (Rosenthal et al., 2004), HGF (Knowles et al., 2009), and MMPs (Johansson et al., 2012).

Takahashi et al. (2015) discovered that CAFs inhibited T cell proliferation, encouraged T cell death, and rapidly converted PBMCs into regulatory T cell as compared to normal fibroblasts, showing that HNSCC-derived CAFs play an important role in immunosuppression. CAFs have greater amounts of IL-6, TGFB1, CXCL8, VEGFA, and TNF than normal fibroblasts, according to their findings (Takahashi et al., 2015). In addition, multiple studies have demonstrated that OSCC cells release IL-1, which causes CAFs to produce TGF and HGF, enhancing cancer cell invasion in vitro (Hasina et al., 1999; Hwang et al., 2012).

1.1.4.4 Endothelial cells

Blood vessels are the main source of tumour nutrients and oxygen and remove waste enabling survival and proliferation (Fitzgerald et al., 2018). Tumour endothelial cells have distinct phenotypic and functional features as compared to normal endothelial cells in terms of metabolism, genetics, and transcriptomic profile (Dudley, 2012). Furthermore, tumour endothelial cells play diverse functional roles, and they are important for inducing tumour angiogenesis (Dudley, 2012). Hypoxia-induced factor-1α (HIF-1α) is the main factor that

initiates sprouting (Matsuda et al., 2010). They also have high levels of proangiogenic factors, including epidermal growth factor (EGF) and platelet-derived growth factor (Tonini et al., 2003; Lamalice et al., 2007).

Endothelial cells have been associated with tumour metastasis in several studies, by allowing invasive cancer cells to translocate into blood vessel lumens via intravasation. This process is a critical step in cancer metastasis (van Zijl et al., 2011). A study in oral cancer revealed that endothelial cells produced proteins that contributed to a distinct aspect of metastasis, such as interleukin 6 (IL6), which generates a chemotactic gradient allowing cancer cells to travel towards arteries (Kim et al., 2017).

The tumour-associated endothelium has been discovered to act as an immunological barrier to T-cells, reducing the efficacy of immunotherapies (Georganaki et al., 2018). Endothelin B receptor overexpression has been discovered in tumour-associated endothelial cells, which reduces T-cell adhesion and tumour targeting when activated by Endothelin-1 (Georganaki et al., 2018). In a study of oral cancer patients, the release of VEGF caused endothelial cells to downregulate the CD8+ T-cell cytotoxic mediators perforin and granzyme B, which might provide tumours with a survival advantage by reducing the T cells' capacity to kill tumour cells (Mulligan et al., 2010).

1.1.4.5 Extracellular matrix

The extracellular matrix (ECM) is a network of macromolecules that exists outside cells and includes glycoproteins, fibrous structural proteins and growth factors, which generate a structure that gives physical and biochemical support to other surrounding cells (Peltanova et al., 2019). ECM is commonly unregulated and disordered in cancer, which directly promotes malignant cell transformation (Provenzano et al., 2006; Levental et al., 2009). This occurs when cancer cells develop large numbers of matrix metalloproteinases, which are capable of degrading basement membrane ECM proteins (Suzuki et al., 1997; Tallant et al., 2010). Harada et al. (1994) discovered that the decreased expression of essential ECM proteins such as vitronectin, laminin, and collagen type IV, as well as the increased production of tenascin and fibronectin, were associated with the invasive nature of primary OSCC tumours (Harada et al., 1994).

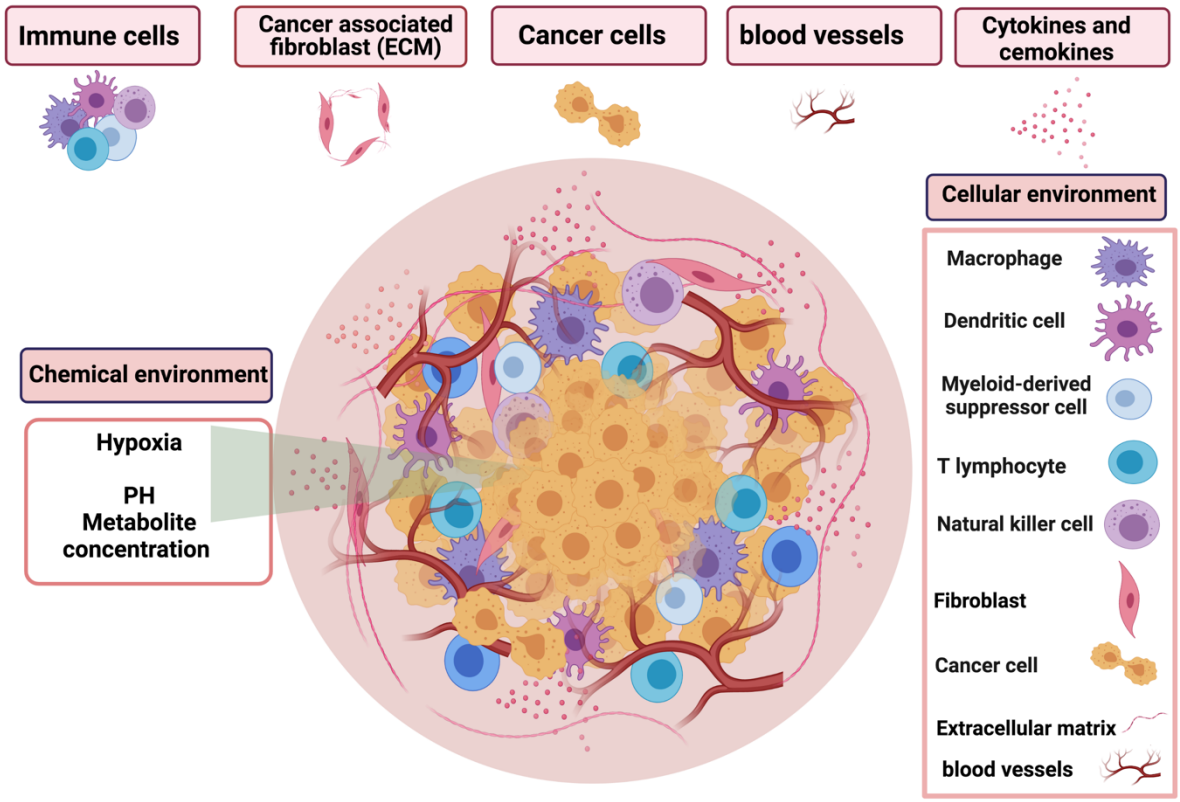

Figure 1. 4 The microenvironment of the tumour. The cancer cells are surrounded by an abundant stroma that aggregates during tumorigenesis; it involves cells such as fibroblasts, endothelial cells of blood vessels and different categories of immune cells such as macrophages, lymphocytes, and neutrophils. Created using BioRender and adapted and modified from (Ho et al., 2020).

1.2 Extracellular vesicles

It has been discovered that the "mutual dialogue" among cells in the TME mediates tumour growth, invasion, and metastatic capacity. Extracellular vesicles (EVs) play a crucial part in this process by transporting chemicals and information among cells in the TME. EVs were first viewed as garbage dumpsters, but were later described as signal boxes capable of redirecting the purpose of a recipient cell, which drew the attention of numerous researchers (Xie et al., 2019).

1.2.1 Discovering EVs

EVs were first observed in different contexts without realizing that they actually represent a universal form of intercellular communication. They were originally detected in normal plasma as platelet-derived particles before being termed "platelet dust" (Chargaff and West, 1946; Wolf, 1967). The release of plasma membrane vesicles, the discovery of

biological vesicles in seminal fluid, as well as the release of virus-like particles in mammalian cultured cells are all described in publications from the 1970s and 1980s (Benz Jr and Moses , 1974; De Broe et al., 1975; Dalton, 1975).

Two groups conducted ultrastructural analyses of transferrin trafficking in reticulocytes in 1983. The researchers discovered that tagged transferrin is taken up by recipient cells via receptor-mediated endocytosis. MVBs or multivesicular endosomes are formed during the production of late endosomes of intraluminal vesicles. MVB were found, unexpectedly, to have the capacity to fuse with plasma cell surfaces and discharge into the extracellular space, rather than fusing with lysosomes to break down intralumenal vesicles (ILVs) and their cargo (Harding et al., 1983; Pan and Johnstone, 1983).

In the late 1960s, the existence of vesicles around cells in mammalian tissues or fluids was first recognised (Wolf, 1967; Anderson, 1969). However, research published in the late 1990s suggested that EVs may be used for intercellular communication, particularly in immunological responses and cancer (Raposo et al., 1996a; Wolfers et al., 2001; Reibel, 2003). In 1987, Johnstone et al. identified exosomes as the vesicles produced by MVB. The first investigation into the functional features of exosomes in intercellular communication was published in 1996. According to Raposo and colleagues, MHC class II-carrying vesicles in B lymphoblastic cells could elicit antigen-specific MHC class II restricted T-cell activation (Raposo et al., 1996a). Following that, several investigations discovered functional significance in tumour and immune biology. Later studies revealed that EVs carried multiple RNA species which could be transferred between cells and impact gene expression in the recipient cell (Ratajczak et al., 2006a; Valadi et al., 2007c). A few years later, it was shown that most cancer cells produced EVs in greater quantities than normal cells (Taylor and Gercel-Taylor, 2008; Logozzi et al., 2009).

1.2.2 Type and nomenclature of EVs

In addition to releasing vesicles through the endocytic pathway (exosomes), cells can also shed vesicles directly from their surface (microvesicles). Vesicles can be released by apoptotic cells (Kim et al., 2003). The nomenclature of EVs is complex; some researchers named EVs depending on their cellular or tissue origin. For instance, vesicles originating from cardiomyocytes are called cardiosomes (Chaturvedi et al., 2015); protostomes are released

from prostate cells (Vlaeminck-Guillem, 2018), EVs with immunogenic properties are named as tolerosomes (Minciacchi et al., 2015). Other studies have used terminologies depending on the physical characteristics of EVs including size and density together with the biological composition CD81/CD63, Annexin A5-stained EVs, or they named them according to the conditions of the cell origin; for example, hypoxic EVs, podocyte EVs, apoptotic bodies, instead of terms such as microvesicles and exosomes (Théry et al., 2018b).

Recently, the International Society for Extracellular Vesicles (ISEV) has supported the study of EV nomenclature (Gould and Raposo, 2013). Exosomes have a diameter of (~30–150) nm while microvesicles have a diameter of (~100–1000) nm, according to the literature. Because of their overlapping sizes and densities, exosomes and microvesicles, together with other smaller vesicle types, cannot be distinguished experimentally. As a result, rather than using the terms exosomes or microvesicles, the majority of ISEV members prefer to refer to vesicles in an experimental environment as EVs (Raposo et al., 1996a; Gould and Raposo, 2013; Théry et al., 2018c).

1.2.3 Biogenesis and characterization of EVs

EV biogenesis research is critical for understanding how a cell creates vesicles. EVs are typically characterised as lipid bilayer-enclosed packets of biomolecules liberated into their neighbouring environment by many types of cells. The term EV is a generic name that encompasses particles such as exosomes, microvesicles, and apoptotic bodies (Doyle and Wang, 2019).

1.2.3.1 Exosomes

Exosomes are the smallest EVs of the three main subgroups, with dimensions ranging from 30 to 150 nm. They are produced as a result of the intraluminal budding of the endosomal compartment, resulting in intraluminal vesicles (ILVs) contained in multivesicular bodies. The formation of ILVs signals marks the start of the exosome biogenesis route. The endosomal sorting complexes required for transport (ESCRT) machinery, which is composed of a series of protein complexes such (ESCRT-0, -I, -II, and -III), is the primary mechanism of ILV synthesis (Schuh and Audhya, 2014).

However, lipid rafts and tetraspanin microdomains can also govern ILV invagination and exosome secretion in an ESCRT-independent way (Garcia et al., 2015; Van Niel et al., 2018; Zhang et al., 2019b). When multivesicular bodies merge with the plasma membrane of the original cell, ILVs are discharged into the extracellular milieu as exosomes. Alternatively, these components are trafficked to lysosomes for degradation (Zhang et al., 2019b). (Figure 1.5)

Several ways for their release have been proposed, including Rab GTPases (Rab27, Rab11/35), tetraspanins, and the SNARE (solubleN-ethylmaleimide-sensitive attachment protein receptor) complex (Kowal et al., 2014). Exosomes exhibit an artefactual cup shaped or biconcave morphology by transmission electron microscopy (Zhang et al., 2019b). Typically, the density of exosomes ranges from 1.13 g/mL up to 1.19 g/ml on sucrose gradients. Exosomes are sedimented using high-speed centrifugation at 100,000 x g (Théry et al., 2006).

Exomeres, a novel particle type found recently, vary in size from 30 to 50 nm and have been shown to contaminate exosome preparations (Zhang et al., 2019b) (Figure 1.6).

1.2.3.2 Microvesicles

Microvesicles, which vary in size from 100 to 1000 nm, are a much more diverse vesicle population formed by outward budding of the plasma membrane, which is why they are also known as shedding vesicles or ectosomes (Cocucci et al., 2009) and microparticles (El Andaloussi et al., 2013). Many enzymes, as well as mitochondrial or calcium signalling, may be involved in outward budding in response to stimuli. Cytoskeleton remodelling and changes in phospholipid symmetry occur during the budding process. These mechanisms can vary greatly amongst cell types (Curtis et al., 2013; Larson et al., 2014). Modifying membrane asymmetry in this way stimulates the transfer of amino phospholipids, particularly phosphatidylserine, to the plasma membrane's outer layer. Microvesicle generation appears to be restricted to the membrane's lipid-rich microdomains, such as lipid rafts and caveolae domains (Del Conde et al., 2005; Morel et al., 2009). Interestingly, alterations in the plasma membrane have been observed to be independent of asymmetry loss in multiple investigations. The ESCRT pathway or tetraspanin microdomains are involved in these activities (Pieterse and van der Vlag, 2014; Kalra et al., 2016).

Multiple complicated pathways are certainly implicated, according to the limited research that has, to date, investigated the biological processes of microvesicle synthesis. Depending on the initial stimulus, these include Rho associated kinase I and II and myosin light chain, nuclear factor-B or p38 mitogen-activated protein kinase, tumour necrosis factor-related apoptosis-inducing ligand (Dignat-George and Boulanger, 2011).

The density of microvesicles is unknown (Castellana et al., 2009); they sediment at lower speeds, usually at 10,000 x g (Heijnen et al., 1999). By using transmission electron microscopy, one can determine that the appearance of microvesicles is heterogeneous in size and morphology (Heijnen et al., 1999; Antonyak et al., 2011).

1.2.3.3 Apoptotic bodies

Apoptotic bodies are EVs formed by caspase-mediated cleavage and subsequent activation of Rho-associated kinase I during the last stages of apoptosis (El Andaloussi et al., 2013; Kalra et al., 2016). They differ from exosomes and microvesicles in that they have an externalised phosphatidylserine and a permeable membrane, and their diameters range from 50 nm up to 5000 nm (Wickman et al., 2012). According to several investigations, apoptotic bodies include a wide range of biological elements, including histones, DNA, Annexin V, membrane/cytosolic components and cellular organelles (Fadeel and Orrenius, 2005). Little is understood regarding their molecular composition, yet only a few recent studies have attempted to characterise them proteomically. Under electron microscopy, the appearance of these vesicles is diverse (Théry et al., 2001; Hristov et al., 2004).

1.2.3.4 Other types of EVs

Apoptotic cells produce very large EVs and neurons, and other cells may create micron-sized EVs. When formed by tumour cells, these particles are known as large oncosomes and can measure up to 20 microns in diameter. They have a functioning cytoskeleton and energy sources (mitochondria), and they might be motile, capable of migrating (Trams et al., 1981; Morello et al., 2013).

When neurons in the model organism *C. elegans* were treated with a dye, it was seen that the dye was sequestered inside a section of the cell and then liberated in a huge EV termed the exopher, which shares similarities with large oncosomes except they are produced by non-cancerous cells (Meehan et al., 2016).

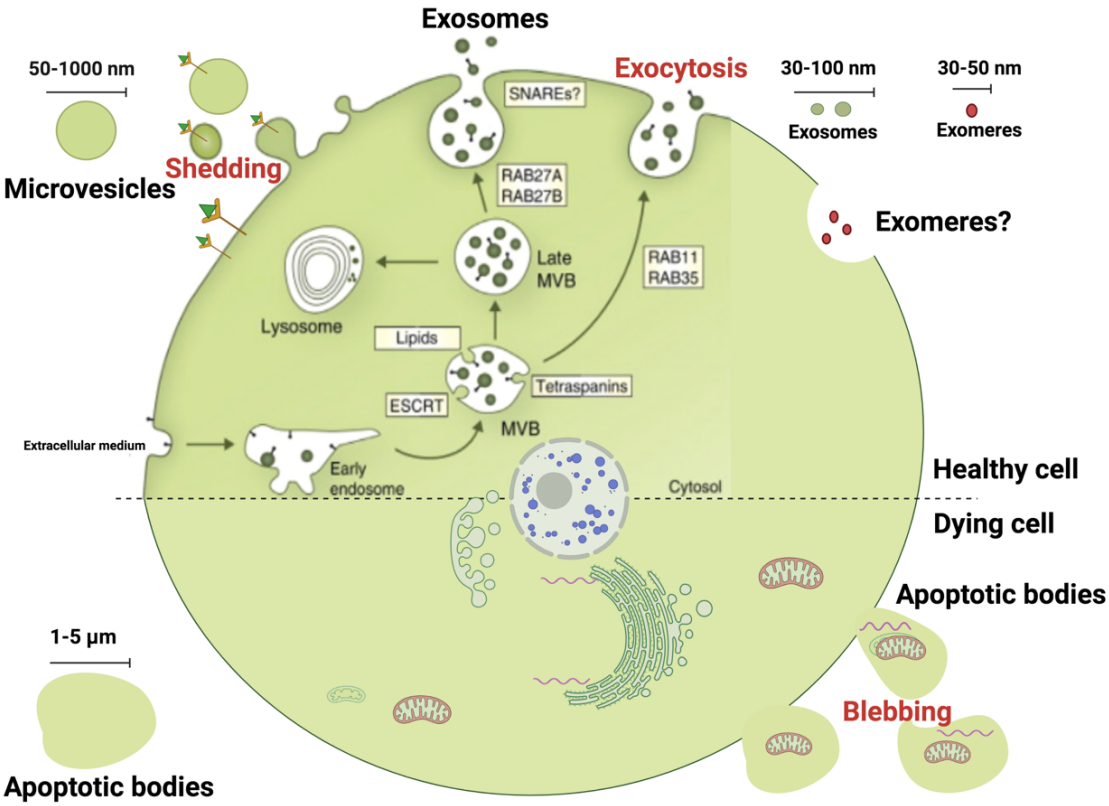

Figure 1. 5 Types of extracellular vesicle and their biogenesis; Exosomes, microvesicles, and apoptotic bodies are illustrated in this diagram, as well as the biogenesis of exosomes, which are generated as ILVs by budding into early endosomes and MVBs. The destination of MVBs can be either fusion with lysosomes or fusion with the plasma membrane, as shown in the diagram above. In the form of apoptotic bodies and microvesicles, some bud straight from the plasma membrane. Biorender was used to make this image, which was adapted from (Kowal et al., 2014).

1.2.4 Composition of Extracellular vesicles

During the biogenesis of EVs, proteins and nucleic acids are captured in the invaginating membrane and sorted into these vesicles (Théry et al., 2002; Johnstone, 2006). Thus, EVs are predominantly made up of lipids, proteins, and nucleic acids, which are all functional when transported into recipient cells; these can be in close proximity to the donor cell or at distant regions in the body via biofluids (Zomer et al., 2016).

1.2.4.1 Nucleic acid cargo

EVs are thought to include a substantial amount of nucleic acid; including ribosomal and transfer RNA, messenger RNA, long noncoding RNA, picoRNA, vaultRNA, microRNA, and Y-RNA (Riazifar et al., 2017). Exosome RNA (ExRNA) cargo may be able to influence the target

cell processes in a variety of ways, including transcriptional and epigenetic post-transcriptional regulation (Riazifar et al., 2017).

ExRNA has been utilised in studies as a more sensitive and specific biomarker that better reflects cell dynamics than DNA (Chiabotto et al., 2019). However, because of their variability, the insufficient description of their many targets and activities, and their stability in diverse bodily fluids, there are still several limits to the use of exRNA as biomarkers (Chiabotto et al., 2019).

One study used opposing series of centrifugation procedures to isolate the various types of vesicles by size to detect the alterations in the RNA profiles of the subclasses. The presence of large quantities of ribosomal RNA in apoptotic bodies was verified, but exosomes had only modest amounts and microvesicles had essentially no rRNA (Crescitelli et al., 2013), which hinted at a selective packing mechanism.

1.2.4.1.1 MicoRNAs (miRNAs)

MicroRNAs (miRNAs) are endogenous, small non coding RNA (20–21nt) in length and One class of frequently detected exRNA is mature miRNA (sometimes referred to as exomiRs) (Yáñez-Mó et al., 2015). MiRNAs are transcript from intron segment of gene by transcriptase enzyme to pri-miRNAs Pri-miRNA are often several kilobases long and form stem loop/hairpin structures by folding to match base pairs along the strand , which are subsequently cleaved into pre-miRNAs by drosh, Primary processing is carried out by Drosha and other proteins cleaving at the base of the structures, producing the 60-70 nucleotide pre-miRNA (Burke et al.,, 2014). Exportin- 5 helps transport pre-miRNA out to the cytoplasm through nuclear pores where it is further processed. Pre-miRNA undergoes further cleavage by Dicer proteins before the 21-25 nt double strand is anchored into and Argonaute protein complexes and the strands are separated (Yi et al., 2003). MiRNAs typically bind to the 3' UTRs of target mRNAs, resulting in mRNA degradation and/or translational repression. MiRNAs may function as either oncogenes or tumor suppressors under certain conditions including amplification or deletion of miRNA genes, abnormal transcriptional control of miRNAs, dysregulated epigenetic changes and defects in the miRNA biogenesis machinery (Peng et al., 2016). MiRNAs are involved in the control of gene expression after transcription and are commonly dysregulated in the pathogenesis of numerous diseases, including cancer (Kosaka et al., 2013). The packaging of nucleic acids into vesicles would require a distinctive mechanism (Bhome et

al., 2018). For example, it has been revealed that RNA-binding proteins such as ribonuclear protein, hnRNPA2B1, might identify a sequence motif and might be accountable for sorting miRNAs into vesicles once sumoylated (Villarroya-Beltri et al., 2013). Y-Box Binding Protein 1 (YBX-1) and major vault protein (MVP) have also been implicated in packaging miRNA into exosomes (Lin et al., 2019; Teng et al., 2017). Furthermore, a link between MVB and RISC has been described raising the possibility that these proteins are involved in exosomal miRNA sorting (Gibbings et al., 2009). Using the neutral sphingomyelinase-2 (nMase-2) inhibitor (GW4869), Kosaka and colleagues were the first to confirm that ceramide altered the content of exosomal miRNA (Kosaka et al., 2010).

It has been postulated that RNA that is intended for vesicles and released from the cell has a signalling pattern; this hypothesis has been verified for miRNA cargo. The researchers employed microarray analysis to recognise miRNAs increased in vesicles (rather than the entire cell) and compared sequence alignments to detect genetic markers (Bhome et al., 2018).

Koppers-Lalic et al. (2014) investigated the function of non-template terminal nucleotide additions at the 3' end in exomiR sorting in B cells. According to RNA sequencing, ExomiRs were considerably more likely to be uridinylated at their 3' end, while cellular miRNAs were more likely to be adenylated. The results were matched in exosomes from healthy urine, indicating that this process is not confined to B cells (Koppers-Lalic et al., 2014).

2.4.1.2 DNA content of EVs

In several investigations, double-stranded genomic DNA (gDNA) has been found in various forms of EVs (Thakur et al., 2014). It is possible that various EV types package distinct portions of DNA. EVs can transport oncogene amplifications, mitochondrial DNA (mtDNA), and single-stranded DNA (Guescini et al., 2010; Balaj et al., 2011; Thakur et al., 2014; Kahlert et al., 2014). MtDNA migration may occur via EVs, and so EVs may constitute an alternate pathway for mutated mtDNA to infiltrate other cells, favouring the spread of different diseases (Guescini et al., 2010). Tumour-EVs include DNA that indicates the tumour's genetic status, such as c-Myc gene amplification (Balaj et al., 2011). In EVs, DNA varying in length from 100 base pairs (bp) to 2.5 kilobase pairs (kB) can be found in EVs (Thakur et al., 2014). EV-carried DNA could be used to identify mutations in primary tumour cells and hence could be

a translational biomarker. However, the physiological relevance of the DNA cargo in EVs is unclear at this time (Thakur et al., 2014).

1.2.4.2 Protein cargo

As ESCRT proteins govern exosomal production and MVB transport, these proteins and their accessory proteins (Alix, TSG101, HSP90 and heat-shock proteins HSC70) are predicted to be present in exosomes regardless of the cell type from which they originate (Doyle and Wang, 2019). As a result, this group of proteins is frequently referred to as exosomal marker proteins. Membrane proteins that create microdomains in the plasma membrane or endosomes are commonly found on EVs (Hemler, 2003). Tetraspanins are a class of more than 30 proteins with four transmembrane domains that are necessary for ILV synthesis and subsequent EV release (Van Niel et al., 2011). In B cell exosomes, tetraspanins such as CD63, CD82, CD81, and CD9 have been described; they may be enriched > 100-fold compared to the transferrin receptor, which may be considered a marker for both the plasma membrane and early endosomes in this cell type (Escola et al., 1998). Tetraspanins have been found in EVs obtained from a variety of sources and can be regarded as common EV markers (Andreu and Yáñez-Mó, 2014; Jankovičová et al., 2020).

Some proteins, such as sumoylated heterogeneous nuclear ribonuclear protein A2B1 (Villarroya-Beltri et al., 2013), annexin a2, and YBX1, have been proposed to have a function in RNA packing (Shurtleff et al., 2016). However, the significance of these and other elements in defining EV content remains to be fully elucidated. Protein cargos delivered by EVs act as regulators in recipient cells, triggering impacts on cell shape, downstream signalling pathways, or other cancer features (Jabalee et al., 2018).

Due to a variety of loaded components, the function and destination of EVs vary. As a result, there are many regulatory systems for loading protein into EVs. Modifications at the plasma membrane start the production of all vesicles. Lipid rafts may have a role in the organisation of those areas, as well as the membrane proteins that reside in them. Stomatin, Lyn, GM1, and flotillin-1 are connected to lipid raft domains and have been found in vesicles (de Gassart et al., 2003). The same finding demonstrated that Lyn in vesicles is controlled after sorting via caspase-3. The fact that post-translational modification happens in vesicles, which are associated with many different kinds of protein, is convincing evidence for the existence

of a purposeful sorting process. It has been proposed, for example, that whole rafts are incorporated into vesicles containing their attached proteins (de Gassart et al., 2003).

Cells use ubiquitination to transport proteins to breakdown pathways, usually by packing them into lysosome-associated vesicles with the aid of the ESCRT complexes (Zhang et al., 2019b). Additional research has revealed that the ubiquitin-dependent pathway is used to degrade receptors in immature dendritic cells. Following cell activation, the ubiquitin-independent technique is used, and the cells release vesicles carrying the MHC-II complex, which has the ability to communicate with T cells (Buschow et al., 2009).

Phosphorylation is involved in selecting proteins that are destined for vesicles. The Tau protein in Alzheimer disease is abnormally phosphorylated; it is added to the vesicles, allowing it to disseminate (Saman et al., 2012). This suggests that there are other components to the system, most likely proteins that bind specifically to the improperly phosphorylated Tau protein and guide it into place inside the EVs.

The common EV markers CD81 and CD63 have been co-localized on membranes with N linked glycans; crucial for the association of CD81 with vesicles (Liang et al., 2014). The concept that glycans designate distinct membrane areas where EVs form is consistent with prior studies on lipid rafts. Proteins are subsequently glycosylated or otherwise changed to target these domains; they are either integrated into or connected to the membrane before inward curvature. (Liang et al., 2014)

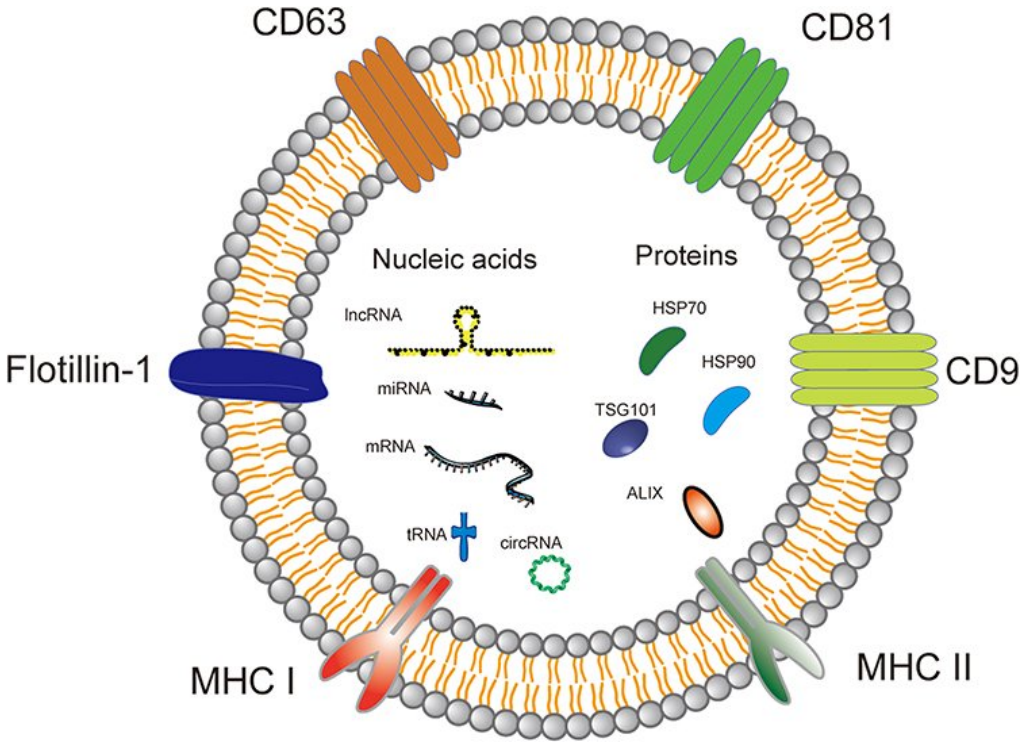

Figure 1. 6 The structure and content of vesicles. The vesicles consist of a phospholipid bilayer and contain proteins, nucleic acids, and lipids. The diagram was created using BioRender as adapted and modified by Fujita et al. (2015).

1.2.5 Uptake of EVs by recipient cells (cell-cell communication)

Several well-established processes exist for internalising materials from extracellular locations via a cell's plasma membrane. Surprisingly, nearly all of these appear to be used in the widespread uptake of EVs (Mulcahy et al., 2014). Clathrin-dependent endocytosis as well as clathrin-independent mechanisms which include caveolin-mediated uptake and lipid raft-mediated internalisation, macropinocytosis, and phagocytosis are examples of EV uptake techniques (Figure 1.7) (Mulcahy et al., 2014).

1.2.5.1 Clathrin-dependent endocytosis

Clathrin-dependent endocytosis is dependent on the formation of clathrin-coated vesicles, which requires the involvement of a number of transmembrane receptors and their ligands (Kirchhausen, 2000). Clathrin is a protein that takes the form of a triskelion with three heavy chains and three light chains. These chains join to create a coated pit, which deforms the membrane, causing this to collapse into a vesicular bud, mature, and pinch off. The next intracellular vesicle is uncoated by clathrin; it subsequently merges with the endosome,

where it discharges its contents (Royle, 2006). It has been shown that reducing dynamin2 (Vallee et al., 1993) or blocking this process with chlorpromazine (Escrevente et al., 2011) limits EV uptake.

1.2.5.2 Clatherin-independent pathways

Caveolae are microscopic cave-like invaginations in the plasma membrane that can be absorbed into the cell (Doherty and McMahon, 2009). Caveolin-1 is a necessary protein; it is required for the formation of caveolae and may be seen clustered within membrane invaginations (Doherty and McMahon, 2009). Caveolae are glycolipid raft subdomains of the plasma membrane that are high in cholesterol, sphingolipids, and caveolins. Caveolin oligomerization (assisted by caveolin oligomerization domains) contributes to the formation of caveolin-rich rafts in the cell membrane (Smart et al., 1999). In one experiment (Nanbo et al., 2013), silencing this protein was shown to reduce EV absorption, whereas in another, it was found to promote EV uptake (Svensson et al., 2013). The causes of this conflict remain unknown; although it has been suggested that this system has some flexibility, it has also been suggested that caveolin-1 silencing produces changes in the membrane composition, perhaps lowering its rigidity, which makes EV uptake more efficient in some cells.

Macropinocytosis is another endocytic mechanism, but it is somewhat distinct. The membrane protrudes from the cell surface in huge characteristic protrusions; it can encircle a region of extracellular environment that is later internalised by fusing with another protrusion or directly fusing with the plasma membrane (Swanson, 2008).
Researchers blocked Na+/H+ exchange or used small molecule antagonists of the rac-related C3 botulinum toxin substrate (rac-1) to disrupt this pathway, which both reduced EV uptake by microglia (Fitzner et al., 2011). In other studies, however, some inhibitors have had no effect on EV uptake (Feng et al., 2010; Christianson et al., 2013; Nanbo et al., 2013).

Phagocytosis is a form of endocytosis that occurs when macrophages internalise large items such as bacteria. Studies using EVs produced from leukaemia cells have shown that they could only be internalised by macrophages and not by other cells, indicating that phagocytosis is involved (Feng et al., 2010). Additional studies, employing PI3K inhibitors to limit phagocytosis and EVs dyed with the pH sensitive dye pHrodo, that might be found within

acidic phagosomes, confirm a phagocytic function in EV absorption (Feng et al., 2010; Montecalvo et al., 2012).

Lipid rafts are microdomains on the cell surface that have modified phospholipid composition and are abundant in receptor proteins and sphingolipids such as sphingomyelin. They represent another alternative uptake strategy. Exosomal ligands that bind to specific receptors on the cellular plasma membrane, as well as the presence of cholesterol- and sphingolipid-rich microdomains on the cell membrane, are both essential for raft-mediated endocytosis (Calder and Yaqoob, 2007). As previously proven, clathrin-independent endocytosis is significantly reliant on cholesterol, which is abundant in lipid rafts. These rafts can also be present in caveolin-1 invaginations or in planar sections of the cellular membranes designated by flotillins, a protein family that mediates endocytosis without the need for clathrin or caveolin (Glebov et al., 2006; Otto and Nichols, 2011).

Many investigations have been carried out to guarantee that lipid rafts are blocked in EV uptake. In one of these experiments, EV uptake in dendritic cells was reduced when EV-producing cells were pre-treated using fumonisin B1 and N-butyldeoxynojirimycin hydrochloride, both of which reduce glycosphingolipid composition in the plasma membrane by blocking its creation (Wang et al., 1991; Platt et al., 1994; Izquierdo-Useros et al., 2009). This demonstrates that EV sphingolipids play an important role in binding and endocytosis, most likely through cholesterol-rich microdomains in dendritic cells (Izquierdo-Useros et al., 2009).

It is also feasible that EVs are adsorbed through direct fusion with the plasma membrane due to the fluid characteristics of the plasma membrane. In an aquatic environment, direct fusion of two lipid bilayers may occur easily, and this way may be seen via fluorescent lipid dequenching. Investigations with this technology have demonstrated that some EV uptake can occur through this pathway (Parolini et al., 2009).

Moreover, several studies have suggested that tetraspanins, which are prevalent on the EV surface, have a role in EV internalisation. As tetraspanins are ubiquitous and play important roles in adhesion, it is probable that EV absorption happens via comparable routes (Rana et al., 2012). Antibodies against the tetraspanins CD81 or CD9 on recipient cells have been shown to decrease EV uptake by dendritic cells (Morelli et al., 2004).

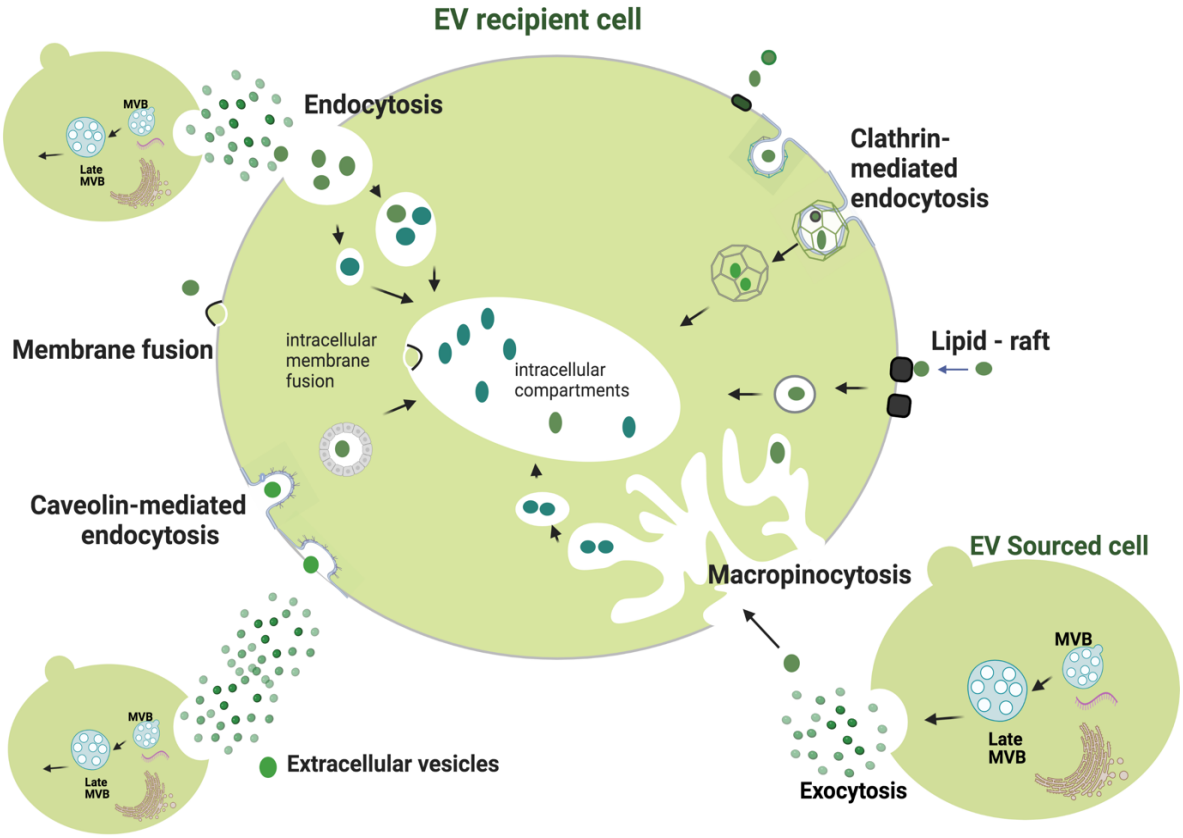

Figure 1. 7 Uptake of extracellular vesicles; The diagram depicts clathrin-dependent endocytosis as well as clathrin-independent pathways such as caveolin-mediated uptake, micropinocytosis, lipid raft-mediated internalisation and phagocytosis. BioRender was used to create this, which was derived and modified from (Mulcahy et al., 2014).

1.2.6 EV effects on tumour microenvironment

It has been demonstrated that tumour-derived EVs facilitate intercellular communication, hence promoting tumour development and metastasis in both local and distant environments (Becker et al., 2016). They promote tumour formation by modulating a variety of important biological activities such as proliferation, angiogenesis, immune reprogramming, as well as activating stromal cells (Ratajczak et al., 2006a; Becker et al., 2016; Kalluri and LeBleu, 2020).

1.2.6.1 Endorsing cell proliferation and apoptosis resistance

Normal cells can be recruited into the tumorigenic process by EVs secreted by cancer cells, which facilitate their phenotypic transition and so contribute to tumour development by increasing proliferative signalling (Xavier et al., 2020). EVs can help cancer cells resist

apoptosis (O'Neill et al., 2019). In melanoma, for example, platelet-derived growth factor receptor beta (PDGFR-β) transfer was facilitated by EVs produced by melanoma (recipient) cells, allowing them to bypass the MAPK pathway on BRAF-mutated (donor) cells, resulting in cell growth and apoptosis suppression (Xavier et al., 2020).

Several studies have confirmed the significance of miRNAs found in EV cargo on cancer cell growth and death. For instance, EVs which are released from an oesophageal cell line transmit miR-93-5p to neighbouring cancer cells, altering phosphatase and tensin homolog (PTEN) expression and its downstream proteins, cyclin D1 and p21and thereby enhancing recipient cell proliferation (Liu et al., 2018). Long non-coding RNAs (lncRNA) contained in cancer-derived EVs have been found to influence cancer cell growth and apoptosis. This has been reported in a variety of tumour cell types, including gastric, colon, and oesophageal cancer (Guo et al., 2017; Zhang et al., 2018).

1.2.6.2 Supporting Angiogenesis

Tumour development and metastasis need the production of *de novo* vasculature, and EVs play an important role in this process. Tumour-derived EVs can promote angiogenesis by allowing cancer cells to communicate with endothelial cells. Tumour-derived exosomes have also been found to impact angiogenesis upregulation (Ludwig et al., 2018).

EVs generated by glioma cells have been shown in several studies to influence angiogenesis by transferring pro-angiogenic factors such as lncRNA CCAT2 and lncRNA POU3F3 (Lang et al., 2017), miR-21 (Sun et al., 2017), or CXCR4 receptor (Giusti et al., 2016), which resulting in an increase in VEGF on recipient endothelial cells. VEGF was also discovered in the cargo of EVs and was found to have a role in angiogenesis activation (Sun et al., 2017; Giusti et al., 2016; Lang et al., 2017).

Furthermore, investigations have revealed that cancer cell-derived EVs transport VEGF and IL-6, two powerful pro-angiogenic factors, as well as other compounds capable of stimulating endothelial cell invasion and organising into tubule-like structures (Kosaka et al., 2013).

A recent study discovered that miR-130a delivered into human umbilical vein endothelial cells (HUVECs) by exosomes from gastric cancer cells encouraged angiogenesis

and tumour growth *in vivo* and *in vitro* by targeting c-MYB; thus, miR-130a packaged in cancer cell exosomes serves as an angiogenesis driver (Yang et al., 2018).

1.2.6.3 Immune suppression

Most tumour cells produce antigens that the immune system can recognise. On the other hand, tumour cells produce vesicles that have the power to suppress immune responses. As a result, exosomes perform a variety of immune suppressive activities, including the induction of apoptosis in activated T lymphocytes via the production of death ligands FasL (Andreola et al., 2002) and the factor-related apoptosis-inducing ligand TRAIL (Taylor and Gercel-Taylor, 2005); dendritic cell differentiation from monocytes is impaired (Clayton and Mason, 2009), as well as the inhibition of cytotoxic responses mediated by NK cells (Clayton et al., 2007).

T-cells were repressed by EVs generated by breast cancer cells according to research conducted by providing TGF- β straight to these immune cells (Rong et al., 2016). Another study found that tumour-derived exosomes can impede NK cell development by releasing the immunosuppressive cytokine transforming growth factor- (TGF- β) (Szczepanski et al., 2011). EV regulation of B-lymphocytes has already been described, despite the fact that it is mostly unexplored. The transformation of naïve B cells into TGF-producing regulatory B cells was encouraged by EVs produced by oesophageal cancer cells, leading to immunological suppressor effects on T-cell proliferation (Li et al., 2015).

1.2.6.4 Involvement in Cancer Cell Invasion and Metastasis

Most cancer cells must be able to pass through the weakened extracellular matrix, necessitating a dramatic reorganisation of the cytoskeleton (Shimoda and Khokha, 2013; Wang et al., 2014a). Both tumours and neighbouring normal cells have indeed been discovered to release vesicles that contain large amounts of proteolytic enzymes, which are involved in the degradation of cell-matrix bonds and cell-cell bonds (Shimoda and Khokha, 2013).

Interestingly, vesicles from distinctive tumour types bear integrins which target EVs to certain tissues and trigger signalling pathways inducing pre-metastatic niche formation (Hoshino et al., 2013). EVs generated by renal cancer cell lines have been shown to reduce

the cell adhesion molecule (EpCAM) in a p-Akt dependent way, encouraging malignancy by boosting cell mobility (Jiang et al., 2014). Further research has revealed that blocking any vesicle formed by deactivating the protein RAB27B inhibited the development of metastatic characteristics (Ostenfeld et al., 2014a).

In addition, function of miRNAs cargo has been investigated *in vitro*. One example is the discovery of miR-205-5p or miR-423-5p in EVs secreted by cholangiocarcinoma or gastric cancer cells (Kitdumrongthum et al., 2018; Yang et al., 2018). A further study showed that exosomes with low levels of CD9 and high levels of CD151 in prostate cancer can drive the migration and invasion of non-cancerous prostate cells, causing metastases (Brzozowski et al., 2018; Bray et al., 2018; Thakur et al., 2022). As a result, the great majority of experimental research confirms that EVs play an important role in encouraging cancer characteristic attributes at various phases of cancer development (Fang et al., 2018).

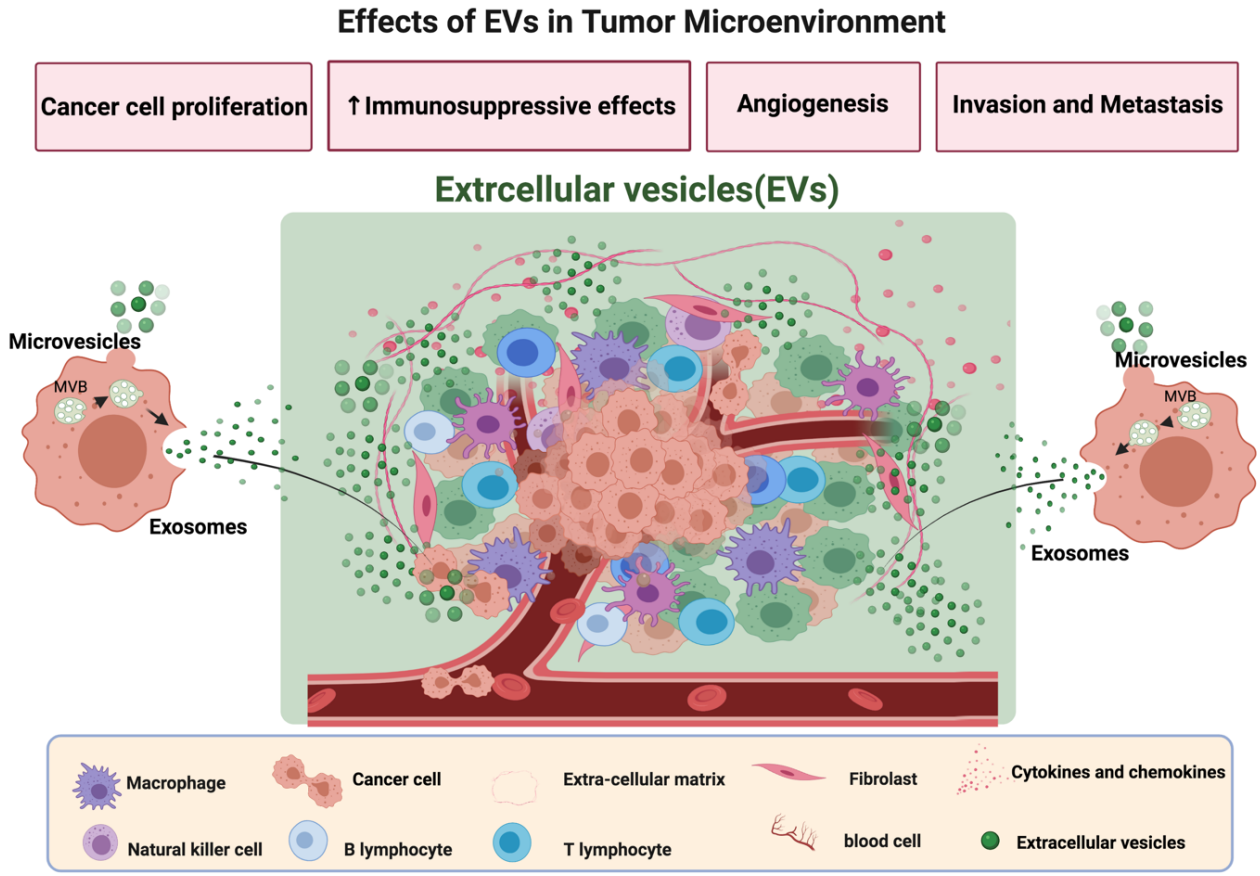

Figure 1. 8 The function of EVs in the tumour microenvironment. The diagram displays different cell types' components with the function of vesicles included in the tumour microenvironment. The image is adapted from Ciardiello et al. (2016) and created by Biorender.

1.2.7 The role of EVs in oral squamous cell carcinoma

EVs have been implicated in cancer progression in OSCC and have been shown to promote cancer growth, proliferation, spread and invasion of tumour. For example, the nuclear factor kappa-light chain-enhancer of activated B cells (NF-B) pathway in monocytes has been found to be stimulated by OSCC-derived EVs, resulting in a cytokine-rich environment that promotes tumour growth (Momen-Heravi and Bala, 2018b).

In addition, recent research has demonstrated that tumour cells have increased Snail and Vimentin protein expression by miRNA-21-enriched in exosomes while decreasing E-cadherin levels, indicating that OSCC might form a niche for distant transfer (Wang et al., 2014b; Li et al., 2016a). Previous research has revealed that EVs generated from OSCC cells carry exosomal proteins such as Sonic Hedgehog (Shh), 6-phosphofructo-2-kinase / fructose-2,6 biphosphatase (PFKFB3) which is angiogenic proteins, activating the relevant model mechanism to provoke endothelial proliferation or tubule formation (Gu et al., 2017; Huaitong et al., 2017). Also, it has been demonstrated that exosomes from the plasma of patients with head and neck squamous cell carcinoma (HNSCC) display PD-L1 on their surface, which interacts with the PD-1 receptor on immune cells, inhibiting T-cell function and so promoting tumour growth (Theodoraki et al., 2018; Thakur et al., 2022).

A study showed that exosomal miRNA-200C-3p and miRNA-1246 can be transported to primary OSCC cells where they target chromodomain helicase DNA 9/Werner and DENN/MADD Domain Containing 2D (DENND2D) increasing tumour cell proliferation, metastasis, and invasion (Kawakubo-Yasukochi et al., 2018).

Furthermore, OSCC cell migration and invasion were increased by exosomes generated by hypoxic OSCC cells in an HIF-1 and HIF-2 dependent manner (Li et al., 2016a).

Additionally, EVs derived from OSCC had an effect on tumour angiogenesis via the ephrin type B receptor 2 (EPHB2), both *in vitro* and in animal models (Sato et al., 2019). Furthermore, angiogenesis was boosted by HNSCC-released vesicles containing interleukin-6 (IL-6) and IL-10, as well as IL-6-dependent inflammatory activation (Moskovitz et al., 2018; Chen et al., 2020a).

1.2.8 EVs in biological fluids

Once discharged from cells, EVs may enter body fluids; thereby EVs can be purified from several biological fluids such as plasma (Caby et al., 2005), nasal fluid (Lässer et al.,

2011b), cerebrospinal fluid (Street et al., 2012; Marzesco et al., 2005), breast milk (Lässer et al., 2011b), urine (Pisitkun et al., 2004), sperm (Sullivan et al., 2005), bronchial lavage fluid (Asef et al., 2018), and other fluids including saliva (Gonzalez-Begne et al., 2009; Ogawa et al., 2011; Sun et al., 2016a). (Figure 1.9)

Salivary EVs were discovered by Gonzalez et al. (2009) during *in vitro* culture of salivary gland epithelial cells. in addition , epithelial cell markers can be detected on saliva-derived EVs and it is likely that these cells are the source of the EVs found in saliva. Suggesting that saliva-derived EVs are mainly from granulocyte and epithelial cells origin (Kapsogeorgou et al., 2005).

Saliva is a combination of secretions that come from three pairs of major salivary glands (submandibular, sublingual and parotid glands) and numerous minor glands spread across the oral mucosa, combined with gingival crevicular fluid, which all affect the composition of saliva (Lamy and Mau, 2012). Saliva performs a lubricative role, such as wetting food, allowing the instigation of swallowing and protecting the mucosal surfaces of the oral cavity from drying (de Almeida et al., 2008). It consists of 99% water and proteins such as enzymes (α-amylase, lingual lipase, and lyzosomes), cell debris, microorganisms, and cytokines. It also contains other important substances, including antibodies, electrolytes, and mucus (Sun et al., 2016a). Many of these components enter saliva via blood, either by active transport, passive diffusion, or extracellular ultrafiltration. As a result, saliva may be viewed as a mirror of the body's physiological activity in many circumstances (Lima et al., 2010).

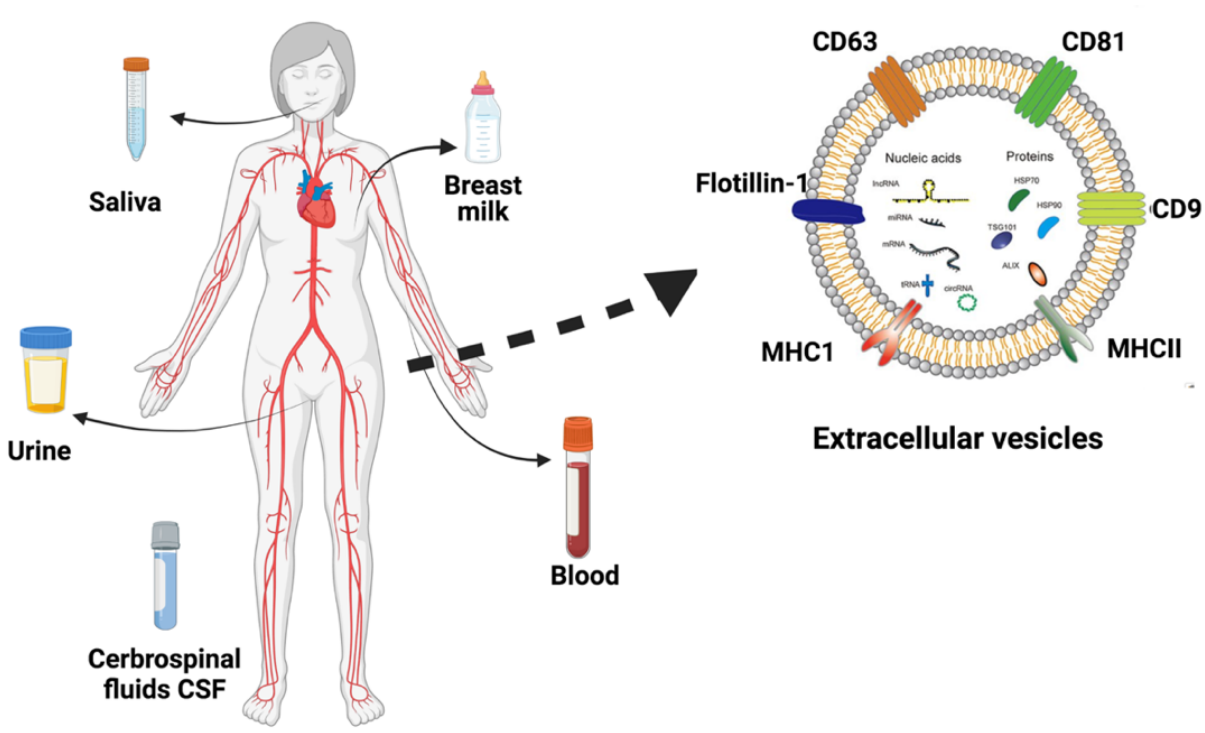

Figure 1. 9 EV in biological fluids. The diagram depicts several sources of EV that may be obtained from biological fluids such as saliva, blood (plasma), urine, CSF, and breast milk. Adapted from (Ciferri et al., 2021) and created by Biorender.

1.2.9 Using saliva as a liquid biopsy

Over the last decade, saliva has been viewed as an attractive bodily fluid for molecular diagnostics. It could be a possible alternative to blood and/or tissue analyses because it contains biological information that is relevant to systemic as well as local diseases. It contains molecules such as RNA, DNA and proteins and it has many different advantages over other bodily fluids like blood (Gai et al., 2018). For example, saliva is easy to obtain by a non-invasive collection method. Consequently, it does not cause discomfort to the patient when repeated collections are required. The collection is also usually economical (Cheng et al., 2019). Saliva has a lower concentration of analytes than blood and so there have been concerns about its use for diagnostic purposes (Miller, 1994). However, this is no longer a constraint due to the improvement of very sensitive molecular tools and nanotechnology (Javaid et al., 2016).

Salivary levels of particular proteins are elevated in OSCC patients. For example,CD44 (a cell surface glycoprotein involved in cell-to-cell contact), Cyfra 21-1 (a cytokeratin 19

fragment), Cancer antigen 125 (CA-125) and tissue polypeptide antigen (TPS), for example, have been proposed as oral cancer biomarkers (Franzmann et al., 2005; Nagler et al., 2006). OSCC-associated saliva RNAs had an 81 percent prediction accuracy rate, indicating their potential as biomarkers for oral cancer diagnosis. Furthermore, Park et al. (2009) found that miR-200a and miR-125a levels were increased in OSCC patients compared to healthy controls, indicating that miRNAs in saliva might be used to identify oral cancer (Park et al., 2009a). In addition, miR-31 was shown to be significantly higher in saliva from patients with oral carcinoma at all clinical stages, including very small tumours, according to Liu et al. (2012), who employed it as a clinical biomarker of OSCC in oral lesions, saliva, and plasma. Salivary miR-31 was shown to be more prevalent than plasma miR-31, which suggests that salivary miR-31 might be utilised to make a more accurate diagnosis of oral cancer. Furthermore, after oral cancer excision, salivary miR-31 levels were substantially lower, indicating that the bulk of the up-regulated salivary miR-31 was sourced from tumour tissues (Liu et al., 2012).

Salivary proteomics is also a useful method for detecting systemic disorders like Sjogren's syndrome (SS). A panel of potential SS salivary biomarkers was recently explored. SS was discovered to have a substantial impact on twenty-eight proteins (Baldini et al., 2011). The salivary proteomic profile of type 2 diabetes patients showed that 52 proteins were differentially increased in the saliva of diabetics compared to controls, as well as greater levels of several diabetes-related inflammatory indicators (Border et al., 2012). According to previous research, 65 of the 487 detected proteins in saliva showed increased amounts in type 2 diabetes patients compared to healthy people (Rao et al., 2009). As a result, saliva protein profiling might be proove to be a useful tool for diagnosing and monitoring disorders.

1.2.10 Salivary EVs as a source of biomarkers

As mentioned previously saliva contains a high concentration of EVs, which are enriched in RNAs and proteins. So, proteomic and transcriptomic analysis of EVs constitutes an emerging and promising avenue for the discovery of biomarkers for systemic and oral diseases (Chiabotto et al., 2019). EVs have been shown to enhance their cargo stability and as a result, they can increase the bioavailability of bioactive chemicals. The EV lipid bilayer membrane that envelops bioactive cargo can survive the activity of digestive enzymes in

bodily fluids, protecting their contents from breakdown until they reach their destination (Boukouris and Mathivanan, 2015).

1.2.10.1 The relationship between salivary EVs and systemic Diseases

Salivary EVs have drawn substantial attention as a potential source of systemic disease and cancer biomarkers, and as a means of observing body health (Becker et al., 2016). The role of salivary EVs for diagnosis is mainly based on two macromolecular substances; RNAs and proteins as biomarkers of cancer (Al-Tarawneh et al., 2011).

EVs were shown to pass through epithelial barriers such as the blood–brain barrier, demonstrating that they may have a role in transferring RNAs from the blood into saliva (Kim et al., 2003). They were also discovered to have a significant key role in the pathogenesis of neurodegenerative disorders, for example, Alzheimer's disease, a disease that has an assembly of pathophysiological and medical correlations with traumatic brain injury (Cheng et al., 2019).

Lau et al. (2012) created a model for analysing a systemic ailment using a non-invasive method. The pancreatic cancer cell line Panc02 was embedded into the pancreas and the reduction of disease-specific salivary biomarkers, by suppressing the biogenesis and formation of tumour-derived exosomes, demonstrated that they have an essential role in the development of salivary tumour-specific biomarkers (Principe et al., 2013). Despite the fact, however, that it is known that saliva contains gingival crevicular fluid, a serum transudate, there was not a clear rationalization for this (Lamster and Ahlo, 2007; Principe et al., 2013). Machida et al. (2016) found that miR-4644 and miR-1246 contained in salivary EVs were hypothetical biomarkers of cancer in the pancreatobiliary tract (Machida et al., 2016).

Numerous proteomics studies of salivary EVs have shown different disease profiles. CD24 peptides are greatly expressed in a range of different diseases, such as hepatitis B and SS in saliva and plasma (Zheng et al., 2014). Furthermore, Zheng et al. (2017) found that salivary EVs produced from patients with inflammatory bowel disease contain high levels of proteasome subunit alpha type 7 (PSMA7)(Zheng et al., 2017). In addition, Cao et al. (2019) discovered Synuclein in salivary EVs, which might be used as a diagnostic biomarker for Parkinson's disease (PD), where the levels of -synOlig, -synOlig/-synTotal in salivary EVs are greater in PD than in controls (Cao et al., 2019). Nik Mohamed Kamal et al. (2020) discovered

that miR-28-5p, and miR-5571-5p were considerably increased in salivary EVs from patients with periodontitis compared to healthy individuals, indicating that they might be potential biomarkers (Nik Mohamed Kamal et al., 2020).

Saliva-derived EV from patients with oesophageal squamous cell carcinoma were strongly abundant with two short RNAs (tRNA-GlyGCC-5 and sRESE), which might be useful as biomarkers for diagnosis and prognosis, as well as for prediction of adjuvant therapy benefits (Li et al., 2022). EV-associated miRNAs have been found in the saliva of patients with ovarian (Gallo et al., 2012) and lung cancer (Sun et al., 2018).

1.2.10.2 Use of Salivary EVs as a source of biomarkers in head and neck cancer

The salivary EV is a useful biomarker for OSCC (Fuller et al., 2015; Dionne et al., 2015), and it has attracted the most interest of researchers in many studies (Valadi et al., 2007c; El Krief et al., 2011; Andaloussi et al., 2013; Wong, 2015; Lötvall et al., 2014; Wang et al., 2020). A study has demonstrated that increased circulating vesicles in cancer patients are associated with poor diagnosis (Kim et al., 2003). The majority of these circulating vesicles appear not to originate from cancer cells but to be derived from activated platelets or megakaryocytic cells (Flaumenhaft et al., 2009) and macrophages, lymphocytes, and erythrocytes (Rak, 2013). Zlotogorski-Hurvitz et al. (2016) showed that saliva from oral cancer patients had a much greater concentration of EVs than healthy persons. Furthermore, the same study found that OSCC patients' salivary EVs had a higher CD63 abundance but less CD9 and CD81, which might be utilised for oral cancer detection (Zlotogorski-Hurvitz et al., 2016).

Salivary EVs derived from patients with HNSCC are larger (ranging from 20 to 400 nm in diameter) than healthy controls (Sharma et al., 2011). They exist in aggregates or more extended agglomerates. This effect was most notable in cases with advanced stages of HNSCC (Sharma et al., 2011).

Fontana et al., (2021) confirmed that protein cargo of salivary EVs define a functional signature through quantitative proteome using the SWATH MS (Sequential Window Acquisition of all Theoretical Mass Spectra method), resulting in quantitative information for 365 proteins differentially characterised by the EVs of analysed clinical conditions, thus having potential value as novel predictor biomarkers for OSCC (Fontana et al., 2021).

Furthermore, certain subsets of miRNAs are detected in salivary EVs from individuals with oral squamous cell carcinoma. MiR-517b-3p and miR-302b-3p were exclusively found in vesicles from OSCC patients, whilst miR-512-3p and miR-412-3p were up-regulated in EVs from OSCC patients. All four miRNAs have the potential to be employed as biomarkers (Gai et al., 2018).

After extracting EVs from conditioned media from four HNSCC cell lines and oral epithelial control cells, Langevin et al. (2017) employed miRNA-sequencing to fully define their miRNA cargo and compare transcripts with salivary EVs in different patients. They observed that numerous candidate miRNAs, including miR-486-5p, miR-486-3p, and miR-10b-5p, were over-expressed in the EVs of a subset of head and neck carcinomas in saliva and tissue as compared to cancer-free controls (Langevin et al., 2017).

When researchers discovered that expression of miR-24-3p was substantially higher in the salivary EVs of OSCC patients compared to healthy people, they established the potential of exosome miRNA cargo as a future investigative biomarker. They also discovered that miR-24-3p levels in OSCC neoplastic tissues were greater, indicating that cancer cells generate circulating miR-24-3p. They also discovered that overexpressing miR-24-3p boosted OSCC cell growth, showing that salivary EV miR-24-3p may be used to detect OSCC (He et al., 2020).

Wang et al. (2020) isolated EVs from HPV-associated oropharyngeal cancer (HPV-OPC) and discovered that HPV 16 DNA is packaged in salivary EVs in 80% of HPV16-positive tissues/biopsies. This result was obtained after previous studies failed to detect human papilloma viral (HPV) DNA in whole saliva and did not show adequate clinical performance (Wang et al., 2020).

Thus, suggesting that cancer-specific proteins, miRNAs and precise antigens in salivary EVs might be useful biomarkers for the detection of premalignant lesions and early-stage cancer (Principe et al., 2013).

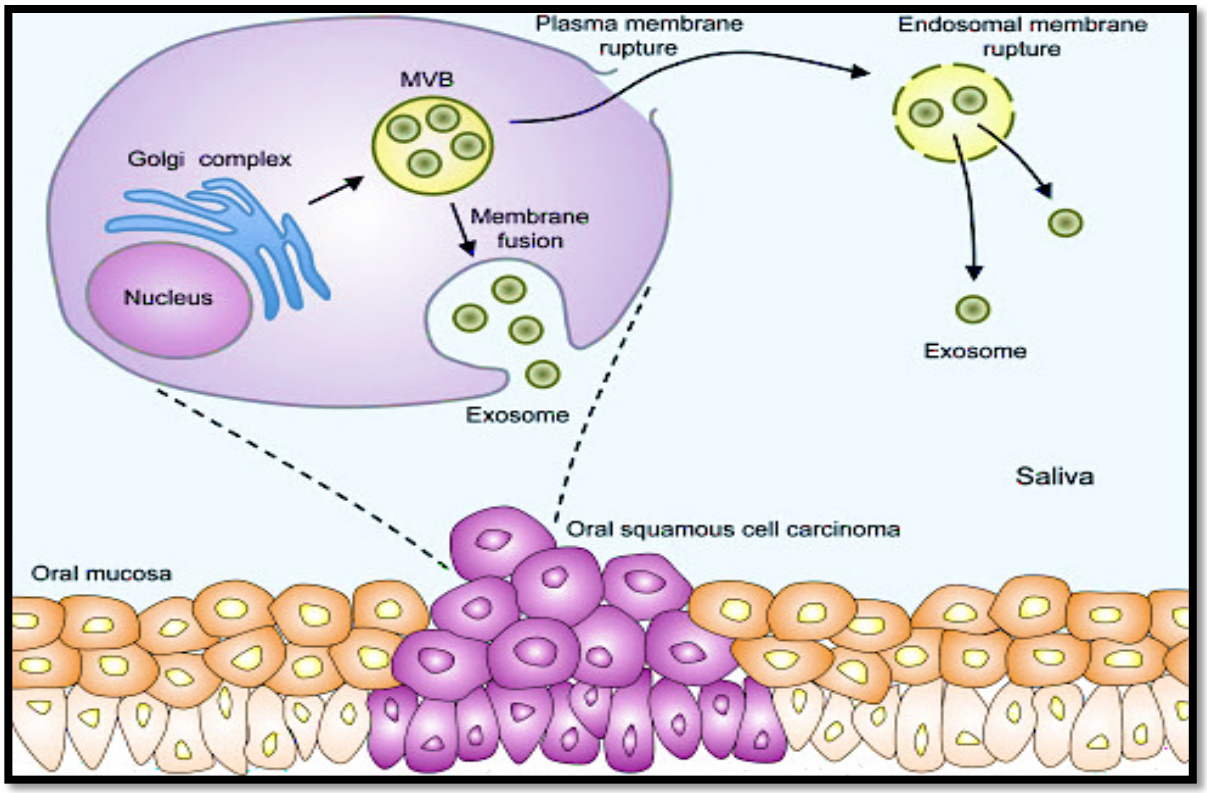

Figure 1. 10 Salivary EVs derived from OSCC cells. The diagram illustrates the release of EV from oral cancer tissue and adapted from (Nonaka and Wong, 2017b).

1.3 Hypothesis and project aims

1.3.1 Hypothesis

The miRNA cargo of salivary EV can be used as a biomarker signature to develop a diagnostic test for OSCC.

1.3.2 Project aims

- Given the complex nature of saliva (viscosity and highly abundant soluble factors), the first aim is to determine a suitable technique for isolation of EVs from saliva for downstream analysis. Common EV isolation methods, such as ultracentrifugation, size exclusion chromatography and Dynabead immunocapture will be compared to determine their suitability. This decision will be based on the purity of the isolated EVs and also the potential to apply the isolation technique to a large number of patient samples as part of a diagnostic test.
- EVs will be characterised according to the MISEV 2018 guidelines by a variety of techniques including nanoparticle tracking analysis, western blotting, transmission electron microscopy and Exoview tetraspanin profiling.
- The impact of the starting volume of saliva and storage of saliva on EV isolation will be assessed.
- Salivary EVs will be isolated for a cohort of patients with OSCC and healthy controls. EV RNA will be extracted and miRNA cargo analysed by small RNA sequencing.
- Differential expression analysis will be conducted to identify up- and down-regulated miRNA. Validation of small RNA sequencing data will be conducted by qRT-PCR.

Chapter two

2. Materials and methods

2 .1 Materials

All laboratory chemicals and reagents were purchased from Merck, UK (previously known as Sigma-Aldrich) and molecular biology reagents were ordered from Thermo Fisher Scientific, UK unless stated otherwise.

2.2 Methods

2.2.1 Saliva samples

2.2.1.1 Saliva collection

Passive drool saliva samples were collected from healthy volunteers (in accordance with University of Sheffield ethics application 003166) or from patients visiting Sheffield Teaching Hospitals Trust (in accordance with NHS ethics application IRAS: 264332/STH: 20945) by asking them to spit into a sterile 50 ml centrifuge tube. Samples were collected between 8 - 10.30 am. Donors were asked to refrain from eating or drinking anything for at least one-hour prior to the collection of saliva.

2.2.1.2 Saliva processing

Saliva was diluted with an equal volume of sterile phosphate buffered saline (PBS) and endogenous protease activity was quenched by the addition of a cOmplete Mini EDTA FREE protease inhibitor tablet (Roche, Germany). Diluted saliva was clarified by centrifugation at 3,000 x *g* for 30 min to pelleted large debris, dead cells and bacteria, followed by 12,000 x *g* for 45 min. A differential centrifugation methodology was adapted from the protocol previously described by Théry et al. (2006) (Figure 2.1). Where concentrated saliva was required, clarified saliva was reduced to ~0.5 ml by centrifugation at 6,000 x *g* in a Vivaspin 20 (100 kDa MWCO) centrifugal concentrator (GE Healthcare Life Sciences, Sweden).

2.2.2 EV isolation methods

2.2.2.1 Isolation of EVs by ultracentrifugation (UC)

Clarified saliva was centrifuged (Optima TLX- Ultracentrifuge) at 100,000 x *g* for 1 hour at 4°C. Pellets were washed with PBS and recentrifuged at 100,000 x *g* for 1 hour. The supernatant was discarded and the pellet resuspended dependent on downstream

application. Resuspended pellets were transferred to a fresh tube and placed on ice until needed or stored at -20°C.

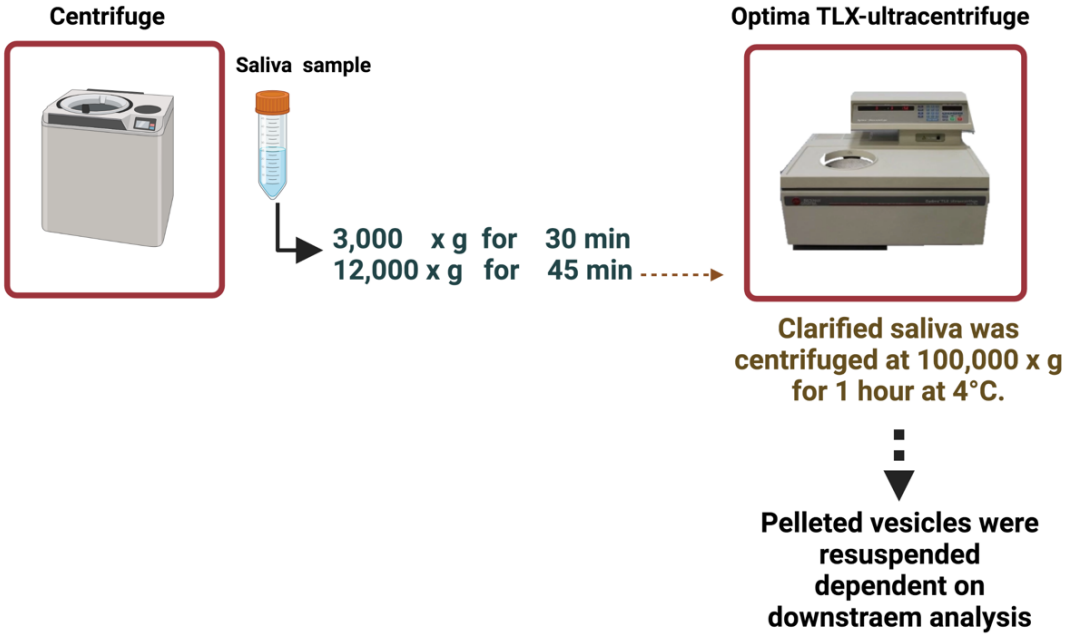

Figure 2. 1 Schematic outlining salivary EV isolation by ultracentrifugation. Saliva was clarified by centrifugation at 3,000 x g, 30 mins and 12,000 x g, 45 mins. The supernatant was centrifuged at 100,000 x g for 1 hour at 4°C. The pellets were collected and resuspended in appropriate buffer for further analysis.

2.2.2.2 Isolation of EVs by Size Exclusion Chromatography (SEC)

14 ml of Sepharose CL-2B slurry (GE Healthcare Life Sciences, Sweden) was added to each Econo-Pac chromatography column (Biorad, US) and left to settle by gravity. Using forceps, a filter disc was added to the top of the stacked Sepharose resin taking care to prevent the formation of bubbles beneath the filter. The plastic column stopper was removed to allow the ethanol to run out of the column and leave behind 10 ml of Sepharose resin. The stacked Sepharose was washed with 30 ml PBS containing 0.03% (v/v) of Tween-20 (PBST) to remove any ethanol remnants. ~0.5 ml concentrated saliva (Section 2.2.1.2) was loaded onto the prepared SEC column. As soon at the sample had completely entered the resin, the column was topped up with PBST and twenty 0.5 ml fractions were collected in 1.5 ml microfuge tubes (Figure 2.2).

Where necessary, individual or multiple combined SEC fractions were centrifuged at 100,000 x *g* for 1 hour at 4°C. The supernatant was then removed, and pelleted vesicles were resuspended in PBS or protein lysis buffer depending on downstream analysis. 1 ml of Protein lysis buffer was made by adding 100 µl of 10x Radio-Immunoprecipitation Assay (RIPA) buffer (Merck Millipore, Massachusetts, USA), 143 µl of 7x protease inhibitor solution, (prepared by dissolving 1 tablet of protease inhibitor in 1.5 ml of distilled water) (Roche, Burgess Hill, UK), and 0.2 µl of universal nuclease (PierceTM Universal Nuclease for Cell Lysis, Thermo Scientific TM, UK), to 757 µl of dH_2O.

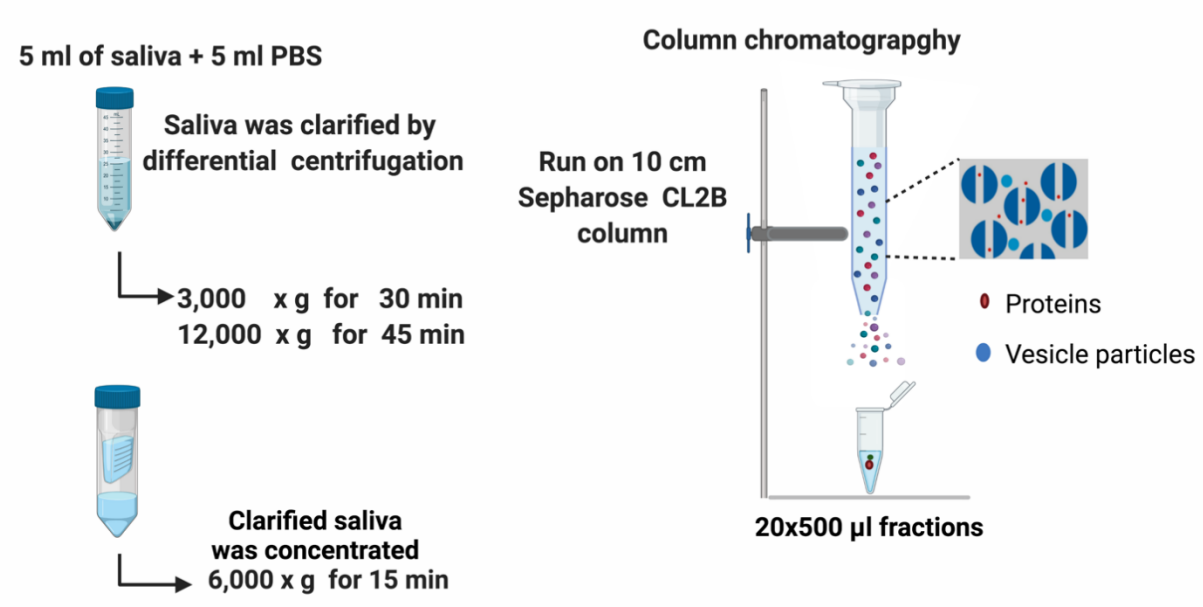

Figure 2. 2 Schematic outlining salivary EV isolation by size exclusion chromatography. Clarified saliva was concentrated to 0.5 ml and fractionated on a 10 ml Sepharose column. Twenty 0.5 ml fractions were collected from the column.

2.2.2.3 Isolation of EVs by Dynabead immunocapture

Dynabeads pre-conjugated with anti-human CD63, CD9, and CD81 antibodies were purchased from Invitrogen (Catalogue numbers: 10606D, 10614D and 10616D). Dynabeads were vortexed for 30 seconds to ensure even suspension. 100 µl of CD63 Dynabeads (1×10^7 beads/ml), 40 µl CD9 (1.3×10^8 beads/ml) and 40 µl CD81 Dynabeads (1.3×10^8 beads/ml) were pipetted into a 2 ml U-bottom microfuge tube. The tetraspanin bead mix was then

washed with 320 µl of Isolation Buffer (PBS with 0.1% (w/v) bovine serum albumin (BSA) filtered through a 0.2 µm filter) and placed on a DynaMag-2 magnet for 1 min. The supernatant was discarded and the beads were ready for sample loading. ~500 µl of concentrated saliva (Section 2.2.1.2) was added to the tube containing the washed tetraspanin bead mix and incubated overnight (18-22 hours) at 4°C with gentle tilting and rotation (Figure 2.3).

After incubation, the tubes were briefly centrifuged for a few seconds to collect the samples at the bottom of the tube, and then placed on the magnetic rack for 1 min. The supernatant containing unbound EVs and other particles was removed and stored in a microfuge tube at -20°C. The remaining bead-EV complexes in the tubes were washed with 500 µl Isolation Buffer, followed by 2 more washes with 500 µl PBS and resuspended in either protein or RNA lysis buffer for downstream isolating and analysis.

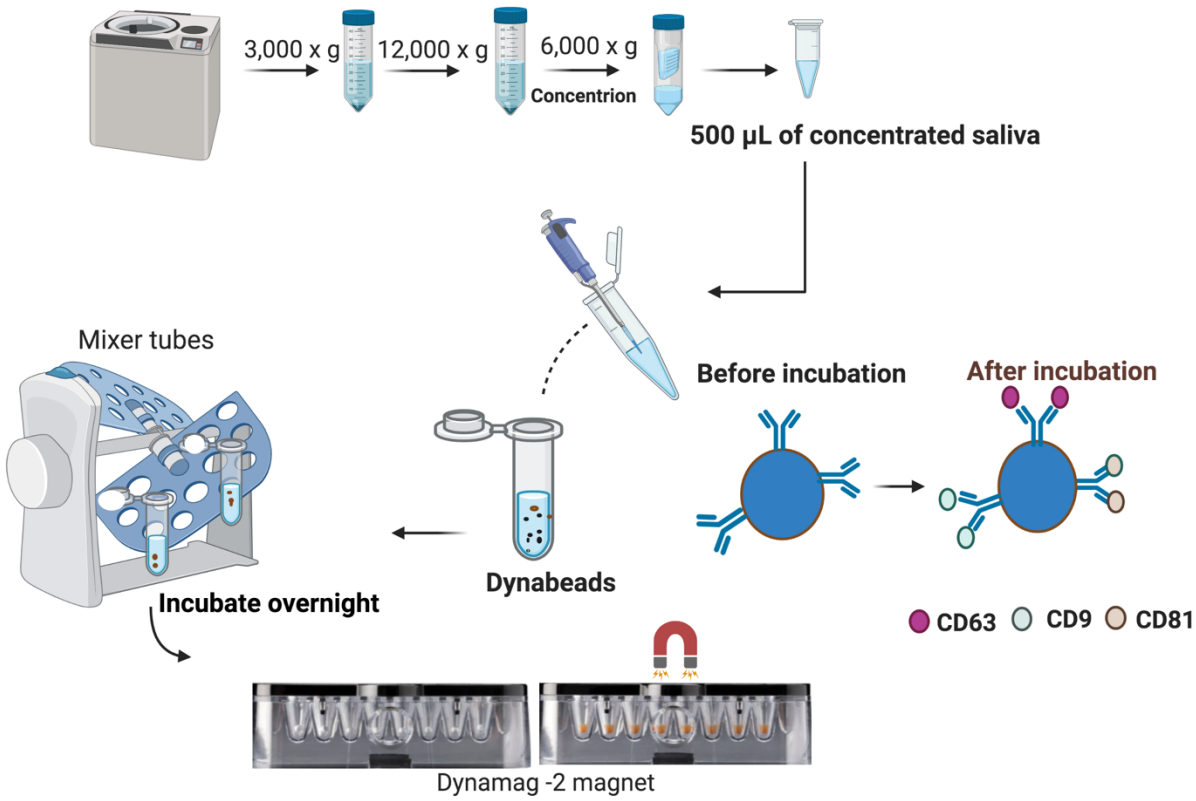

Figure 2. 3 Schematic outlining salivary EV isolation by Dynabead immunocapture. Diagram illustrating the steps to isolate EVs from 500µl of concentrated saliva using Dynabeads coated with anti-CD81, anti-CD9 and anti-CD63 antibodies.

2.2.4 Salivary EV characterisation methods

2.2.4.1 Nanoparticle Tracking Analysis (NTA)

NTA was performed by using a ZetaView instrument, which was calibrated using 100 nm polystyrene calibration particles (Metrix Gmbh, Germany) diluted at 1:250,000 in Milli-Q water. Samples were diluted in Milli-Q water to bring them within optimal concentration parameters (1:20 – 1:200). The data was analysed using the software that was supplied with the ZetaView instrument. To run samples, 3 ml of sample was injected into the instrument, followed by acquisition by the instrument and automatic analysis to remove any outliers. Each sample was run 3 times and video was captured for 60 s each time (Table 2.1). Settings were kept constant within each experiment and between experiments. Particle size and concentration values for technical and biological replicates were averaged.

Table 2. 1 ZetaView setting used for measurement of small particles.

Parameter	Setting for particles (~100nm)
Sensitivity	85
Shutter	70
Min brightness	25 pixels
Max area(size)	500 pixels
Min area (size)	20 pixels
Framerate	30 frames per second(fps)
Tracelength	15
Video quality	Medium
Positions	11 Positions

2.2.4.2 Characterization of salivary EVs by ExoView

EVs were enriched by SEC, pelleted by UC (section 2.2.2.2) and resuspended in 50 µl PBS. After that they were diluted 1 in 4 using proprietary incubation solution. 35 µl of diluted sample was then pipetted directly onto a tetraspanin array chip. The chip was incubated in a humidified environment at room temperature, in the dark, overnight. The chip was washed three times for 5 min using proprietary washing solution at room temperature. Secondary antibody, conjugated to a fluorophore, was added and the chip and incubated for 1 hour at room temperature. The chip was washed three times for 5 min using proprietary washing solution at room temperature and was allowed to dry before being loaded into a metal cassette. The cassette was placed in the ExoView R100. High resolution imaging was then carried out to detect label-free and fluorescent particles bound to the chip. Images were gathered using proprietary software. ExoView analysis was conducted by Dr Alex Shephard (NanoView Biosciences) as part of an instrument demonstration.

2.2.4.3 Characterization of salivary EVs by Transmission Electron microscopy

2.2.4.3.1 Transmission electron microscopy of EVs in suspension

Five microlitres of EV suspension (section 2.2.2.2) was absorbed on air glow-discharged carbon-coated copper-palladium grids for 1 min and stained with 0.75% (w/v) uranyl formate. Imaging was performed on a Philips CM100 TEM, operating at 100 kV, using a Gatan MultiScan 794 1K x 1K CCD camera (Gatan, Pleasanton, CA, USA). Preparation and imaging of TEM grids was performed by Dr Svet Tzokov at the Electron Microscopy Facility, The University of Sheffield.

2.2.4.3.2 Transmission electron microscopy of resin embedded EV-Dynabead complexes

Washed Dynabead-EV complexes (section 2.2.2.3) were resuspended in 20 µl of Hanks' Balanced Salt Solution (HBSS), transferred to a microfuge tube and pre-fixed with 2% (w/v) glutaraldehyde in 100 mM phosphate buffer (pH 7.4) at room temperature for at least 2 h, followed by post-fixation with 2% (w/v) osmium tetroxide in 100 mM phosphate buffer (pH 7.4). The fixed samples were subjected to several washes in distilled water to remove excess phosphate ions prior to dehydration through a series of ethanol concentrations (30%, 50%, 70%, 90%, v/v) for 15 min each, followed with 100% (v/v) ethanol for 30 min with 3

changes of solution, and finally in propylene oxide for 15 min with 2 changes of solution. Quetol 812 epoxy resin (Nissin EM) was infiltrated by mixing propylene oxide and the resin, as 2:1, 1:1, 1:2 ratios, and samples were left for 1 h in each solution and in 100% resin overnight. The sample embedding was completed the following day by placing in fresh resin for 1 h with polymerisation. The embedded samples were trimmed to have a block face of 1-2 mm in diameter and were sectioned into 100 nm ultra-thin slices with a Leica EM UC6 ultramicrotome (Leica). Each section was carefully collected onto a grid and left to dry before being stained with 2% (w/v) uranyl acetate in distilled water for 15 min and washed twice with distilled water. The stained grids were imaged on the Tecnai T12 Spirit TEM at 80 kV. Resin-embedded samples were processed and imaged by Mr Chris Hill at the Electron Microscopy Facility, The University of Sheffield.

2.2.5 Protein methods

2.2.5.1 Bicinchoninic acid assay (BCA)

Protein concentrations were determined using the Pierce BCA protein assay kit (catalogue number 23225, Thermo Fisher Scientific, UK), according to the following protocol. Standards of known concentrations of bovine serum albumin (BSA) were prepared in the same buffer as the samples to be assayed ranging from 0 to 1 mg/ml. All samples were tested in triplicate with 10 µl of sample or standard added to a 96-well plate. 200 µl of the working reagent A and B solutions combined in a 50:1 ratio added to each well, the plate covered and incubated for 30 min at 37°C. Following incubation, the absorbance was measured at 560 nm using a spectrophotometer plate reader TECAN (Magellan V7.2 software, Infinite M200). The absorbance values were plotted against the known concentrations of the standards and a polynomial equation used to determine the concentration of samples.

2.2.5.2 SDS-PAGE

Samples (20 µl) were mixed with 5µl 5x loading buffer, heated at 95°C for 5 minutes using a heat block (Techne) and briefly centrifuged. SDS-PAGE gels mixtures were made according to table 2.2. Once the resolving gel was poured, isopropanol was used as overlay whilst the stacking gel was assembled. After the resolving gel had polymerized isopropanol was poured off and rinsed away with water.

The stacking gel was poured on top of the set resolving gel and a sample comb was inserted before allowing the gel to polymerize for 10 minutes. The comb was then removed and each well washed out with copious amounts of distilled water to remove any unpolymerized gel. Gels were then placed in BIO-RAD tanks filled with 1x Tris glycine running buffer (192 mM glycine, 0.1% SDS, 25 mM Tris Base pH 8.3).

Table 2. 2 Reagents for two 1.0 mm, 12% polyacrylamide resolving gels and stacking gels

Stacking		**Resolving**	
40% polyacrylamide (ml)	**0.975**	40% polyacrylamide (ml)	**3**
1M Tris (pH6,8) (ml)	**2.1**	1.5 M Tris (pH8.8) (ml)	**2.5**
10% Ammonium persulfate (µl)	**100**	10% Ammonium persulfate (µl)	**350**
TEMED (µl)	**17**	TEMED (µL)	**5**
H_2O (ml)	**4.725**	H_2O (ml)	**4.3**

Samples were loaded alongside 5 µl prestained proteins standard (Precision plus proteins standard Bio-Rad) and proteins were separated at 150 volts for 70 minutes.

2.2.5.3 Western blotting

Proteins separated by SDS-PAGE were transferred using a mini format TURBO transfer kit, (Bio-Rad). The SDS-PAGE gel was placed on top of the membrane in the correct orientation in the cassette. This was covered with filter paper, taking care to remove all air bubbles using a blotting roller and the cassette closed. Proteins was transferred at 25 V for 7-minute. The transfer sandwich was disassembled and the membrane was blocked in 5% (w/v) skimmed milk prepared of 2.5g powder was weighted out and dissolved in 1x Tris buffered saline supplemented with 0.1% (v/v) Tween-20 (TBST), for 1 hour on a rocking shaker at room temperature.

Primary antibodies were diluted in blocking buffer (Table 2.3) and incubated with the membrane on a rocking shaker at 4°C overnight. Following incubation with primary antibody the membrane was washed three times with TBST for 10 minutes, secondary antibodies were diluted in blocking buffer (Table 2.4) and incubated with the membrane on a rocking shaker for one hour at room temperature. The membrane was washed three times for 10 minutes in

TBST and then the membrane was transferred to a small plastic box containing Westar supernova (CYNAGEN Srl, Italy). The membrane was wrapped in cling film and placed in an x-ray cassette for exposure to x-ray film (Thermo scientific, USA) and developed with an automated processor (Xograph Compact X4). Where necessary, nitrocellulose membranes were stripped of antibody complexes by incubating the membrane in Restore TM western blot stripping buffer (Thermo Fisher Scientific) for 10 min at room temperature on a shaker, followed by three washes (10 min each) with 1× TBST. The stripped membrane was then ready for blocking and antibody incubation.

Table 2. 3 Details of all primary antibodies used in western blotting experiments.

Target	Clone	Dilution	Manufacturer and catalogue number	Expected weight (kDa)
Anti-CD63 antibody (Rabbit)	EPR5702	1:1000	Abcam, ab134045	30-60
Anti-CD9 antibody (Rabbit)	EPR2949	1:2000	Abcam, ab92726	24-27
Anti-CD81 antibody (Mouse)	5A6	1:200	Santa Cruz, Sc-23962	22-26
Anti-TSG101 antibody (Mouse)	EPR713618	1:500	Abcam, ab125011	44
Anti-Alpha-amylase (Rabbit)	EPR19605	1:5000	Abcam, ab201450	50-60
Anti-Apolipoprotein AI (Rabbit)	EPSISR27	1:1000	Abcam, ab151710	30
Anti-Apolipoproteins B (Rabbit)	EPR2914	1:1000	Abcam, ab139401	250
Anti- MVP antibody (Rabbit)	EPR13227(B)	1:2000	Abcam, ab175239	100

Table 2. 4 Details of HRP conjugated secondary antibodies used in western blot experiments.

Antibody	Dilution	Catalogue number and supplier
Anti-mouse	1:3000	7076S - Cell Signalling (New England Biosciences)
Anti-rabbit	1:3000	7074S - Cell Signalling (New England Biosciences)

2.2.6 RNA, DNA and protein extraction

2.2.6.1 Sample preparation

The RNA/DNA/Protein Purification Plus Kit (Norgen, UK, Cat; 47700) was used to isolate nucleic acids and protein from the same sample. Washed EVs bound to Dynabeads as described (section 2.2.2.3.2) were resuspended in 300 µl SKP buffer and vortexed. The lysate was placed on a magnet for 1 min, the supernatant transferred to a fresh RNAse free tube and then stored at -80°C until the protocol was completed.

2.2.6.2 Genomic DNA purification

Genomic DNA (gDNA) was purified by adding 300 µL lysate to a gDNA purification column and centrifuging at 5,200 x *g* for 1 minute. All of the flowthrough was retained for RNA purification (section 2.2.6.3). 500 µL wash solution A was added to the gDNA column, which was centrifuged at 3,500 x g for 1 minute. The wash step was repeated again and the flowthrough discarded. The column was centrifuged at 14,000 x *g* for 2 minutes in order to thoroughly dry the resin.

gDNA was eluted into a fresh 1.7 mL elution tube provided with the kit. 100 µL elution buffer F was added to the column and incubated at room temperature for 2 minutes. The column was centrifuged for 2 minutes at 200 x *g* followed by 1 minute at 14,000 x *g*. The purified DNA sample was stored at -20°C.

2.2.6.3 RNA purification

The 300 µl retained flowthrough (section 2.2.6.2) was combined with 180 µl 100% Ethanol mixed by vortexing, applied to an RNA/Protein Purification Column and centrifuged for 2 minutes at 3,500 x g. The flowthrough was retained for Protein Purification (section

2.2.6.4). RNA was washed by applying 400 µL wash solution A to the column and centrifuged at 3,500 x g for 2 minutes. The flowthrough was discarded and then the column was treated with 100 µl DNase solution for 15 minutes at 25°C as per the manufacturer's instructions. The column was washed two more times with 400 µl wash solution A and centrifuged at 3,500 x g for 1 minute. After the third wash, the flowthrough was discarded and the column centrifuged at 14,000 x g for 2 minutes to dry the resin. The RNA was eluted into a fresh tube by adding 50 µl Elution Solution A and centrifugation at 200 x g for 2 minutes, followed by 14,000 x g for 1 minute. The RNA was stored at -80°C.

2.2.6.4 Protein purification

The 480 µl retained flowthrough (section 2.2.6.3) was diluted with an equal volume of molecular biology grade water and 40 µl Binding Buffer A was added. This was applied to the same column previously used for RNA purification and centrifuged at 5,200 x *g* for 2 minutes. The flowthrough was discarded and the column was washed with 500 µl Wash Solution C and centrifuged at 5,200 x *g* for 2 minutes. Protein was eluted into a tube that contained 9.3 µl Protein Neutralizer by adding 100 µl Elution Buffer C to the column and centrifugation at 5,200 x *g* for 2 minutes. The protein was stored at -20°C.

2.2.7 Measurement of RNA concentration

RNA concentration was determined by Agilent 2100 Bioanalyzer (Agilent Technologies) with an RNA 6000 Pico kit (Agilent Technologies) by Dr Paul Heath (SiTraN, The University of Sheffield) following the manufacturer's instructions. Briefly, 9 µl of gel-dye mix composed of filtered gel and dye (65:1) was added into the Pico chip and the plunger depressed for 60 s. After 9 µl conditioning solution, 5 µl of marker, and 1µl ladder were added, 1 µl of ladder and extracted EV total RNA were added in appropriate wells on the RNA chip. RNA concentrations were then calculated according to the electropherogram profiles.

2.2.8 Small RNA sequencing

RNA was extracted from salivary EV samples (section 2.2.6) and quantified by Bioanalyzer (section 2.2.7).

2.2.8.1 Library preparation and sequencing

An input of 3 ng RNA (or a maximum 3 µl volume where this wasn't possible) was used for the creation of sequencing libraries using the Real Seq-AC miRNA Library Kit for Illumina sequencing. Library quality was determined by Qubit 2.0 fluorometer (coupled with a High Sensitivity dsDNA kit) and Agilent 2200 Tape station System.

Pooled libraries were loaded onto the HiSeq 2500 using the cBOT system and HiSeq Rapid Duo CBOT sample loading kit. Paired end reads (2x 50bp) were generated using HiSeq PE Rapid Cluster Kit v2 and HiSeq Rapid SBS Kit v2 (200 cycles), with the instrument in Rapid Mode. Data was exported in FASTQ format for subsequent bioinformatics analysis. Library preparation and sequencing were performed by Mr Timothy Wright (Sheffield Children's NHS Foundation Trust).

2.2.8.2 Bioinformatics analysis

The raw sequencing reads from small-RNA sequencing were processed using the nfcore (Ewels et al., 2020) smrnaseq workflow. This involves generating QC of raw sequencing reads using FASTQC, adapter trimming with TrimGalore and alignment to mature miRNA using Bowtie1 (Langmead et al., 2009). Raw counts from mature miRNA were imported into DESeq2 for normalisation and differential expression analysis (Love et al., 2014). Other small-RNA species were analysed using the nfcore rnaseq pipeline, which aligns samples to a reference genome using STAR (Magoč and Salzberg, 2011), and produces gene-based counts using salmon (Patro et al., 2017). DESeq2 was used again for differential expression. Bioinformatics analysis was performed by Dr Mark Dunning (Bioinformatics Core Director, The University of Sheffield).

2.2.9 Quantitative real-time PCR (qPCR)

2.2.9.1 Complementary DNA (cDNA) synthesis

RNA samples were transcribed to the complementary DNA (cDNA) using the reverse transcription kit (Thermo Fisher Scientific, Cat number; 4366596). The reactions were set up on ice following the manufacturer's instructions. All RNA experiments were carried out using RNase-free microfuge tubes and filtered pipette tips. Extra care was paid not to introduce RNase and other contaminants during sample handling. 1 ng of EV total RNA was used as a

template per reaction. The reverse transcription was performed on an Applied Biosystems 2720 Thermal Cycler (Table 2.8), cDNA was stored at -20°C and used within 4 weeks.

The RT reaction with single-stranded small RNA was prepared by mixing 7 µL of RT reaction mix, which was prepared as described in (Table 2.5), with 5 µL (containing 1 ng) of total RNA in a reaction tube. 3 µL of 5X RT Primer (Thermo Fisher Scientific) was added to each reaction tube and sealed and placed into a thermal cycler, then incubated using standard cycling as described in (Table 2.6).

Table 2. 5 Composition of RT Reaction Mix.

Component	Component Volume (1 reaction)
100mM dNTPs (with dTTP)	0.15 µL
MultiScribe™ Reverse Transcriptase, 50 U/µL	1.00 µL
10x Reverse Transcription Buffer	1.50 µL
RNase Inhibitor, 20 U/µL	0.19 µL
Nuclease-free Water	4.16 µL
Total RT Reaction Mix volume	**7.00 µL**

Table 2. 6 Conditions used for reverse transcription reaction

Step	Temperature	Time
Reverse transcription	16 C	30 minutes
	42 C	30 minutes
Stop reaction	85 C	5 minutes
Hold	4 C	Hold

Table 2.7 TaqMan primer/probes used for PCR.

Target	Assay ID
miR-29a-3p	002112
miR-92a-3p	000431
miR-181a-5p	000480
miR-21-5p	000397

2.2.9.2 TaqMan qPCR reaction

The reaction mix for miRNA qPCR was composed of 5 µl 2X qPCR Bio Probe mastermix, 0.5 µl Taqman probe (Thermo Fisher Scientific), 0.5 µl cDNA synthesised with the corresponding microRNA RT primer (Table 2.7), and 4 µl nuclease free water H_2O in each sample (Table 2.8). All qPCR reactions were assembled on ice and handled with RNase-free equipment according to the manufacturer's instructions. Each reaction was assayed in triplicate to minimise variation due to pipetting errors. In a Rotor- Gene Q 2plex real-time PCR cycler (QIAGEN), a two-step run was conducted and programmed as follows: 10 min at 95 °C for initial denaturation, 15 s at 95 °C for denaturing and 60 s at 60 °C for annealing and extension for 40 cycles.

Table 2. 8 Real time qPCR TaqMan master mix components.

Real time qPCR master mix Volume	(total volume 10 µl)
Taqman probe	0.5 µl
cDNA	0.5 µl
Nuclease free water	4 µl
2X qPCR Bio Probe master mix (Applied Biosystems, Cat; PB20.25-05, Thermo Fisher Scientific)	5 µl

2.2.9.3 Data analysis

Data was reported as mean Ct values ± standard deviation (mean ± STDV). Student's t-test was utilised to verify the statistical significance of findings as indicated in individual figure legends. A p-value of less than 0.05 was considered significant.

Chapter Three

3. Isolation of salivary EVs by differential centrifugation and size exclusion chromatography

3.1 Introduction

Salivary EV cargo is altered in diseases such as cancer, leading to a considerable amount of research focused on EV related biomarker identification (Bebelman et al., 2018). Several approaches have been used for the isolation of EVs from biological fluids, such as differential centrifugation, size exclusion chromatography (SEC), density gradient centrifugation, precipitation, and immune-affinity capture. Due to the heterogeneous nature of EVs, there is no universally agreed isolation strategy (Théry et al., 2006; Webber and Clayton, 2013; Dominkuš et al., 2018; Dong et al., 2020; Stam et al., 2021).

Saliva is one of the most challenging bodily fluids to work with due to its variable nature (e.g., viscosity) and endogenous contamination. Saliva does not only contain EVs but it also holds cell and food debris, bacterial cells, highly abundant soluble proteins (e.g. α-amylase), protein aggregates, and lipoproteins (Ferguson, 1968; van Stegeren et al., 2006; Deutsch et al., 2008). Standardised approaches must be used to reduce variability and diurnal fluctuations when examining saliva composition for disease biomarker identification. As emphasized by the minimal information from studies of EVs 2018 (MISEV2018) (Théry et al., 2018a) and other position papers from the International Society for EVs (ISEV) (Lener et al., 2015; Mateescu et al., 2017a; Russell et al., 2019), isolation/enrichment of EVs is one of the most important and difficult prerequisites prior to any subsequent analyses.

Salivary α-amylase is a highly abundant digestive enzyme found in the oral cavity (Scannapieco et al., 1993), which catalyzes the hydrolysis of starch into maltose and dextrin (Butterworth et al,. 2011). The elimination of α-amylase and other soluble proteins during EV isolation might help with downstream proteomic analysis of salivary EV cargo (van Stegeren et al., 2006; Sun et al., 2016b). In addition, the lipoprotein particles composed of low-density and high-density lipoproteins (LDL and HDL, respectively) are often co-purified with EVs (Mänttäri et al., 2001). These particles can interfere with particle counts and downstream biomarker analysis. While HDL particles are ~10 nm in diameter and appreciably smaller than EVs, their density overlaps with that of EVs (1.13 –1.19 g/ml) (Vickers et al., 2011). HDLs have been proven to transport RNAs so contamination of EVs with these particles may result in biased findings (Vickers and Remaley, 2012). As a result, separating salivary EVs from soluble

proteins and non-EV lipid particles is vital for developing biomarker discovery and validation methodologies.

Differential centrifugation and ultracentrifugation are two of the most extensively utilised techniques for isolating EVs (Raposo et al., 1996b; Théry et al., 2006; Gardiner et al., 2016b). Differential centrifugation utilises increasing sedimentation speeds. Large particles (e.g. apoptotic bodies and cell debris) are pelleted at low speeds, whereas small particles (e.g. exosomes) are typically pelleted at high speeds (Théry et al., 2006). SEC is another advancement that is utilised for the separation and enrichment of EVs, and there has been a considerable growth in SEC applications from 2010 to 2020 (Liangsupree et al., 2021). SEC has the advantage of not requiring specialised equipment such as an ultracentrifuge. This technique operates by passing samples through a chromatography column that includes a resin such as Sepharose. The EVs pass around the Sepharose beads and elute in the first several fractions before the passage of the soluble components such as proteins, which take a tortuous route through the beads and elute in the later fractions (Shah et al., 2013; Coumans et al., 2017a). Many studies have demonstrated that SEC as part of a combined methodology improves EV purity from different biological fluids (Böing et al., 2014; Yu et al., 2018). In 2020, 60% of EV isolations by SEC were performed in combination with other isolation methods (Stam et al., 2021).

The latest MISEV2018 guidelines define the recommended steps for EV characterisation. Quantification and characterization of enriched EVs after isolation is one of the most challenging aspects in EV research. Nanoparticle tracking analysis is commonly used to determine the size and concentration of the sub-micrometre particles in suspension by tracking their Brownian motion with a dark field microscope (Filipe et al., 2010; Szatanek et al., 2017; Stam et al., 2021).

Other characterization methods often applied to EVs are focused on detecting EV-specific markers and non-EV markers using bulk immunoassays such as western blots and/or enzyme-linked immunosorbent assays (ELISAs) (Coumans et al., 2017b). EVs are also commonly characterized by electron microscopy (EM) methods such as transmission electron microscopy (TEM), scanning EM or cryo-EM that are able to reveal EV morphology; however, they can also indicate EV size, concentration and purity (Chuo et al., 2018).

3.2 Aim and objectives

Given the complex nature of saliva (viscosity and highly abundant soluble factors), the main aim of this chapter was to determine a suitable technique for isolation of EVs from saliva for downstream analysis. To meet this aim, the following objectives were addressed:

- Determining if differential centrifugation is a suitable technique for the enrichment of salivary EVs.
- Deciding whether SEC is a suitable technique for the enrichment of salivary EVs.
- Determining whether SEC is sufficient to isolate salivary EVs with minimal contamination from soluble proteins and other nanoparticles.
- Characterising the particles isolated by SEC, NTA, western blotting, Exo-View analysis and transmission of electron microscopy.

3.3. Results

3.3.1 Enrichment of salivary EVs by differential centrifugation

The first EV isolation technique tested in our study was differential centrifugation due to the fact that it is the most commonly used methodology amongst the EV research community (Raposo et al., 1996a; Théry et al., 2006; Witwer et al., 2013a). We utilised the protocol developed by (Thery et al., 2006). Passive drool samples were collected from healthy volunteers under standardised conditions (Section 2.2.1.1). The saliva was first diluted with an equal volume of sterile PBS to reduce viscosity and then it was clarified (debris and bacteria were removed) by centrifugation at 3,000 x *g* for 30 mins and 12,000 x *g* for 45 mins. Small particles were then pelleted by ultra-centrifugation at 100,000 x *g* for 1 hour. The pellet was washed with PBS and then recentrifuged at 100,000 x *g* for 1 hour. This produced a viscous/sticky pellet that was difficult to resuspend. The pellet adhered to the plastic pipette tip and to the wall of the tube (Figure 3.1A and B). Nanoparticle tracking analysis (NTA) of the resuspended pellet detected the presence of 1.14 x 10^{10} particles/ml (Figure 3.1C), which measured on average 270 nm diameter (Figure 3.1D).

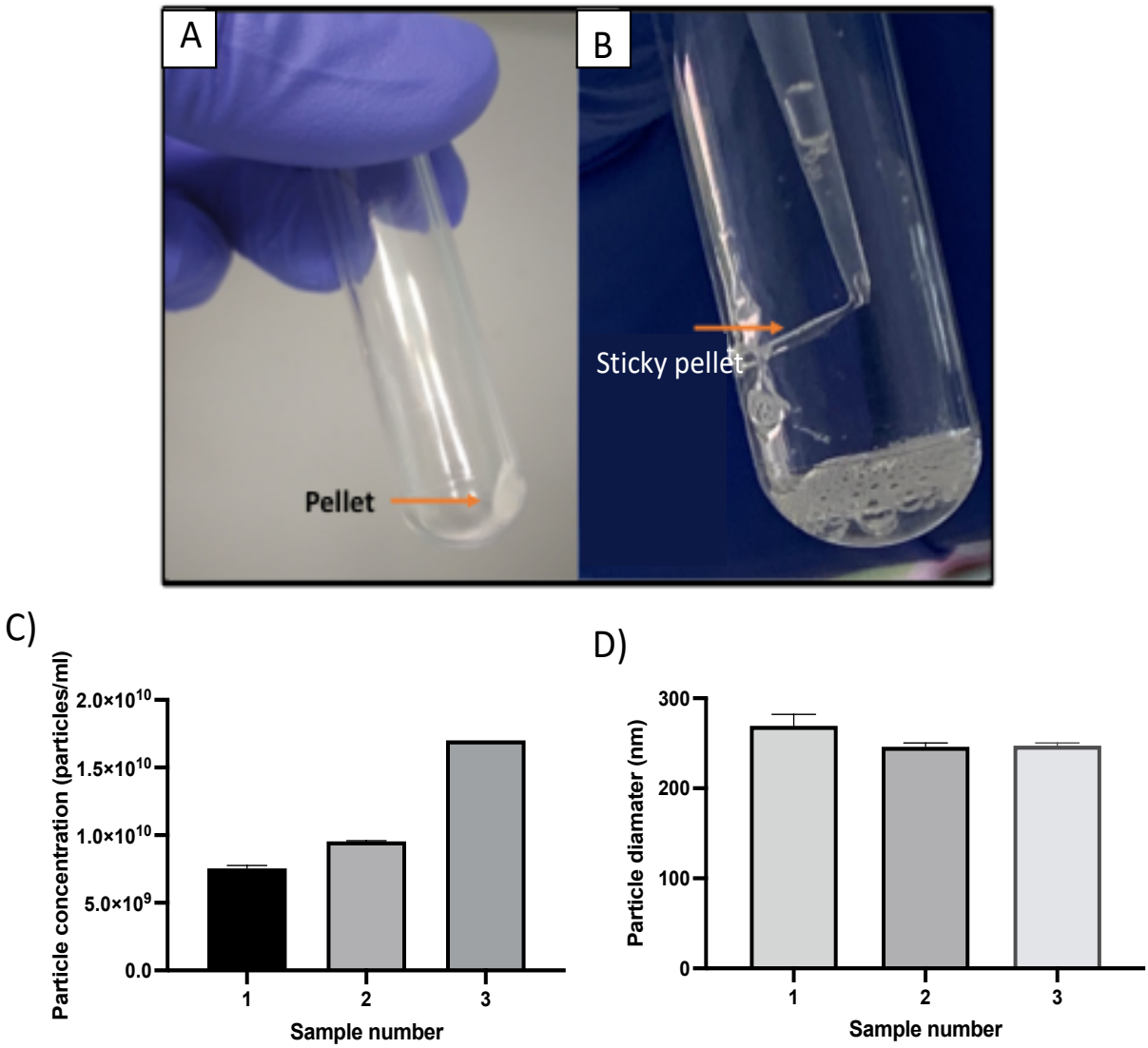

Figure 3.1 Isolation by ultracentrifugation. A) Pelleted material obtained by ultracentrifugation of saliva. **B**) Resuspension of pellet revealed it to be viscous/sticky. **C)** The concentration of particles in each sample was measured by NTA. **D)** The mean diameter of particles per sample was assessed by NTA. Graphed data are averaged triplicate technical repeats ± SD for each biological sample.

3.3.2 Enrichment of salivary EVs by size exclusion chromatography

The viscous/sticky nature of the pellet produced by ultracentrifugation made us question the suitability of this technique for enrichment of salivary EVs. Therefore, we compared it to the efficacy of SEC.

3.3.2.1 Elution profile

Previous work in the Hunt lab has found that SEC is a suitable technique to separate EVs from soluble protein in complex mixtures, ready for downstream characterisation (Peacock et al., 2018). Here, SEC was used to fractionate concentrated saliva samples and the elution profile was carefully examined. NTA revealed that particles were eluted in fractions 5-10 (Figure 3.2A). The particles in each fraction were on average ~150 nm diameter (Figure 3.2C). Protein quantification revealed that soluble proteins were eluted from the column in fractions 11-20 (Figure 3.2A).

We next used western blotting to confirm the identity of particles detected in SEC fractions. EV markers (CD81, TSG101) were present in fractions 5 to 12 (Figure 3.2B). As lipoprotein particles are frequently reported to be co-purified with EVs, we blotted for ApoAI and ApoB, which are present in HDL and LDL particles, respectively. ApoAI was detected in fractions 6-10 (Figure 3.2B), but we could not detect ApoB in any fraction (not shown). Vault particle proteins, such as major vault protein (MVP), are frequently identified in EV preparations from diverse bodily fluids, including saliva (Gonzalez-Begne et al., 2009). Ongoing work in our lab is currently exploring if vault particles are common contaminants of EV preparations. Therefore, we blotted for MVP, which is the major structural protein of vaults. MVP was detected in fractions 5-8 (Figure 3.2B), suggesting that EVs, lipoprotein particles and MVP/vault particles co-elute in overlapping SEC fractions. The presence of α-amylase (a highly abundant, soluble salivary protein) was detected in fractions 11-20 (Figure 3.2B), which mirrored the elution of soluble protein from the column (Figure 3.2A).

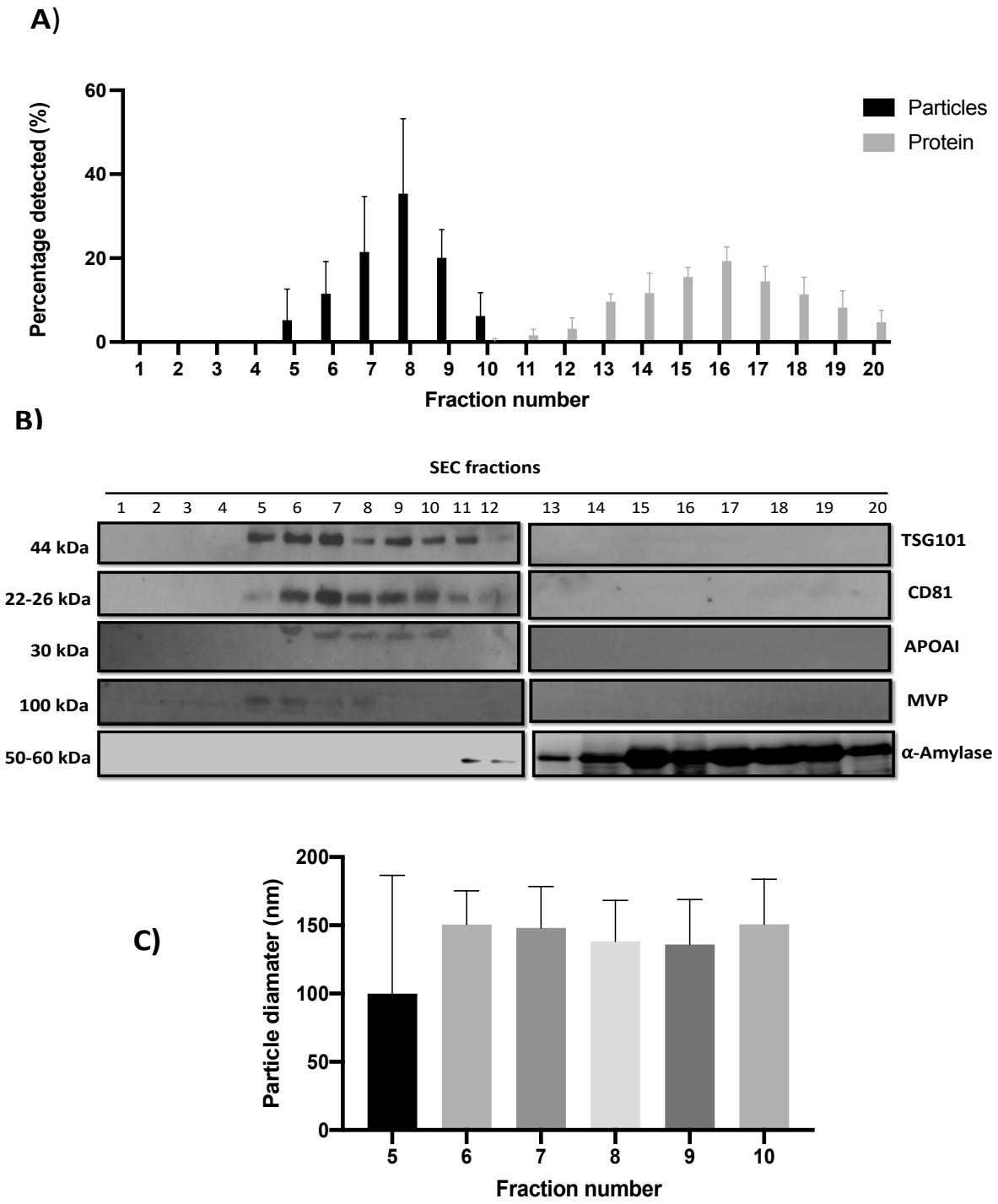

Figure 3. 2 SEC elution profile. A) Twenty 0.5 ml SEC fractions were collected. Samples were subjected to BCA and NTA to measure soluble protein and particle concentration, respectively. Data was expressed as percentage of the total detected. **B**) Western blotting to detect EV markers (CD81 and TSG101), α-amylase, lipoprotein ApoAI, and MVP in SEC fractions. Blots are representative of three independent repeats. **C**) The mean diameter of particles in EV rich fractions was measured by NTA. Graphed data is averaged from n=3 biological repeats ± SD. The western blot image is representative of three biological repeats.

3.3.4 The yield of salivary EVs after purification by SEC and ultracentrifugation

Although SEC was able to separate EVs from abundant soluble protein, it resulted in EVs/particles being eluted across multiple fractions. Here we applied 0.5 ml concentrated saliva to each SEC column, which resulted in seven 0.5 ml fractions that were positive for EV markers by western blot (Figure 3.2B). We therefore aimed to assess the yield of EVs that had been purified by SEC and then pelleted by UC to re-concentrate them. Fractions that were EV rich but that contained low amounts of soluble proteins (fractions 5-10) were combined and a small aliquot was taken for NTA. The remaining volume was ultracentrifuged to pellet EVs, which were then resuspended in PBS ready for NTA.

NTA was performed to determine the total number of particles (Figure 3.3A-C) before and after UC. The average number of particles before UC was 5.3 $x10^8$, whereas the number of particles after UC was 3.0 $x10^8$, which represented a significant decrease in particle number (p= 0.044). We used this data to calculate the percentage yield after UC, which was 58% on average (Figure 3.3D). NTA revealed that the mean diameter of particles before and after UC was around ~150 nm and that it was not significantly different (p= 0.171) (Figure 3.3C).

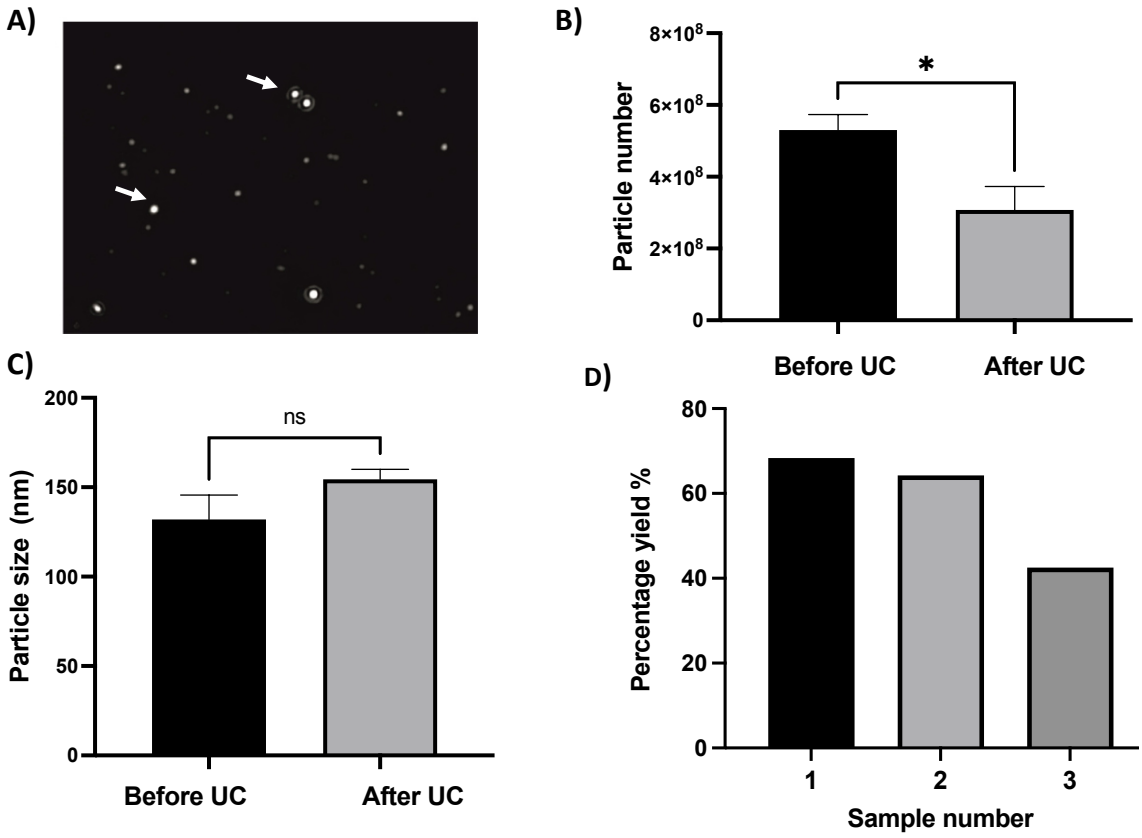

Figure 3. 3 The yield of SEC purified particles before and after UC. A) Visualization of particles on the NTA live view screen with white arrows indicating particles. **B)** The number of particles in combined SEC fractions before and after UC. Data is the average n=3 ± SD. **C)** Mean diameter of particles was measured by NTA. Data is the average n=3 ± SD. **D)** Recovery of particles after UC. Data expressed as percentage yield for individual samples. Pairwise comparisons were conducted by Student's t-test ns=not significant, *= $p<0.05$.

3.3.5 Characterization of salivary EVs by TEM

We detected the presence of EV sized nanoparticles and EV protein markers (as well as markers related to contaminating nanoparticles) in our SEC preparations. We next sought to visually confirm the presence of EVs in pelleted SEC fractions by TEM, which confirmed the presence of numerous particles bearing the artefactual cup-shaped morphology that is typical of EVs (Figure 3.4).

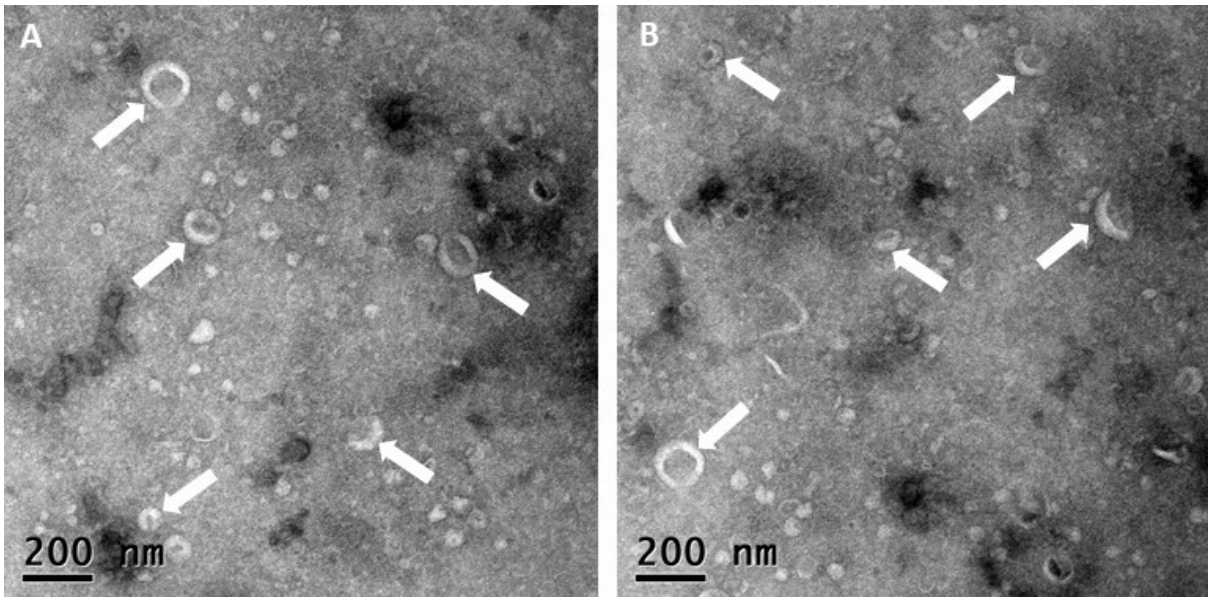

Figure 3. 4 Visualisation of salivary EVs by TEM. A,B) Representative transmission electron microscopy images of salivary EVs isolated by SEC and pelleted by UC. Artefactual cup-shaped structures (indicated by arrows) were clearly visible. Scale bars reflect 200 nm.

3.3.6 Detection of salivary EV tetraspanin profile

Having confirmed the presence of salivary EVs in our preparations by TEM, our next objective was to determine the tetraspanin profile of EVs isolated by combined SEC and UC. We previously detected the CD81 tetraspanin marker by western blotting (Figure 3.2B). As part of an on-site ExoView instrument demonstration, we were able to expand the tetraspanin profiling of our samples. Salivary EV samples were diluted and pipetted directly onto a tetraspanin array chip before incubation overnight at room temperature (section 2.2.4.2). EVs were captured by antibodies targeting CD9, CD63, and CD81 that were immobilised on the array produced by the manufacturers of the ExoView platform (Nanoview Biosciences).

After hybridisation, arrays were washed and incubated with a 3-colour fluorescent cocktail of antibodies against CD63, CD81 and CD9. Labelled arrays were then scanned using the ExoView R100 platform to produce high resolution fluorescent images (Figure 3.5). Red spots are vesicles that are positive for CD63; blue Spots are vesicles that are positive for CD9 and green Spots are vesicles that are positive for CD81. Other colours are vesicles that express various combinations of the fluorescent signals and represent co-localisation of markers.
Image data was converted to numerical data to exhibit the abundance of tetraspanin markers (Figure.3.5B,D). As expected, CD63-captured EVs stain strongly with the CD63 fluorescent antibody (red). A small proportion of CD63-captured EVs are also positive for CD9. CD9-captured EVs are highly labelled with the CD9 fluorescent antibody (blue). A large proportion of CD9-captured EVs are also CD63 positive. Very few EVs were captured by the immobilised CD81 antibody and there was little staining of EVs with the CD81 fluorescent antibody (green) across all spots on the chip. Negligible numbers of EVs were bound to the negative control mouse IgG spots (Figure 3.5A/C). In summary, Exoview analysis revealed that salivary EVs were abundant with CD63 and CD9 protein, but unexpectedly appeared to be mostly CD81 negative.

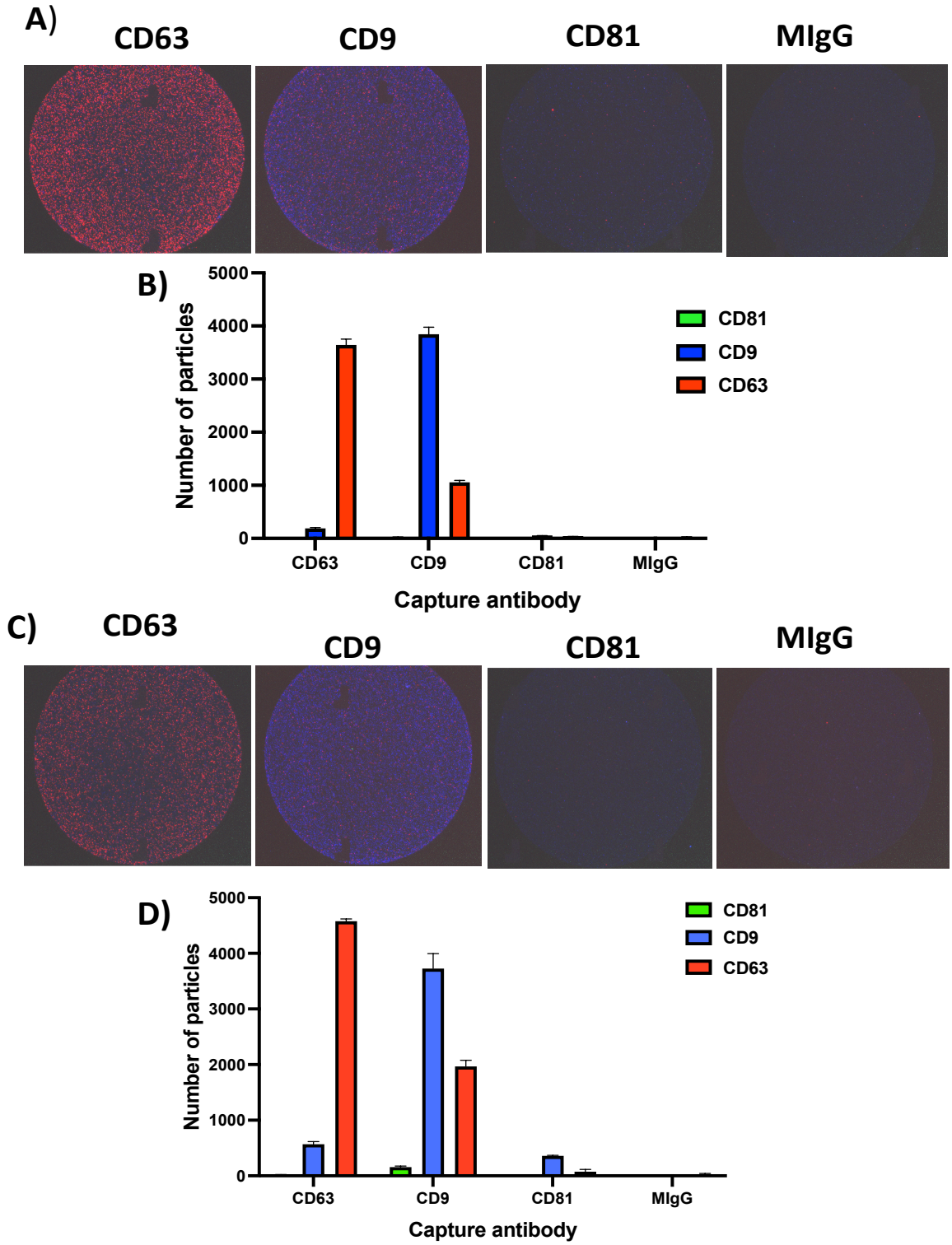

Figure 3. 5 ExoView analysis. A, C) The samples were incubated on tetraspanin array chips coated with anti-CD63, anti-CD9, anti-CD81 capture antibodies and a mouse IgG negative control. Captured EVs were labelled with 3-colour fluorescent cocktail of antibodies against CD63 (red), CD9 (blue) and CD81 (green) and were scanned using the ExoView R100 reader and the Exo-Scan acquisition software. **B, D)** Numerical data showing the number of fluorescent EVs bound to tetraspanin capture spots. Data is shown for two independent biological repeats. Graphs represent the average of the technical triplicate capture spots on each array, with error bars indicating standard deviation.

3.3.7 Validation of salivary EV tetraspanin profile by western blotting

We next sought to validate the data obtained by ExoView analysis by western blotting in a larger panel of samples. EVs were isolated by combined SEC and UC before solubilisation in protein lysis buffer and lysates were analysed using antibodies against CD63, CD81, CD9 and additional EV marker, TSG101. A variable expression of tetraspanins CD9 and CD63 was noted across the six different biological samples whereas expression of CD81 was detectable in all the samples. TSG101 was detected in the majority of samples (Figure 3.6A).

Though salivary EVs were isolated from the same volume of saliva, which was collected under standardised conditions, there appeared to be variability in the expression of protein markers among the different samples. We then further examined the samples to attempt to explain these differences. We conducted NTA on the combined SEC fractions prior to UC and also quantified the amount of protein in the resulting lysates by BCA.

NTA data revealed that the particle concentration in each sample appeared to correlate with the detection of markers by western blot. For example, sample 2 had the highest particle concentration and it was the only sample in which all protein markers were detected (Figure 3.6A/B). The size of the EVs isolated after UC, was ~150 nm; which is compatible with the previous experiments (Figure 3.6C). The two samples with the highest particle concertation (samples 2 and 3), also had the highest amount of protein (Figure 3.6D).

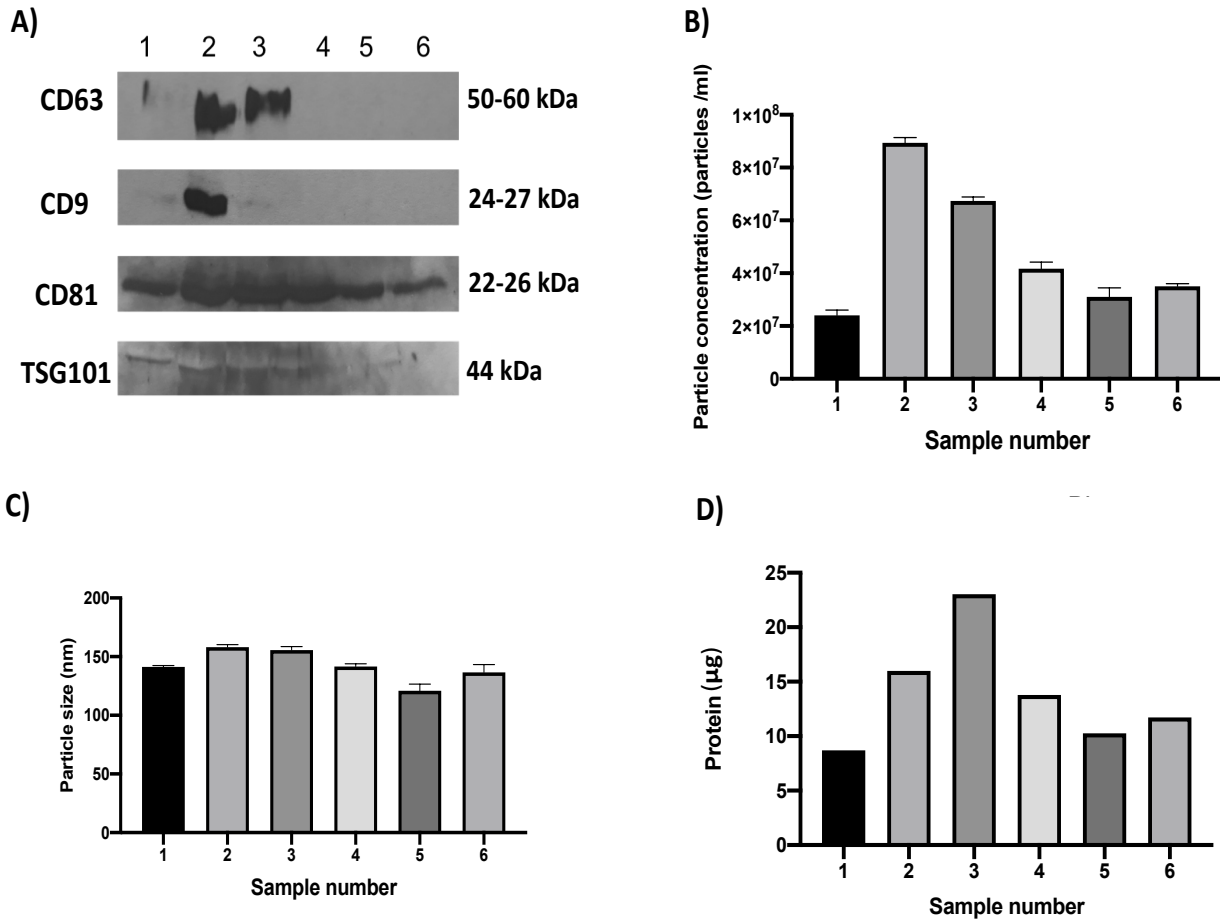

Figure 3. 6 Salivary EV protein markers. A) EV pellets were resuspended in RIPA buffer containing protease inhibitors to solubilise EV protein. 20 µl of each sample was separated by SDS-PAGE and transferred to a nitrocellulose membrane for subsequent western blot analysis. **B)** Particle concentration and **C)** size in each sample was measured by NTA. The data had averaged values of 3 technical repeats per biological sample and the error bars indicated standard deviation. **D)** The amount of protein (µg) analysed by western blotting for each sample was measured by BCA.

3.4 Discussion

Saliva is a viscous complex biofluid, due to high concentrations of glycoproteins including mucins that are secreted by the sublingual, submandibular and palatal glands (Ljungberg et al., 2007), which needs to be considered during the EV isolation process. In addition, some studies stated that saliva might differ depending on the sampling time and location in the mouth of collection (Bhattarai et al., 2018). Therefore, in this study, passive drool samples were collected at a set time (early morning) from volunteers who consented to refrain from eating or drinking for at least one hour before collection.

3.4.1 Differential centrifugation

Although differential centrifugation has been used in many studies to isolate EVs from a variety of biological fluids and cell culture media (Théry et al., 2006; Linares et al., 2015), this approach co-precipitates proteins, lipoproteins, and other contaminants (Yuana et al., 2014). In addition, the viscosity of biofluids can affect the sedimentation of particles by UC (Momen-Heravi et al., 2012; Gardiner et al., 2016a). Our study has shown that UC of saliva produces a sticky pellet that adheres to the plastic pipette tip and the wall of the tube, making it difficult to resuspend. This finding is consistent with another study in which isolated EVs from saliva were found to be extremely sticky by UC (Zlotogorski-Hurvitz et al., 2015). In addition, NTA of resuspended pellets detected large particles with an average diameter of 270 nm, suggesting particle aggregation. This finding is documented by several studies, where EVs were isolated from diverse biofluids, reporting that UC resulted in clumping of EVs and aggregates, which can often be observed in EV preparations (Witwer et al., 2013a; Böing et al., 2014; Yuana et al., 2015; Linares et al., 2015; Konoshenko et al., 2018). Other studies have proved that membranes of exosome particles may adhere to certain ultra-centrifugation tubes, such as Beckman ultra-clear tubes. In addition, the size and number of EVs within aggregates are very variable (Théry et al., 2006; Issman et al., 2013; Erdbrügger et al., 2014; Linares et al., 2015). Momen-Heravi et al. (2012) confirmed that the size of EVs/particles in more viscous biofluids may increase significantly after UC (Momen-Heravi et al., 2012). Hence, it was concluded that UC was not a suitable method for EV preparation in our study and so we decided to evaluate SEC as an alternative method to overcome the issues of UC.

3.4.2 SEC

We investigated the possibility that SEC could enrich EVs from healthy saliva, in quantities sufficient for downstream analysis. We also wanted to determine if we could separate EVs from major impurities including highly abundant proteins such as α-amylase, MVP, and lipoproteins (ApoAI/ApoB). We used a hybrid isolation method that incorporated SEC with UC, which builds on previous studies that used these protocols (in isolation) for EV purification (Théry et al., 2006; Böing et al., 2014; Onódi et al., 2018; Yu et al., 2018). The chromatographic technique separates particles/molecules based on their size while conserving the integrity and biological activity of the molecules being separated (Wang et al., 2010), including EVs (Gámez-Valero et al., 2016).

Our data shows that particles are detectable in SEC fractions 5–10, whilst EV markers were detected in fractions 5-12. Soluble proteins were eluted in fractions 11 and above. The findings from the current study were consistent with several other published findings where SEC was used. Gámez-Valero et al., (2016) described the application of 10 ml Sepharose CL-2B columns for the efficient isolation of EVs from small volumes of plasma, demonstrating that low levels of protein become detectable from fraction 15 onwards, whereas vesicles were mainly present in fraction 5-14. Moreover, the study by Karimi et al. (2018) demonstrated by NTA that most particles which were purified from plasma by Sepharose CL-2B columns were present in fractions 8–12, while the bulk of the plasma proteins were present in fractions 11 onward. Vesicle markers peaked in fractions 7–11 (Karimi et al., 2018a). When compared to our data, the difference in elution profile could be attributed to column height and diameter, or to sample input amount, all of which can be optimised to improve the separation of vesicles from contaminating factors (Gaspar et al., 2020b).

One of the obstacles to salivary EV preparation is the interference of α-amylase in the identification and characterization of salivary EV proteins (Amado et al., 2014). For this reason, many studies related to salivary EVs, attempt to exclude α-amylase from EV preparations. (Deutsch et al., 2008; Gallo et al., 2012; Punyani and Sathawane, 2013; Sun et al., 2016a; Han et al., 2018). By encapsulating and adhering globules with membrane structures and viscous proteins, α-amylase may obstruct the extraction and separation of EVs, hence decreasing the yield of EV extraction. Thus, removing α-amylase and other viscous proteins from saliva before extracting EVs should aid downstream proteome analysis of salivary EVs and help with potential cancer biomarker profiling (Sun et al., 2016). Deutsch et

al. (2008) used affinity adsorption and an Amylase activity assay to confirm removal of α-amylase from saliva prior to proteomic analysis. In our study, we confirmed the separation of salivary EVs from α-amylase by SEC.

Lipids in saliva are mostly glandular in origin (Karjalainen et al., 1997), which means they pass directly from plasma to saliva (Slomiany et al., 1985; Mänttäri et al., 2001; AL-Rawi and Atiyah, 2008). There are two main types of cholesterol in saliva: high-density lipoprotein (HDL) and low-density lipoprotein (LDL). ApoB is the primary protein component of low-density lipoprotein (LDL). ApoAI is the primary protein component of high-density lipoprotein (HDL) (Feingold and Grunfeld, 2015). Excluding lipoproteins from EV preparations is critical as they have also been shown to be associated with RNA (Vickers et al., 2011; Yuana et al., 2014), which could confound RNA sequencing studies. Moreover, lipoproteins may account for particle number overestimation as NTA does not distinguish between EVs and similarly sized structures (Théry et al., 2018a; Karimi et al., 2018; Ramirez et al., 2018; Gaspar et al., 2020a). We found that ApoAI co-purified with EVs in fraction 6-10. The finding was compatible with that of Gaspar et al. (2020), where EV- derived plasma were isolated by SEC, which showed the presence of ApoAI in fractions 7–10 (Gaspar et al., 2020a), indicating that the separation of EVs and lipoproteins by SEC was unsuccessful. This finding was also comparable with those of many previous studies which showed that SEC alone is unable to completely separate EVs from lipoprotein particles (Sódar et al., 2016; Simonsen, 2017; Karimi et al., 2018a; Gaspar et al., 2020b). Stranska et al. (2018) confirmed that SEC-derived EVs from human plasma have also been shown to be contaminated with albumin and lipoproteins (Stranska et al., 2018). Furthermore, Neuberger et al. (2021) confirmed the presence of ApoAI in EV-rich fractions from plasma, indicating lipoprotein co-isolation (Neuberger et al., 2021). ApoB was not detected in any fraction in our study, which may be due to the fact that the levels of ApoB in saliva are lower than those of ApoA when compared with plasma (Karjalainen et al., 1997; Hirtz et al., 2016;).

Although MVP (and other vault components) have been reported as EV cargo multiple times in the literature, vault particles were first found to be non-vesicular contaminants in 2019 (Jeppesen et al., 2019). They had also previously been shown to contaminate intracellular vesicle preparations (Kedersha and Rome, 1986). However, it has been claimed that MVP is involved in facilitating the transport of RNA into exosomes (Teng et al., 2017; Statello et al., 2018). The size of these barrel-shaped particles (73 x 41 nm) is similar to that

of EVs and the vault components have been detected in a variety of bodily fluids and tissues (Admyre et al., 2007;Skogberg et al., 2013; Pienimaeki-Roemer et al., 2015), including saliva (Gonzalez-Begne et al., 2009). However, there have been no reports of active export or release of these particles, so the mechanism of how and why these particles are released by cells into the extracellular environment remains unknown. In our study, we have demonstrated that MVP is found in the EV-rich SEC fractions 5–8. Our data suggests that MVP/vault particles co-eluted with EVs, likely due to their similarity in size. A previous study identified MVP in EV fractions of plasma isolated by UC/Optiprep Density Gradient (Arab et al., 2019). Hence, researchers should be aware of the possibility of contaminants such as vault particles when enriching EVs.

3.4.3 Characterization of salivary EVs

NTA was performed to measure the particle size and concentration in each SEC fraction. The elution profile data and the peak elution were similar to those of the commercially available SEC columns, which also eluted the highest number of particles in fraction 8 (www.izon.com). The median diameter of particles in SEC fractions was 150 nm, which is consistent with studies, isolating small particles that range between 50-150 nm from saliva by SEC (Ogawa et al., 2008; Sharma et al., 2010; Sharma et al., 2011; Zlotogorski-Hurvitz et al., 2016; Iwai et al., 2016;; Ogawa et al., 2016; Han et al., 2020).

Particles that were spread across multiple SEC fractions were concentrated by ultracentrifugation, which resulted in a 58% yield. Other studies have displayed that further purification leads to increased purity of EVs but it also decreases their quantity (Livshits et al., 2015Wei et al., 2020). In addition, the size of particles was compared before and after UC as some studies have reported that the size of particles could be affected by this isolation technique (van der Pol, Edwin, 2012). However, the size of EVs remained unaltered at ~150 nm after UC. This finding was consistent with that of studies that demonstrated significant separation efficiency of small EVs from plasma with greater purity by using the SEC followed by UC (Wei et al., 2020; Alameldin et al., 2021). The identity of particles isolated by SEC was confirmed by TEM, which revealed numerous structures typical of extracellular vesicles. This finding conforms to previous reports of salivary EVs from healthy patients, which demonstrated by TEM that EVs isolated by SEC were cup-shaped and had intact membrane

structures and were of diverse sizes, indicating that the preparation contained a heterogeneous population of EVs (Ogawa et al., 2008; Palanisamy et al., 2010; He et al., 2020; Han et al., 2020).

Exoview analysis of SEC purified EVs showed that the majority of EVs were CD63-positive with another population of CD9/CD63-positive EVs; very few CD81-positive EVs were detected. Comfort et al. (2021) confirmed the co-expression of the three tetraspanins CD81, CD9, and CD63 by Exoview in EVs derived from healthy saliva (Comfort et al., 2021), suggesting that the discrepancy in our data is likely due to experimental error. We aimed to further validate our data by western blotting and added an additional EV marker, TSG101. The detection of CD63 and CD9 was variable amongst 6 different biological samples. However, CD81 and TSG101 were consistently detected. Variability of EV marker expression has been shown in many studies (Kowal et al., 2016; Newman et al., 2021) but it has also been suggested that CD63 is a highly reliable EV marker; CD9 and TSG101 are often found at varying levels and are often not detected in EV samples (Kadota et al., 2018). The western blot findings of my study are similar to previously published studies in which all EVs markers (CD63, CD81, and CD9) were detected in salivary EVs (Zlotogorski-Hurvitz et al., 2015; Iwai et al., 2016; Sun et al., 2018; Yu et al., 2019; Nik Mohamed Kamal et al., 2020; Conzelmann et al., 2020; Li et al., 2021; Han et al., 2021; Comfort et al., 2021). The reason for the discrepancy of CD81 abundance between Exoview/western blot analysis remains to be elucidated.

Due to the variability in CD63 and CD9 expression between the different samples, we attempted to retrospectively correlate the EV concentration in the sample before UC and the amount of protein used for the western blot. NTA data showed that samples 2 and 3 had a higher particle concentration than that of others. This was also compatible with BCA data which showed that these samples had the highest protein concentration. This suggests that the detection of CD63 and CD9 is dependent on the particle/protein yield of the sample whereas CD81 and TSG101 are more readily detected in less abundant samples. The study conducted by Wei et al. (2020) revealed that the pellets isolated from plasma by the combined SEC/UC method had the minimum total protein content compared to that of SEC alone and/or UC alone. By applying western blotting, they showed that not all EV markers were detected at the same level in the fractions separated by the combination method under the premise of the same protein quantity; however, they revealed the successful EV recovery by a combined SEC and UC isolation procedure (Wei et al., 2020).

3.4.4 Conclusion

Taking together, although SEC appeared suitable for isolating salivary EVs, the technique is time consuming and low-throughput, which constitutes a problem when dealing with many clinical samples. The current study also provides evidence that EV preparations using the SEC technique may be frequently contaminated with lipoproteins and MVP/vault particles. Without further characterisation and investigation, they could be classified as EV-associated molecules, identified by the MISEV2018 guidelines as one of the main challenges that EV research encounters.

Chapter four

Chapter 4. Isolation of salivary EVs by Dynabead immunocapture

4.1 Introduction

After realising the limitations of size-based separation techniques and ultracentrifugation (Chapter 3), we needed an improved method that could consistently generate pure and intact EVs to provide reproducibility for biomarker studies. Recently, several alternative methods have been introduced and utilised for the isolation and purification of EVs. We investigated commercially available Dynabeads that capture EVs by immunoaffinity to particular surface markers (such as tetraspanins), which should minimise contamination of EVs with particles that have similar size/density characteristics (Oksvold et al., 2015; Cocozza et al., 2020).

Dynabeads are superparamagnetic polystyrene beads that are coated with a primary monoclonal antibody specific for a variety of antigens including CD63, CD9, and CD81, which are present on salivary EVs according to western blot data (Chapter 3). Captured EVs can be eluted from the beads or lysed directly for subsequent analysis (Figure 4.1). Dynabeads are known for their sensitivity, reproducibility and stability (Wang et al., 2013). Another advantage is that the magnetic handling allows you to "see" your sample due to the light brown colour of the beads. When the sample tube is placed on the magnet, the bead-bound EVs are pulled to the side of the tube, allowing for easy separation and purification (Théry et al.,2006).

EV isolation by immunocapture has been developed to improve EV enrichment efficiency and make the isolation process faster and less complex (Oksvold et al., 2015). The method isolates a more homogenous population of vesicles in terms of size, morphology, and protein content (Tauro et al., 2012). Resulting EVs are devoid of contamination with proteins and protein aggregates and have been proven to be of higher purity by many studies (Zhang et al., 2019a; Jeppesen et al., 2019; Huang et al., 2020; Chen et al., 2020a; Liangsupree et al., 2021) and it works efficiently even if the input sample volume is small (Konoshenko et al., 2018). However, such techniques are less popular due to high cost, and where selecting specific EV subtypes is not desirable (Peterson et al., 2015). In addition, immunocapture is not suited for processing large sample volumes (Théry et al., 2006; Li et al., 2017b).

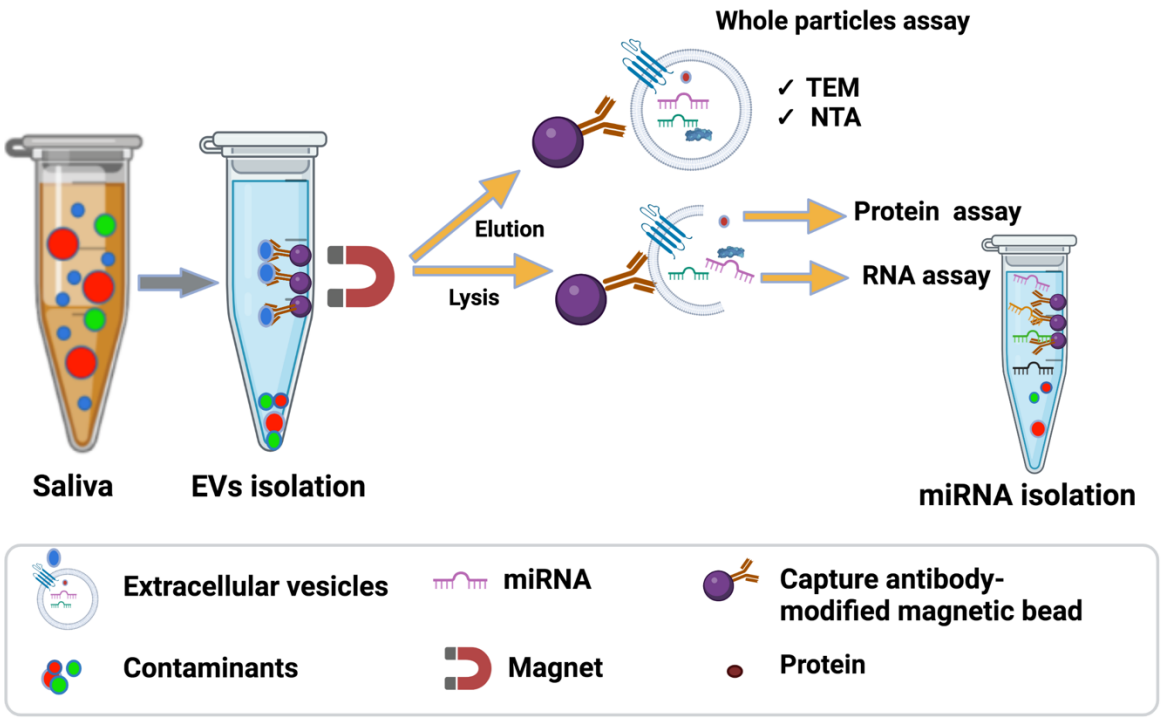

Figure 4. 1 Dynabead immunocapture procedure. Captured EVs can be eluted for whole particle assays, such as transmission electron microscopy (TEM) and nanoparticle tracking analysis (NTA). Alternatively, captured EVs can be lysed to study their molecular contents, including proteins and RNAs. Adapted from Chen et al. (2020) and created by Biorender.

Several optimization parameters are required for each biological fluid and isolation method, (such as testing the optimal input volume), which should be carefully tested because of their significance in the validation stages of any EV biomarkers (Soekmadji et al., 2018; Clayton et al., 2019), as emphasized by MISEV 2018 guidelines (Thery et al., 2018).

The sample storage conditions for EV-based research is necessary to acquire results that reproduce the original physiological state of EVs (Ayers et al., 2011). The effects of storage conditions (temperature and duration) on EVs can affect properties such as size, integrity, content, particle number, aggregation, and function (Bæk et al., 2016; Muller et al., 2014; Jeyaram and Jay, 2018).

According to the literature, currently there is no consensus on the storage of fluids because the effects of storage appear to vary with sample source (Théry et al., 2018a; Clayton et al., 2019). Storage before EV purification may be convenient to allow simultaneous processing of samples from different patients or sources (Witwer et al., 2013c), however, this may be unavoidable in cases where the samples are obtained from a biobank (Yuan et al.,

2021). At the same time, there is some consensus that fresh samples of biological fluid are preferred (Ayers et al., 2011; Szatanek et al., 2015).

According to the MISEV2018 guidelines, western blotting is commonly used to confirm the presence of vesicle markers, in which at least three distinct marker proteins should be examined. Since none of the common markers are unique to a single EV subtype, it is recommended that researchers choose adequate isolation techniques to rule out other EV types rather than relying just on characterised markers (Théry et al., 2018). In our study, TSG101 (a luminal EV protein), and CD63, CD9, and CD81 (typical transmembrane EVs markers) were used to optimise the Dynabead protocol (Jankovičová et al., 2020).

4.2 Aims and objectives

The aims of this chapter were to determine if Dynabead immunocapture was a more suitable salivary EV isolation technique and to explore the impact of storage of saliva on subsequent EV isolation. To meet these aims, the following objectives will be addressed:

- Compare the efficiency of Dynabead immunocapture to SEC.
- Evaluate input sample volume and stability of EV-bead complexes post-capture.
- Quantify unbound particles after immunocapture.
- Assess the effect of storage of saliva on the capture of salivary EVs.

4.3 Results

4.3.1 Compare isolation of Salivary EVs by SEC and Dynabead immunocapture

The first aim in this chapter was to isolate salivary EVs by both SEC and immunocapture to compare efficiency. 10 ml saliva was obtained from six volunteers under standardised conditions. The saliva was clarified as previously described in (Section 2.2.1.2) and concentrated to 1 ml. At this point the samples were divided, 0.5 ml was processed by SEC and 0.5 ml processed by Dynabead immunocapture. The resulting EV pellets from SEC (followed by UC) and Dynabead-EV complexes were solubilised in RIPA buffer and analysed by western blot for EV markers. The signal intensity of EV tetraspanin markers (CD63, CD9, and CD81) was much stronger with Dynabead isolation, which indicates that Dynabead isolation is more efficient than SEC (Figure 4.2).

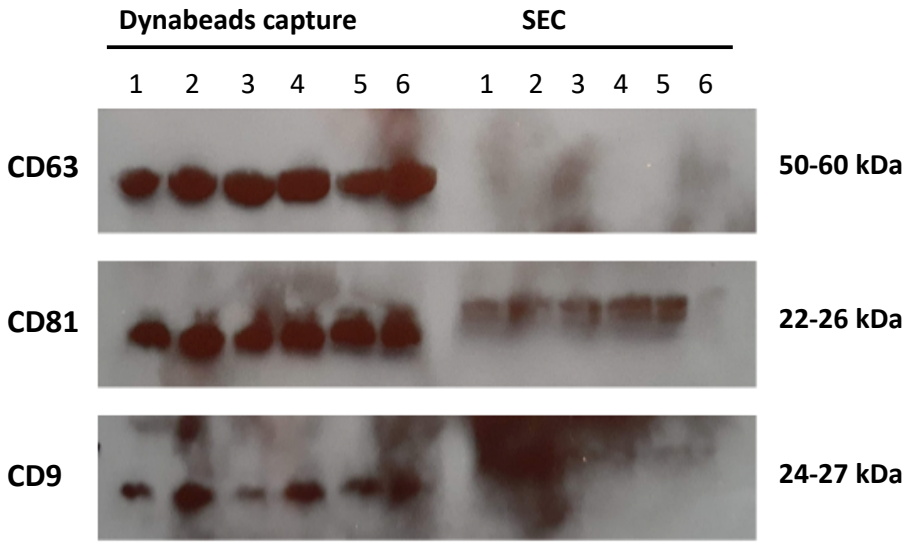

Figure 4. 2 Comparison of Dynabead isolation and SEC. EVs were isolated from equal volumes of saliva and solubilised in RIPA buffer, separated by SDS-PAGE and subsequent western blot analysis. EV lysates were probed for CD63, CD81 and CD9. The western blot images show six independent biological samples.

4.3.2 Optimization of Dynabead immuno-capture isolation method

4.3.2.1 Evaluating the efficiency of Dynabead immunocapture

We next sought to evaluate how consistent Dynabead immunocapture was at capturing salivary EVs from equivalent volumes of saliva. EV-Dynabead complexes were pulled out of solution and solubilised for analysis by western blot. The concentration/size of particles before and after capture (that remained in the unbound fraction) was measured by NTA (Figure 4.3A). Blotting for CD9, CD63, and CD81 suggested that EV capture was broadly similar between different biological samples (Figure 4.3B). The average number of particles in samples prior to immunocapture was 8.98 x 10^{10} particles. Whereas the average particle number in unbound fractions was 9.83x 10^{9}, which represents a significant decrease in particle number (p=0.0313) (Figure 4.3C) and capture of 89% of particles present in the input sample. NTA revealed that the mean diameter of particles in the input sample and in the unbound fraction was around ~200 nm and not significantly different (p=0.2200) (Figure 4.3D).

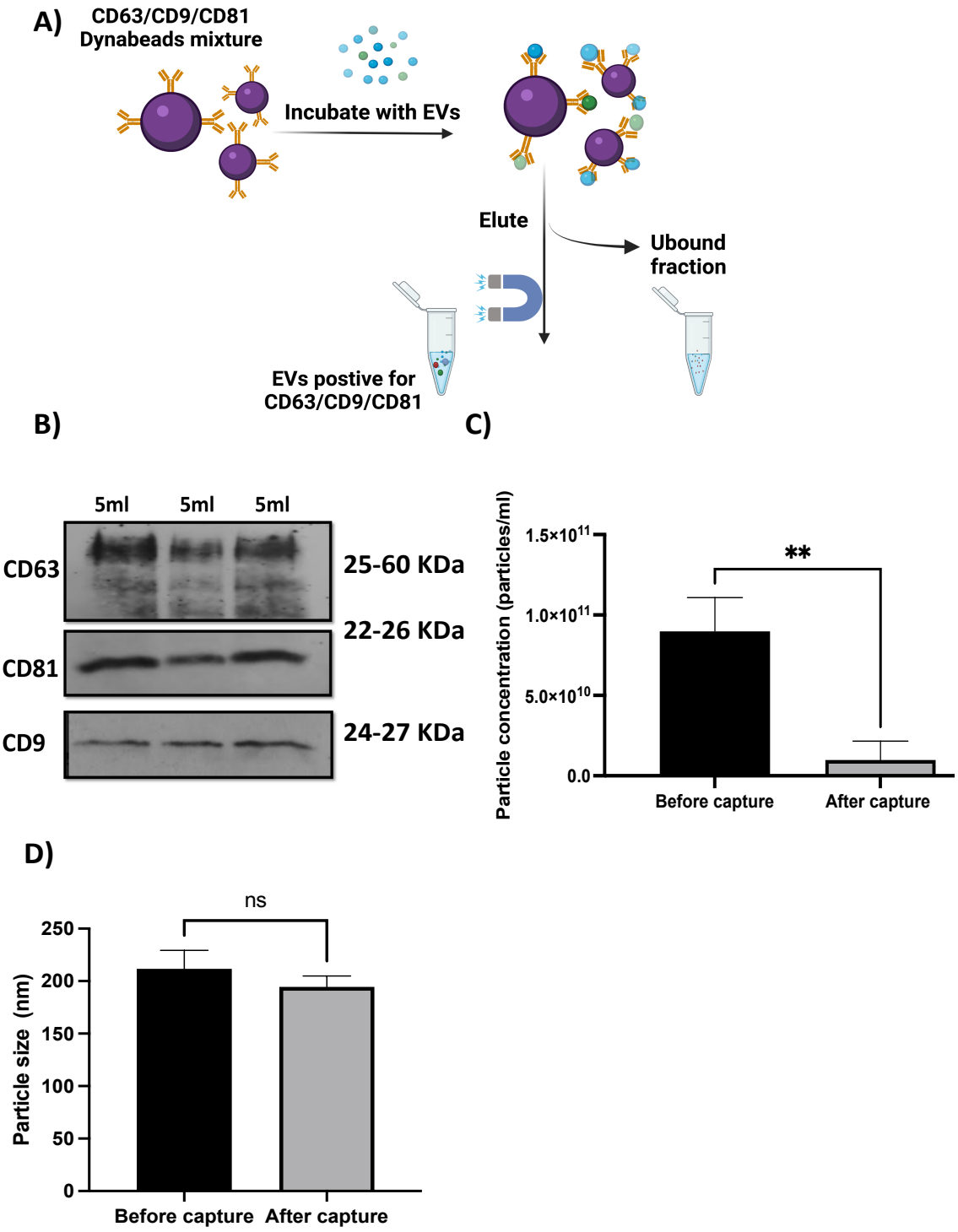

Figure 4. 3 Assessing the efficiency of Dynabead immunocapture. A) Schematic depicting the experimental design of incubating saliva with a CD9/CD63/CD81 Dynabead cocktail, followed by separation of marker-positive EVs from unbound fraction using a magnet. B) Western blotting to detect EV markers (CD81, CD63, and CD9). The western blot image shows three independent biological samples. C) The number of particles before and after capture determined by NTA. Data is the average n=3 ± SD. D) The mean diameter of particles measured by NTA. Data is the average n=3 ± SD. Pairwise comparisons were conducted by Student's t-test ns=not significant, **= $p<0.05$.

4.3.2.2 Assessing the input volume of saliva for Dynabead immunocapture

After determining the high efficiency and reproducibility of immunocapture using 5 ml saliva (Figure 4.3), we next tried to determine the minimum input volume of saliva that provided a detectable yield of captured EVs. Increasing concentrations of saliva (equivalent of 1 to 5 ml) were incubated with a fixed quantity of CD9/CD63/CD81 Dynabeads. Western blotting using solubilised Dynabead-EV complexes showed increasing signal intensity as the saliva input increased (Figure 4.4A). All EV markers (CD63, CD81, CD9 and TSG101) were detectable when the saliva input was ≥2 ml. Only CD9 and TSG101 were detectable when the saliva input volume was 1 ml. In parallel to western blotting, we quantified the number of particles that were added to the beads and how many did not bind to the beads to determine if they became saturated as saliva input volume increased. As the number of particles incubated with the beads increased so did the number of particles in the unbound fraction (Figure 4.4B). However, the increase appeared proportional to the input quantity rather than a rapid increase that might suggest bead saturation.

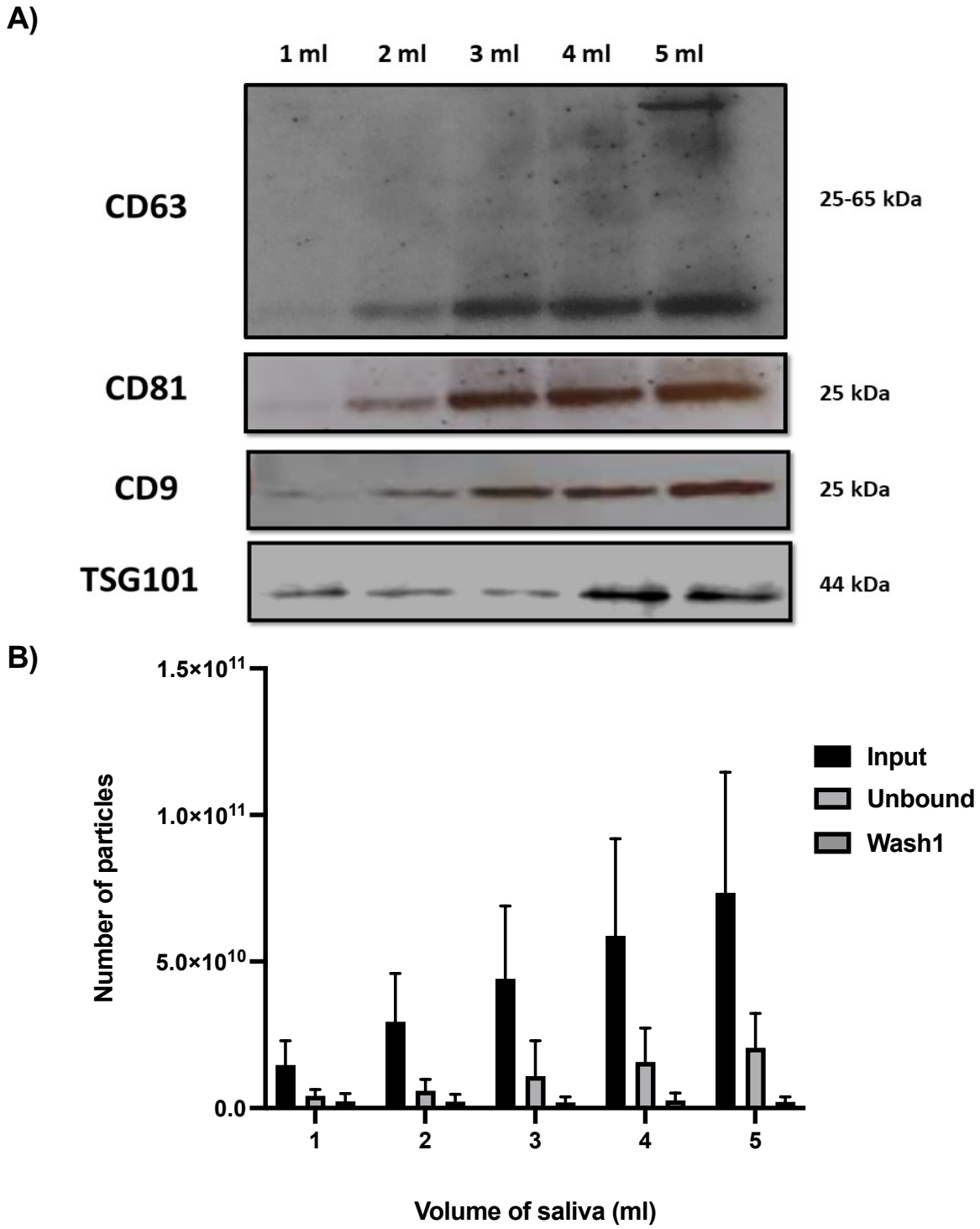

Figure 4. 4 Optimum volume of saliva for Dynabead isolation. A) Western blotting to detect EV markers (CD81, CD63, and CD9, TSG101) after incubating Dynabeads with 1 to 5 ml saliva. The blots are representative of 3 experiments. B) NTA was used to determine the number of particles in the input sample, the unbound fraction and the first PBS wash. Bars show average of 3 experiments with error bars representing standard deviation.

4.3.2.3 Visualisation of Dynabead-EV complexes by TEM

One technical difficulty related to immunocapture is particle analysis of captured EVs by NTA or similar techniques. To perform NTA the EVs must be released from the Dynabeads, but this methodology is not included in the Manufacturer's instructions. Instead, we attempted to confirm the presence of salivary EVs bound to Dynabeads by TEM. Images of Dynabeads incubated with PBS (negative control) and with concentrated saliva were captured and showed that the beads were round with an irregular surface (Figure 4.5A). Occasional EV-like structures were visualised on the surface of the Dynabeads with a spherical shape and measuring ~50 nm diameter (Figure 4.5B). These structures were not observed on negative control beads (Figure 4.7A).

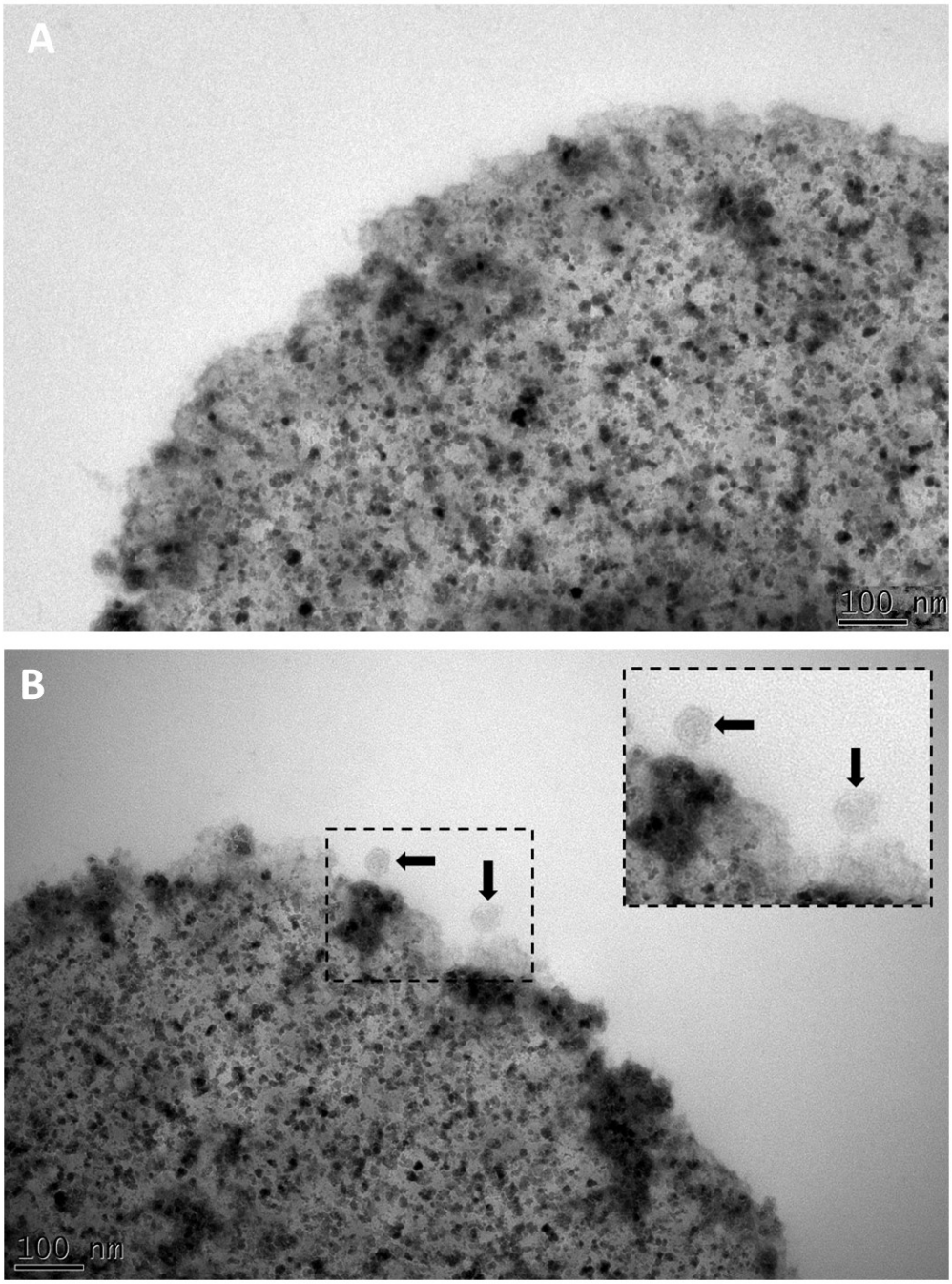

Figure 4. 5 Imaging of Dynabead-EV complexes by TEM. A) Tetraspanin Dynabeads incubated with PBS (negative control). B) Tetraspanin Dynabeads incubated with saliva. Images were obtained by negatively stained, resin embedded TEM. Black arrows indicated EV-like structures on the surface of Dynabeads. Scale bars represent 100 nm.

4.3.2.4 Effect of storage time on captured salivary EVs

We next wanted to determine if Dynabead-EV complexes could be stored at 4°C, which may be an advantage for downstream biomarker studies. EVs were isolated from 5 ml saliva and after the final wash step were stored in PBS at 4°C for up to 14 days. Western blotting for common EV markers showed similar band intensity at 1- and 2-day timepoints, however, by day 7 there was a noticeable decrease in TSG101 signal intensity suggesting a decrease in EV integrity and loss of luminal cargo (Figure 4.6).

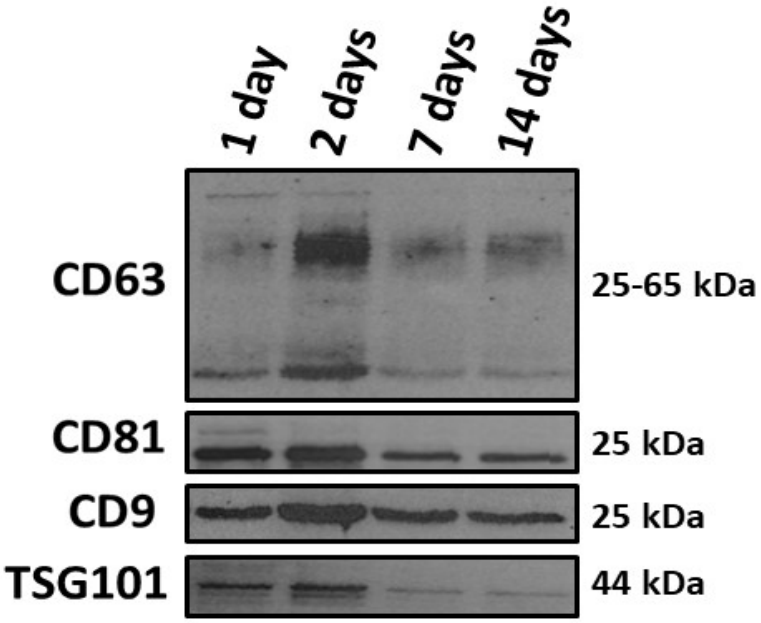

Figure 4. 6 Effect of storage time on captured salivary EVs. EVs incubated with Dynabeads and after the final wash step were incubated at 4°C for up to 14 days. Dynabead-EV complexes were lysed in 20 µl of lysis buffer and separated by 12% SDS-PAGE. After transferring them to a nitrocellulose membrane, they were blocked and incubated overnight with the primary antibodies. Blots were developed by incubation with appropriate HRP conjugated secondary antibodies and incubated with Supernova reagent before exposure to X-ray film and developed on a Xograph X4. The blots shown are representative of three independent experiments.

4.3.2.5 Effect of storage of saliva on capture of EVs

Next, we sought to determine if saliva could be stored before EV isolation. This would inform if saliva samples needed to be processed fresh or could be stored for batch processing. EVs were either isolated immediately (control) or saliva was stored overnight at 4°C or -20°C prior to EV isolation by Dynabead immunocapture. Western blotting of Dynabead-EV complex lysates showed a decrease in TSG101 signal intensity after storage at 4°C and -20°C, suggesting a decrease in EV integrity and loss of luminal cargo (Figure 4.7).

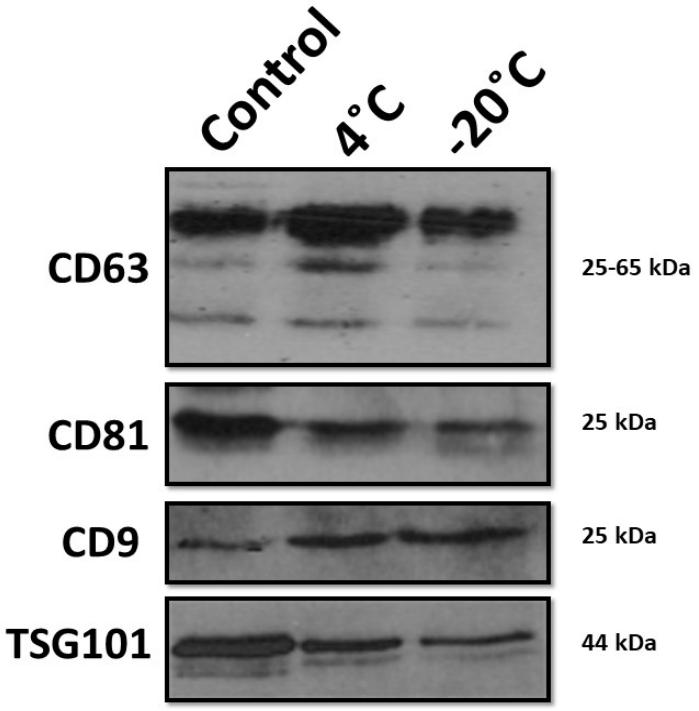

Figure 4. 7 Storage of saliva prior to immunocapture of salivary EV. EVs were either isolated immediately (control) or saliva was stored overnight at 4°C or - 20°C prior to EV isolation, then Dynabead-EV complexes were resuspended in RIPA buffer containing protease inhibitors to solubilise EV protein. 20 µl of each sample was separated by SDS-PAGE and transferred to a nitrocellulose membrane for subsequent western blot analysis. Representative blot from 3 independent experiments.

4.4 Discussion

4.4.1 Dynabead EV isolation is more efficient than SEC

In this chapter, we demonstrated an immunoaffinity-based isolation strategy using Dynabeads that successfully isolates salivary EVs. Western blotting suggested that the capture technique yielded more EVs for downstream analysis compared to SEC. Although SEC appears suitable for isolating salivary EVs, the technique is time-consuming and low-throughput, which is a problem when dealing with many clinical samples. Isolation of EVs based on size alone is not optimal due to contamination with similar sized particles (Brennan et al., 2020). Therefore, affinity-based capture is as an option for improving recovery and purity of EVs. The success of this approach depends on the stable presence on the EV surface of a marker or markers that can strongly bind a detection reagent such as a marker-specific antibody. In our experiments, we were able to pull out the marker-positive EVs (CD63/CD9/CD81) using magnetic bead/antibody complexes against specific well-defined EV markers, which should leave contaminating particles behind in the unbound fraction.

Many studies have demonstrated the high efficacy of Dynabeads in capturing EVs from biofluids using tetraspanin markers (Caby et al., 2005; Jakobsen et al., 2015; Zhang et al., 2019a; Chen et al., 2020a; Karimi et al., 2022b). Immunoselection has improved efficacy to isolate EV from biological fluids compared to ultracentrifugation and density gradient centrifugation, making them highly attractive and suitable for clinical applications and diagnostic purposes (Caby et al., 2005; Tauro et al., 2012). Hinzman et al. (2022) found that immunocapture yielded smaller vesicles of a more uniform size when compared with UC and SEC (Hinzman et al., 2022). When compared to UC, Zhang et al. (2019) discovered that EVs isolated using Dynabeads have much narrower size distribution after releasing EVs from the magnetic beads. Since most body fluid-EVs are currently isolated using precipitation methods, which are frequently prone to being crude and contain aggregated contaminants (Musante et al., 2012; Kim et al., 2012; Paolini et al., 2016; Gámez-Valero et al., 2016a), Dynabeads can be especially helpful in EV isolation from biological fluids. While Dynabead isolation addresses the aforementioned issues, it unavoidably has the disadvantage of being marker-specific and only isolating a certain subpopulation of EVs (Alvarez et al., 2012; Ji et al., 2013; Rutter and Innes, 2017). For example, when isolated from various biological sources or utilising various enrichment methods, EVs express various markers (Alvarez et al., 2012; Ji et al., 2013; Karimi et al., 2022a), or when cells are in a different state (e.g. stressed vs actively growing) (Rutter

and Innes, 2017), which can result in inconsistent EV yield and EV content between experiments. In addition, due to the heterogeneity of tumours, it is possible that not all cells within a tumour may express the target antigen, meaning that EVs derived from those cells may not be captured (O'Loghlen, 2018). Furthermore, antigen modulation can occur as cancers advance, so that a tumour may initially produce the target antigen but that expression may decrease with time or the antigenic epitope may be blocked or masked (Beatty and Gladney, 2015). However, with the continuous discovery of new EV markers, a Dynabead cocktail comprising antibodies against numerous EV markers may be a feasible alternative. This separation method may benefit studies on EV cargo in marker-positive EV subpopulations, and it might also be employed as a negative selection strategy to facilitate larger investigations into other non-vesicular extracellular particles (Tauro et al., 2012; Taylor and Shah, 2015).

Here, in our study, we found that 89% of salivary EVs were captured from input samples. Moreover, NTA data from the input sample and the unbound fraction revealed a similar mean particle diameter size of ~200 nm. This is broadly in agreement with the study by Zhang et al. (2019) that tested the efficiency of Dynabead EV isolation from plasma, which showed a high recovery efficiency (78%). In addition, they measured the size of EVs in the input sample before and after Dynabead isolation and found that they were the same, at ~200 nm (Zhang et al., 2019). Immunocaptured EVs appeared morphologically intact and had a typical spherical-shaped morphology by TEM, measuring ~50 nm diameter. However, the number of imaged particles was too low to conduct any meaningful size analysis. With more time for protocol optimisation, additional images with better contrast could have been generated. This might allow more EVs to be imaged and for their size to be quantified.

4.4.2 Saliva input volume and storage conditions affect EV yield and integrity

In accordance with the MISEV 2018 guidelines, different factors that may affect the binding efficiency of Dynabeads were carefully examined, including input volume and sample storage conditions. The optimum input volume of different biological fluids when choosing an EV enrichment protocol is important, as some biofluids may need to be concentrated prior to EV isolation to allow downstream analysis, for example, proteomic and transcriptomic analysis (Caby et al., 2005; Kim et al., 2012).

The current study showed that among different input volumes of saliva (1-5 ml), all EV markers were detected by western blot for ≥2 ml. NTA data revealed that Dynabeads did not show signs of saturation when up to 5 ml saliva was used as input volume. El-Khoury et al. (2016) used increasing amounts of starting material to investigate the impact on miRNA extracted from cells, plasma, and urine/plasma-derived exosomes. They showed that miRNA recovery was largely influenced by the amount of input material and by the isolation method (El-Khoury et al., 2016). Zarovni et al. (2015) showed that magnetic beads demonstrated linear titration of captured exosomes when incubated with 100 µl to 1000 µl plasma (Zarovni et al., 2015). Another study found that increasing the protein levels of the input exosomes linearly correlated with the protein level of $CD34^+$ exosomes captured from plasma. However, they found the unbound fraction still contained $CD34^+$ EVs (Hong et al., 2014). In contrast, the maximum input volume of urine for EV isolation by immunocapture was found to be 10 ml, at which point the beads became saturated (Reithmair et al., 2022).

The optimisation of sample storage conditions for EV-based research is necessary to obtain results that reflect the original physiological state of EVs (Ayers et al., 2011). Storage of biofluids seems to be inevitable before isolating EVs as many samples are obtained from biobanks and cannot be processed at collection to allow simultaneous processing of samples from different patients or sources (Witwer et al., 2013c). Many studies have suggested that it is advisable to proceed to vesicle isolation immediately after collecting the biofluid. Thus, fresh samples are often preferable, but not always practical (Ayers et al., 2011). The effects of storage conditions (temperature and duration) on EVs can affect properties such as size, integrity, content, particle number, aggregation, and function (Bæk et al., 2016; Muller et al., 2014; Jeyaram and Jay, 2018). In our study, the appropriate handling of saliva was investigated. We have shown through western blot analysis of four EVs markers that the integrity of the EVs decreased when saliva was stored at 4°C and -20°C. Processing the saliva immediately gave the best yield of intact EVs for biomarker studies. Other studies have published contrasting findings that suggest saliva can be stored prior to EV isolation. The total protein, morphology, and expression of EV markers (CD9, ALIX, and TSG101) were stable when human saliva was stored at 4°C for 7 days, but evidence of minor degradation of certain proteins was also found after storage (Kumeda et al., 2017). Freezing samples at -80°C has been reported to preserve most EV particles derived from blood, but incubation at 4°C and 20°C caused significant loss of EV numbers (Lőrincz et al., 2014). The effects of storage might

change depending on the sample source (Clayton et al., 2019; Théry et al., 2018c). Duration of storage could also have an impact on RNA biomarker studies if RNA cargo is lost from EVs upon freezing (Debey et al., 2004; Sourvinou et al., 2013; Lee et al., 2016). Hu et al. (2020) have found that EVs isolated and stored for the short-term (2 weeks) at 4 °C would decrease the EV RNA level, whereas freezing at -80°C or -20°C for the long term showed no change in RNA or protein levels (Hu et al., 2020a). Our results show that Dynabead-EV complexes were stable at 4°C for at least 2 days. However, at 7-14 days there was a decrease in EV integrity and loss of luminal cargo. According to MISEV 2018 guidelines isolated EVs should only be stored in the short-term at 4 °C. For long-term storage, isolated EVs should be stored at −80 °C (Witwer et al., 2013c; Théry et al., 2018c).

4.4.3 Conclusion

Altogether, this chapter demonstrates that Dynabead immunocapture is more efficacious than SEC isolation for capture salivary EVs. Though Dynabead capture appears to be less cost-effective when compared to traditional techniques such as DC and SEC, it isolated EVs that were detectable by western blotting from as little as 2 ml of saliva. The captured EVs were stable for up to 2 days once bound to Dynabeads, but extended storage led to degradation. In addition, isolation of salivary EV worked best from fresh saliva. The findings from this chapter inform the handling of clinical samples that will be utilised in the subsequent chapter.

Chapter Five

5. Characterisation of OSCC patient salivary EV miRNA cargo

5.1 Introduction

It is generally recognised that EVs contain a wide range of molecular cargo, including protein, lipid, DNA, and RNA (Abels and Breakefield, 2016) with RNA being the most extensively studied. Deep sequencing of RNA cargos obtained from immune cell EVs revealed a diverse group of protein-coding and non-coding RNAs (Nolte-'t Hoen et al., 2012). The fact that EV RNA cargo differs from total cellular RNA suggests that packing mechanisms are selective (Nolte'T Hoen et al., 2012). Multiple RNA species have been found as EV cargo, with new RNA species being gradually discovered. Ratajczak et al. (2006) proposed that RNA might be transferred horizontally between donor and recipient cells via EVs (Ratajczak et al., 2006b). In 2007, Valadi et al. presented one of the instances of EV RNA exchange between cells. It was demonstrated that EVs transported messenger RNA (mRNA) into recipient cells, where the mRNAs were translated into proteins (Valadi et al., 2007a). Since then, the use of CRE recombinase-controlled reporter systems has demonstrated EV mRNA transport in vivo (Ridder et al., 2015).

EVs also contain non-coding RNAs, which are of great interest because of how they regulate gene expression. Small nucleolar RNAs (snoRNAs), transfer RNAs (tRNAs), ribosomal RNAs (rRNAs), long non-coding RNAs (lncRNAs), piwi-interacting RNAs (piRNAs), and vtRNAs are some of the several forms of RNA that comprise this population (Nolte-'t Hoen et al., 2012). Among all these, miRNAs represent a highly conserved class of RNA molecules. These small (19–22 nucleotides long) RNA molecules usually bind to their mRNA targets' 3' untranslated region (3'UTR), causing post-transcriptional gene regulation through translation inhibition or mRNA degradation (Momen-Heravi and Bala, 2018a; Li et al., 2018). It has also been shown that the secondary structure of the 5' untranslated region (5'UTR) of mRNA is important for miRNA-mediated gene regulation in humans (Gu et al., 2014). The presence of both mRNAs and miRNAs in EVs was first reported in 2007 (Valadi et al., 2007a).

It has been demonstrated that the EVs released by tumour cells are different from those of normal cells (Tűzesi et al., 2017). EV RNA cargo has been shown to contribute to multiple pro-tumorigenic phenotypes such as increased proliferation, angiogenesis, and metastasis (Li et al., 2016b; Cai et al., 2019; Hu et al., 2020b; Baig et al., 2020). There are two main possible impacts of packaging RNA into EVs: removal of RNA from the cellular

environment and functional impact on recipient cells. A CRE recombinase-controlled reporter system was used to demonstrate that cancer EVs may spread oncogenic RNA species to nearby cells, suggesting a physiological function for EV RNA transfer (Zomer et al., 2015). Others have demonstrated that tumour suppressor miRNAs may be concentrated in cancer EVs, and that when EV release is inhibited, tumorigenic phenotypes of the cells are repressed (Ostenfeld et al., 2014b).

Oral cancer screening has been proposed to employ particular salivary miRNAs as disease indicators (Liu et al., 2012b; Duz et al., 2016). Currently, characterising small EV RNA content is a main topic of research. It was discovered that RNA cargo is sorted differently into various types of EV because EVs are a highly diverse population (O'Brien et al., 2020). Numerous studies have suggested that miRNAs in salivary exosomes could be a potential resource for the diagnosis of oral cancer and may become a new oral cancer biomarker (Michael et al., 2010; Machida et al., 2016; Chiabotto et al., 2019). Langevin et al. (2017) detected differences in miRNA expression levels in salivary exosomes from patients with head and neck squamous cell carcinoma when compared to comparable controls using miRNA microarrays (Langevin et al., 2017). He et al. (2020) demonstrated differences expression in miRNA 24-3p expression in salivary exosomes from patients with OSCC compared to the corresponding control saliva samples by using microarray analysis and subsequent qRT-PCR validation (He et al., 2020). EV miRNA cargo are protected from RNases in body fluids by encapsulation within the phospholipid bilayer membrane (Mumford et al., 2018). Therefore, examination of EV miRNA from saliva, which is in contact with tumor tissue, could be exploited as a valuable source of biomarkers for oral cancer (Teng et al., 2021).

Previous studies that have profiled salivary EV RNA have utilised EV isolation techniques such as UC that, in our laboratory, gave sub-optimal results (Langevin et al., 2017; Farag et al., 2021). Here we build on knowledge and expertise from our preliminary studies and employ our pre-optimised Dynabead EV isolation strategy. We also use an unbiased small RNA sequencing approach to determine EV miRNA cargo.

5.2 Aims and objectives

The main aim of this chapter was to compare the miRNA cargo of salivary EVs isolated from patients with OSCC compared to healthy controls. To address this aim, the following objectives will be addressed:

- Isolate salivary EVs from patient saliva samples using Dynabead immunocapture and extract EV RNA
- Quantify salivary EV RNA by Bioanalyzer analysis.
- Conduct small RNA sequencing on a subset of RNA samples to determine differentially expressed miRNA
- Validate small RNA sequencing data in the whole cohort using qRT-PCR.

5.3 Results

5.3.1 Study participants

A cohort of 17 newly diagnosed patients with OSCC (11 men and 6 women) were recruited. Although all cancer patients were diagnosed with OSCC, tumours were situated in different anatomical sites within the oral cavity: seven within the tongue, three within the retromolar region, one of the maxilla, two associated with the palate, one of the alveolar ridge, and three affecting the floor of the mouth. A cohort of 7 healthy patients (5 men and 2 women) were also recruited from routine dental clinics. All patients were recruited in accordance with NHS ethics application IRAS: 264332/STH: 20945, during their treatment at Sheffield Teaching Hospitals Trust. Saliva collection from OSCC patients was carried out prior to cancer treatments such as surgical resection. Anonymised details of the study participants are provided below (Table 5.1).

Table 5. 1 Clinical details of OSCC patients and healthy controls.

Sample number	Site	Gender	Age	Smoking status (cigarettes per day)	Drinking Status (units per week)	Disease status (healthy or cancer)
C01	Tongue	Male	63	-	-	Cancer
C02	Left retromolar region	Male	70	15	37.8	Cancer
C03	Right retromolar region	Male	56	10-12	50	Cancer
C04	Left lateral tongue	Male	72	0 (stopped 1996)	14	Cancer
C06	Left floor of mouth	Female	67	0	14	Cancer
CO7	Right lateral tongue and floor of mouth	Male	53	20	42	Cancer
C08	Right ventral tongue	Female	52	15	42	Cancer
C09	Maxilla	Male	76	0	23	Cancer
C10	Right alveolar ridge	Male	60	15-20	0	Cancer
C11	Flour of mouth	Female	61	5 (reduced from 20)	None for 1 year	Cancer
C12	Retromolar region	Male	71	20	18	Cancer
C13	Tongue	Male	71	30	8.7	Cancer
C14	Ventral tongue	Female	58	20	113.4	Cancer
C15	Palate	Male	62	20	120	Cancer

C16	Ventral tongue	Male	75	0	13.53	Cancer
C17	Palate	Female	45	10	10	Cancer
C20	Floor of mouth	Female	59	Stopped 10 ago	21	Cancer
H06	NA	Male	42	0	12	Healthy
H07	NA	Female	41	10 + 1 pipe of cannabis	Occasional	Healthy
H10	NA	Male	57	0	12	Healthy
H11	NA	Female	71	0	8	Healthy
H12	NA	Female	66	0 (Stopped 15 years ago)	14	Healthy
H13	NA	Female	66	0	1.5	Healthy
H14	NA	Female	71	0	0	Healthy

5.3.2 Transcriptomic analysis of clinical samples

5.3.2.1 EV-RNA isolation and Bioanalyzer analysis

To determine differences in small RNA cargo in salivary EVs produced by healthy and cancer patients, EVs were isolated by Dynabead immunocapture from up to 5ml of saliva. Total RNA was extracted from EV-Dynabead complexes and the integrity of isolated RNA was characterised using an Agilent 2100 Bioanalyzer coupled with an RNA 6000 Pico LabChip. The Bioanalyzer traces showed abundant small RNA species 25 to 200 nucleotides in length across all samples (except C10, C11, and C12, which failed Bioanalyzer analysis and were excluded from further analysis). This indicates the enrichment of small RNA species in EV RNA samples (Figure 5.1). There was an absence of ribosomal RNA peaks (18S, 28S) that are expected in cellular RNA samples. No differences were observed between the RNA profiles of OSCC patients and healthy controls (Figure 5.1 A,B). EV-RNA concentrations were automatically calculated based on the area under the curve from cancer samples and control samples (Table 5.2).

A) Healthy controls

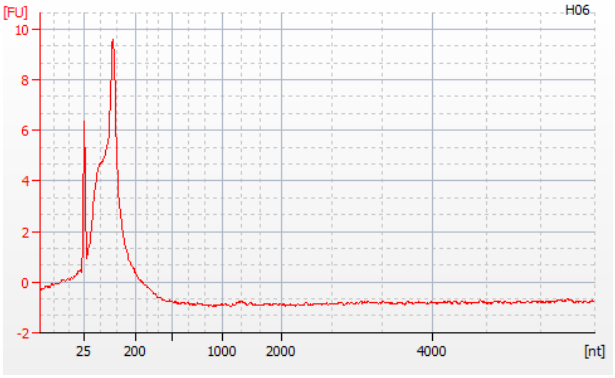

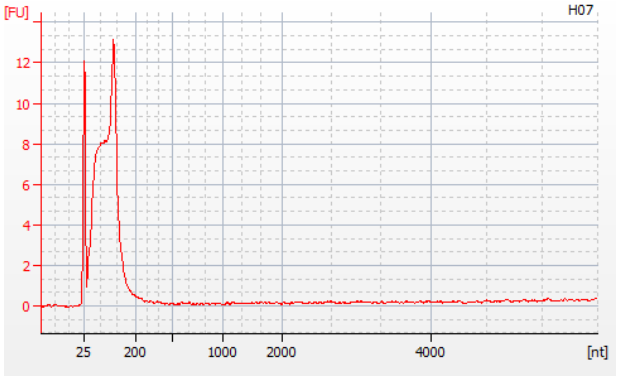

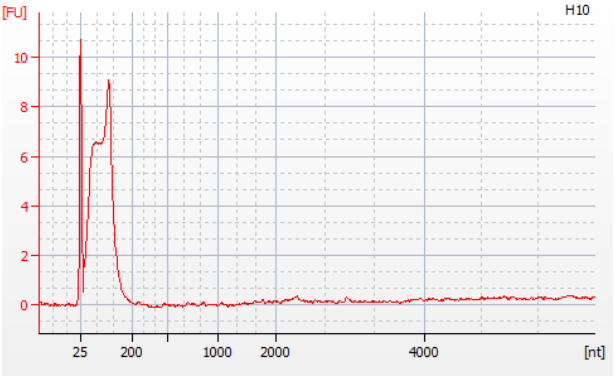

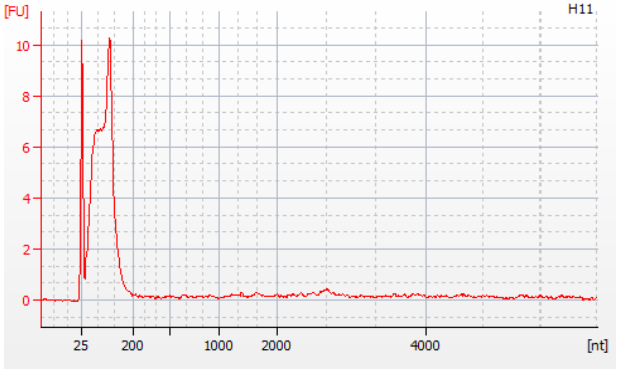

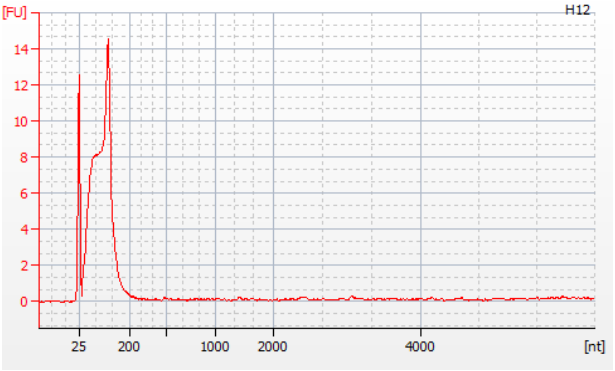

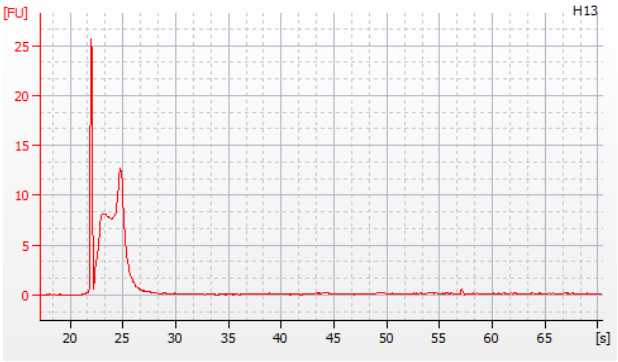

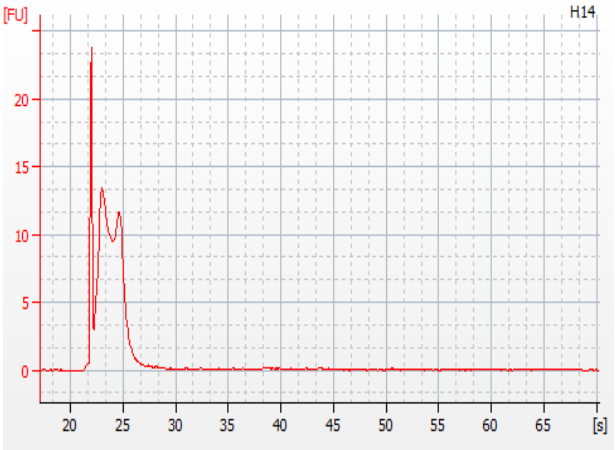

B) Cancer groups

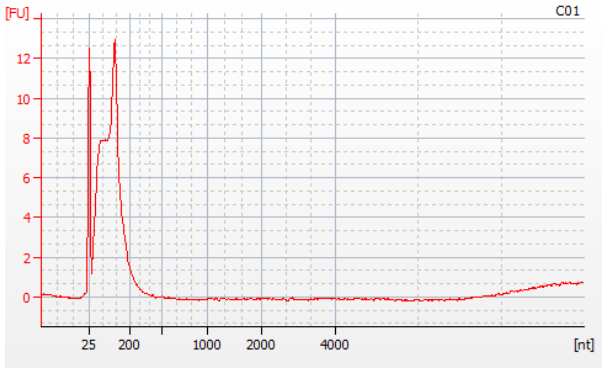

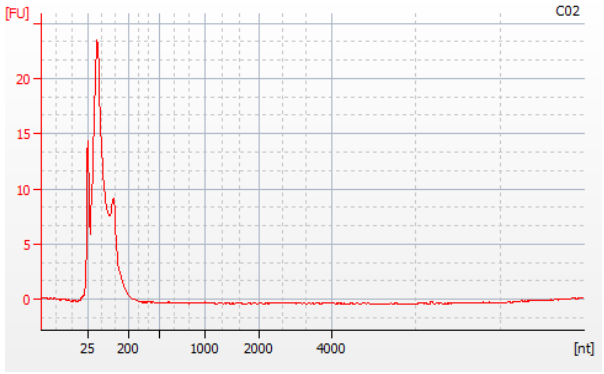

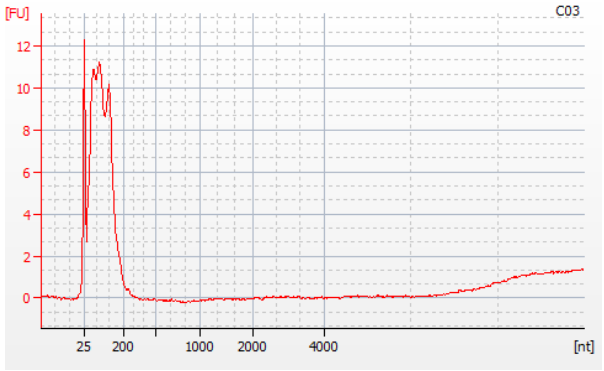

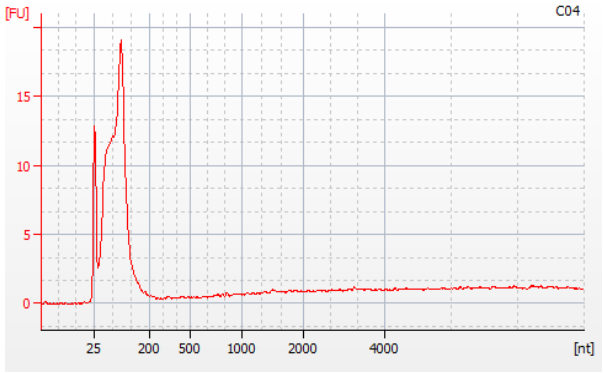

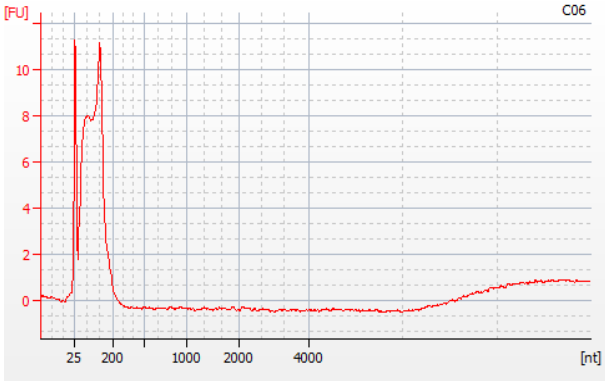

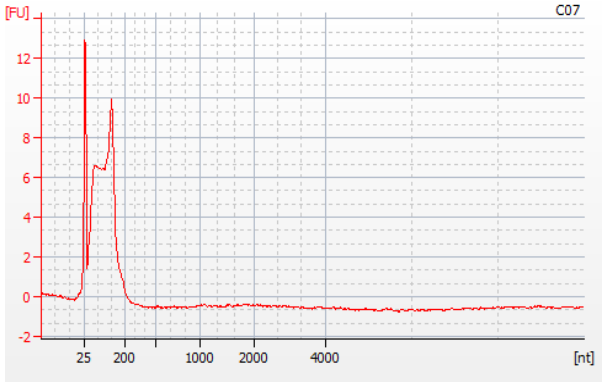

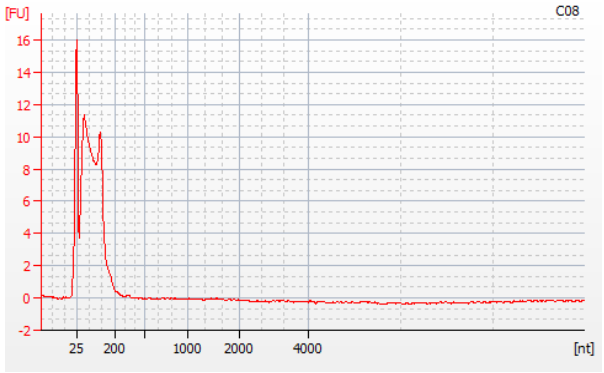

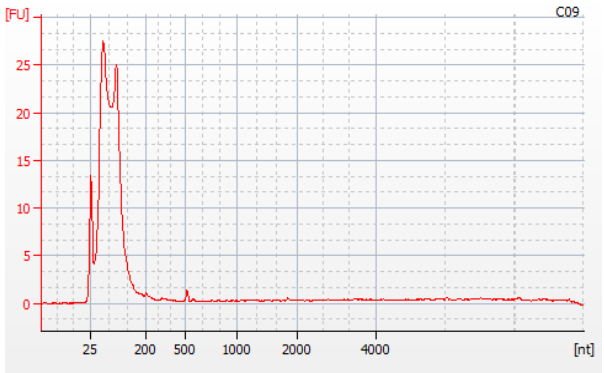

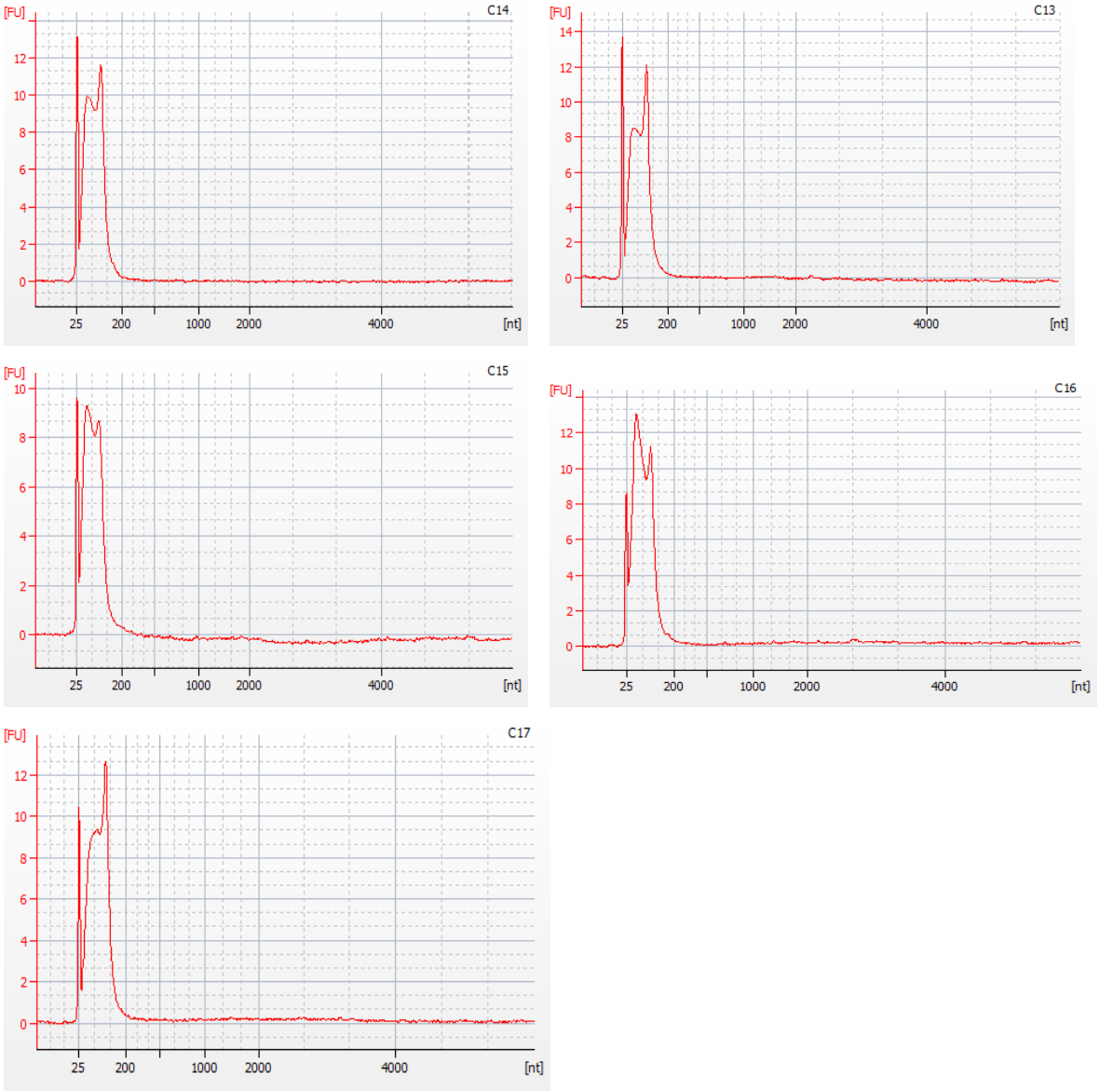

Figure 5. 1 Bioanalyzer traces of salivary EV-RNA. EVs were isolated from the saliva of cancer patients and healthy individuals by Dynabead immunocapture and resuspended in RNA lysis buffer followed by RNA extraction. 1 µl of each purified RNA sample was used for RNA quantification on an RNA 6000 Pico LabChip on an Agilent 2100 Bioanalyzer. The histograms show the RNA distributions range from 25-200 nucleotides. The X axis shows the number of nucleotides (nt). The Y axis shows fluorescence units (FU).

Table 5. 2 EV RNA concentration determined by Bioanalyzer.

Sample	RNA concentration (pg/µl)
H06	594
H07	903
H10	671
H11	760
H12	912
H13	570
H14	693
C01	482
C02	670
C03	522
C04	706
C06	438
C07	378
C08	486
C09	1102
C10	0
C11	0
C12	0
C13	842
C14	925
C15	788
C16	1100
C17	1057
C20	633

5.3.2.2 Small RNA sequencing of salivary EV cargo

At the time samples were sent for RNA sequencing not all patients had been recruited due to delays caused by the COVID pandemic and prolonged suspension of clinical research projects. We had originally planned to sequence age/sex matched samples and select healthy patients with similar smoking/drinking status to the OSCC patients. However, recruiting healthy patients became very difficult due to reduced routine dental treatment in the Charles Clifford Dental Hospital. The frequency of OSCC surgeries also reduced due to the impacts of the COVID pandemic. No patients (healthy or cancer) were recruited to this study for almost 12 months. We therefore selected RNA samples derived from healthy patients (H06, H10 and H11) and OSCC patients (C02, C04, C06, C07 and C09) for sequencing that were available at the time. The healthy patients were selected and all drank alcohol which a common risk factor shared with the OSCC patients. The OSCC patients were selected to examine a variety of tumour locations within the oral cavity (retromolar region, tongue, floor of the mouth and maxilla).

The salivary EV RNA from the cohort of five patients with OSCC and three healthy controls was analysed by small RNA sequencing, which showed that no miRNAs were significantly downregulated, but 17 out of 1398 miRNAs were significantly upregulated in OSCC patient-derived salivary EVs compared with the healthy group (Figure 5.2). The upregulated miRNA were: miR-92a-3p, miR-21-5p, miR-1273h-3p, miR-181a-5p, miR-16-5p, miR-22-3p, miR-29a-3p, miR-23a-3p, miR-320a-3p, miR-3184-5p, miR-1290, miR-101-3p, miR-221-3p, miR-30d-5p, miR-186-5p, miR-1246, and miR-7847-3p. The largest fold change observed was for miR-1273h-3p (58.2-fold) and the smallest fold change was observed for miR-1290 (8.7-fold) (Table 5.3).

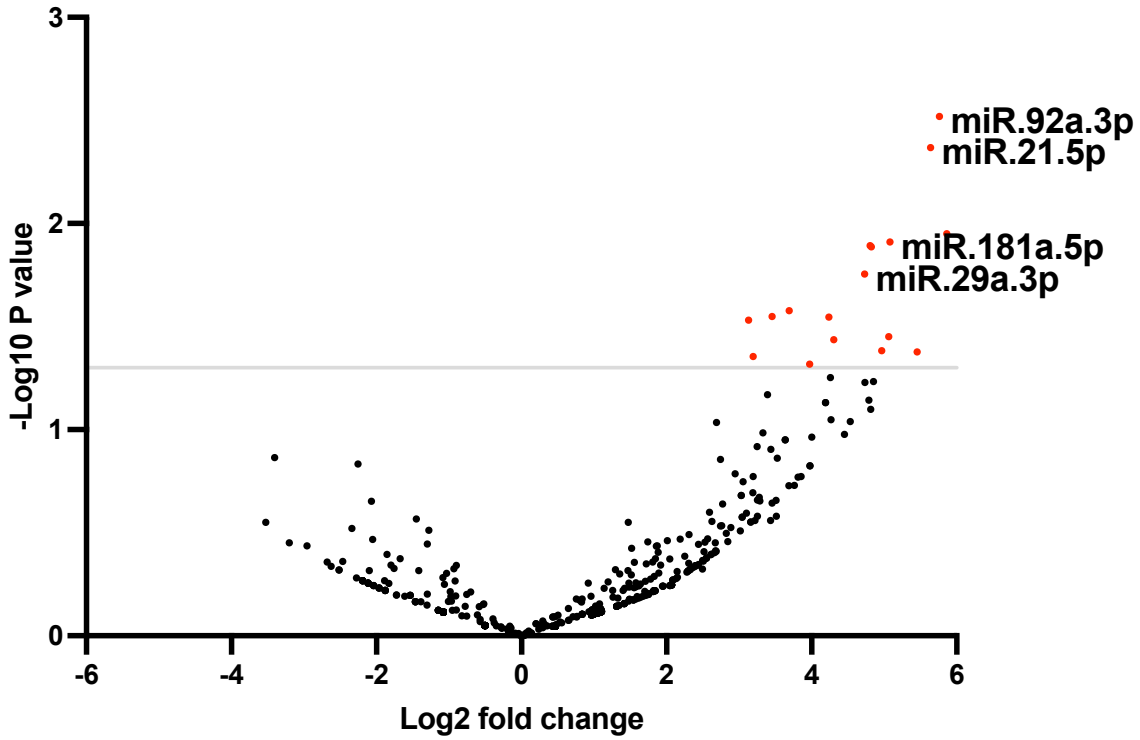

Figure 5. 2 Relative abundance of miRNA in salivary EVs from OSCC cancer patients compared to healthy patients. Cut offs for Log2 fold change was set at -1 and 1 (2-fold change in either direction) and -Log10 P value > 1.3 (P value <0.05), which is denoted by the grey line. MiRNA reaching the fold change and P value cut-offs are highlighted in red. Named microRNA were selected for validation by qRT-PCR.

Table 5. 3 Significantly upregulated miRNAs in OSCC salivary EVs. MiRNA are ordered by P value.

Name	Fold change	P value
miR-92a-3p	54.3	0.003
miR-21-5p	49.8	0.004
miR-1273h-3p	58.2	0.011
miR-181a-5p	33.8	0.012
miR-16-5p	28.0	0.013
miR-22-3p	28.3	0.013
miR-29a-3p	26.5	0.018
miR-23a-3p	12.9	0.026
miR-320a-3p	11.0	0.028
miR-3184-5p	18.9	0.028
miR-1290	8.7	0.029
miR-101-3p	33.4	0.035
miR-221-3p	19.8	0.037
miR-30d-5p	31.3	0.041
miR-186-5p	43.8	0.042
miR-1246	9.1	0.044
miR-7847-3p	15.7	0.048

5.3.2.2.1 Cluster analysis

Principal component analysis (PCA) was performed according to the EV miRNA expression data to highlight the degree of similarity between each sample by converting complex data into a 2D format to find patterns or clustering.

The PCA plot shows that healthy samples (H06, H10 and H11) cluster together (Figure 5.3). The cancer samples (C02, C04 and C09) are separated along PC1 and PC2 axes, exhibiting greater expression dissimilarity. However, C06 and C07 are clustered close together and adjacent to H06 (Figure 5.3). Both C06 and C07 were derived from saliva from patients with OSCC involving the floor of the mouth. Whereas sample C09 (OSCC of the maxilla), C02 (OSCC of the retromolar region), and C04 (OSCC of the tongue) were clustered separately (Figure 5.3).

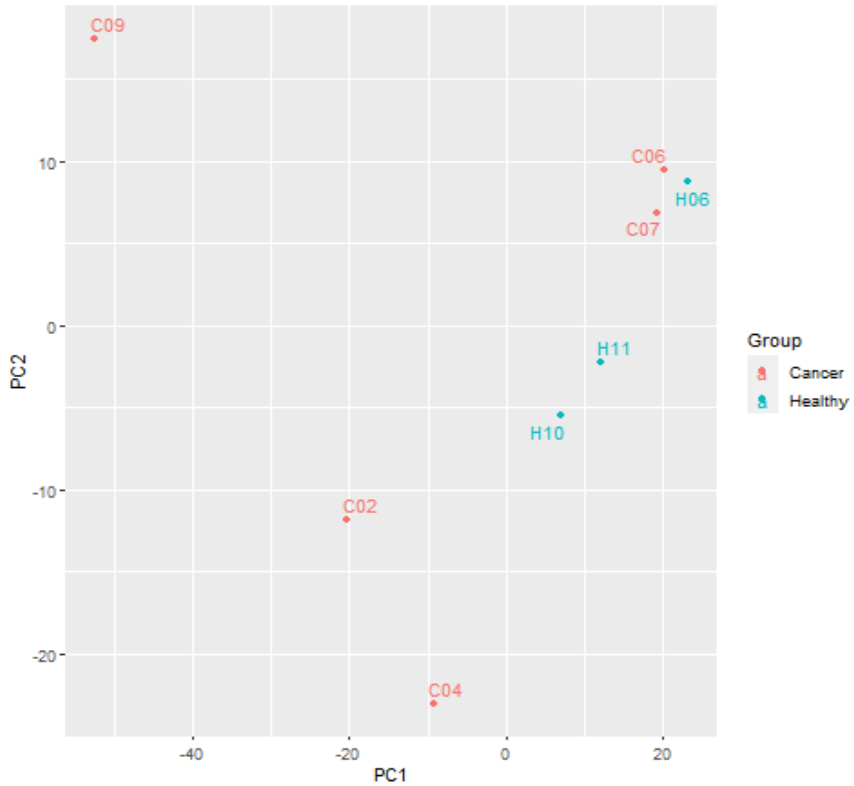

Figure 5. 3 Principal component analysis of EV miRNA abundance. Each dot represents an individual sample. Green dots represent the healthy samples and red dots represent the OSCC samples.

5.3.2.2.2 Visualising miRNA families

Here, we sought to visualise the entire EV miRNA dataset as a network using miRViz. MiRNAs are often redundant in the sense that many miRNAs can target the same mRNAs. As a result, miRNAs that are highly connected in the network might be interesting to study together. MiRViz (http://mirviz.prabi.fr/) is a webserver application designed to identify miRNA from the primary sequence and classify them into miRNA families, allowing direct visualization of miRNA families by connecting pairs of miRNA nodes that share the same seed sequence.

Differentially expressed miRNAs present in salivary EV from OSCC and healthy patients were visualised on a colour scale, with red nodes indicating upregulation and green nodes indicating downregulation. This analysis was based on Log2 fold change for the entire miRNA dataset and no P value cut-off was applied. MirViz allowed global inspection of the dataset and also closer inspection of individual miRNA families and nodes (Figure 5.4). In the human genome, the miR-181 family is composed of four different 5p mature forms, namely miR-181a-5p; miR-181b-5p; miR-181c-5p; and miR-181d-5p. miRViz showed that three members of the miR-181 family were upregulated in EV RNA from OSCC patients (Figure 5.4). The miR-29 family contains three members: miR-29a-3p, miR-29b-3p, and miR-29c-3p. Two of the miR-29 family and an associated miRNA (miR-6871-3p) were upregulated in OSCC derived EVs compared to healthy controls (Figure 5.4). Two members of the miR-23 family were also found to be upregulated in OSCC EV RNA samples (Figure 5.4). In contrast, despite miR-1273h-3p being the most upregulated miRNA in the small RNA sequencing dataset, no other related miRNA were increased (Figure 5.4).

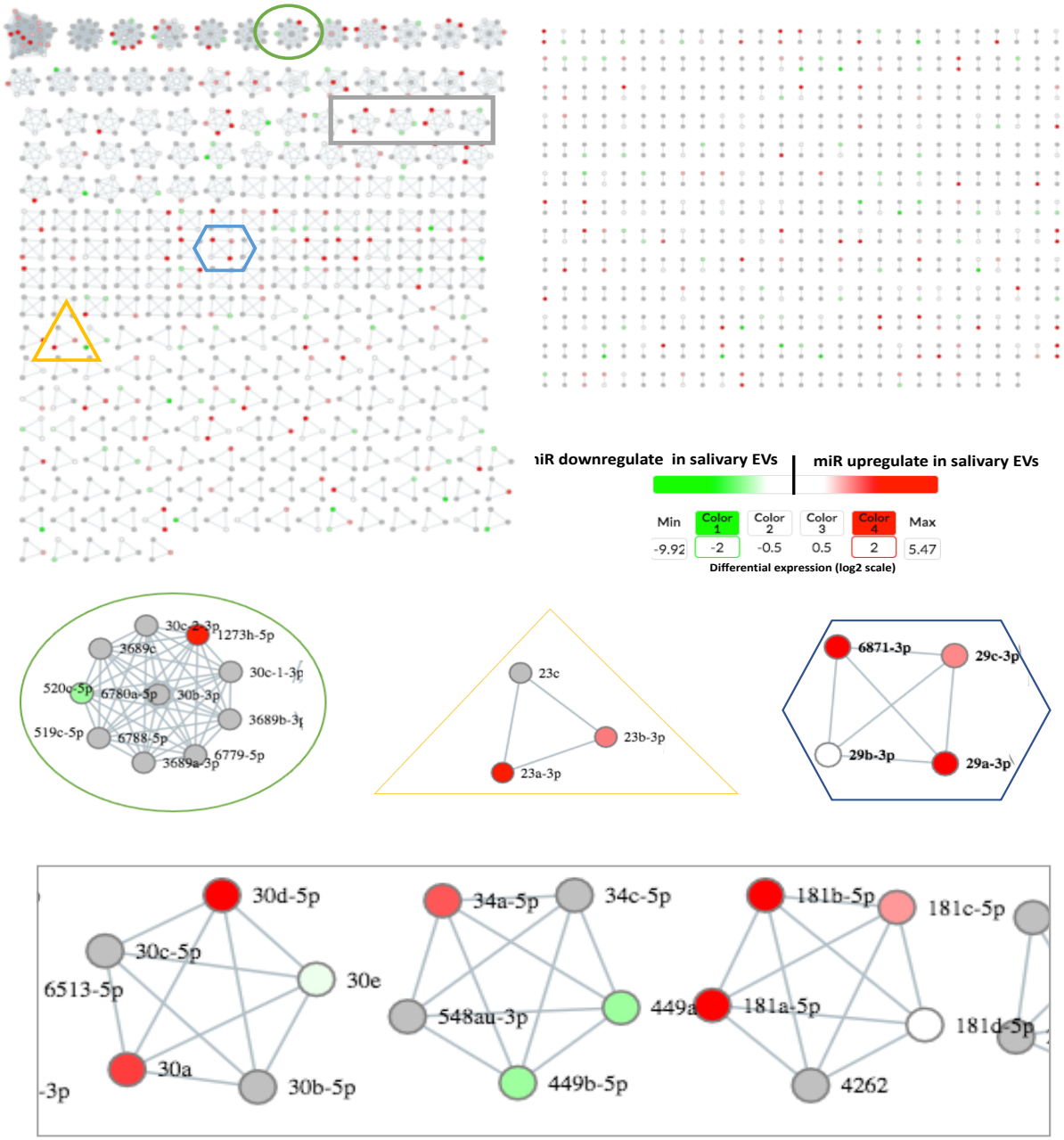

Figure 5. 4 Colour scale representation of the differentially expressed EV miRNAs grouped by seed sequence. Lines between individual nodes show similarity based on seed sequence. Red and green nodes correspond to miRNAs upregulated and downregulated in OSCC salivary EVs, respectively. The miRNA cluster in the black square corresponds to the miR-181 family, the purple hexagon corresponds to the miR-29 family, the green circle to the miR-1237 family, and the yellow triangular to the miR-23 family. Analysis performed and images generated by miRViz.

5.3.2.3 Validation of upregulated miRNAs by qRT-PCR

We next attempted to validate small RNA sequencing data by qRT-PCR. Four miRNAs were selected for validation (miR-21-5p, miR-29a-3p, miR-92a-3p and miR-181a-5p) from the list of significantly upregulated miRNA (Table 5.3) based on reports that they were upregulated in previous studies of OSCC. The small RNA sequencing data was inspected for miRNA present in equal quantities across all samples that could be used as an endogenous control, but no suitable candidates were found. Therefore qRT-PCR data is presented as Ct values, where a lower Ct value represents higher expression of the target miRNA.

All 21 samples that yielded RNA (n = 14 cancer patients and n = 7 healthy controls) were included in the qRT-PCR analysis. A comparison of cancer and healthy samples showed there was no statistically significant difference for any of the target miRNA (Figure 5.5). There was variation in Ct value between the groups and within each group. Apart from miR-29a-3p (where Ct values were more similar between groups), there was a trend that a proportion of cancer samples displayed higher expression (lower Ct value) for the target miRNA. However, due to the large amount of variation within the cancer group this did not reach statistical significance.

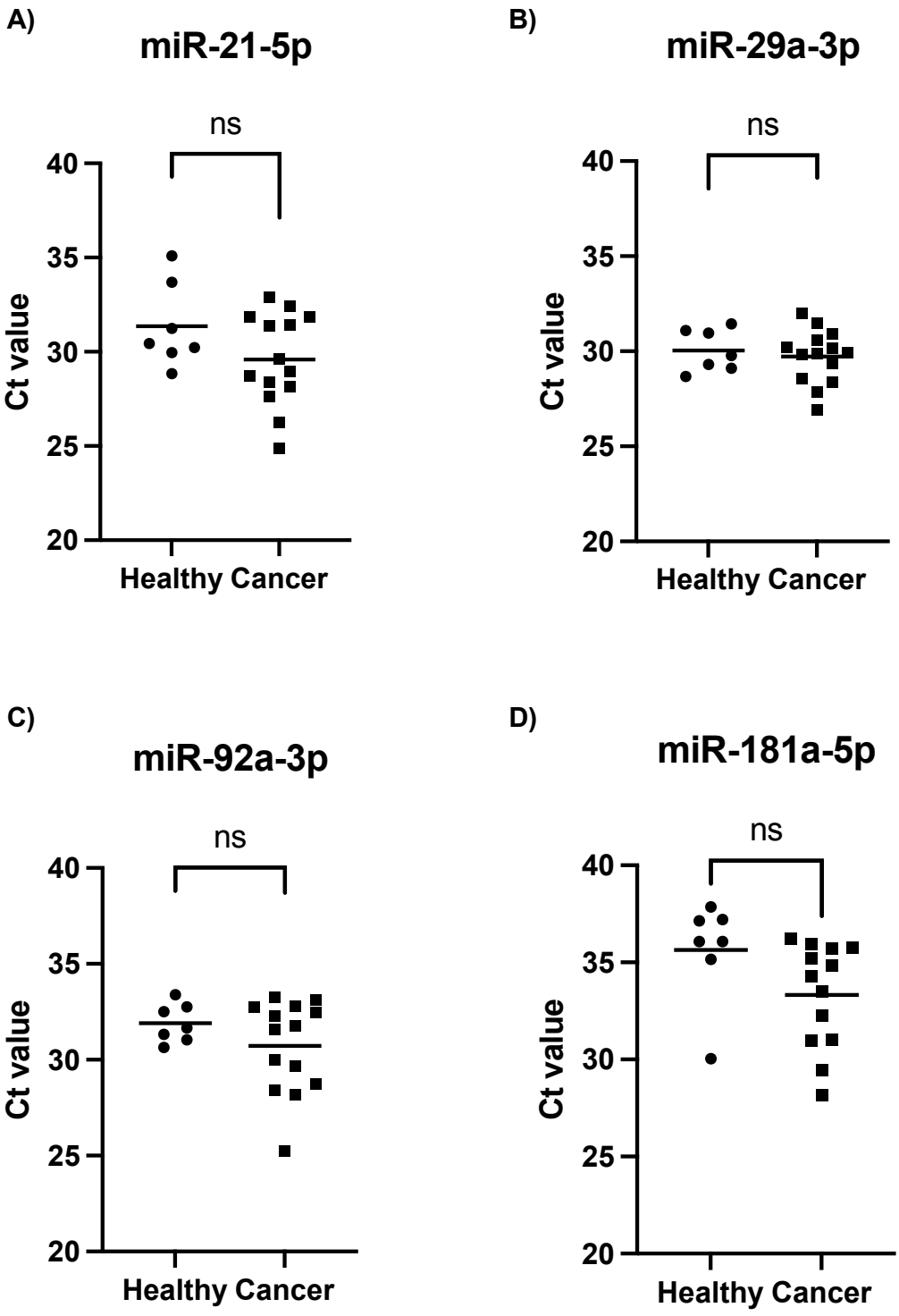

Figure 5. 5 Validation of small RNA sequencing by qRT-PCR. The study cohort of 14 cancer patients and 7 healthy controls were analysed. The Ct value of miRNA from cancer and a healthy control were plotted. An individual dot indicates one sample. P value > 0.05 by Student's t-test is considered not significant (ns).

5.4. Discussion

5.4.1 Integrity and quantity of RNA in salivary EVs

Due to low RNA amounts and a lack of standards, such as those developed for cellular RNA, measuring the quantity and quality of EV-associated RNA is challenging. This is true for EVs derived from *in vitro* cell cultures in general, but it is especially true for those derived from patient samples, where high sample quantities may be difficult to obtain. Many of them are caused by the fact that research involving EV-RNA often involves working with minimal amounts of RNA in comparison to the quantities seen in cells (Mateescu et al., 2017b). EV samples largely lack complete large and small ribosomal RNA subunits, in contrast to cellular RNA, where intact ribosomal RNA predominates in the pool of RNA. As a result, the amount of RNA needed for certain analytical techniques (such as sequencing, microarrays, or qRT-PCR) may differ from the guidelines for cellular RNA samples (Mateescu et al., 2017b).

There are numerous RNA detection methods for quantifying EV-RNA, with the Bioanalyzer being one of the most useful for determining total RNA content and length distribution. Some groups isolating EVs from fluids such as blood plasma or urine report the enrichment of small RNA species and absence of 18s and 28s (Huang et al., 2013). In another study, Bioanalyzer traces showed enrichment of small RNAs in EVs and plasma of patients with OSCC (Momen-Heravi and Bala, 2018b). Here, the Bioanalyzer traces showed salivary EVs were enriched with small RNA species with the absence of intact 18s and 28s rRNA, which is in agreement with previous reports (Wei et al., 2017; Eldh et al., 2012). We did not observe any difference in EV RNA Bioanalyzer profiles between the different groups. Overall, our total EV RNA profiles seemed to be consistent with those stated in the literature and were of sufficient quantity for small RNA sequencing.

5.4.2 Salivary EV miRNA biomarker profiles

Here we attempted to build on previous studies that have attempted to use EV RNA signatures as biomarkers for oral cancer. Previous studies had utilised techniques such as differential ultracentrifugation (Langevin et al., 2017; Farag et al., 2021) and precipitation (ExoQuick) (Byun et al., 2015; He et al., 2020) to enrich salivary EVs. However, these methods are not able to separate salivary EVs from other extracellular particles (Yuana et al., 2015; Zlotogorski-Hurvitz et al., 2015). In addition, methods such as UC can be time-consuming and

are not suitable for processing large numbers of clinical samples. Therefore, we previously optimised a Dynabead salivary EV immunocapture protocol (Chapter 4), which could be adapted to a high throughput diagnostic lab setting. We hypothesised that salivary EVs (captured using our Dynabead protocol) derived from OSCC patients contain oncogenic miRNAs that can be used as diagnostic biomarkers. Small RNA sequencing has advantages over microarray and qRT-PCR screening of miRNA because it offers high-throughput and unbiased analysis to discover low abundance and novel miRNA variants (Liu et al., 2011).

In our study, small RNA sequencing was performed on a cohort of 5 patients with OSCC cancer and 3 healthy controls, which identified 17 miRNA that were upregulated in OSCC samples. Many of these miRNAs had previously been linked to OSCC in previous studies (summarised in Table 5.4). Some of these miRNAs are discussed in detail below.

Table 5. 4 MiRNA that were upregulated in OSCC patients in previous studies.

Name	Sources	References
MiR-92a-3p	Serum	(MacLellan et al., 2012)
MiR-21-5p	Saliva/tissue	(Jadhav et al., 2022)
	Blood	(Ren et al., 2014)
	Plasma/tissue	(Schneider et al., 2018)
	OSCC tissue	(Hui et al., 2010b)
	EVs derived from oral cancer cell line	(Chen et al., 2019)
MiR-1246	EVs derived from oral cancer cell line	(Sakha et al., 2016)
	Salivary EVs	(He et al., 2020)
	OSCC tissue	(Liao et al., 2015)
Mi181a-5p	OSSC tissue	(Zheng et al., 2018)
	Tumour tissues/plasma	(Yang et al., 2011)
MiR-29a-3p	OSSC tissue	(Manikandan et al., 2016)
	EVs derived from oral cancer tissue	(Hulsmans and Holvoet, 2013)
	OSCC tissue EVs derived from oral cancer cell line/ Blood	(Cai et al., 2019)
MiR-1290	OSCC cell line	(Qin et al., 2019)
	OSCC Cell line	(Janiszewska et al., 2015)
	OSCC Tissue/cell line	(Chen et al., 2020b)
MiR-23a-3p	EVs derived from oral cancer cell line.	(Masaoka et al., 2021)
	EVs derived serum/OSCC tissue	(Bao et al., 2018)
MiR-186-5p	Plasma	(Summerer et al., 2015)
MiR-16-5p	OSCC cells/tissue	(Hui et al., 2010)

5.4.2.1 MiR-92a-3p

Previously miR-92a has been identified as an oncogenic member of the miR-17-92 family (Sandhu et al., 2013) and it has been shown to act on the proliferation of cancer cells and tumour growth, inhibit cell apoptosis and promote metastasis (Li et al., 2014). Yang et al. (2020) found enriched exosomal miR-92a-3p in the plasma of hepatocellular carcinoma patients with high-metastatic potential (Yang et al., 2020). Jinghua et al. showed that miR-92a-3p expression was enhanced in breast cancer tissues and cells (Jinghua et al., 2021).

Groups have identified upregulation of miR-92a-3p in biological fluids for example, MacLellan et al. (2012) found an upregulation of miR-92a-3p in the serum of HNSCC patients, Fassan et al. (2020) revealed miR-92a-3p as a biomarker that was over-expressed in the blood of precancerous lesions of esophageal adenocarcinoma compared to normal squamous esophageal mucosa and Shin et al. (2015) observed elevated levels of miR-92a-3p in the plasma of breast cancer patients compared with healthy individuals. In addition, up-regulation of miR-92a-3p has been reported in gastric cancer patients' sera (Li et al., 2017a). Overall, miR-92a-3p appears to be upregulated in biological fluid derived-exosomes. Progression of cancer appears to be a major function targeted by miR-92a-3p and may be responsible for development of cancer.

5.4.2.2 MiR-21-5p

MiR-21 is one of the most abundant and well-conserved miRNAs identified (Jenike and Halushka, 2021). It is overexpressed in a number of solid malignant tumours and has been shown to be a strong prognostic marker in head and neck cancer (Childs et al., 2009; Fu et al., 2011; Sannigrahi et al., 2018; Dioguardi et al., 2020). MiR-21 is a critical regulator of cell proliferation, migration, invasion, apoptosis, metastasis, and the epithelial to mesenchymal transition during cancer progression in a variety of cancers (Chan et al., 2005; Li et al., 2009; Hermansen et al., 2013; Cappellesso et al., 2014), and it has been postulated that miR-21 expression might indicate a worse prognosis (Asangani et al., 2008; Hwang et al., 2010).

Previous studies have demonstrated a statistically significant correlation between miR-21-5p expression in the saliva and tumour tissue of patients with OSCC with cervical lymph node metastasis with a diagnostic accuracy of 65% to 71.54% in saliva and 69% to 81.54% in tumour tissue (Jadhav et al., 2022). Higher levels of miR-21 expression have been shown in HNSCC tissue (Shen et al., 2022), and in tongue cancer have been linked to advanced

clinical stage, poor differentiation, and lymph node metastasis (Avissar et al., 2009; Ganci et al., 2016); increased expression of mi-21-5p in HNSCC tissue has also been shown (Shen et al., 2022). Another study found that miR-21 promotes oral tongue squamous cell carcinoma invasion via the Wnt/-catenin pathway by targeting DKK2 *in vitro* (Kawakita et al., 2014) while Zhang et al. showed exosomal delivery of miR-21-5p to human umbilical vein endothelial cells increased angiogenesis via inhibiting CXCL10 (Zhang et al., 2022). Chen et al. (2019) revealed that OSCC EVs are enriched with miR-21-5p and are associated with increased metastasis, stemness, chemoresistance, and poor survival in patients with OSCC (Chen et al., 2019).

Bodily-fluid-based miRNA studies have revealed higher expression of miR-21-5p in the blood of OSCC patients (Ren et al., 2014; Schneider et al., 2018). Furthermore, miR-21-5p expression in circulating exosomes was markedly higher in colorectal cancer patients than in healthy donors (He et al., 2021).

Overall, miR-21-5p is a critically important miRNA in the development of many cancers. It was shown to be up-regulated in a variety of cancers, mainly in the biological fluid of OSCC cancer.

5.4.2.3 MiR-181a-5p

MiR-181a-5p belongs to the miR-181 family, which plays an important role in malignant diseases (Zekri et al., 2018). It has been suggested that MiR-181a-5p acts as a tumour suppressor gene in many cancers (Shen et al., 2018), however, Zheng et al. (2018) found miR-181a-5p was significantly upregulated in OSCC tissue and was linked to tumour proliferation in a variety of cancers with roles in cell cycle, apoptosis, proliferation, migration, and invasion (Zheng et al., 2018). In addition, miR-181a-5p is widely known to be associated with the development and differentiation of blood vascular endothelial cells (Kazenwadel et al., 2010) and lymphocytes (Li et al., 2007). miR-181a-5p was found to be associated with lymph node metastasis and poor OSCC patient survival (Childs et al., 2009; Chang et al., 2013). Yang et al. (2011) discovered over-expression of miR-181 correlated with lymph-node metastasis of OSCC, vascular invasion, and poor survival. Up-regulation of miR-181 has been reported in OSCC transformation from dysplasia (leucoplakia) to invasive tumour (Liu et al., 2020).

MiRNA-181-5p was found to be overexpressed in the plasma exosomes of patients with thyroid cancer (Samsonov et al., 2016), colon cancer (Shtam et al., 2017) and lung cancer (Tian et al., 2017). Gao et al. (2014) found that miR-181-5p was highly expressed in the salivary supernatant of patients with pancreatic cancer (Gao et al., 2014). In addition, elevated expression of miR-181a was identified as a negative prognostic molecular marker in HNSCC (Jamali et al., 2015) in a meta-analysis of 21 studies involving 1,685 patients,.

Overall, miR-181a-5p plays a key role in the development of cancer and upregulation of miR-181a-5p has been identified in exosomes derived from biological fluid.

5.4.2.4 MiR-16-5p

MiR-16-5p has been shown to be a vital component of the intracellular miRNA regulatory network, causing an inhibitory effect on the growth and invasion of cancer, including breast cancer and osteosarcoma. Qu et al. (2017) showed overexpression of miR-16-5p contributes to growth inhibition *in vitro* and *in vivo*, cell apoptosis, and a decrease in the invasiove capacity of breast carcinoma cells (Qu et al., 2017). Gu et al. (2020) found that overexpression of miR-16-5p resulted in the inhibition of the proliferation, migration, and invasion of osteosarcoma cells (Gu et al., 2020).

MiR-16 has been reported to be one of the most stably expressed miRNAs in body fluids (Bryzgunova et al., 2016; Romani et al., 2021). Fan et al. showed overexpression of miR-16-5p in the serum of early breast cancer patients (Fan et al., 2018). In lung cancer patients, levels of miR-16-5p were elevated in the plasma of two subclasses of lung cancer, adenocarcinoma and squamous cell carcinoma, in comparison with healthy controls (Wang et al., 2018a). Furthermore, upregulated miR-16-5p was identified in tissue samples of HNSCC (Hui et al., 2010a). Overexpression in exosomes derived from the tissue of oesophageal squamous cell carcinoma has been shown by Chen et al. (2019).

Overall, miR-16-5p appears to inhibit the growth and metastasis of cancer and is overexpressed in biological fluids and tissue of a number of cancers.

5.4.2.5 MiR-22-3p

MiR-22 has been shown to have a significant impact on cancer phenotypes such as proliferation, cell cycle and apoptosis, invasion, and metastasis (Yang et al., 2015; Luo et al.,

2017). MiR-22 has also been shown to accelerate cell senescence, suppress energy metabolism and angiogenesis, and slow the EMT process in various cancers (Xu et al., 2011; Yamakuchi et al., 2011). The mechanisms of miR-22-induced tumour progression are complex (Landgraf et al., 2007) and may involve numerous regulated genes, such as PTEN, Sp1, SIRT-1, CD147, and E-cadherin (Luo et al., 2017; Dhar et al., 2017; Xia et al., 2017). Zuo et al. (2015) discovered overexpression of miR-22-3p markedly suppressed the proliferation, invasion, and migration of gastric cancer cells (Zuo et al., 2015). Thereby, miR-22 could play a tumour suppressor or oncogenic role in different tumour types (Nejati et al., 2021).

In miRNA-EVs studies, miR-22-3p has been detected as one of the top 20 most abundant miRs in plasma-derived EVs (Sundar et al., 2019). Petkevich et al. (2021) investigated non-exosomal and exosomal miRNA expression levels of miR-22-3p in blood plasma of liver cancer patients and showed that miR-22-3p was detected in both plasma amd plasma exsomes (Petkevich et al., 2021). Also, Naakka et al. (2022) found significant overexpression of miR-22-3p in tissue samples of mucoepidermoid carcinoma (Naakka et al., 2022). MiR-22-3p was highly up-regulated in cervical cancer tissues (Lv et al., 2018).

Generally, MiR-22-3p appears to have both tumour suppressor and oncogenic activities in several tumour types and has been shown to be overexpressed in biological samples of different cancers.

5.4.2.6 MiR-29a-3p

MiR-29a regulates several hallmarks of cancer, including cell growth, migration, and tumour formation. MiR-29a has recently been in the spotlight as a tumour oncogene that is frequently increased in cancers (Li et al., 2017c). Upregulation of miR-29a-3p is observed in OSCC-derived exosomes, promoting M2 subtype macrophage polarization, which subsequently promoted the proliferation and invasion of SCC-9 and CAL-27 cells (Cai et al., 2019). Overexpressed miR-29a-3p in exosomes was also demonstrated in ovarian cancer cell lines, which promoted ovarian cancer cell proliferation and immune escape and also correlated with poor prognosis of patients (Lu et al., 2021).

Focusing on the tight connection between miR-29 and the incidence and development of OSCC, miR-29 represents a miRNA family with three members, including miR-29a-3p, miR-29b-3p, and miR-29c-3p. A significant level of its expression was discovered in OSCC tissue (Manikandan et al., 2016). Also, Hulsmans and Holvoet, (2013) found that the

expression of miR-29a-3p was detected in exosomes secreted by tumour cells (Hulsmans and Holvoet, 2013).

Circulating levels of miR-29a-3p increased in exosomes derived from the plasma of lung cancer patients (Dinh et al., 2016). Li et al. (2020) found that the increased miR-29a-3p in serum-derived-exosomes plays a crucial role in hepatocellular carcinoma progression (Li et al., 2020). Overall, miR-29a-3p has been shown to mediate either tumour suppressive or oncogenic functions in distinct malignancies. It was upregulated in EVs derived from biological fluids.

5.4.2.7 MiR-23a-3p

MiR-23a is one of the most thoroughly investigated miRNAs in many forms of human cancer, and it has a variety of functions in tumour genesis, development, invasion, and metastasis (Wang et al., 2018b). Many studies have shown that miR-23a-3p is upregulated in a variety of cancers and is closely related to the development of cancer (Ma et al., 2022). Advances in cancer research have highlighted the cancer-promoting function of miR-23a in regulating cell proliferation, apoptosis, EMT and angiogenesis progress (Lee et al., 2020; Liu et al., 2016). High expression of miR-23a in tumour tissue was shown to be linked with advanced clinical stage and lymph node metastases in laryngeal carcinoma (Zhang et al., 2015). It has been reported, that miR-23a-3p promotes the development of prostate cancer (Wen et al., 2015b), gastric cancer (Liu et al., 2018) and gliomas (Hu et al., 2013). This research implies that miR-23a is important in terms of cancer stage, differentiation, and metastasis.

Masaoka et al. (2021) recognised upregulated miR-23a-3p in exosomal miRNAs in the OSCC-derived cell lines compared to human normal keratinocytes (Masaoka et al., 2021). Additionally, it has been noted that esophageal squamous cell carcinoma tissue has enhanced miR-23a-3p expression (Zhu et al., 2013). According to Ma et al., miR-23a expression was considerably greater in breast tumour tissues (Ma et al., 2017). Bao et al. found that miR-23a-3p expression was up-regulated in the tumour tissue of nasopharyngeal carcinoma (Bao et al., 2018)

In bodily-fluid-based miRNA studies, it has been shown that there is overexpression of miR-23a-3p in serum samples from patients with colon cancer (Jahid et al., 2012).

Generally, miR-23a-3p appears to be upregulated in serum and has a promoting role in several cancer types.

5.4.2.8 MiR-1290

MiR-1290 has been found in a variety of cancers, including colon, pancreatic, lung, and liver cancer; hence, its position as an oncomir is well established (Manikandan et al., 2016; Guz et al., 2022). Upregulation of miR-1290 was associated with clinicopathological characteristics and poor prognosis in OSCC patients and promoted cell metastasis and epithelial-mesenchymal transition (EMT) (Qin et al., 2019). Over-expression of miR-1290 has enhanced proliferation of lung adenocarcinoma cells and induced cell cycle progression and invasiveness (Xiao et al., 2018). All of these studies indicated that miR-1290 was a tumour promoter in some human cancers. Li and colleagues reported that patients with elevated circulating miR-1290 expression level had a poorer outcome after resection of their pancreatic cancer (Li et al., 2013). In addition, Mo and colleagues reported that high miR-1290 levels in lung carcinoma tissue and serum correlated with a poor prognosis (Mo et al., 2015).

Circulating miR-1290 is a novel and promising biomarker for the early detection of colorectal cancer as it is overexpressed in plasma derived exosomes (Ma et al., 2018). Furthermore, upregulation of exosomal miR-1290 was shown in the blood plasma of gastric cancer patients (Huang et al., 2019) and the serum of hepatocellular carcinoma (Wang et al., 2021). In addition, in previous studies, upregulation of miR-1290 has been identified in esophageal squamous cell carcinoma tissue (Xie et al., 2017), and laryngeal carcinoma cell lines (Janiszewska et al., 2015) and also in nasopharyngeal carcinoma tissue (Chen et al., 2020b).

Overall, miR-1290 appears to enhance the proliferation, migration, and invasiveness of many tumors, and it was upregulated in exosomal miRs of biological fluids.

5.4.2.9 MiR-1246

MiR-1246 has been found to exert oncogenic roles in oral, colorectal, breast, renal, laryngeal, pancreatic and ovarian cancers as well as melanoma and glioma. The expression of miR-1246 has shown also to be increased in OSCC tissues and a high level of miR-1246 was associated with tumour grade (Liao et al., 2015). Furthermore, miR-1246 has been identified

as a novel target of p53 (Liao et al., 2012). Sakha et al. (2016) have demonstrated miR-1246 in exosomes derived from oral cancer cell line induced a pro-metastatic phenotype, including increase cell motility and invasion through the regulation of DENND2D in oral squamous cell carcinoma (Sakha et al., 2016). Recently, miR-1246 was shown to have crucial roles in tumour initiation and metastasis (Kim et al., 2016; Zhang et al., 2016). Chen et al. reported that upregulation of serum miR-1246 expression could predict lymph node metastasis in patients with early-stage cervical squamous cell carcinoma (Chen et al., 2013).

He et al. (2020) discovered that miR-1246 was highly upregulated in salivary EVs from OSCC patients (He et al., 2020). Furthermore, Machida et al. (2016) found levels of miR-1246 in salivary exosomes were higher in pancreatic cancer patients than in healthy control participants (Machida et al., 2016). The miR-1246 biomarker contained in circulating exosomes has been well-evaluated as a biomarker for early detection of pancreatic cancer (Xu et al., 2017), breast cancer (Hannafon et al., 2016), prostate cancer (Bhagirath et al., 2018), and hepatocellular carcinoma (Wang et al., 2018c). The serum exosomal levels of miR-1246 were significantly higher in colorectal cancer (Ogata-Kawata et al., 2014).

Overall, MiR-1246 is widely regarded as an oncogenic miRNA in human cancers, and it was found to be upregulated in many EV derived from many biological fluids such as saliva.

5.4.2.10 MiR-186-5p

MiR-186 was documented as a tumor suppressor miRNA by targeting multiple oncogenes in the majority of studies (Xiang et al., 2020), while conflicting reports verified miR-186 as an oncomir (Xiang et al., 2020). Alterations of miR-186 expression were demonstrated in numerous cancer tissues or cell lines, and it has been shown to play a vital role in oncogenesis, invasion, metastasis, apoptosis, and drug resistance (Xiang et al., 2020). One report showed the levels of miR-186 were increased in metastatic prostate cancer cells (Jones et al., 2018). However, Chen and Zhang (2022) found that overexpression of miR-186-5p suppressed the proliferation and migration of OSCC cells and tissue (Chen and Zhang, 2022). Summerer et al. (2015) identified an upregulation of miR-186-5p in the plasma of HNSCC patients (Summerer et al., 2015). A study reported that miR-186-5p was overexpressed in not only tumour tissues and blood, but also urine from bladder cancer patients (He et al., 2017).

Islam et al. (2017) revealed that miR-186 was significantly upregulated in colorectal cancer tissues and cells.

On the basis of the identified functions, it could be concluded that the altered expression of miR-186 might also play a critical part in oral carcinogenesis and prognosis.

5.4.2.11 MiR-320a-3p

MiR-320 has been shown to be an oncogenic miRNA in breast cancer, brain tumours, and biliary tract cancer (Yang et al., 2014), but in gastric cancer, colon cancer, ovarian cancer, esophageal cancer, and clear cell renal cell carcinoma it is reported to be a tumor suppressor (Gutschner et al., 2013; Zhao et al., 2014; Serguienko et al., 2015). MiR-320a has different expression levels and roles in multiple malignancies (Peng et al., 2021). Notably, miR-320a was identified as a metastatic suppressor in colorectal cancer and high expression of miR-320a-3p in stage II tumours was associated with better disease-free survival in colorectal cancer patients (Schepeler et al., 2008). Hence, miR-320a is an important suppressive miRNA in colorectal cancer development and metastasis.

In bodily-fluid-based EV-miRNA studies, miR-320a-3p was upregulated in serum exosomes of hepatocellular carcinoma (Wen et al., 2015a). Navarro et al. (2019) reported upregulated expression of miR-320a-3p in the plasma of pancreatic cancer patients. Similarly, miR-320a-3p has been shown to be significantly increased in the plasma of osteosarcoma patients (Lian et al., 2015). Overall, miR-320a-3p appears to be upregulated in biological fluids and has a dual oncogenic and suppressor effect in different cancers.

5.3 Clustering

OSCC is a group of diverse heterogeneous cancers that arise from a variety of anatomical sites and are associated with a variety of risk factors related to both behaviour and genetic background, making OSCC one of the most complex cancers (Marcu and Yeoh, 2009). Many studies have shown that the clinical features of OSCC, as well as prognosis and treatment, vary with different anatomical locations and stages (Manikandan et al., 2016). This emphasises the importance of using large patient cohorts for profiling to illustrate the diversity among the different OSCCs (Lajer et al., 2011). In addition, there is a considerable variation in the miRNA profiles across different studies of head and neck cancer, which might

reflect differences in stage, grade and sampling from multiple anatomical sites (Lajer et al., 2011).

Priciple component analysis (PCA) has been used to obtain an overview of the differences and similarities of the tissue miRNA expression profile among different cancers and normal patient groups (Manikandan et al., 2016). Manikandan et al. (2016) showed that clustering of OSCC samples with moderately or well differentiated histology was scattered in all quadrants of a PCA plot, demonstrating the molecular heterogeneity of OSCC. They suggested that different staging did not correlate with miRNA expression and also suggested the need for more studies with a larger cohorts to uncover patterns (Manikandan et al., 2016). Also, Nunvar et al. (2021) revealed that miRNA expression pattern of head and neck cancer samples was most significantly associated with anatomical location (Nunvar et al., 2021). Some studies have shown overlapping clustering of normal controls and cancer samples (Lajer et al., 2011), whilst others show distinct clustering between groups (Schneider et al., 2018).

The present study showed by PCA that healthy samples clustered together, whereas cancer samples were more scattered. However, CO6 and CO7 (both floor of the mouth) clustered together and closer to the healthy controls than the other cancer samples. It has been suggested that anatomical sites might play a dominant role in changing the miRNA expression patterns (Nunvar et al., 2021). Another explanation could be the embryological origin of the tissues that the tumours are derived from. The mucosa of the oral cavity, such as the anterior two thirds of the tongue and all of the hard palate, has an ectodermic origin, whereas the mucosa of the floor of the mouth is of endodermic origin (Hughes and Chuong, 2003). Alternatively, C06 and C07 could cluster with the healthy samples because those tumours were smaller and released fewer extracellular vesicles into the saliva. However, we have no data relating to the size of the tumours and so this remains speculative. If we had a larger cohort of cancer patients the samples could have been analysed based on anatomical location or other relevant clinical parameters (tumour size, grade etc), but this was not possible with the number of patients recruited and the data collected.

5.4 Validation by RT-QPCR

Validation of small RNA sequencing data was attempted by qRT-PCR analysis of four miRNAs (miR-21-5p, miR-29a-3p, miR-92a-3p and miR-181a-5p) that were significantly

upregulated. However, none of these miRNAs were significantly upregulated based on the qRT-PCR data.

Many studies have reported that some miRNAs fail as cancer biomarkers in validation studies (Sapre et al., 2014). Our finding was consistent with the Koppers-Lalic study (2016), where miRNAs were validated by qRT-PCR in prostate cancer associated miRNAs in urinary EVs. miR-21, miR-375, and miR-204 failed to robustly discriminate for disease in a validation study with qRT-PCR-detection of mature miRNA sequences. They confirmed that detection of mature miRNA sequences using qRT-PCR does not always correspond with RNA sequencing data. The majority of the previous studies have not included validation of significant miRNAs and hence they lack the ability to demonstrate reproducibility of data (Mahn et al., 2011; Moltzahn et al., 2011; Shen et al., 2012).

Many studies have reported that in order to achieve accurate, reproducible, and biologically relevant miRNA qRT-PCR data, experimental variation (technical and biological) should be corrected for by using reference genes (Chang et al., 2010). However, use of unreliable reference genes for normalisation may lead to inaccurate quantitation of miRNAs of interest (Davoren et al., 2008; Peltier and Latham, 2008).

The lack of statistical significance in our qRT-PCR data could be due to inaccurate quantification of EV RNA, which is reflected in the large variation of Ct values. As mentioned previously, quantification of EV RNA is challenging. A previous study has reported that variability observed in Ct value between samples are commonly due to PCR efficiency, starting material, pipetting errors and biological variation (Ruiz-Villalba et al., 2021). Normally a references gene would also be used to correct for any differences in RNA input (Ruiz-Villalba et al., 2021). Gouin et al. (2017) have proved that identification of reference genes for EVs remains challenging, especially as the source of the EVs becomes more complex such as those isolated from bodily fluids (Gouin et al., 2017). Also, it has been noted that identified reference genes for specific EV populations, including liver carcinoma (Li and Li, 2015), colorectal cancer (Chiba et al., 2012) and cerebrospinal fluid (Zanello and SB, 2014), in the majority of these studies, one reference gene is not sufficient but rather the mean of multiple genes is necessary. One alternative to using reference genes is absolute quantification of copy number (Bracht et al., 2021). However, this would still rely on accurate quantification of EV RNA to produce reliable data.

5.5 Conclusion

In this study, we demonstrated the possibility of using Dynabead immunocapture to isolate salivary EVs from OSCC patient samples for downstream biomarker screening. Using a small RNA sequencing approach we identified 17 miRNA were significantly enriched in salivary EVs from OSCC patients. Many of these miRNAs have been previously identified as potential biomarkers for OSCC, which is encouraging. Despite the difficulty with validating these miRNA by traditional qRT-PCR, it would be worth evaluating other methods for validation, such as absolute quantification of copy number.

Chapter Six

6. Final discussion

6.1 The challenges of using saliva in EV biomarker studies

EVs have been isolated from diverse biofluids including blood (Caby et al., 2005), urine (Bryzgunova et al., 2016), breast milk (Lässer et al., 2011a), cerebrospinal (Akers et al., 2015), ascitic fluids (Cappellesso et al., 2014), bronchoalveolar lavage (Wahlund et al., 2017), semen (Madison et al., 2017), tears (Grigor'eva et al., 2016) and saliva (Ogawa et al., 2008). The viscosity of these fluids, as well as their fat and protein content, are highly variable, which may affect EV purity and yield (Mallia et al., 2020). Standardized pre-analytical steps are critically important for the successful experimental outcome of any experiment and to minimize artefacts in EV-analysis, particularly when EVs are derived from complex body fluids such as saliva (Witwer et al., 2013b). Saliva is produced by three major paired glands (the sublingual, submandibular, and parotid) and additional smaller glands lining the oral cavity. The salivary glands secrete fluid transported from serum as well as tissues surrounding the glands. Other human saliva constituents are derived from the oral mucosa, periodontium, and the oral microbiome (Caporossi et al., 2010).

For the last two decades, saliva has been used as a non-invasive source of biomarkers, which can be collected easily and could be a substitute for blood. However, when compared to other biofluids, saliva has limitations and challenges, including composition variability and high viscosity due to mucins (Humphrey and Williamson, 2001), and the presence of α-amylase, which masks low-abundance salivary protein biomarkers that have the potential to be useful for diagnosis (Deutsch et al., 2008). In addition, low RNA abundance, small sample volumes, highly fragmented RNA, and high abundance of bacterial content, all create challenges for downstream RNA sequencing assays (Faur et al., 2021).

Successful measurement of salivary analytes such as EV-associated miRNA requires optimal collection, processing, and storage procedures (Witwer et al., 2013b). In previous studies, a number of factors were considered relevant to the collection of saliva samples such as: location, sampling time, instruction to participants and the method of collection, while various levels of salivary constituents could be produced via the distinctive glands (Zakowski and Bruns, 1985). EV production and composition would possibly vary between each salivary gland (Ogawa et al., 2008 Lässer et al., 2011a; Gallo et al., 2012). In addition, the composition of whole saliva may be influenced by extraneous factors which may limit its use as a

biomarker, such as social habits (e.g. smoking, drinking alcohol and diet). Therefore it is common to ask saliva donors to abstain from smoking or consuming food or drink (except water) for an hour before the sample is taken (Iwai et al., 2016; Gai et al., 2018). Oral hygiene could also impact the composition of saliva at the time of collection (Pernot et al., 2014). Furthermore, the content of saliva may alter with response to stress due to physical activity (Simkin et al., 2012). Hence, donors also need to refrain from vigorous physical exercise before the collection of saliva (Rohleder and Nater, 2009).

There are two main ways to collect saliva: unstimulated or stimulated saliva, which varies from study to study. Unstimulated saliva is collected by draining or drooling, spitting, suction, or swabbing. Stimulated saliva is collected by providing the patients with a stimulant agent, such as citric acid, paraffin, or a gum base (Yakob et al., 2014). Unstimulated saliva collection is the most common method and was used prior to EV isolation in many studies due to its ability to reflect the status of the body (Liangsupree et al., 2021). Collection of stimulated saliva samples is significantly faster and more comfortable for the patient than collection of unstimulated saliva, which may make it preferable for screening of larger populations. However, downstream analysis has revealed dilution of the components in stimulated saliva (Yakob et al., 2014; Schafer et al., 2014). With stimulated collection, saliva is obtained primarily from the parotid gland, whereas unstimulated (resting) saliva is produced primarily by the submandibular gland, with minor contributions from the parotid and sublingual glands (Dodds et al., 2005; de Almeida et al., 2008). Thus, unstimulated saliva is more favourable for biomarker discovery and has been used in most diagnostic studies (Principe et al., 2013).

In the current study, we followed the accepted best practice for saliva collection (passive drool) based on the factors described above. Healthy volunteers (donating saliva for the initial optimisation experiments) and healthy control patients (attending the Charles Clifford Dental Hospital for routine procedures) were asked to refrain from eating or drinking anything for at least one hour prior to the collection of saliva. Collection of saliva from OSCC patients was standardised as the samples were collected on the morning of surgery, therefore the patients were all nil by mouth. However, this presented an additional challenge. Patients often struggled to produce a large volume of saliva due to dry mouth, which was likely a result of fasting and pre-surgery anxiety. We currently do not know how this might have affected the composition of the collected saliva and the EVs contained within.

The MISEV 2018 guidelines emphasise the importance of biological fluid storage in the validation stages of any EV biomarker (Thery et al., 2018). Storage of biological fluids before EV isolation may affect EV characteristics, including stability, number of particles, aggregation, and function (Muller et al., 2014; Bæk et al., 2016). According to literature searches, there is no definite consensus about the storage of fluids because the effects of storage appear to vary with sample source (Théry et al., 2018a; Clayton et al., 2019). In the current study we showed the signal intensity of salivary EV luminal protein TSG101 was more stable without saliva storage suggesting that fresh saliva is more suitable for biomarker studies. However, the analysis of TSG101 is a surrogate marker for EV RNA cargo and our goal was to extract RNA from salivary EVs for downstream analysis. Therefore, measurement of RNA cargo in response to storage of saliva prior to EV isolation could have provided valuable information. As mentioned previously, however, accurate quantification of EV RNA provides its own challenges.

Further studies by using TEM to detect intact EVs are required to fully elucidate the effect of saliva storage on EV biomarkers. Standardisation of sample collection and storage conditions are vital to allow comparison between studies conducted by different research groups.

6.2 Technical challenges of working with extracellular vesicles

Due to the pervasive participation of EVs in a variety of cellular functions and their potential utility in translational disease applications, including screening, diagnosis, and treatment development, there has been a rapid increase in scientific interest in EVs (Wiklander et al., 2019). Well-defined, intact, and high-purity EV isolation is necessary to accomplish these requirements. The development of EV subclass research has been limited by the fact that EVs are heterogeneous and current EV isolation techniques are unable to discriminate between different EV subpopulations (Willms et al., 2018). Traditional EV purification approaches rely on EV biophysical parameters (such as size and density), which might cause the co-purification of other extracellular particles with similar qualities (Cocozza et al., 2020a). Exomeres (Karimi et al., 2018b; Mathieu et al., 2019) and lipoproteins (high density lipoprotein, low density lipoprotein) are lipid-based but non-vesicular components of these particles, the latter was discovered, and its size range is comparable to that of small EVs

(Scheinberg et al., 1954). Other protein complexes discovered in EV preparations include argonautes, nucleosomes, and vault particles, none of which are associated with EVs (Jeppesen et al., 2019).

In the current study, we assessed the suitability of three commonly used isolation techniques, ultracentrifugation, SEC and Dynabead immunocapture, to isolate salivary EVs (Figure 6.1). According to literature, one of the limitations in using ultracentrifugation for isolation of EVs is co-precipitation of protein aggregates and nucleosome fragments, which can lead to decreased sample purity and may affect downstream analysis (Furi et al., 2017). In the current study, we showed that UC was not suitable to isolate salivary EVs, due to the production of a sticky pellet, making it difficult to resuspend, suggesting particle aggregation. Despite abandoning the use of UC early in the project, it would have been useful to conduct some preliminary analysis on the resulting pellets. Western blotting of pellet lysates could have revealed the identity of any co-isolated particles.

Preservation of vesicle integrity and prevention of EV aggregation are notable advantages of using SEC (Liangsupree et al., 2021). We showed that this technique was effective at fractionating EVs and soluble factors, as demonstrated by separation of EVs and α-amylase (one of the most abundant proteins in saliva). However, our data suggested the EV rich fractions were contaminated with other particles such as vault particles (MVP) and high-density lipoprotein particles (APOA). Whilst the detection of these proteins by western blotting suggests the presence of the mentioned particles, additional analysis by electron microscopy could have demonstrated the presence of these particles in SEC isolates.

Finally, we evaluated Dynabead immunocapture. This approach is a quick, simple, and effective EV purification technique that is more feasible in clinical applications (Chen et al., 2022). In the current study, we demonstrated that immunocapture was more efficient than SEC at enriching $CD63^+$ $CD9^+$ $CD81^+$ EVs. Immunocapture offers unique advantages for the recovery of EVs from complex and viscous fluids in terms of increased efficiency and specificity of capture, integrity, and selective origin of isolated vesicles. The immunocapture approach has the disadvantage of only picking particular EV populations that are positive for the selection markers, despite the fact that it has been demonstrated to produce purer EVs than traditional methods (Chen et al., 2020). Therefore, EVs without surface identifiers or with different surface markers won't be purified. Furthermore, EVs may display distinct markers when separated from different biological sources (Alvarez et al., 2012; Ji et al., 2013),

or when cells are in a different state (for example, stressed vs. actively developing), which may induce changes in EV yield and EV content across experiments (Rutter and Innes, 2017). In addition, due to the heterogeneity of tumours, it is possible that not all cells within a tumour may express the target antigen, such that EVs derived from those cells will not be captured (O'Loghlen, 2018). Furthermore, antigen modulation can occur as cancers advance, so that a tumour may initially produce the target antigen but that expression may decrease with time or the antigenic epitope may be blocked or masked (Beatty and Gladney, 2015). It would have been valuable to characterise what was present in the unbound fraction from Dynabead isolations. Other common EV markers (such as EpCAM) could have been probed by western blotting to determine if there were additional populations that had not bound to the beads. Additionally, probing for markers of other extracellular particles such as vaults (MVP) and lipoprotein particles (ApoA) could indicate their successful separation from EVs.

More advanced isolation approaches have been devised in order to address the aforementioned problems and enable improved isolation of EV subtypes. These innovative methods utilise size, charge, and affinity to better resolve and produce the separation of various EV subpopulations, producing EVs with the purity and integrity required for the intended applications (Liangsupree et al., 2021). For instance, field-flow fractionation (FFF), which separates macromolecules depending on their diffusion coefficients, is the most popular of the modern size-based isolation techniques (Sitar et al., 2015). Besides, FFF might also give an accurate assessment of EV size distribution, size morphology, and aggregation states when used in combination with light scattering detectors (Liangsupree et al., 2021). However, even this method falls short of completely separating distinct EV subtypes, necessitating further concentrating processes and minimal loading amounts to prevent self-association and overloading effects (Liangsupree et al., 2021).

A strategy to accomplish EV separation with better purity and specificity than any currently existing approach might be produced by the combination of isolation techniques based on several biophysical features, even if it is impossible to completely purify EVs from other entities (Multia et al., 2020). For instance, utilising immunoaffinity chromatography in combination with the FFF approach to separate EV subpopulations produced EVs that were extremely pure, intact, and concentrated (Multia et al., 2020). The EV yield is heavily

dependent on the selective markers and size ranges, and it also has the drawback of requiring extremely specialised equipment and trained operators. Electric field-induced release and measurement, a recently created revolutionary diagnostic tool, can detect EV RNA directly with only 40 µL of bodily fluid (Wei et al., 2014; Tu et al., 2015; Pu et al., 2016). More research and deployment of saliva-based point-of-care technology may enable improved rapid clinical treatment.

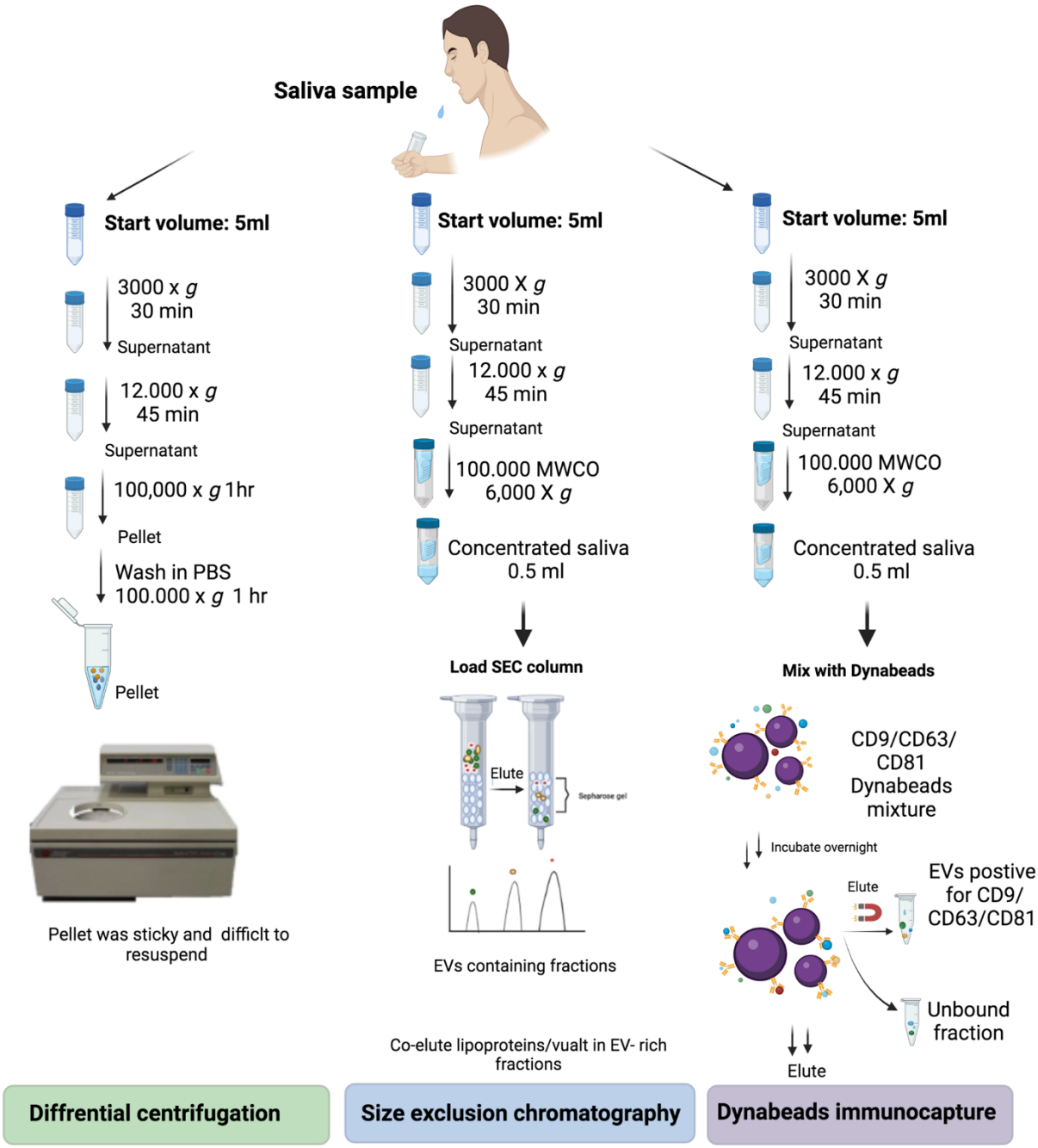

Figure 6. 1 Diagram of the EV isolation techniques used in this study and their outcomes. In this study, EVs from saliva were isolated by three techniques: DC, SEC, and Dynabead immunocapture. In which, purification of DC-derived pellets resulted in EVs with particle aggregation and sticky pellet, SEC co-purified vault particles (MVP) and lipoprotein (ApoAI) with EVs. However, capturing from concentrated saliva using Dynabeads led to improved enrichment of CD9+CD63+CD81+ EVs, compared to SEC.

6.3 Can small RNA in salivary EVs be used as a biomarker signature for oral cancer?

MiRNAs are small (19–22 nucleotides long) non-coding RNAs that interact with the RNA-induced silencing complex (RISC), binding to the 3'UTR of mRNA to induce either mRNA degradation or mRNA translation inhibition (Mohr and Mott, 2015). MiRNA influence vital processes such as cell cycle, apoptosis, proliferation, and differentiation by regulating target gene expression (Guo et al., 2014), and any dysregulation of miRNA expression contributes to cancer tumorigenesis, such as invasion, angiogenesis, progression, metastasis, and chemoresistance (Valadi et al., 2007c).

MiRNA were identified in salivary EVs, which have attracted the interest of many researchers due to their potential as a source of biomarkers in the diagnosis of oral cancer and oral disease (Faur et al., 2021). Sampling salivary EVs offers a promising and alternative way to measure disease in real-time (Sui et al., 2021). The salivary EV cargo originates from the lavage process and blood stream, from where EVs passively pass into saliva through gingival sulcus fluid and are also secreted from the oral epithelial layer. As a consequence, the concentration of EV miRNA in saliva is higher than in blood and act as mediators of intercellular signalling through RNA and functional protein exchange (Sui et al., 2021), in which they are protected by an EV lipid barrier against enzymatic degradation. As a result, they are more stable in the extracellular environment compared with cell-free miRNA. Thus, the accuracy of EV miRNA-based cancer detection increases, making them attractive diagnostic tools for clinical application (Ingenito et al., 2019).

Based on differences between the salivary EVs originating from healthy subjects compared to patients with cancer, it is possible that disease-specific EVs may differ in functional properties (Nonaka and Wong, 2017a). It has been shown that the amount and content of salivary EVs are highly variable even in patients with the same tumour types and stages (Nonaka and Wong, 2018). The increased number of EVs, as well as the change in shape and expression of EV cargo such as RNA, were most noticeable in cancer-derived EVs (Rak and Guha, 2012). RNA species such as miRNAs are the best-studied and annotated, particularly regarding current EV research. According to a search of Google Scholar/Pubmed between 2010-2021, five articles were included for salivary EV-miRNA, four focused on oral cancer and one on premalignant lesion detection (Byun et al., 2015; Langevin et al., 2017; Gai et al., 2018; He et al., 2020; Farag et al., 2021). These studies analysed twelve salivary EV miRNA, presenting different techniques of EV and miRNA identification for HNSCC detection and all

five articles presented a low bias risk and high applicability (Faur et al., 2021). The current study was built on these previous studies that have attempted to use EV RNA signatures as biomarkers for oral cancer.

In the studies evaluated, the size of salivary samples utilised for EV miRNA detection varied. Gallo et al. demonstrated that a small amount of saliva contains enough EV miRNA for proper analysis (Gallo et al., 2012). EV miRNA expression was analysed by various methods, which could cause heterogeneous results. The main miRNA profiling methods are next-generation sequencing, miRNA microarray analysis, qRT-PCR and digital PCR (dPCR) (Yoshizawa and Wong, 2013). Small RNA sequencing has advantages over microarray and qRT-PCR screening of miRNA because it offers high-throughput and unbiased analysis to discover low abundance and novel miRNA variants (Liu et al., 2011). However, disadvantages include high cost and complicated data manipulation is required for analysis (Nonaka and Wong, 2018).

Complications of miRNA-based cancer detection can be related to other factors, such as lifestyle (smoking), inflammation, and the ageing process, which may alter the miRNA expression and further interfere with the cancer diagnosis process (Takahashi et al., 2013). For example, alcohol consumption induces changes in EV characteristics (He et al., 2020). This is particularly relevant to our study as alcohol is a major risk factor for developing OSCC. As can be seen in the clinical information gathered from our OSCC cohort, the majority consume alcohol (in combination with smoking). It is challenging to find healthy controls with an alcohol and smoking consumption similar to the OSCC group. Some miRNA (e.g. miR-24-3p) are expressed differently in older people compared to younger people (He et al., 2020). Lack of a standardised technique will result in reduced concordance between results and, moreover, insufficient laboratory validation (Gallo et al., 2012). MiRNAs have been shown to degrade at various rates in various fluids. For instance, miR-124a is rapidly reduced in saliva samples (less than 10% detectable after 3 min) in comparison to miR-191 (about 30% detectable after 30 min) (Park et al., 2009b; Fălămaş et al., 2020). MiRNA degradation rates are likely related to if they are free in solution, part of a protein complex or shielded within an EV membrane.

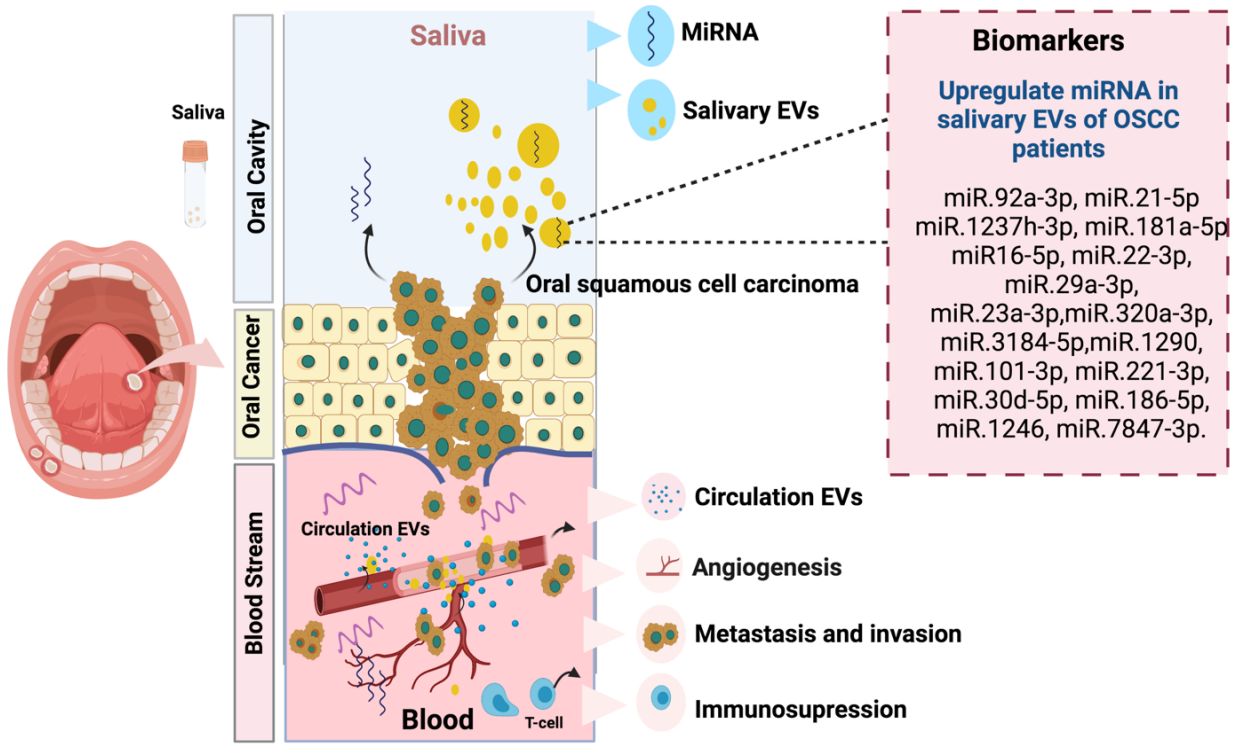

Figure 6. 2 Salivary EVs as a source of miRNA biomarkers for OSCC diagnosis.

6.4. Limitations, future work and conclusion

6.4.1 Limitations

The findings of this study have to be seen in light of some limitations that need to be addressed. In particular, the COVID-19 pandemic disrupted many plans. We were unable to achieve several of the project's intended objectives due to lockdown of our laboratories from March 2020 to August 2020 and limited lab access with a maximum of 10 hours per week from August 2020 to April 2021. Because of the reduction in conventional dental care at the Charles Clifford Dental Hospital, recruiting healthy patients became exceptionally challenging. In addition, the number of OSCC surgical resections was decreased. For over a year, no patients (healthy or cancer) were enrolled in this study. Certain experiments were delayed or interrupted as a result of this. We needed to have a sufficient sample size in order to draw valid results from small RNA sequencing analysis. However, time restraints meant that this analysis was conducted on a smaller number of samples than intended. As mentioned in the previous studies, the composition of salivary EV miRNAs in healthy subjects may vary with external risk factors such as HPV infection, alcohol consumption, cigarette smoking, etc. The diagnostic bias caused by the patients' exposure to the above-mentioned risk factors should be considered. There are limitations regarding clinical samples, such as large variation between subjects in terms of sex, age, drinking and smoking status, where controls and OSCC samples were not completely matched. Also, insufficient patient data was collected (e.g. tumour size, grade, etc.). We also chose to conduct small RNA sequencing on a cohort of patient samples with OSCC affecting different anatomical locations in the oral cavity. In hindsight, it might have been advantageous to focus on a particular OSCC location such as the tongue. The other patient samples could have then been included in qRT-PCR validation. However, due to COVID related impacts on the project, there was not sufficient time to recruit all the patients before selecting samples for small RNA sequencing.

Characterisation of salivary EVs from cancer patients and comparison with healthy controls (NTA, TEM and western blotting) would have been desirable. This would have allowed detection in changes in size, concentration, morphology and protein markers of EVs. However, due to the limited sample volumes obtained it was not possible to conduct this additional analysis. The priority was to obtain sufficient RNA for downstream analysis.

6.4.2 Future work

The immediate priority for further work should be to validate the current small RNA sequencing data using alternative methods such as digital PCR for absolute copy number quantification. Future small RNA sequencing studies should include a larger cohort size, which would allow better matching of controls and OSCC samples. Analysis of a larger cohort would also allow samples to be grouped based on anatomical location of the tumour. In addition, the inclusion of more OSCC samples would reveal if the miRNA profiles of OSCC EVs could continue to be differentiated into specific groups by unbiased PCA clustering. More clinical information such as tumour grade and size, etc., should be collected, which may help with setting cut-offs for samples to be included in initial biomarker discovery.

Future studies may evaluate if the upregulated miRNA identified in salivary EVs are upregulated in OSCC cell lines by using qRT-PCR. This would allow experiments to be performed to determine if these miRNA have any functional effects *in vitro*. If the function of these miRNA in the tumour microenvironment can be elucidated, they may prove to be novel therapeutic targets as well as diagnostic biomarkers.

Several studies suggest morphological differences between EVs isolated from healthy individuals and patients with OSCC. Future work by using (NTA,TEM and WB) should aim to further characterise these differences and to identify specific surface markers, which might inform immunoaffinity EV isolation strategies. Further characterization of the unbound fraction from Dynabead preparations is required to determine if there are EVs and/or other unbound extracellular particles present.

6.4.3 Conclusion

Currently, a complete clinical oral examination is used to detect OSCC, along with a biopsy for a histological investigation if an abnormal region is found. For histological confirmation of the oral cancer, the site from which the biopsy sample is collected is essential. However, because malignant and precancerous lesions don't occur uniformly, choosing the best place can be challenging. This study provides further evidence that saliva presents a rich and accessible source of biomarkers for cancer diagnosis. Isolation of salivary EVs represents

a way to enrich intact biomarkers (protected by an EV membrane) that might otherwise be masked by higher abundance molecules or may be degraded in whole saliva.

Overall, this was the first study to use Dynabead immunocapture to enrich salivary EVs for downstream small RNA sequencing analysis. This strategy could one day be applied to an automated diagnostic lab setting. The miRNAs contained within salivary EVs are promising biomarkers for OSCC. They can be detected in relatively small amounts of saliva, which is necessary for a rapid and non-invasive cancer diagnostic test. Once appropriate RNA biomarkers are validated they could be used in the detection of premalignant lesions and early-stage oral cancers, which would significantly improve patient outcomes. Such biomarkers could also be used to predict and monitor responses to therapy.

10. References

ABELS, E. R. & BREAKEFIELD, X. O. 2016. Introduction to extracellular vesicles: biogenesis, RNA cargo selection, content, release, and uptake. *Cellular and molecular neurobiology,* 36**,** 301-312.

ACCOMANDO, W. P., WIENCKE, J. K., HOUSEMAN, E. A., BUTLER, R. A., ZHENG, S., NELSON, H. H. & KELSEY, K. T. 2012. Decreased NK Cells in Patients with Head and Neck Cancer Determined in Archival DNA. *Clinical Cancer Research,* 18**,** 6147-6154.

ADMYRE, C., JOHANSSON, S. M., QAZI, K. R., FILÉN, J.-J., LAHESMAA, R., NORMAN, M., NEVE, E. P., SCHEYNIUS, A. & GABRIELSSON, S. 2007. Exosomes with immune modulatory features are present in human breast milk. *The Journal of immunology,* 179**,** 1969-1978.

AGARWAL, R., CHAUDHARY, M., BOHRA, S. & BAJAJ, S. 2016. Evaluation of natural killer cell (CD57) as a prognostic marker in oral squamous cell carcinoma: An immunohistochemistry study. *Journal of oral and maxillofacial pathology: JOMFP,* 20**,** 173.

AKERS, J. C., RAMAKRISHNAN, V., KIM, R., PHILLIPS, S., KAIMAL, V., MAO, Y., HUA, W., YANG, I., FU, C.-C. & NOLAN, J. 2015. miRNA contents of cerebrospinal fluid extracellular vesicles in glioblastoma patients. *Journal of Neuro-oncology,* 123**,** 205-216.

AL-RAWI, N. & ATIYAH, K. 2008. Assessment of salivary lipid profiles in patients with ischemic stroke and patients at risk of having stroke among Iraqi sample. *Internet Journal of Third World Medicine,* 7.

AL-TARAWNEH, S. K., BORDER, M. B., DIBBLE, C. F. & BENCHARIT, S. 2011. Defining salivary biomarkers using mass spectrometry-based proteomics: a systematic review. *Omics: a journal of integrative biology,* 15**,** 353-361.

ALAMELDIN, S., COSTINA, V., ABDEL-BASET, H. A., NITSCHKE, K., NUHN, P., NEUMAIER, M. & HEDTKE, M. 2021. Coupling size exclusion chromatography to ultracentrifugation improves detection of exosomal proteins from human plasma by LC-MS. *Practical Laboratory Medicine,* 26**,** e00241.

ALFAROUK, K. O., MUDDATHIR, A. K. & SHAYOUB, M. E. 2011. Tumor acidity as evolutionary spite. *Cancers,* 3**,** 408-414.

ALVAREZ, M. L., KHOSROHEIDARI, M., RAVI, R. K. & DISTEFANO, J. K. 2012. Comparison of protein, microRNA, and mRNA yields using different methods of urinary exosome isolation for the discovery of kidney disease biomarkers. *Kidney international,* 82**,** 1024-1032.

ÁLVAREZ-TEIJEIRO, S., GARCÍA-INCLÁN, C., VILLARONGA, M., CASADO, P., HERMIDA-PRADO, F., GRANDA-DÍAZ, R., RODRIGO, J. P., CALVO, F., DEL-RÍO-IBISATE, N. & GANDARILLAS, A. 2018. Factors secreted by cancer-associated fibroblasts that sustain cancer stem properties in head and neck squamous carcinoma cells as potential therapeutic targets. *Cancers,* 10**,** 334.

AMADO, F. M. L., VITORINO, R. M. P., DOMINGUES, P. M. D. N., LOBO, M. J. C. & DUARTE, J. A. R. 2014. Analysis of the human saliva proteome. *http://dx.doi.org/10.1586/14789450.2.4.521*.

ANDERSON, H. C. 1969. Vesicles associated with calcification in the matrix of epiphyseal cartilage. *The Journal of cell biology,* 41**,** 59-72.

ANDREOLA, G., RIVOLTINI, L., CASTELLI, C., HUBER, V., PEREGO, P., DEHO, P., SQUARCINA, P., ACCORNERO, P., LOZUPONE, F. & LUGINI, L. 2002. Induction of lymphocyte apoptosis by tumor cell secretion of FasL-bearing microvesicles. *The Journal of experimental medicine,* 195**,** 1303-1316.

ANDREU, Z. & YÁÑEZ-MÓ, M. 2014. Tetraspanins in extracellular vesicle formation and function. *Frontiers in immunology,* 5**,** 442.

ANTONYAK, M. A., LI, B., BOROUGHS, L. K., JOHNSON, J. L., DRUSO, J. E., BRYANT, K. L., HOLOWKA, D. A. & CERIONE, R. A. 2011. Cancer cell-derived microvesicles induce transformation by transferring tissue transglutaminase and fibronectin to recipient cells. *Proceedings of the National Academy of Sciences,* 108**,** 4852-4857.

ARAB, T., RAFFO-ROMERO, A., VAN CAMP, C., LEMAIRE, Q., LE MARREC-CROQ, F., DRAGO, F., ABOULOUARD, S., SLOMIANNY, C., LACOSTE, A. & GUIGON, I. 2019. Proteomic characterisation of leech microglia extracellular vesicles (EVs): comparison between differential ultracentrifugation and Optiprep™ density gradient isolation. *Journal of extracellular vesicles,* 8**,** 1603048.

ARGIRION, I., ZARINS, K. R., DEFEVER, K., SUWANRUNGRUANG, K., CHANG, J. T., PONGNIKORN, D., CHITAPANARUX, I., SRIPLUNG, H., VATANASAPT, P. & ROZEK, L. S. 2019. Temporal changes in head and neck cancer incidence in Thailand suggest changing oropharyngeal epidemiology in the region. *Journal of Global Oncology,* 5**,** 1-11.

ASANGANI, I. A., RASHEED, S. A., NIKOLOVA, D., LEUPOLD, J., COLBURN, N., POST, S. & ALLGAYER, H. 2008. MicroRNA-21 (miR-21) post-transcriptionally downregulates tumor suppressor Pdcd4 and stimulates invasion, intravasation and metastasis in colorectal cancer. *Oncogene,* 27**,** 2128-2136.

ASEF, A., MORTAZ, E., JAMAATI, H. & VELAYATI, A. 2018. Immunologic role of extracellular vesicles and exosomes in the pathogenesis of cystic fibrosis. *Tanaffos,* 17**,** 66.

AVISSAR, M., MCCLEAN, M. D., KELSEY, K. T. & MARSIT, C. J. 2009. MicroRNA expression in head and neck cancer associates with alcohol consumption and survival. *Carcinogenesis,* 30**,** 2059-2063.

AYERS, L., KOHLER, M., HARRISON, P., SARGENT, I., DRAGOVIC, R., SCHAAP, M., NIEUWLAND, R., BROOKS, S. A. & FERRY, B. 2011. Measurement of circulating cell-derived microparticles by flow cytometry: sources of variability within the assay. *Thrombosis research,* 127**,** 370-377.

BÆK, R., SØNDERGAARD, E. K., VARMING, K. & JØRGENSEN, M. M. 2016. The impact of various preanalytical treatments on the phenotype of small extracellular vesicles in blood analyzed by protein microarray. *Journal of Immunological Methods,* 438**,** 11-20.

BAIG, M. S., ROY, A., RAJPOOT, S., LIU, D., SAVAI, R., BANERJEE, S., KAWADA, M., FAISAL, S. M., SALUJA, R. & SAQIB, U. 2020. Tumor-derived exosomes in the regulation of macrophage polarization. *Inflammation Research,* 69**,** 435-451.

BALAJ, L., LESSARD, R., DAI, L., CHO, Y.-J., POMEROY, S. L., BREAKEFIELD, X. O. & SKOG, J. 2011. Tumour microvesicles contain retrotransposon elements and amplified oncogene sequences. *Nature communications,* 2**,** 1-9.

BALDINI, C., GIUSTI, L., CIREGIA, F., DA VALLE, Y., GIACOMELLI, C., DONADIO, E., SERNISSI, F., BAZZICHI, L., GIANNACCINI, G. & BOMBARDIERI, S. 2011. Proteomic analysis of saliva: a unique tool to distinguish primary Sjögren's syndrome from secondary Sjögren's syndrome and other sicca syndromes. *Arthritis research & therapy,* 13**,** 1-16.

BAO, L., YOU, B., SHI, S., SHAN, Y., ZHANG, Q., YUE, H., ZHANG, J., ZHANG, W., SHI, Y., LIU, Y., WANG, X., LIU, D. & YOU, Y. 2018. Metastasis-associated miR-23a from nasopharyngeal carcinoma-derived exosomes mediates angiogenesis by repressing a novel target gene TSGA10. *Oncogene,* 37**,** 2873-2889.

BEATTY, G. L. & GLADNEY, W. L. 2015. Immune escape mechanisms as a guide for cancer immunotherapy. *Clin Cancer Res,* 21**,** 687-92.

BEBELMAN, M. P., SMIT, M. J., PEGTEL, D. M. & BAGLIO, S. R. 2018. Biogenesis and function of extracellular vesicles in cancer. *Pharmacology & therapeutics,* 188**,** 1-11.

BECKER, A., THAKUR, B. K., WEISS, J. M., KIM, H. S., PEINADO, H. & LYDEN, D. 2016. Extracellular vesicles in cancer: cell-to-cell mediators of metastasis. *Cancer cell,* 30**,** 836-848.

BELLO, I. O., VERED, M., DAYAN, D., DOBRIYAN, A., YAHALOM, R., ALANEN, K., NIEMINEN, P., KANTOLA, S., LÄÄRÄ, E. & SALO, T. 2011. Cancer-associated fibroblasts, a parameter of the tumor microenvironment, overcomes carcinoma-associated parameters in the prognosis of patients with mobile tongue cancer. *Oral oncology,* 47**,** 33-38.

BENZ JR, E. W. & MOSES, H. L. 1974. Brief Communication: Small, Virus-Like Particles Detected in Bovine Sera by Electron Microscopy. *Journal of the National Cancer Institute,* 52**,** 1931-1934.

BHAGIRATH, D., YANG, T. L., BUCAY, N., SEKHON, K., MAJID, S., SHAHRYARI, V., DAHIYA, R., TANAKA, Y. & SAINI, S. 2018. microRNA-1246 Is an Exosomal Biomarker for Aggressive Prostate CancerExosomal microRNA in Aggressive Prostate Cancer. *Cancer research,* 78**,** 1833-1844.

BHOME, R., DEL VECCHIO, F., LEE, G.-H., BULLOCK, M. D., PRIMROSE, J. N., SAYAN, A. E. & MIRNEZAMI, A. H. 2018. Exosomal microRNAs (exomiRs): Small molecules with a big role in cancer. *Cancer letters,* 420**,** 228-235.

BLATT, S., KRÜGER, M., ZIEBART, T., SAGHEB, K., SCHIEGNITZ, E., GOETZE, E., AL-NAWAS, B. & PABST, A. M. 2017. Biomarkers in diagnosis and therapy of oral squamous cell carcinoma: a review of the literature. *Journal of Cranio-Maxillofacial Surgery,* 45**,** 722-730.

BÖING, A. N., VAN DER POL, E., GROOTEMAAT, A. E., COUMANS, F. A., STURK, A. & NIEUWLAND, R. 2014. Single-step isolation of extracellular vesicles by size-exclusion chromatography. *Journal of extracellular vesicles,* 3**,** 23430.

BORDER, M. B., SCHWARTZ, S., CARLSON, J., DIBBLE, C. F., KOHLTFARBER, H., OFFENBACHER, S., BUSE, J. B. & BENCHARIT, S. 2012. Exploring salivary proteomes in edentulous patients with type 2 diabetes. *Molecular BioSystems,* 8**,** 1304-1310.

BOSE, A., CHAKRABORTY, T., CHAKRABORTY, K., PAL, S. & BARAL, R. 2008. Dysregulation in immune functions is reflected in tumor cell cytotoxicity by peripheral blood mononuclear cells from head and neck squamous cell carcinoma patients. *Cancer Immunity Archive,* 8.

BOUKOURIS, S. & MATHIVANAN, S. 2015. Exosomes in bodily fluids are a highly stable resource of disease biomarkers. *Proteomics–Clinical Applications,* 9**,** 358-367.

BRACHT, J. W. P., GIMENEZ-CAPITAN, A., HUANG, C.-Y., POTIE, N., PEDRAZ-VALDUNCIEL, C., WARREN, S., ROSELL, R. & MOLINA-VILA, M. A. 2021. Analysis of extracellular vesicle mRNA derived from plasma using the nCounter platform. *Scientific Reports,* 11.

BRAY, F., FERLAY, J., SOERJOMATARAM, I., SIEGEL, R. L., TORRE, L. A. & JEMAL, A. 2018. Global cancer statistics 2018: GLOBOCAN estimates of incidence and mortality worldwide for 36 cancers in 185 countries. *CA: a cancer journal for clinicians,* 68**,** 394-424.

BRENNAN, K., MARTIN, K., FITZGERALD, S. P., O'SULLIVAN, J., WU, Y., BLANCO, A., RICHARDSON, C. & MC GEE, M. M. 2020. A comparison of methods for the isolation and separation of extracellular vesicles from protein and lipid particles in human serum. *Scientific Reports,* 10.

BRYZGUNOVA, O. E., ZARIPOV, M. M., SKVORTSOVA, T. E., LEKCHNOV, E. A., GRIGOR'EVA, A. E., ZAPOROZHCHENKO, I. A., MOROZKIN, E. S., RYABCHIKOVA, E. I., YURCHENKO, Y. B. & VOITSITSKIY, V. E. 2016. Comparative study of extracellular vesicles from the urine of healthy individuals and prostate cancer patients. *PLoS One,* 11**,** e0157566.

BRZOZOWSKI, J. S., BOND, D. R., JANKOWSKI, H., GOLDIE, B. J., BURCHELL, R., NAUDIN, C., SMITH, N. D., SCARLETT, C. J., LARSEN, M. R. & DUN, M. D. 2018. Extracellular vesicles with altered tetraspanin CD9 and CD151 levels confer increased prostate cell motility and invasion. *Scientific reports,* 8**,** 1-13.

BUSCHOW, S. I., NOLTE-'T HOEN, E. N., VAN NIEL, G., POLS, M. S., TEN BROEKE, T., LAUWEN, M., OSSENDORP, F., MELIEF, C. J., RAPOSO, G. & WUBBOLTS, R. 2009. MHC II in dendritic cells is targeted to lysosomes or T cell-induced exosomes via distinct multivesicular body pathways. Traffic, 10, 1528-1542.

Burke, J.M., Kelenis, D.P., Kincaid, R.P. and Sullivan, C.S., 2014. A central role for the primary microRNA stem in guiding the position and efficiency of Drosha processing of a viral pri miRNA. Rna, 20(7), pp.1068-1077.

BYUN, J. S., HONG, S. H., CHOI, J. K., JUNG, J. K. & LEE, H. J. 2015. Diagnostic profiling of salivary exosomal micro RNA s in oral lichen planus patients. *Oral Diseases,* 21**,** 987-993.

CABY, M.-P., LANKAR, D., VINCENDEAU-SCHERRER, C., RAPOSO, G. & BONNEROT, C. 2005. Exosomal-like vesicles are present in human blood plasma. *International immunology,* 17**,** 879-887.

CAI, J., QIAO, B., GAO, N., LIN, N. & HE, W. 2019. Oral squamous cell carcinoma-derived exosomes promote M2 subtype macrophage polarization mediated by exosome-enclosed miR-29a-3p. *American Journal of Physiology-Cell Physiology,* 316**,** C731-C740.

CALDER, P. C. & YAQOOB, P. 2007. Lipid rafts—composition, characterization, and controversies. *The Journal of nutrition,* 137**,** 545-547.

Cancer Research UK (2018) Head and neck cancers incidence statistics | Cancer Research UK. Available at: https://www.cancerresearchuk.org/health-professional/cancer-statistics/statistics-by- cancer-type/head-and-neck-cancers/incidence (Accessed: 31 August 2021).

Cancer Research UK (2020) Head and neck cancers incidence statistics | Cancer Research UK. Available at: https://www.cancerresearchuk.org/health-professional/cancer-statistics/statistics-by- cancer-type/head-and-neck-cancers/incidence#ref-2 (Accessed: 31 August 2021).

CAO, Z., WU, Y., LIU, G., JIANG, Y., WANG, X., WANG, Z. & FENG, T. 2019. α-Synuclein in salivary extracellular vesicles as a potential biomarker of Parkinson's disease. *Neuroscience letters,* 696**,** 114-120.

CAPOROSSI, L., SANTORO, A. & PAPALEO, B. 2010. Saliva as an analytical matrix: state of the art and application for biomonitoring. *Biomarkers,* 15**,** 475-487.

CAPPELLESSO, R., TINAZZI, A., GIURICI, T., SIMONATO, F., GUZZARDO, V., VENTURA, L., CRESCENZI, M., CHIARELLI, S. & FASSINA, A. 2014. Programmed cell death 4 and micro RNA 21 inverse expression is maintained in cells and exosomes from ovarian serous carcinoma effusions. *Cancer cytopathology,* 122**,** 685-693.

CASTELLANA, D., ZOBAIRI, F., MARTINEZ, M. C., PANARO, M. A., MITOLO, V., FREYSSINET, J.-M. & KUNZELMANN, C. 2009. Membrane microvesicles as actors in the establishment of a favorable prostatic tumoral niche: a role for activated fibroblasts and CX3CL1-CX3CR1 axis. *Cancer research,* 69**,** 785-793.

CHAN, J. A., KRICHEVSKY, A. M. & KOSIK, K. S. 2005. MicroRNA-21 is an antiapoptotic factor in human glioblastoma cells. *Cancer research,* 65**,** 6029-6033.

CHANG, C.-C., YANG, Y.-J., LI, Y.-J., CHEN, S.-T., LIN, B.-R., WU, T.-S., LIN, S.-K., KUO, M. Y.-P. & TAN, C.-T. 2013. MicroRNA-17/20a functions to inhibit cell migration and can be used a prognostic marker in oral squamous cell carcinoma. *Oral oncology,* 49**,** 923-931.

CHANG, K. H., MESTDAGH, P., VANDESOMPELE, J., KERIN, M. J. & MILLER, N. 2010. MicroRNA expression profiling to identify and validate reference genes for relative quantification in colorectal cancer. *BMC Cancer,* 10**,** 173.

CHARGAFF, E. & WEST, R. 1946. The biological significance of the thromboplastic protein of blood. *J Biol Chem,* 166**,** 189-197.

CHATURVEDI, P., KALANI, A., MEDINA, I., FAMILTSEVA, A. & TYAGI, S. C. 2015. Cardiosome mediated regulation of MMP9 in diabetic heart: role of mir29b and mir455 in exercise. *J Cell Mol Med,* 19**,** 2153-61.

CHEN, J., LI, P., ZHANG, T., XU, Z., HUANG, X., WANG, R. & DU, L. 2022. Review on strategies and technologies for exosome isolation and purification. *Frontiers in Bioengineering and Biotechnology,* 9**,** 811971.

CHEN, J., YAO, D., LI, Y., CHEN, H., HE, C., DING, N., LU, Y., OU, T., ZHAO, S., LI, L. & LONG, F. 2013. Serum microRNA expression levels can predict lymph node metastasis in patients with early-stage cervical squamous cell carcinoma. *International Journal of Molecular Medicine,* 32**,** 557-567.

CHEN, J.-H., WU, A. T. H., BAMODU, O. A., YADAV, V. K., CHAO, T.-Y., TZENG, Y.-M., MUKHOPADHYAY, D., HSIAO, M. & LEE, J.-C. 2019. Ovatodiolide Suppresses Oral Cancer Malignancy by Down-Regulating Exosomal Mir-21/STAT3/β-Catenin Cargo and Preventing Oncogenic Transformation of Normal Gingival Fibroblasts. *Cancers,* 12**,** 56.

CHEN, M. & ZHANG, J. 2022. miR-186-5p inhibits the progression of oral squamous cell carcinoma by targeting ITGA6 to impair the activity of the PI3K/AKT pathway. *J Oral Pathol Med,* 51**,** 322-331.

CHEN, R., LU, X., LI, Z., SUN, Y., HE, Z. & LI, X. 2020a. Dihydroartemisinin prevents progression and metastasis of head and neck squamous cell carcinoma by inhibiting polarization of macrophages in tumor microenvironment. *OncoTargets and therapy,* 13**,** 3375.

CHEN, X., HUANG, Y., SHI, D., NIE, C., LUO, Y., GUO, L., ZOU, Y. & XIE, C. 2020b. LncRNA ZNF667-AS1 promotes ABLIM1 expression by adsorbing microRNA-1290 to suppress nasopharyngeal carcinoma cell progression. *OncoTargets and therapy,* 13**,** 4397.

CHENG, J., NONAKA, T. & WONG, D. T. 2019. Salivary exosomes as nanocarriers for cancer biomarker delivery. *Materials,* 12**,** 654.

CHIABOTTO, G., GAI, C., DEREGIBUS, M. C. & CAMUSSI, G. 2019. Salivary extracellular vesicle-associated exRNA as cancer biomarker. *Cancers,* 11**,** 891.

CHIBA, M., KIMURA, M. & ASARI, S. 2012. Exosomes secreted from human colorectal cancer cell lines contain mRNAs, microRNAs and natural antisense RNAs, that can transfer into the human hepatoma HepG2 and lung cancer A549 cell lines. *Oncology reports,* 28**,** 1551-1558.

CHILDS, G., FAZZARI, M., KUNG, G., KAWACHI, N., BRANDWEIN-GENSLER, M., MCLEMORE, M., CHEN, Q., BURK, R. D., SMITH, R. V. & PRYSTOWSKY, M. B. 2009. Low-level expression

of microRNAs let-7d and miR-205 are prognostic markers of head and neck squamous cell carcinoma. *The American journal of pathology,* 174**,** 736-745.

CHOI, D., LEE, T. H., SPINELLI, C., CHENNAKRISHNAIAH, S., D'ASTI, E. & RAK, J. Extracellular vesicle communication pathways as regulatory targets of oncogenic transformation. Seminars in cell & developmental biology, 2017. Elsevier, 11-22.

CHRISTIANSON, H. C., SVENSSON, K. J., VAN KUPPEVELT, T. H., LI, J.-P. & BELTING, M. 2013. Cancer cell exosomes depend on cell-surface heparan sulfate proteoglycans for their internalization and functional activity. *Proceedings of the National Academy of Sciences,* 110**,** 17380-17385.

CHUO, S. T.-Y., CHIEN, J. C.-Y. & LAI, C. P.-K. 2018. Imaging extracellular vesicles: current and emerging methods. *Journal of biomedical science,* 25**,** 1-10.

CLAYTON, A., BOILARD, E., BUZAS, E. I., CHENG, L., FALCÓN-PEREZ, J. M., GARDINER, C., GUSTAFSON, D., GUALERZI, A., HENDRIX, A. & HOFFMAN, A. 2019. Considerations towards a roadmap for collection, handling and storage of blood extracellular vesicles. *Journal of extracellular vesicles,* 8**,** 1647027.

CLAYTON, A. & MASON, M. D. 2009. Exosomes in tumour immunity. *Current oncology,* 16**,** 46-49.

CLAYTON, A., MITCHELL, J. P., MASON, M. D. & TABI, Z. 2007. Human tumor-derived exosomes selectively impair lymphocyte responses to interleukin-2. *Cancer research,* 67**,** 7458-7466.

COCOZZA, F., GRISARD, E., MARTIN-JAULAR, L., MATHIEU, M. & THÉRY, C. 2020. SnapShot: extracellular vesicles. *Cell,* 182**,** 262-262. e1.

COCUCCI, E., RACCHETTI, G. & MELDOLESI, J. 2009. Shedding microvesicles: artefacts no more. *Trends in cell biology,* 19**,** 43-51.

COLLINS, L. & DAWES, C. 1987. The surface area of the adult human mouth and thickness of the salivary film covering the teeth and oral mucosa. *Journal of dental research,* 66**,** 1300-1302.

COMFORT, N., BLOOMQUIST, T. R., SHEPHARD, A. P., PETTY, C. R., CUNNINGHAM, A., HAUPTMAN, M., PHIPATANAKUL, W. & BACCARELLI, A. 2021. Isolation and characterization of extracellular vesicles in saliva of children with asthma. *Extracellular Vesicles and Circulating Nucleic Acids*.

CONZELMANN, C., GROS, R., ZOU, M., KRÜGER, F., GÖRGENS, A., GUSTAFSSON, M. O., EL ANDALOUSSI, S., MÜNCH, J. & MÜLLER, J. A. 2020. Salivary extracellular vesicles inhibit Zika virus but not SARS-CoV-2 infection. *Journal of Extracellular Vesicles,* 9**,** 1808281.

COUMANS, F. A., BRISSON, A. R., BUZAS, E. I., DIGNAT-GEORGE, F., DREES, E. E., EL-ANDALOUSSI, S., EMANUELI, C., GASECKA, A., HENDRIX, A. & HILL, A. F. 2017a. Methodological guidelines to study extracellular vesicles. *Circulation research,* 120**,** 1632-1648.

COUMANS, F. A., GOOL, E. L. & NIEUWLAND, R. 2017b. Bulk immunoassays for analysis of extracellular vesicles. *Platelets,* 28**,** 242-248.

CRESCITELLI, R., LÄSSER, C., SZABÓ, T. G., KITTEL, A., ELDH, M., DIANZANI, I., BUZÁS, E. I. & LÖTVALL, J. 2013. Distinct RNA profiles in subpopulations of extracellular vesicles: apoptotic bodies, microvesicles and exosomes. *Journal of extracellular vesicles,* 2**,** 20677.

CURRY, J. M., SPRANDIO, J., COGNETTI, D., LUGINBUHL, A., BAR-AD, V., PRIBITKIN, E. & TULUC, M. 2014. Tumor Microenvironment in Head and Neck Squamous Cell Carcinoma. *Seminars in Oncology,* 41**,** 217-234.

CURTIS, A. M., EDELBERG, J., JONAS, R., ROGERS, W. T., MOORE, J. S., SYED, W. & MOHLER III, E. R. 2013. Endothelial microparticles: sophisticated vesicles modulating vascular function. *Vascular medicine,* 18**,** 204-214.

DALTON, A. J. 1975. Microvesicles and vesicles of multivesicular bodies versus "virus-like" particles. *Journal of the National Cancer Institute,* 54**,** 1137-1148.

DAVOREN, P. A., MCNEILL, R. E., LOWERY, A. J., KERIN, M. J. & MILLER, N. 2008. Identification of suitable endogenous control genes for microRNA gene expression analysis in human breast cancer. *BMC molecular biology,* 9**,** 1-11.

DE ALMEIDA, P. D. V., GREGIO, A., MACHADO, M., DE LIMA, A. & AZEVEDO, L. R. 2008. Saliva composition and functions: a comprehensive review. *J contemp dent pract,* 9**,** 72-80.

DE BROE, M., WIEME, R. & ROELS, F. 1975. Membrane fragments with koinozymic properties released from villous adenoma of the rectum. *The Lancet,* 306**,** 1214-1215.

DE GASSART, A., GÉMINARD, C., FÉVRIER, B., RAPOSO, G. & VIDAL, M. 2003. Lipid raft-associated protein sorting in exosomes. *Blood,* 102**,** 4336-4344.

DEBEY, S., SCHOENBECK, U., HELLMICH, M., GATHOF, B., PILLAI, R., ZANDER, T. & SCHULTZE, J. 2004. Comparison of different isolation techniques prior gene expression profiling of blood derived cells: impact on physiological responses, on overall expression and the role of different cell types. *The pharmacogenomics journal,* 4**,** 193-207.

DEL CONDE, I., SHRIMPTON, C. N., THIAGARAJAN, P. & LÓPEZ, J. A. 2005. Tissue-factor–bearing microvesicles arise from lipid rafts and fuse with activated platelets to initiate coagulation. *Blood,* 106**,** 1604-1611.

DEUTSCH, O., FLEISSIG, Y., ZAKS, B., KRIEF, G., AFRAMIAN, D. J. & PALMON, A. 2008. An approach to remove alpha amylase for proteomic analysis of low abundance biomarkers in human saliva. *Electrophoresis,* 29**,** 4150-4157.

DHAR, S., KUMAR, A., GOMEZ, C. R., AKHTAR, I., HANCOCK, J. C., LAGE, J. M., POUND, C. R. & LEVENSON, A. S. 2017. MTA 1-activated Epi-micro RNA-22 regulates E-cadherin and prostate cancer invasiveness. *FEBS letters,* 591**,** 924-933.

DIGNAT-GEORGE, F. & BOULANGER, C. M. 2011. The many faces of endothelial microparticles. *Arteriosclerosis, thrombosis, and vascular biology,* 31**,** 27-33.

DINH, T.-K. T., FENDLER, W., CHAŁUBIŃSKA-FENDLER, J., ACHARYA, S. S., O'LEARY, C., DERASKA, P. V., D'ANDREA, A. D., CHOWDHURY, D. & KOZONO, D. 2016. Circulating miR-29a and miR-150 correlate with delivered dose during thoracic radiation therapy for non-small cell lung cancer. *Radiation Oncology,* 11.

DIOGUARDI, M., CALORO, G. A., LAINO, L., ALOVISI, M., SOVERETO, D., CRINCOLI, V., AIUTO, R., COCCIA, E., TROIANO, G. & LO MUZIO, L. 2020. Circulating miR-21 as a potential biomarker for the diagnosis of oral cancer: A systematic review with meta-analysis. *Cancers,* 12**,** 936.

DIONNE, K. R., WARNAKULASURIYA, S., BINTI ZAIN, R. & CHEONG, S. C. 2015. Potentially malignant disorders of the oral cavity: Current practice and future directions in the clinic and laboratory. *International journal of cancer,* 136**,** 503-515.

DODDS, M. W., JOHNSON, D. A. & YEH, C.-K. 2005. Health benefits of saliva: a review. *Journal of dentistry,* 33**,** 223-233.

DOHERTY, G. J. & MCMAHON, H. T. 2009. Mechanisms of endocytosis. *Annual review of biochemistry,* 78**,** 857-902.

DOMINKUŠ, P. P., STENOVEC, M., SITAR, S., LASIČ, E., ZOREC, R., PLEMENITAŠ, A., ŽAGAR, E., KREFT, M. & LENASSI, M. 2018. PKH26 labeling of extracellular vesicles:

Characterization and cellular internalization of contaminating PKH26 nanoparticles. *Biochimica et Biophysica Acta (BBA)-Biomembranes,* 1860**,** 1350-1361.

DONG, L., ZIEREN, R. C., HORIE, K., KIM, C. J., MALLICK, E., JING, Y., FENG, M., KUCZLER, M. D., GREEN, J. & AMEND, S. R. 2020. Comprehensive evaluation of methods for small extracellular vesicles separation from human plasma, urine and cell culture medium. *Journal of extracellular vesicles,* 10**,** e12044.

DOYLE, L. M. & WANG, M. Z. 2019. Overview of extracellular vesicles, their origin, composition, purpose, and methods for exosome isolation and analysis. *Cells,* 8**,** 727.

DUDLEY, A. C. 2012. Tumor endothelial cells. *Cold Spring Harbor perspectives in medicine,* 2**,** a006536.

DUZ, M. B., KARATAS, O. F., GUZEL, E., TURGUT, N. F., YILMAZ, M., CREIGHTON, C. J. & OZEN, M. 2016. Identification of miR-139-5p as a saliva biomarker for tongue squamous cell carcinoma: a pilot study. *Cellular Oncology,* 39**,** 187-193.

ECONOMOPOULOU, P. & PSYRRI, A. 2017. Epidemiology, risk factors and pathogenesis of squamous cell tumours. *Head and Neck Cancers: Essentials for clnicians. https://oncologypro. esmo. org/content/download/113133/1971849/file/2017-ESMO-Essentials-for-Clinicians-Head-Neck-Cancers*.

EL ANDALOUSSI, S., MÄGER, I., BREAKEFIELD, X. O. & WOOD, M. J. 2013. Extracellular vesicles: biology and emerging therapeutic opportunities. *Nature reviews Drug discovery,* 12**,** 347-357.

EL-KHOURY, V., PIERSON, S., KAOMA, T., BERNARDIN, F. & BERCHEM, G. 2016. Assessing cellular and circulating miRNA recovery: the impact of the RNA isolation method and the quantity of input material. *Scientific Reports,* 6**,** 19529.

ELDH, M., LÖTVALL, J., MALMHÄLL, C. & EKSTRÖM, K. 2012. Importance of RNA isolation methods for analysis of exosomal RNA: evaluation of different methods. *Molecular immunology,* 50**,** 278-286.

ERDBRÜGGER, U., RUDY, C. K., E. ETTER, M., DRYDEN, K. A., YEAGER, M., KLIBANOV, A. L. & LANNIGAN, J. 2014. Imaging flow cytometry elucidates limitations of microparticle analysis by conventional flow cytometry. *Cytometry Part A,* 85**,** 756-770.

ESCOLA, J.-M., KLEIJMEER, M. J., STOORVOGEL, W., GRIFFITH, J. M., YOSHIE, O. & GEUZE, H. J. 1998. CARBOHYDRATES, LIPIDS, AND OTHER NATURAL PRODUCTS-Selective enrichment of tetraspan proteins on the internal vesicles of multivesicular endosomes and on exosomes secreted by human B-lymphocytes. *Journal of Biological Chemistry,* 273**,** 20121-20127.

ESCREVENTE, C., KELLER, S., ALTEVOGT, P. & COSTA, J. 2011. Interaction and uptake of exosomes by ovarian cancer cells. *BMC cancer,* 11**,** 1-10.

EWELS, P. A., PELTZER, A., FILLINGER, S., PATEL, H., ALNEBERG, J., WILM, A., GARCIA, M. U., DI TOMMASO, P. & NAHNSEN, S. 2020. The nf-core framework for community-curated bioinformatics pipelines. *Nature biotechnology,* 38**,** 276-278.

FADEEL, B. & ORRENIUS, S. 2005. Apoptosis: a basic biological phenomenon with wide-ranging implications in human disease. *Journal of internal medicine,* 258**,** 479-517.

FĂLĂMAȘ, A., ROTARU, H. & HEDEȘIU, M. 2020. Surface-enhanced Raman spectroscopy (SERS) investigations of saliva for oral cancer diagnosis. *Lasers in Medical Science,* 35**,** 1393-1401.

FAN, T., MAO, Y., SUN, Q., LIU, F., LIN, J. S., LIU, Y., CUI, J. & JIANG, Y. 2018. Branched rolling circle amplification method for measuring serum circulating micro RNA levels for early breast cancer detection. *Cancer Science,* 109**,** 2897-2906.

FANG, J. H., ZHANG, Z. J., SHANG, L. R., LUO, Y. W., LIN, Y. F., YUAN, Y. & ZHUANG, S. M. 2018. Hepatoma cell-secreted exosomal microRNA-103 increases vascular permeability and promotes metastasis by targeting junction proteins. *Hepatology,* 68**,** 1459-1475.

FARAG, A. F., SABRY, D., HASSABOU, N. F. & ALAA EL-DIN, Y. 2021. MicroRNA-134/microRNA-200a derived salivary exosomes are novel diagnostic biomarkers of oral squamous cell carcinoma. *Egyptian Dental Journal,* 67**,** 367-377.

FASSAN, M., REALDON, S., CASCIONE, L., HAHNE, J. C., MUNARI, G., GUZZARDO, V., ARCIDIACONO, D., LAMPIS, A., BRIGNOLA, S. & DAL SANTO, L. 2020. Circulating microRNA expression profiling revealed miR-92a-3p as a novel biomarker of Barrett's carcinogenesis. *Pathology-Research and Practice,* 216**,** 152907.

FAUR, C. I., ROTARU, H., OSAN, C., JURJ, A., ROMAN, R. C., MOLDOVAN, M., CHIRILA, M. & HEDESIU, M. 2021. Salivary exosomal microRNAs as biomarkers for head and neck cancer detection—a literature review. *Maxillofacial Plastic and Reconstructive Surgery,* 43.

FEINGOLD, K. R. & GRUNFELD, C. 2015. Introduction to lipids and lipoproteins.

FELLER, L. L., KHAMMISSA, R. R., KRAMER, B. B. & LEMMER, J. J. 2013. Oral squamous cell carcinoma in relation to field precancerisation: pathobiology. *Cancer cell international,* 13**,** 1-8.

FENG, D., ZHAO, W. L., YE, Y. Y., BAI, X. C., LIU, R. Q., CHANG, L. F., ZHOU, Q. & SUI, S. F. 2010. Cellular internalization of exosomes occurs through phagocytosis. *Traffic,* 11**,** 675-687.

FERGUSON, D. 1968. Dehydrogenase enzymes in human saliva. *Archives of Oral Biology,* 13**,** 583-588.

FERLAY, J., COLOMBET, M., SOERJOMATARAM, I., MATHERS, C., PARKIN, D., PIÑEROS, M., ZNAOR, A. & BRAY, F. 2019. Estimating the global cancer incidence and mortality in 2018: GLOBOCAN sources and methods. *International journal of cancer,* 144**,** 1941-1953.

FERLAY, J., ERVIK, M., LAM, F., COLOMBET, M., MERY, L., PIÑEROS, M., ZNAOR, A., SOERJOMATARAM, I. & BRAY, F. 2020. Global cancer observatory: cancer today. Lyon: International Agency for Research on Cancer; 2018.

FERLAY, J., SHIN, H. R., BRAY, F., FORMAN, D., MATHERS, C. & PARKIN, D. M. 2010. Estimates of worldwide burden of cancer in 2008: GLOBOCAN 2008. *International journal of cancer,* 127**,** 2893-2917.

FILIPE, V., HAWE, A. & JISKOOT, W. 2010. Critical evaluation of Nanoparticle Tracking Analysis (NTA) by NanoSight for the measurement of nanoparticles and protein aggregates. *Pharmaceutical research,* 27**,** 796-810.

FITZGERALD, G., SORO-ARNAIZ, I. & DE BOCK, K. 2018. The Warburg effect in endothelial cells and its potential as an anti-angiogenic target in cancer. *Frontiers in cell and developmental biology,* 6**,** 100.

FITZNER, D., SCHNAARS, M., VAN ROSSUM, D., KRISHNAMOORTHY, G., DIBAJ, P., BAKHTI, M., REGEN, T., HANISCH, U.-K. & SIMONS, M. 2011. Selective transfer of exosomes from oligodendrocytes to microglia by macropinocytosis. *Journal of cell science,* 124**,** 447-458.

FLAUMENHAFT, R., DILKS, J. R., RICHARDSON, J., ALDEN, E., PATEL-HETT, S. R., BATTINELLI, E., KLEMENT, G. L., SOLA-VISNER, M. & ITALIANO JR, J. E. 2009. Megakaryocyte-derived microparticles: direct visualization and distinction from platelet-derived microparticles. *Blood, The Journal of the American Society of Hematology,* 113**,** 1112-1121.

FONTANA, S., MAUCERI, R., NOVARA, M. E., ALESSANDRO, R. & CAMPISI, G. 2021. Protein Cargo of Salivary Small Extracellular Vesicles as Potential Functional Signature of Oral Squamous Cell Carcinoma. *International Journal of Molecular Sciences,* 22**,** 11160.

FRANZMANN, E. J., REATEGUI, E. P., CARRAWAY, K. L., HAMILTON, K. L., WEED, D. T. & GOODWIN, W. J. 2005. Salivary soluble CD44: a potential molecular marker for head and neck cancer. *Cancer Epidemiology and Prevention Biomarkers,* 14**,** 735-739.

FU, X., HAN, Y., WU, Y., ZHU, X., LU, X., MAO, F., WANG, X., HE, X., ZHAO, Y. & ZHAO, Y. 2011. Prognostic role of microRNA-21 in various carcinomas: a systematic review and meta-analysis. *European journal of clinical investigation,* 41**,** 1245-1253.

FUJII, N., SHOMORI, K., SHIOMI, T., NAKABAYASHI, M., TAKEDA, C., RYOKE, K. & ITO, H. 2012. Cancer-associated fibroblasts and CD163-positive macrophages in oral squamous cell carcinoma: their clinicopathological and prognostic significance. *Journal of oral pathology & medicine,* 41**,** 444-451.

FUKUDA, M., OHMORI, Y. & SAKASHITA, H. 2012. *The role of tumor microenvironment in oral cancer*, IntechOpen.

FULLER, C., CAMILON, R., NGUYEN, S., JENNINGS, J., DAY, T. & GILLESPIE, M. B. 2015. Adjunctive diagnostic techniques for oral lesions of unknown malignant potential: Systematic review with meta-analysis. *Head & neck,* 37**,** 755-762.

FURI, I., MOMEN-HERAVI, F. & SZABO, G. 2017. Extracellular vesicle isolation: present and future. *Ann Transl Med,* 5**,** 263.

GAI, C., CAMUSSI, F., BROCCOLETTI, R., GAMBINO, A., CABRAS, M., MOLINARO, L., CAROSSA, S., CAMUSSI, G. & ARDUINO, P. G. 2018. Salivary extracellular vesicle-associated miRNAs as potential biomarkers in oral squamous cell carcinoma. *BMC cancer,* 18**,** 1-11.

GALLO, A., TANDON, M., ALEVIZOS, I. & ILLEI, G. G. 2012. The majority of microRNAs detectable in serum and saliva is concentrated in exosomes. *PloS one,* 7**,** e30679.

GÁMEZ-VALERO, A., MONGUIÓ-TORTAJADA, M., CARRERAS-PLANELLA, L., FRANQUESA, M. L., BEYER, K. & BORRÀS, F. E. 2016. Size-Exclusion Chromatography-based isolation minimally alters Extracellular Vesicles' characteristics compared to precipitating agents. *Scientific Reports,* 6**,** 1-9.

GANCI, F., SACCONI, A., MANCIOCCO, V., SPERDUTI, I., BATTAGLIA, P., COVELLO, R., MUTI, P., STRANO, S., SPRIANO, G. & FONTEMAGGI, G. 2016. MicroRNA expression as predictor of local recurrence risk in oral squamous cell carcinoma. *Head & neck,* 38**,** E189-E197.

GAO, S., CHEN, L.-Y., WANG, P., LIU, L.-M. & CHEN, Z. 2014. MicroRNA Expression in Salivary Supernatant of Patients with Pancreatic Cancer and Its Relationship with ZHENG. *BioMed Research International,* 2014**,** 1-8.

GARCIA, N. A., ONTORIA-OVIEDO, I., GONZÁLEZ-KING, H., DIEZ-JUAN, A. & SEPÚLVEDA, P. 2015. Glucose Starvation in Cardiomyocytes Enhances Exosome Secretion and Promotes Angiogenesis in Endothelial Cells. *PLOS ONE,* 10**,** e0138849.

GARDINER, C., KIYOKO, K., PATEL, I., LANE, P., MACHIN, S. J. & MACKIE, I. 2016a. A performance evaluation of a novel human recombinant tissue factor prothrombin time reagent.

GARDINER, C., VIZIO, D. D., SAHOO, S., THÉRY, C., WITWER, K. W., WAUBEN, M. & HILL, A. F. 2016b. Techniques used for the isolation and characterization of extracellular vesicles: results of a worldwide survey. *Journal of extracellular vesicles,* 5**,** 32945.

GASPAR, L. S., SANTANA, M. M., HENRIQUES, C., PINTO, M. M., RIBEIRO-RODRIGUES, T. M., GIRÃO, H., NOBRE, R. J. & DE ALMEIDA, L. P. 2020a. Simple and fast sec-based protocol

to isolate human plasma-derived extracellular vesicles for transcriptional research. *Molecular Therapy-Methods & Clinical Development,* 18**,** 723-737.

GASPAR, L. S., SANTANA, M. M., HENRIQUES, C., PINTO, M. M., RIBEIRO-RODRIGUES, T. M., GIRÃO, H., NOBRE, R. J. & PEREIRA DE ALMEIDA, L. 2020b. Simple and Fast SEC-Based Protocol to Isolate Human Plasma-Derived Extracellular Vesicles for Transcriptional Research. *Molecular Therapy - Methods & Clinical Development,* 18**,** 723-737.

GEORGANAKI, M., VAN HOOREN, L. & DIMBERG, A. 2018. Vascular targeting to increase the efficiency of immune checkpoint blockade in cancer. *Frontiers in immunology***,** 3081.

GIBBINGS, D. J., CIAUDO, C., ERHARDT, M. & VOINNET, O. 2009. Multivesicular bodies associate with components of miRNA effector complexes and modulate miRNA activity. *Nature cell biology,* 11**,** 1143-1149.

GIUSTI, I., DELLE MONACHE, S., DI FRANCESCO, M., SANITÀ, P., D'ASCENZO, S., GRAVINA, G. L., FESTUCCIA, C. & DOLO, V. 2016. From glioblastoma to endothelial cells through extracellular vesicles: messages for angiogenesis. *Tumor Biology,* 37**,** 12743-12753.

GLEBOV, O. O., BRIGHT, N. A. & NICHOLS, B. J. 2006. Flotillin-1 defines a clathrin-independent endocytic pathway in mammalian cells. *Nature cell biology,* 8**,** 46-54.

GONZALEZ-BEGNE, M., LU, B., HAN, X., HAGEN, F. K., HAND, A. R., MELVIN, J. E. & YATES III, J. R. 2009. Proteomic analysis of human parotid gland exosomes by multidimensional protein identification technology (MudPIT). *Journal of proteome research,* 8**,** 1304-1314.

GOUIN, K., PECK, K., ANTES, T., JOHNSON, J. L., LI, C., VATURI, S. D., MIDDLETON, R., COUTO, G., WALRAVENS, A. S., RODRIGUEZ-BORLADO, L., SMITH, R. R., MARBÁN, L., MARBÁN, E. & IBRAHIM, A. G. E. 2017. A comprehensive method for identification of suitable reference genes in extracellular vesicles. *Journal of Extracellular Vesicles,* 6**,** 1347019.

GOULD, S. J. & RAPOSO, G. 2013. As we wait: coping with an imperfect nomenclature for extracellular vesicles. *J Extracell Vesicles,* 2.

GRIGOR'EVA, A., TAMKOVICH, S., EREMINA, A., TUPIKIN, A., KABILOV, M., CHERNYKH, V., VLASSOV, V., LAKTIONOV, P. & RYABCHIKOVA, E. 2016. Characteristics of exosomes andmicroparticles discovered in human tears. *Biomeditsinskaia khimiia,* 62**,** 99-106.

GU, M., LI, L., ZHANG, Z., CHEN, J., ZHANG, W., ZHANG, J., HAN, L., TANG, M., YOU, B. & ZHANG, Q. 2017. PFKFB3 promotes proliferation, migration and angiogenesis in nasopharyngeal carcinoma. *Journal of Cancer,* 8**,** 3887.

GU, W., XU, Y., XIE, X., WANG, T., KO, J.-H. & ZHOU, T. 2014. The role of RNA structure at 5′ untranslated region in microRNA-mediated gene regulation. *Rna,* 20**,** 1369-1375.

GU, Z., LI, Z., XU, R., ZHU, X., HU, R., XUE, Y. & XU, W. 2020. miR-16-5p suppresses progression and invasion of osteosarcoma via targeting at Smad3. *Frontiers in Pharmacology,* 11**,** 1324.

GUESCINI, M., GENEDANI, S., STOCCHI, V. & AGNATI, L. F. 2010. Astrocytes and Glioblastoma cells release exosomes carrying mtDNA. *Journal of neural transmission,* 117**,** 1-4.

GUO, D., LI, Q., LV, Q., WEI, Q., CAO, S. & GU, J. 2014. MiR-27a targets sFRP1 in hFOB cells to regulate proliferation, apoptosis and differentiation. *PloS one,* 9**,** e91354.

GUO, K., YAO, J., YU, Q., LI, Z., HUANG, H., CHENG, J., WANG, Z. & ZHU, Y. 2017. The expression pattern of long non-coding RNA PVT1 in tumor tissues and in extracellular vesicles of colorectal cancer correlates with cancer progression. *Tumor biology,* 39**,** 1010428317699122.

GUTSCHNER, T., HÄMMERLE, M., EISSMAN, M., HSU, J., KIM, Y., HUNG, G., REVENKO, A., ARUN, G., STENTRUP, M. & GROS, M. 2013. The Noncoding RNA MALAT1 Is a Critical

Regulator of the Metastasis Phenotype of Lung Cancer CellsMALAT1 Is Important for Metastasis. *Cancer research,* 73**,** 1180-1189.

GUZ, M., JELENIEWICZ, W. & CYBULSKI, M. 2022. An insight into miR-1290: an oncogenic miRNA with diagnostic potential. *International Journal of Molecular Sciences,* 23**,** 1234.

HAN, P., BARTOLD, P. M., SALOMON, C. & IVANOVSKI, S. 2021. Salivary outer membrane vesicles and DNA methylation of small extracellular vesicles as biomarkers for periodontal status: a pilot study. *International Journal of Molecular Sciences,* 22**,** 2423.

HAN, P., LAI, A., SALOMON, C. & IVANOVSKI, S. 2020. Detection of Salivary Small Extracellular Vesicles Associated Inflammatory Cytokines Gene Methylation in Gingivitis. *International Journal of Molecular Sciences,* 21**,** 5273.

HAN, Y., JIA, L., ZHENG, Y. & LI, W. 2018. Salivary exosomes: emerging roles in systemic disease.

HANNAFON, B. N., TRIGOSO, Y. D., CALLOWAY, C. L., ZHAO, Y. D., LUM, D. H., WELM, A. L., ZHAO, Z. J., BLICK, K. E., DOOLEY, W. C. & DING, W. 2016. Plasma exosome microRNAs are indicative of breast cancer. *Breast cancer research,* 18**,** 1-14.

HARADA, T., SHINOHARA, M., NAKAMURA, S. & OKA, M. 1994. An immunohistochemical study of the extracellular matrix in oral squamous cell carcinoma and its association with invasive and metastatic potential. *Virchows Archiv,* 424**,** 257-266.

HARDING, C., HEUSER, J. & STAHL, P. 1983. Receptor-mediated endocytosis of transferrin and recycling of the transferrin receptor in rat reticulocytes. *The Journal of cell biology,* 97**,** 329-339.

HASINA, R., MATSUMOTO, K., MATSUMOTO-TANIURA, N., KATO, I., SAKUDA, M. & NAKAMURA, T. 1999. Autocrine and paracrine motility factors and their involvement in invasiveness in a human oral carcinoma cell line. *British journal of cancer,* 80**,** 1708-1717.

HE, L., PING, F., FAN, Z., ZHANG, C., DENG, M., CHENG, B. & XIA, J. 2020. Salivary exosomal miR-24-3p serves as a potential detective biomarker for oral squamous cell carcinoma screening. *Biomedicine & Pharmacotherapy,* 121**,** 109553.

HE, Q., YE, A., YE, W., LIAO, X., QIN, G., XU, Y., YIN, Y., LUO, H., YI, M., XIAN, L., ZHANG, S., QIN, X., ZHU, W. & LI, Y. 2021. Cancer-secreted exosomal miR-21-5p induces angiogenesis and vascular permeability by targeting KRIT1. *Cell Death & Disease,* 12.

HE, X., PING, J. & WEN, D. 2017. MicroRNA-186 regulates the invasion and metastasis of bladder cancer via vascular endothelial growth factor C. *Experimental and Therapeutic Medicine,* 14**,** 3253-3258.

HEIJNEN, H. F., SCHIEL, A. E., FIJNHEER, R., GEUZE, H. J. & SIXMA, J. J. 1999. Activated Platelets Release Two Types of Membrane Vesicles: Microvesicles by Surface Shedding and Exosomes Derived From Exocytosis of Multivesicular Bodies and-Granules. *Blood, The Journal of the American Society of Hematology,* 94**,** 3791-3799.

HEMLER, M. E. 2003. Tetraspanin proteins mediate cellular penetration, invasion, and fusion events and define a novel type of membrane microdomain. *Annual review of cell and developmental biology,* 19**,** 397-422.

HERMANSEN, S. K., DAHLROT, R. H., NIELSEN, B. S., HANSEN, S. & KRISTENSEN, B. W. 2013. MiR-21 expression in the tumor cell compartment holds unfavorable prognostic value in gliomas. *Journal of neuro-oncology,* 111**,** 71-81.

HINZMAN, C. P., JAYATILAKE, M., BANSAL, S., FISH, B. L., LI, Y., ZHANG, Y., BANSAL, S., GIRGIS, M., ILIUK, A. & XU, X. 2022. An optimized method for the isolation of urinary

extracellular vesicles for molecular phenotyping: detection of biomarkers for radiation exposure. *Journal of translational medicine,* 20**,** 1-12.

HIRTZ, C., VIALARET, J., NOWAK, N., GABELLE, A., DEVILLE DE PÉRIÈRE, D. & LEHMANN, S. 2016. Absolute quantification of 35 plasma biomarkers in human saliva using targeted MS. *Bioanalysis,* 8**,** 43-53.

HO, W. J., JAFFEE, E. M. & ZHENG, L. 2020. The tumour microenvironment in pancreatic cancer — clinical challenges and opportunities. *Nature Reviews Clinical Oncology,* 17**,** 527-540.

HONG, C. S., MULLER, L., BOYIADZIS, M. & WHITESIDE, T. L. 2014. Isolation and Characterization of CD34+ Blast-Derived Exosomes in Acute Myeloid Leukemia. *PLoS ONE,* 9**,** e103310.

HOSHINO, D., KIRKBRIDE, K. C., COSTELLO, K., CLARK, E. S., SINHA, S., GREGA-LARSON, N., TYSKA, M. J. & WEAVER, A. M. 2013. Exosome secretion is enhanced by invadopodia and drives invasive behavior. *Cell reports,* 5**,** 1159-1168.

HRISTOV, M., ERL, W., LINDER, S. & WEBER, P. C. 2004. Apoptotic bodies from endothelial cells enhance the number and initiate the differentiation of human endothelial progenitor cells in vitro. *Blood,* 104**,** 2761-2766.

HU, J., LIU, D., DU, C., YAN, F. & LV, C. 2020a. Intelligent energy management strategy of hybrid energy storage system for electric vehicle based on driving pattern recognition. *Energy,* 198**,** 117298.

HU, W., LIU, C., BI, Z.-Y., ZHOU, Q., ZHANG, H., LI, L.-L., ZHANG, J., ZHU, W., SONG, Y.-Y.-Y. & ZHANG, F. 2020b. Comprehensive landscape of extracellular vesicle-derived RNAs in cancer initiation, progression, metastasis and cancer immunology. *Molecular cancer,* 19**,** 1-23.

HU, X., CHEN, D., CUI, Y., LI, Z. & HUANG, J. 2013. Targeting microRNA-23a to inhibit glioma cell invasion via HOXD10. *Scientific reports,* 3**,** 1-6.

HUAITONG, X., YUANYONG, F., YUEQIN, T., PENG, Z., WEI, S. & KAI, S. 2017. Microvesicles releasing by oral cancer cells enhance endothelial cell angiogenesis via Shh/RhoA signaling pathway. *Cancer biology & therapy,* 18**,** 783-791.

HUANG, J., SHEN, M., YAN, M., CUI, Y., GAO, Z. & MENG, X. 2019. Exosome-mediated transfer of miR-1290 promotes cell proliferation and invasion in gastric cancer via NKD1. *Acta Biochimica et Biophysica Sinica,* 51**,** 900-907.

HUANG, X., SUN, L., WEN, S., DENG, D., WAN, F., HE, X., TIAN, L., LIANG, L., WEI, C. & GAO, K. 2020. RNA sequencing of plasma exosomes revealed novel functional long noncoding RNAs in hepatocellular carcinoma. *Cancer science,* 111**,** 3338-3349.

HUANG, X., YUAN, T., TSCHANNEN, M., SUN, Z., JACOB, H., DU, M., LIANG, M., DITTMAR, R. L., LIU, Y. & LIANG, M. 2013. Characterization of human plasma-derived exosomal RNAs by deep sequencing. *BMC genomics,* 14**,** 1-14.

HUGHES, M. W. & CHUONG, C. M. 2003. A mouthful of epithelial-mesenchymal interactions. *J Invest Dermatol,* 121**,** vii-viii.

HUI, A. B. Y., LENARDUZZI, M., KRUSHEL, T., WALDRON, L., PINTILIE, M., SHI, W., PEREZ-ORDONEZ, B., JURISICA, I., O'SULLIVAN, B., WALDRON, J., GULLANE, P., CUMMINGS, B. & LIU, F.-F. 2010. Comprehensive MicroRNA Profiling for Head and Neck Squamous Cell Carcinomas. *Clinical Cancer Research,* 16**,** 1129-1139.

HULSMANS, M. & HOLVOET, P. 2013. MicroRNA-containing microvesicles regulating inflammation in association with atherosclerotic disease. *Cardiovasc Res,* 100**,** 7-18.

HUMPHREY, S. P. & WILLIAMSON, R. T. 2001. A review of saliva: normal composition, flow, and function. *The Journal of prosthetic dentistry,* 85**,** 162-169.

HWANG, J.-H., VOORTMAN, J., GIOVANNETTI, E., STEINBERG, S. M., LEON, L. G., KIM, Y.-T., FUNEL, N., PARK, J. K., KIM, M. A. & KANG, G. H. 2010. Identification of microRNA-21 as a biomarker for chemoresistance and clinical outcome following adjuvant therapy in resectable pancreatic cancer. *PloS one,* 5**,** e10630.

HWANG, Y. S., XIANGLAN, Z., PARK, K.-K. & CHUNG, W.-Y. 2012. Functional invadopodia formation through stabilization of the PDPN transcript by IMP-3 and cancer-stromal crosstalk for PDPN expression. *Carcinogenesis,* 33**,** 2135-2146.

ICARD, P., KAFARA, P., STEYAERT, J.-M., SCHWARTZ, L. & LINCET, H. 2014. The metabolic cooperation between cells in solid cancer tumors. *Biochimica et Biophysica Acta (BBA)-Reviews on Cancer,* 1846**,** 216-225.

INGENITO, F., ROSCIGNO, G., AFFINITO, A., NUZZO, S., SCOGNAMIGLIO, I., QUINTAVALLE, C. & CONDORELLI, G. 2019. The Role of Exo-miRNAs in Cancer: A Focus on Therapeutic and Diagnostic Applications. *Int J Mol Sci,* 20.

ISLAM, F., GOPALAN, V., VIDER, J., WAHAB, R., EBRAHIMI, F., LU, C.-T., KASEM, K. & LAM, A. K. 2017. MicroRNA-186-5p overexpression modulates colon cancer growth by repressing the expression of the FAM134B tumour inhibitor. *Experimental cell research,* 357**,** 260-270.

ISSMAN, L., BRENNER, B., TALMON, Y. & AHARON, A. 2013. Cryogenic transmission electron microscopy nanostructural study of shed microparticles. *PLoS One,* 8**,** e83680.

IWAI, K., MINAMISAWA, T., SUGA, K., YAJIMA, Y. & SHIBA, K. 2016. Isolation of human salivary extracellular vesicles by iodixanol density gradient ultracentrifugation and their characterizations. *Journal of extracellular vesicles,* 5**,** 30829.

IZQUIERDO-USEROS, N., NARANJO-GÓMEZ, M., ARCHER, J., HATCH, S. C., ERKIZIA, I., BLANCO, J., BORRÀS, F. E., PUERTAS, M. C., CONNOR, J. H. & FERNÁNDEZ-FIGUERAS, M. T. 2009. Capture and transfer of HIV-1 particles by mature dendritic cells converges with the exosome-dissemination pathway. *Blood, The Journal of the American Society of Hematology,* 113**,** 2732-2741.

JABALEE, J., TOWLE, R. & GARNIS, C. 2018. The role of extracellular vesicles in cancer: Cargo, function, and therapeutic implications. *Cells,* 7**,** 93.

JABLONSKA, J., LESCHNER, S., WESTPHAL, K., LIENENKLAUS, S. & WEISS, S. 2010. Neutrophils responsive to endogenous IFN-β regulate tumor angiogenesis and growth in a mouse tumor model. *Journal of Clinical Investigation,* 120**,** 1151-1164.

JADHAV, K. B., SHAH, V., CHAUHAN, N., SHAH, N. & PARMAR, G. 2022. Expression of microRNA-21 in saliva and tumor tissue of patients with oral squamous cell carcinoma: a predictor of cervical lymph node metastasis. *Oral Surg Oral Med Oral Pathol Oral Radiol,* 133**,** 60-69.

JAHID, S., SUN, J., EDWARDS, R. A., DIZON, D., PANARELLI, N. C., MILSOM, J. W., SIKANDAR, S. S., GÜMÜŞ, Z. H. & LIPKIN, S. M. 2012. miR-23a Promotes the Transition from Indolent to Invasive Colorectal CancermiR-23a Accelerates Colorectal Cancer Progression. *Cancer discovery,* 2**,** 540-553.

JAKOBSEN, K. R., PAULSEN, B. S., BÆK, R., VARMING, K., SORENSEN, B. S. & JØRGENSEN, M. M. 2015. Exosomal proteins as potential diagnostic markers in advanced non-small cell lung carcinoma. *Journal of extracellular vesicles,* 4**,** 26659.

JAMALI, Z., AMINABADI, N. A., ATTARAN, R., POURNAGIAZAR, F., OSKOUEI, S. G. & AHMADPOUR, F. 2015. MicroRNAs as prognostic molecular signatures in human head

and neck squamous cell carcinoma: a systematic review and meta-analysis. *Oral oncology,* 51**,** 321-331.

JANISZEWSKA, J., SZAUMKESSEL, M., KOSTRZEWSKA-POCZEKAJ, M., BEDNAREK, K., PACZKOWSKA, J., JACKOWSKA, J., GRENMAN, R., SZYFTER, K., WIERZBICKA, M. & GIEFING, M. 2015. Global miRNA expression profiling identifies miR-1290 as novel potential oncomiR in laryngeal carcinoma. *PLoS One,* 10**,** e0144924.

JANKOVIČOVÁ, J., SEČOVÁ, P., MICHALKOVÁ, K. & ANTALÍKOVÁ, J. 2020. Tetraspanins, More than Markers of Extracellular Vesicles in Reproduction. *International Journal of Molecular Sciences,* 21**,** 7568.

JAVAID, M. A., AHMED, A. S., DURAND, R. & TRAN, S. D. 2016. Saliva as a diagnostic tool for oral and systemic diseases. *Journal of oral biology and craniofacial research,* 6**,** 67-76.

JENIKE, A. E. & HALUSHKA, M. K. 2021. miR-21: a non-specific biomarker of all maladies. *Biomarker Research,* 9.

JEPPESEN, D. K., FENIX, A. M., FRANKLIN, J. L., HIGGINBOTHAM, J. N., ZHANG, Q., ZIMMERMAN, L. J., LIEBLER, D. C., PING, J., LIU, Q. & EVANS, R. 2019. Reassessment of exosome composition. *Cell,* 177**,** 428-445. e18.

JEYARAM, A. & JAY, S. M. 2018. Preservation and storage stability of extracellular vesicles for therapeutic applications. *The AAPS journal,* 20**,** 1-7.

JI, H., GREENING, D. W., BARNES, T. W., LIM, J. W., TAURO, B. J., RAI, A., XU, R., ADDA, C., MATHIVANAN, S. & ZHAO, W. 2013. Proteome profiling of exosomes derived from human primary and metastatic colorectal cancer cells reveal differential expression of key metastatic factors and signal transduction components. *Proteomics,* 13**,** 1672-1686.

JIANG, X., ZHANG, Y., TAN, B., LUO, C. & WU, X. 2014. Renal tumor-derived exosomes inhibit hepaCAM expression of renal carcinoma cells in a p-AKT-dependent manner. *Neoplasma,* 61**,** 416-423.

JINGHUA, H., QINGHUA, Z., CHENCHEN, C., LILI, C., XIAO, X., YUNFEI, W., ZHENGZHE, A., CHANGXIU, L. & HUI, H. 2021. MicroRNA miR-92a-3p regulates breast cancer cell proliferation and metastasis via regulating B-cell translocation gene 2 (BTG2). *Bioengineered,* 12**,** 2033-2044.

JOHANSSON, A.-C., ANSELL, A., JERHAMMAR, F., LINDH, M. B., GRÉNMAN, R., MUNCK-WIKLAND, E., ÖSTMAN, A. & ROBERG, K. 2012. Cancer-associated fibroblasts induce matrix metalloproteinase–mediated cetuximab resistance in head and neck squamous cell carcinoma cells. *Molecular Cancer Research,* 10**,** 1158-1168.

JOHNSON, D. E., BURTNESS, B., LEEMANS, C. R., LUI, V. W. Y., BAUMAN, J. E. & GRANDIS, J. R. 2020. Head and neck squamous cell carcinoma. *Nature Reviews Disease Primers,* 6.

JOHNSTONE, R. M. 2006. Exosomes biological significance: a concise review. *Blood Cells, Molecules, and Diseases,* 36**,** 315-321.

JONES, D. Z., SCHMIDT, M. L., SUMAN, S., HOBBING, K. R., BARVE, S. S., GOBEJISHVILI, L., BROCK, G., KLINGE, C. M., RAI, S. N. & PARK, J. 2018. Micro-RNA-186-5p inhibition attenuates proliferation, anchorage independent growth and invasion in metastatic prostate cancer cells. *BMC cancer,* 18**,** 1-16.

JOYCE, J. A. & FEARON, D. T. 2015. T cell exclusion, immune privilege, and the tumor microenvironment. *Science,* 348**,** 74-80.

KAHLERT, C., MELO, S. A., PROTOPOPOV, A., TANG, J., SETH, S., KOCH, M., ZHANG, J., WEITZ, J., CHIN, L. & FUTREAL, A. 2014. Identification of double-stranded genomic DNA

spanning all chromosomes with mutated KRAS and p53 DNA in the serum exosomes of patients with pancreatic cancer. *Journal of Biological Chemistry,* 289**,** 3869-3875.

KALLURI, R. & LEBLEU, V. S. 2020. The biology, function, and biomedical applications of exosomes. *Science,* 367**,** eaau6977.

KALRA, H., DRUMMEN, G. P. & MATHIVANAN, S. 2016. Focus on extracellular vesicles: introducing the next small big thing. *International journal of molecular sciences,* 17**,** 170.

KAMINAGAKURA, E., VILLA, L. L., ANDREOLI, M. A., SOBRINHO, J. S., VARTANIAN, J. G., SOARES, F. A., NISHIMOTO, I. N., ROCHA, R. & KOWALSKI, L. P. 2012. High-risk human papillomavirus in oral squamous cell carcinoma of young patients. *International journal of cancer,* 130**,** 1726-1732.

KAPSOGEORGOU, E. K., ABU-HELU, R. F., MOUTSOPOULOS, H. M. & MANOUSSAKIS, M. N. 2005. Salivary gland epithelial cell exosomes: a source of autoantigenic ribonucleoproteins. *Arthritis & Rheumatism,* 52**,** 1517-1521.

KARIMI, N., CVJETKOVIC, A., JANG, S. C., CRESCITELLI, R., HOSSEINPOUR FEIZI, M. A., NIEUWLAND, R., LÖTVALL, J. & LÄSSER, C. 2018. Detailed analysis of the plasma extracellular vesicle proteome after separation from lipoproteins. *Cellular and molecular life sciences,* 75**,** 2873-2886.

KARIMI, N., DALIRFARDOUEI, R., DIAS, T., LÖTVALL, J. & LÄSSER, C. 2022. Tetraspanins distinguish separate extracellular vesicle subpopulations in human serum and plasma – Contributions of platelet extracellular vesicles in plasma samples. *Journal of Extracellular Vesicles,* 11.

KARJALAINEN, S. R., SEWÛN, L., SODERLING, E., LARSSON, B., JOHANSSON, I., SIMELL, O., LAPINLEIMU, H. & SEPP‰NEN, R. 1997. Salivary Cholesterol of Healthy Adults in Relation to Serum Cholesterol Concentration and Oral Health. *Journal of Dental Research,* 76**,** 1637 - 1643.

KAWAKUBO-YASUKOCHI, T., MORIOKA, M., HAZEKAWA, M., YASUKOCHI, A., NISHINAKAGAWA, T., ONO, K., KAWANO, S., NAKAMURA, S. & NAKASHIMA, M. 2018. miR-200c-3p spreads invasive capacity in human oral squamous cell carcinoma microenvironment. *Molecular carcinogenesis,* 57**,** 295-302.

KAZENWADEL, J., MICHAEL, M. Z. & HARVEY, N. L. 2010. Prox1 expression is negatively regulated by miR-181 in endothelial cells. *Blood, The Journal of the American Society of Hematology,* 116**,** 2395-2401.

KEDERSHA, N. L. & ROME, L. H. 1986. Isolation and characterization of a novel ribonucleoprotein particle: large structures contain a single species of small RNA. *The Journal of cell biology,* 103**,** 699-709.

KIM, G., AN, H.-J., LEE, M.-J., SONG, J.-Y., JEONG, J.-Y., LEE, J.-H. & JEONG, H.-C. 2016. Hsa-miR-1246 and hsa-miR-1290 are associated with stemness and invasiveness of non-small cell lung cancer. *Lung cancer,* 91**,** 15-22.

KIM, G., YOO, C. E., KIM, M., KANG, H. J., PARK, D., LEE, M. & HUH, N. 2012. Noble Polymeric Surface Conjugated with Zwitterionic Moieties and Antibodies for the Isolation of Exosomes from Human Serum. *Bioconjugate Chemistry,* 23**,** 2114-2120.

KIM, H., SONG, K., PARK, Y., KANG, Y., LEE, Y., LEE, K., RYU, K., BAE, J. & KIM, S. 2003. Elevated levels of circulating platelet microparticles, VEGF, IL-6 and RANTES in patients with gastric cancer: possible role of a metastasis predictor. *European journal of cancer,* 39**,** 184-191.

KIM, J., SHIN, H. & PARK, J. 2017. RNA in salivary extracellular vesicles as a possible tool for systemic disease diagnosis. *Journal of dental research,* 96**,** 938-944.

KIRCHHAUSEN, T. 2000. Clathrin. *Annual review of biochemistry,* 69**,** 699-727.

KITDUMRONGTHUM, S., METHEETRAIRUT, C., CHAROENSAWAN, V., OUNJAI, P., JANPIPATKUL, K., PANVONGSA, W., WEERACHAYAPHORN, J., PIYACHATURAWAT, P. & CHAIROUNGDUA, A. 2018. Dysregulated microRNA expression profiles in cholangiocarcinoma cell-derived exosomes. *Life sciences,* 210**,** 65-75.

KNOWLES, L. M., STABILE, L. P., EGLOFF, A. M., ROTHSTEIN, M. E., THOMAS, S. M., GUBISH, C. T., LERNER, E. C., SEETHALA, R. R., SUZUKI, S. & QUESNELLE, K. M. 2009. HGF and c-Met participate in paracrine tumorigenic pathways in head and neck squamous cell cancer. *Clinical Cancer Research,* 15**,** 3740-3750.

KONOSHENKO, M. Y., LEKCHNOV, E. A., VLASSOV, A. V. & LAKTIONOV, P. P. 2018. Isolation of extracellular vesicles: general methodologies and latest trends. *BioMed research international,* 2018.

KOPPERS-LALIC, D., HACKENBERG, M., BIJNSDORP, I. V., VAN EIJNDHOVEN, M. A., SADEK, P., SIE, D., ZINI, N., MIDDELDORP, J. M., YLSTRA, B. & DE MENEZES, R. X. 2014. Nontemplated nucleotide additions distinguish the small RNA composition in cells from exosomes. *Cell reports,* 8**,** 1649-1658.

KOPPERS-LALIC, D., HACKENBERG, M., DE MENEZES, R., MISOVIC, B., WACHALSKA, M., GELDOF, A., ZINI, N., DE REIJKE, T., WURDINGER, T. & VIS, A. 2016. Non-invasive prostate cancer detection by measuring miRNA variants (isomiRs) in urine extracellular vesicles. *Oncotarget,* 7**,** 22566.

KOSAKA, N., IGUCHI, H., HAGIWARA, K., YOSHIOKA, Y., TAKESHITA, F. & OCHIYA, T. 2013. Neutral sphingomyelinase 2 (nSMase2)-dependent exosomal transfer of angiogenic microRNAs regulate cancer cell metastasis. *Journal of Biological Chemistry,* 288**,** 10849-10859.

KOSAKA, N., IGUCHI, H., YOSHIOKA, Y., TAKESHITA, F., MATSUKI, Y. & OCHIYA, T. 2010. Secretory mechanisms and intercellular transfer of microRNAs in living cells*♦. *Journal of Biological Chemistry,* 285**,** 17442-17452.

KOWAL, J., ARRAS, G., COLOMBO, M., JOUVE, M., MORATH, J. P., PRIMDAL-BENGTSON, B., DINGLI, F., LOEW, D., TKACH, M. & THÉRY, C. 2016. Proteomic comparison defines novel markers to characterize heterogeneous populations of extracellular vesicle subtypes. *Proceedings of the National Academy of Sciences,* 113**,** E968-E977.

KOWAL, J., TKACH, M. & THÉRY, C. 2014. Biogenesis and secretion of exosomes. *Current Opinion in Cell Biology,* 29**,** 116-125.

Knops, A.M., South, A., Rodeck, U., Martinez-Outschoorn, U., Harshyne, L.A., Johnson, J., Luginbuhl, A.J. and Curry, J.M., 2020. Cancer-associated fibroblast density, prognostic characteristics, and recurrence in head and neck squamous cell carcinoma: A meta-analysis. Frontiers in Oncology, 10, p.565306.

KRIEF, G., DEUTSCH, O., GARIBA, S., ZAKS, B., AFRAMIAN, D. & PALMON, A. 2011. Improved visualization of low abundance oral fluid proteins after triple depletion of alpha amylase, albumin and IgG. *Oral Diseases,* 17**,** 45-52.

KUMAR, A. T., KNOPS, A., SWENDSEID, B., MARTINEZ-OUTSCHOOM, U., HARSHYNE, L., PHILP, N., RODECK, U., LUGINBUHL, A., COGNETTI, D. & JOHNSON, J. 2019. Prognostic significance of tumor-associated macrophage content in head and neck squamous cell carcinoma: a meta-analysis. *Frontiers in Oncology,* 9**,** 656.

KUMEDA, N., OGAWA, Y., AKIMOTO, Y., KAWAKAMI, H., TSUJIMOTO, M. & YANOSHITA, R. 2017. Characterization of membrane integrity and morphological stability of human salivary exosomes. *Biological and Pharmaceutical Bulletin,* 40**,** 1183-1191.

LAJER, C. B., NIELSEN, F. C., FRIIS-HANSEN, L., NORRILD, B., BORUP, R., GARNÆS, E., ROSSING, M., SPECHT, L., THERKILDSEN, M. H., NAUNTOFTE, B., DABELSTEEN, S. & VON BUCHWALD, C. 2011. Different miRNA signatures of oral and pharyngeal squamous cell carcinomas: a prospective translational study. *British Journal of Cancer,* 104**,** 830-840.

LAMALICE, L., LE BOEUF, F. & HUOT, J. 2007. Endothelial cell migration during angiogenesis. *Circulation research,* 100**,** 782-794.

LAMSTER, I. B. & AHLO, J. K. 2007. Analysis of gingival crevicular fluid as applied to the diagnosis of oral and systemic diseases. *Annals of the New York Academy of Sciences,* 1098**,** 216-229.

LAMY, E. & MAU, M. 2012. Saliva proteomics as an emerging, non-invasive tool to study livestock physiology, nutrition and diseases. *Journal of proteomics,* 75**,** 4251-4258.

LANDGRAF, P., RUSU, M., SHERIDAN, R., SEWER, A., IOVINO, N., ARAVIN, A., PFEFFER, S., RICE, A., KAMPHORST, A. O. & LANDTHALER, M. 2007. A mammalian microRNA expression atlas based on small RNA library sequencing. *Cell,* 129**,** 1401-1414.

LANG, H.-L., HU, G.-W., ZHANG, B., KUANG, W., CHEN, Y., WU, L. & XU, G.-H. 2017. Glioma cells enhance angiogenesis and inhibit endothelial cell apoptosis through the release of exosomes that contain long non-coding RNA CCAT2. *Oncology reports,* 38**,** 785-798.

LANGEVIN, S., KUHNELL, D., PARRY, T., BIESIADA, J., HUANG, S., WISE-DRAPER, T., CASPER, K., ZHANG, X., MEDVEDOVIC, M. & KASPER, S. 2017. Comprehensive microRNA-sequencing of exosomes derived from head and neck carcinoma cells in vitro reveals common secretion profiles and potential utility as salivary biomarkers. *Oncotarget,* 8**,** 82459.

LANGMEAD, B., TRAPNELL, C., POP, M. & SALZBERG, S. L. 2009. Ultrafast and memory-efficient alignment of short DNA sequences to the human genome. *Genome biology,* 10**,** 1-10.

LARSON, M. C., HILLERY, C. A. & HOGG, N. 2014. Circulating membrane-derived microvesicles in redox biology. *Free Radical Biology and Medicine,* 73**,** 214-228.

LÄSSER, C., ALIKHANI, V. S., EKSTRÖM, K., ELDH, M., PAREDES, P. T., BOSSIOS, A., SJÖSTRAND, M., GABRIELSSON, S., LÖTVALL, J. & VALADI, H. 2011. Human saliva, plasma and breast milk exosomes contain RNA: uptake by macrophages. *J Transl Med,* 9**,** 9.

LEE, M., BAN, J.-J., IM, W. & KIM, M. 2016. Influence of storage condition on exosome recovery. *Biotechnology and Bioprocess Engineering,* 21**,** 299-304.

LEE, Y., KIM, S. J., CHOO, J., HEO, G., YOO, J.-W., JUNG, Y., RHEE, S. H. & IM, E. 2020. miR-23a-3p is a key regulator of IL-17C-induced tumor angiogenesis in colorectal cancer. *Cells,* 9**,** 1363.

LENER, T., GIMONA, M., AIGNER, L., BÖRGER, V., BUZAS, E., CAMUSSI, G., CHAPUT, N., CHATTERJEE, D., COURT, F. A., DEL PORTILLO, H. A., O'DRISCOLL, L., FAIS, S., FALCON-PEREZ, J. M., FELDERHOFF-MUESER, U., FRAILE, L., GHO, Y. S., GÖRGENS, A., GUPTA, R. C., HENDRIX, A., HERMANN, D. M., HILL, A. F., HOCHBERG, F., HORN, P. A., DE KLEIJN, D., KORDELAS, L., KRAMER, B. W., KRÄMER-ALBERS, E. M., LANER-PLAMBERGER, S., LAITINEN, S., LEONARDI, T., LORENOWICZ, M. J., LIM, S. K., LÖTVALL, J., MAGUIRE, C. A., MARCILLA, A., NAZARENKO, I., OCHIYA, T., PATEL, T., PEDERSEN, S., POCSFALVI, G., PLUCHINO, S., QUESENBERRY, P., REISCHL, I. G., RIVERA, F. J., SANZENBACHER, R.,

SCHALLMOSER, K., SLAPER-CORTENBACH, I., STRUNK, D., TONN, T., VADER, P., VAN BALKOM, B. W., WAUBEN, M., ANDALOUSSI, S. E., THÉRY, C., ROHDE, E. & GIEBEL, B. 2015. Applying extracellular vesicles based therapeutics in clinical trials - an ISEV position paper. *J Extracell Vesicles,* 4**,** 30087.

LEVENTAL, K. R., YU, H., KASS, L., LAKINS, J. N., EGEBLAD, M., ERLER, J. T., FONG, S. F., CSISZAR, K., GIACCIA, A. & WENINGER, W. 2009. Matrix crosslinking forces tumor progression by enhancing integrin signaling. *Cell,* 139**,** 891-906.

LI, A., YU, J., KIM, H., WOLFGANG, C. L., CANTO, M. I., HRUBAN, R. H. & GOGGINS, M. 2013. MicroRNA Array Analysis Finds Elevated Serum miR-1290 Accurately Distinguishes Patients with Low-Stage Pancreatic Cancer from Healthy and Disease ControlsSerum miR-1290 as a Marker of Pancreatic Cancer. *Clinical cancer research,* 19**,** 3600-3610.

LI, H., WU, Q., LI, T., LIU, C., XUE, L., DING, J., SHI, Y. & FAN, D. 2017a. The miR-17-92 cluster as a potential biomarker for the early diagnosis of gastric cancer: evidence and literature review. *Oncotarget,* 8**,** 45060.

LI, J., HUANG, H., SUN, L., YANG, M., PAN, C., CHEN, W., WU, D., LIN, Z., ZENG, C., YAO, Y., ZHANG, P. & SONG, E. 2009. MiR-21 Indicates Poor Prognosis in Tongue Squamous Cell Carcinomas as an Apoptosis Inhibitor. *Clinical Cancer Research,* 15**,** 3998-4008.

LI, K., LIN, Y., LUO, Y., XIONG, X., WANG, L., DURANTE, K., LI, J., ZHOU, F., GUO, Y. & CHEN, S. 2022. A signature of saliva-derived exosomal small RNAs as predicting biomarker for esophageal carcinoma: a multicenter prospective study. *Molecular cancer,* 21**,** 1-13.

LI, L., LI, C., WANG, S., WANG, Z., JIANG, J., WANG, W., LI, X., CHEN, J., LIU, K. & LI, C. 2016. Exosomes derived from hypoxic oral squamous cell carcinoma cells deliver miR-21 to normoxic cells to elicit a prometastatic phenotype. *Cancer research,* 76**,** 1770-1780.

LI, M., GUAN, X., SUN, Y., MI, J., SHU, X., LIU, F. & LI, C. 2014. miR-92a family and their target genes in tumorigenesis and metastasis. *Experimental cell research,* 323**,** 1-6.

LI, M., LOU, D., CHEN, J., SHI, K., WANG, Y., ZHU, Q., LIU, F. & ZHANG, Y. 2021. Deep dive on the proteome of salivary extracellular vesicles: comparison between ultracentrifugation and polymer-based precipitation isolation. *Analytical and Bioanalytical Chemistry,* 413**,** 365-375.

LI, N. & LI, Q. 2015. Identification and characterization of endogenous viral elements for the three key schistosomes of humans. *Pakistan journal of pharmaceutical sciences,* 28.

LI, P., KASLAN, M., LEE, S., YAO, J. & GAO, Z. 2017. Progress in exosome isolation techniques. Theranostics 7, 789–804.

LI, Q.-J., CHAU, J., EBERT, P. J., SYLVESTER, G., MIN, H., LIU, G., BRAICH, R., MANOHARAN, M., SOUTSCHEK, J. & SKARE, P. 2007. miR-181a is an intrinsic modulator of T cell sensitivity and selection. *Cell,* 129**,** 147-161.

LI, Y., AN, J., HUANG, S., HE, J. & ZHANG, J. 2015. Esophageal cancer-derived microvesicles induce regulatory B cells. *Cell biochemistry and function,* 33**,** 308-313.

LI, Y., WANG, Z., LI, Y. & JING, R. 2017c. MicroRNA-29a functions as a potential tumor suppressor through directly targeting CDC42 in non-small cell lung cancer. *Oncol Lett,* 13**,** 3896-3904.

LI, Y., ZANG, H., ZHANG, X. & HUANG, G. 2020. Exosomal Circ-ZNF652 Promotes Cell Proliferation, Migration, Invasion and Glycolysis in Hepatocellular Carcinoma via miR-29a-3p/GUCD1 Axis . *Cancer Management and Research,* Volume 12**,** 7739-7751.

LI, Y.-Y., TAO, Y.-W., GAO, S., LI, P., ZHENG, J.-M., ZHANG, S.-E., LIANG, J. & ZHANG, Y. 2018. Cancer-associated fibroblasts contribute to oral cancer cells proliferation and metastasis via exosome-mediated paracrine miR-34a-5p. *EBioMedicine,* 36**,** 209-220.

LIAN, F., CUI, Y., ZHOU, C., GAO, K. & WU, L. 2015. Identification of a Plasma Four-microRNA Panel as Potential Noninvasive Biomarker for Osteosarcoma. *PLOS ONE,* 10**,** e0121499.

LIANG, Y., ENG, W. S., COLQUHOUN, D. R., DINGLASAN, R. R., GRAHAM, D. R. & MAHAL, L. K. 2014. Complex N-linked glycans serve as a determinant for exosome/microvesicle cargo recruitment. *Journal of Biological Chemistry,* 289**,** 32526-32537.

LIANGSUPREE, T., MULTIA, E. & RIEKKOLA, M.-L. 2021. Modern isolation and separation techniques for extracellular vesicles. *Journal of Chromatography A,* 1636**,** 461773.

LIAO, J. M., ZHOU, X., ZHANG, Y. & LU, H. 2012. MiR-1246: a new link of the p53 family with cancer and Down syndrome. *Cell Cycle,* 11**,** 2624-30.

LIAO, L., WANG, J., OUYANG, S., ZHANG, P., WANG, J. & ZHANG, M. 2015. Expression and clinical significance of microRNA-1246 in human oral squamous cell carcinoma. *Med Sci Monit,* 21**,** 776-81.

LIMA, D. P., DINIZ, D. G., MOIMAZ, S. A. S., SUMIDA, D. H. & OKAMOTO, A. C. 2010. Saliva: reflection of the body. *International Journal of Infectious Diseases,* 14**,** e184-e188.

LIN, F., ZENG, Z., SONG, Y., LI, L., WU, Z., ZHANG, X., LI, Z., KE, X. & HU, X. 2019. YBX-1 mediated sorting of miR-133 into hypoxia/reoxygenation-induced EPC-derived exosomes to increase fibroblast angiogenesis and MEndoT. *Stem Cell Research & Therapy,* 10**,** 1-13.

LINARES, R., TAN, S., GOUNOU, C., ARRAUD, N. & BRISSON, A. R. 2015. High-speed centrifugation induces aggregation of extracellular vesicles. *Journal of extracellular vesicles,* 4**,** 29509.

LIU, C. J., LIN, S. C., YANG, C. C., CHENG, H. W. & CHANG, K. W. 2012. Exploiting salivary miR-31 as a clinical biomarker of oral squamous cell carcinoma. *Head Neck,* 34**,** 219-24.

LIU, J., JENNINGS, S. F., TONG, W. & HONG, H. 2011. Next generation sequencing for profiling expression of miRNAs: technical progress and applications in drug development. *J Biomed Sci Eng,* 4**,** 666-676.

LIU, K. Y. P., ZHU, S. Y., BROOKS, D., BOWLBY, R., DURHAM, J. S., MA, Y., MOORE, R. A., MUNGALL, A. J., JONES, S. & POH, C. F. 2020. Tumor microRNA profile and prognostic value for lymph node metastasis in oral squamous cell carcinoma patients. *Oncotarget,* 11**,** 2204-2215.

LIU, M. X., JUAN, L., MING, X., GAO, Z. K., WANG, X. H., ZHANG, Y., SHANG, M. H., YIN, L. H., PU, Y. P. & RAN, L. 2018. miR-93-5p transferred by exosomes promotes the proliferation of esophageal cancer cells via intercellular communication by targeting PTEN. *Biomedical and environmental sciences,* 31**,** 171-185.

LIU, P., WANG, C., MA, C., WU, Q., ZHANG, W. & LAO, G. 2016. MicroRNA-23a regulates epithelial-to-mesenchymal transition in endometrial endometrioid adenocarcinoma by targeting SMAD3. *Cancer cell international,* 16**,** 1-9.

LIVSHITS, M. A., KHOMYAKOVA, E., EVTUSHENKO, E. G., LAZAREV, V. N., KULEMIN, N. A., SEMINA, S. E., GENEROZOV, E. V. & GOVORUN, V. M. 2015. Isolation of exosomes by differential centrifugation: Theoretical analysis of a commonly used protocol. *Scientific reports,* 5**,** 1-14.

LOGOZZI, M., DE MILITO, A., LUGINI, L., BORGHI, M., CALABRÒ, L., SPADA, M., PERDICCHIO, M., MARINO, M. L., FEDERICI, C., IESSI, E., BRAMBILLA, D., VENTURI, G., LOZUPONE, F., SANTINAMI, M., HUBER, V., MAIO, M., RIVOLTINI, L. & FAIS, S. 2009. High levels of exosomes expressing CD63 and caveolin-1 in plasma of melanoma patients. *PLoS One,* 4**,** e5219.

LŐRINCZ, Á. M., TIMÁR, C. I., MAROSVÁRI, K. A., VERES, D. S., OTROKOCSI, L., KITTEL, Á. & LIGETI, E. 2014. Effect of storage on physical and functional properties of extracellular vesicles derived from neutrophilic granulocytes. *Journal of extracellular vesicles,* 3**,** 25465.

LÖTVALL, J., HILL, A. F., HOCHBERG, F., BUZÁS, E. I., DI VIZIO, D., GARDINER, C., GHO, Y. S., KUROCHKIN, I. V., MATHIVANAN, S. & QUESENBERRY, P. 2014. Minimal experimental requirements for definition of extracellular vesicles and their functions: a position statement from the International Society for Extracellular Vesicles. Taylor & Francis.

LOVE, M. I., HUBER, W. & ANDERS, S. 2014. Moderated estimation of fold change and dispersion for RNA-seq data with DESeq2. *Genome biology,* 15**,** 1-21.

LU, L., LING, W. & RUAN, Z. 2021. TAM-derived extracellular vesicles containing microRNA-29a-3p explain the deterioration of ovarian cancer. *Molecular Therapy - Nucleic Acids,* 25**,** 468-482.

LUDWIG, N., YERNENI, S. S., RAZZO, B. M. & WHITESIDE, T. L. 2018. Exosomes from HNSCC promote angiogenesis through reprogramming of endothelial cells. *Molecular Cancer Research,* 16**,** 1798-1808.

LUO, L.-J., ZHANG, L.-P., DUAN, C.-Y., WANG, B., HE, N.-N., ABULIMITI, P. & LIN, Y. 2017. The inhibition role of miR-22 in hepatocellular carcinoma cell migration and invasion via targeting CD147. *Cancer Cell International,* 17**,** 1-9.

LV, K. T., LIU, Z., FENG, J., ZHAO, W., HAO, T., DING, W. Y., CHU, J. P. & GAO, L. J. 2018. MiR-22-3p Regulates Cell Proliferation and Inhibits Cell Apoptosis through Targeting the eIF4EBP3 Gene in Human Cervical Squamous Carcinoma Cells. *Int J Med Sci,* 15**,** 142-152.

MA, F., LI, W., LIU, C., LI, W., YU, H., LEI, B., REN, Y., LI, Z., PANG, D. & QIAN, C. 2017. MiR-23a promotes TGF-β1-induced EMT and tumor metastasis in breast cancer cells by directly targeting CDH1 and activating Wnt/β-catenin signaling. *Oncotarget,* 8**,** 69538-69550.

MA, P., WANG, H., SUN, J., LIU, H., ZHENG, C., ZHOU, X. & LU, Z. 2018. LINC00152 promotes cell cycle progression in hepatocellular carcinoma via miR-193a/b-3p/CCND1 axis. *Cell cycle,* 17**,** 974-984.

MA, Y., GAO, J. & GUO, H. 2022. miR-23a-3p Regulates Runx2 to Inhibit the Proliferation and Metastasis of Oral Squamous Cell Carcinoma. *Journal of Oncology,* 2022**,** 1-11.

MACHIDA, T., TOMOFUJI, T., MARUYAMA, T., YONEDA, T., EKUNI, D., AZUMA, T., MIYAI, H., MIZUNO, H., KATO, H. & TSUTSUMI, K. 2016. miR-1246 and miR-4644 in salivary exosome as potential biomarkers for pancreatobiliary tract cancer. *Oncology reports,* 36**,** 2375-2381.

MACLELLAN, S. A., LAWSON, J., BAIK, J., GUILLAUD, M., POH, C. F. Y. & GARNIS, C. 2012. Differential expression of mi RNAs in the serum of patients with high-risk oral lesions. *Cancer medicine,* 1**,** 268-274.

MADISON, M. N., WELCH, J. L. & OKEOMA, C. M. 2017. Isolation of Exosomes from Semen for in vitro Uptake and HIV-1 Infection Assays. *Bio-protocol,* 7**,** e2216-e2216.

MAGOČ, T. & SALZBERG, S. L. 2011. FLASH: fast length adjustment of short reads to improve genome assemblies. *Bioinformatics,* 27**,** 2957-2963.

MAHN, R., HEUKAMP, L. C., ROGENHOFER, S., VON RUECKER, A., MÜLLER, S. C. & ELLINGER, J. 2011. Circulating microRNAs (miRNA) in serum of patients with prostate cancer. *Urology,* 77**,** 1265. e9-1265. e16.

MALLIA, A., GIANAZZA, E., ZOANNI, B., BRIOSCHI, M., BARBIERI, S. S. & BANFI, C. 2020. Proteomics of Extracellular Vesicles: Update on Their Composition, Biological Roles

and Potential Use as Diagnostic Tools in Atherosclerotic Cardiovascular Diseases. *Diagnostics (Basel),* 10.

MANIKANDAN, M., DEVA MAGENDHRA RAO, A. K., ARUNKUMAR, G., MANICKAVASAGAM, M., RAJKUMAR, K. S., RAJARAMAN, R. & MUNIRAJAN, A. K. 2016. Oral squamous cell carcinoma: microRNA expression profiling and integrative analyses for elucidation of tumourigenesis mechanism. *Molecular Cancer,* 15.

MÄNTTÄRI, M., MANNINEN, V., PALOSUO, T. & CH, E. 2001. Apolipoprotein E polymorphism and C-reactive protein in dyslipidemic middle-aged men.

MARCU, L. G. & YEOH, E. 2009. A review of risk factors and genetic alterations in head and neck carcinogenesis and implications for current and future approaches to treatment. *Journal of cancer research and clinical oncology,* 135**,** 1303-1314.

MARCUS, B., ARENBERG, D., LEE, J., KLEER, C., CHEPEHA, D. B., SCHMALBACH, C. E., ISLAM, M., PAUL, S., PAN, Q. & HANASH, S. 2004. Prognostic factors in oral cavity and oropharyngeal squamous cell carcinoma: The impact of tumor-associated macrophages. *Cancer: Interdisciplinary International Journal of the American Cancer Society,* 101**,** 2779-2787.

MARZESCO, A.-M., JANICH, P., WILSCH-BRÄUNINGER, M., DUBREUIL, V., LANGENFELD, K., CORBEIL, D. & HUTTNER, W. B. 2005. Release of extracellular membrane particles carrying the stem cell marker prominin-1 (CD133) from neural progenitors and other epithelial cells. *Journal of cell science,* 118**,** 2849-2858.

MASAOKA, T., SHINOZUKA, K., OHARA, K., TSUDA, H., IMAI, K. & TONOGI, M. 2021. Bioinformatics analysis of dysregulated exosomal microRNAs derived from oral squamous cell carcinoma cells. *Journal of Oral Science,* 63**,** 174-178.

MATEESCU, B., KOWAL, E. J., VAN BALKOM, B. W., BARTEL, S., BHATTACHARYYA, S. N., BUZÁS, E. I., BUCK, A. H., DE CANDIA, P., CHOW, F. W. & DAS, S. 2017a. Obstacles and opportunities in the functional analysis of extracellular vesicle RNA–an ISEV position paper. *Journal of extracellular vesicles,* 6**,** 1286095.

MATSUDA, N., SATO, S., SHIBA, K., OKATSU, K., SAISHO, K., GAUTIER, C. A., SOU, Y.-S., SAIKI, S., KAWAJIRI, S. & SATO, F. 2010. PINK1 stabilized by mitochondrial depolarization recruits Parkin to damaged mitochondria and activates latent Parkin for mitophagy. *Journal of Cell Biology,* 189**,** 211-221.

MEEHAN, B., RAK, J. & DI VIZIO, D. 2016. Oncosomes–large and small: what are they, where they came from? *Journal of extracellular vesicles,* 5**,** 33109.

MICHAEL, A., BAJRACHARYA, S. D., YUEN, P. S., ZHOU, H., STAR, R. A., ILLEI, G. G. & ALEVIZOS, I. 2010. Exosomes from human saliva as a source of microRNA biomarkers. *Oral diseases,* 16**,** 34-38.

MILLER, S. 1994. Saliva testing--a nontraditional diagnostic tool. *Clinical laboratory science: journal of the American Society for Medical Technology,* 7**,** 39-44.

MINCIACCHI, V. R., FREEMAN, M. R. & DI VIZIO, D. 2015. Extracellular vesicles in cancer: exosomes, microvesicles and the emerging role of large oncosomes. *Semin Cell Dev Biol,* 40**,** 41-51.

MO, D., GU, B., GONG, X., WU, L., WANG, H., JIANG, Y., ZHANG, B., ZHANG, M., ZHANG, Y. & XU, J. 2015. miR-1290 is a potential prognostic biomarker in non-small cell lung cancer. *Journal of Thoracic Disease,* 7**,** 1570.

MOHR, A. M. & MOTT, J. L. Overview of microRNA biology. Seminars in liver disease, 2015. Thieme Medical Publishers, 003-011.

MOLTZAHN, F., OLSHEN, A. B., BAEHNER, L., PEEK, A., FONG, L., STÖPPLER, H., SIMKO, J., HILTON, J. F., CARROLL, P. & BLELLOCH, R. 2011. Microfluidic-Based Multiplex qRT-PCR Identifies Diagnostic and Prognostic microRNA Signatures in the Sera of Prostate Cancer PatientsSerum miRNAs in Prostate Cancer. *Cancer research,* 71**,** 550-560.

MOMEN-HERAVI, F. & BALA, S. 2018. Extracellular vesicles in oral squamous carcinoma carry oncogenic miRNA profile and reprogram monocytes via NF-κB pathway. *Oncotarget,* 9**,** 34838.

MOMEN-HERAVI, F., BALAJ, L., ALIAN, S., TRACHTENBERG, A. J., HOCHBERG, F. H., SKOG, J. & KUO, W. P. 2012. Impact of biofluid viscosity on size and sedimentation efficiency of the isolated microvesicles. *Frontiers in physiology,* 3**,** 162.

MONTECALVO, A., LARREGINA, A. T., SHUFESKY, W. J., BEER STOLZ, D., SULLIVAN, M. L., KARLSSON, J. M., BATY, C. J., GIBSON, G. A., ERDOS, G. & WANG, Z. 2012. Mechanism of transfer of functional microRNAs between mouse dendritic cells via exosomes. *Blood, The Journal of the American Society of Hematology,* 119**,** 756-766.

MONTERO, P. H. & PATEL, S. G. 2015. Cancer of the oral cavity. *Surg Oncol Clin N Am,* 24**,** 491-508.

MOREL, O., TOTI, F., MOREL, N. & FREYSSINET, J.-M. 2009. Microparticles in endothelial cell and vascular homeostasis: are they really noxious *haematologica,* 94**,** 313.

MORELLI, A. E., LARREGINA, A. T., SHUFESKY, W. J., SULLIVAN, M. L., STOLZ, D. B., PAPWORTH, G. D., ZAHORCHAK, A. F., LOGAR, A. J., WANG, Z. & WATKINS, S. C. 2004. Endocytosis, intracellular sorting, and processing of exosomes by dendritic cells. *Blood,* 104**,** 3257-3266.

MORELLO, M., MINCIACCHI, V., DE CANDIA, P., YANG, J., POSADAS, E., KIM, H., GRIFFITHS, D., BHOWMICK, N., CHUNG, L. & GANDELLINI, P. 2013. Large oncosomes mediate intercellular transfer of functional microRNA. *Cell cycle,* 12**,** 3526-3536.

MORFIT, H. M. 1956. Cancer of the Mouth and Neck. *Postgraduate medicine,* 20**,** 283-291.

MORI, K., HIROI, M., SHIMADA, J. & OHMORI, Y. 2011. Infiltration of m2 tumor-associated macrophages in oral squamous cell carcinoma correlates with tumor malignancy. *Cancers,* 3**,** 3726-3739.

MOSKOVITZ, J., MOY, J. & FERRIS, R. L. 2018. Immunotherapy for head and neck squamous cell carcinoma. *Current oncology reports,* 20**,** 1-7.

MULCAHY, L. A., PINK, R. C. & CARTER, D. R. F. 2014. Routes and mechanisms of extracellular vesicle uptake. *Journal of extracellular vesicles,* 3**,** 24641.

MULLER, L., HONG, C.-S., STOLZ, D. B., WATKINS, S. C. & WHITESIDE, T. L. 2014. Isolation of biologically-active exosomes from human plasma. *Journal of immunological methods,* 411**,** 55-65.

MULLIGAN, J. K., ROSENZWEIG, S. A. & YOUNG, M. R. I. 2010. Tumor secretion of VEGF induces endothelial cells to suppress T cell functions through the production of PGE2. *Journal of Immunotherapy (Hagerstown, Md.: 1997),* 33**,** 126.

MUMFORD, S. L., TOWLER, B. P., PASHLER, A. L., GILLEARD, O., MARTIN, Y. & NEWBURY, S. F. 2018. Circulating microRNA biomarkers in melanoma: tools and challenges in personalised medicine. *Biomolecules,* 8**,** 21.

NAAKKA, E., BARROS-FILHO, M. C., ADNAN-AWAD, S., AL-SAMADI, A., MARCHI, F. A., KUASNE, H., KORELIN, K., SULEYMANOVA, I., BROWN, A. L., SCAPULATEMPO-NETO, C., LOURENÇO, S. V., CASTILHO, R. M., KOWALSKI, L. P., MÄKITIE, A., ARAÚJO, V. C., LEIVO, I., ROGATTO, S. R., SALO, T. & PASSADOR-SANTOS, F. 2022. miR-22 and miR-205 Drive

Tumor Aggressiveness of Mucoepidermoid Carcinomas of Salivary Glands. *Frontiers in Oncology,* 11.

NAGLER, R., BAHAR, G., SHPITZER, T. & FEINMESSER, R. 2006. Concomitant analysis of salivary tumor markers—a new diagnostic tool for oral cancer. *Clinical Cancer Research,* 12**,** 3979-3984.

NANBO, A., KAWANISHI, E., YOSHIDA, R. & YOSHIYAMA, H. 2013. Exosomes derived from Epstein-Barr virus-infected cells are internalized via caveola-dependent endocytosis and promote phenotypic modulation in target cells. *Journal of virology,* 87**,** 10334-10347.

NEJATI, K., ALIVAND, M. & ARABZADEH, A. 2021. MicroRNA-22 in female malignancies: focusing on breast, cervical, and ovarian cancers. *Pathology-Research and Practice,* 223**,** 153452.

NEUBERGER, E. W. I., HILLEN, B., MAYR, K., SIMON, P., KRÄMER-ALBERS, E.-M. & BRAHMER, A. 2021. Kinetics and Topology of DNA Associated with Circulating Extracellular Vesicles Released during Exercise. *Genes,* 12**,** 522.

NEVILLE, B., DAMM, D. & ALLEN, C. 2009. Melanotic neuroectodermal tumor of infancy. *Oral and maxillofacial pathology, 3rd edn. Saunders/Elsevier, St. Louis,* 533534.

NEWMAN, L. A., FAHMY, A., SORICH, M. J., BEST, O. G., ROWLAND, A. & USECKAITE, Z. 2021. Importance of between and within Subject Variability in Extracellular Vesicle Abundance and Cargo when Performing Biomarker Analyses. *Cells,* 10**,** 485.

NIK MOHAMED KAMAL, N. N. S., AWANG, R. A. R., MOHAMAD, S. & SHAHIDAN, W. N. S. 2020. Plasma-and saliva exosome profile reveals a distinct MicroRNA signature in chronic periodontitis. *Frontiers in physiology***,** 1561.

NOLTE-'T HOEN, E. N., BUERMANS, H. P., WAASDORP, M., STOORVOGEL, W., WAUBEN, M. H. & T HOEN, P. A. 2012. Deep sequencing of RNA from immune cell-derived vesicles uncovers the selective incorporation of small non-coding RNA biotypes with potential regulatory functions. *Nucleic Acids Res,* 40**,** 9272-85.

NONAKA, T. & WONG, D. 2018. Liquid biopsy in head and neck cancer: promises and challenges. *Journal of dental research,* 97**,** 701-708.

NONAKA, T. & WONG, D. T. W. 2017. Saliva-Exosomics in Cancer: Molecular Characterization of Cancer-Derived Exosomes in Saliva. *Enzymes,* 42**,** 125-151.

NUNVAR, J., PAGACOVA, L., VOJTECHOVA, Z., AZEVEDO, N. T. D. D., SMAHELOVA, J., SALAKOVA, M. & TACHEZY, R. 2021. Lack of Conserved miRNA Deregulation in HPV-Induced Squamous Cell Carcinomas. *Biomolecules,* 11**,** 764.

O'LOGHLEN, A. 2018. Role for extracellular vesicles in the tumour microenvironment. *Philosophical Transactions of the Royal Society B: Biological Sciences,* 373**,** 20160488.

O'NEILL, C. P., GILLIGAN, K. E. & DWYER, R. M. 2019. Role of extracellular vesicles (EVs) in cell stress response and resistance to cancer therapy. *Cancers,* 11**,** 136.

OGATA-KAWATA, H., IZUMIYA, M., KURIOKA, D., HONMA, Y., YAMADA, Y., FURUTA, K., GUNJI, T., OHTA, H., OKAMOTO, H. & SONODA, H. 2014. Circulating exosomal microRNAs as biomarkers of colon cancer. *PloS one,* 9**,** e92921.

OGAWA, Y., KANAI-AZUMA, M., AKIMOTO, Y., KAWAKAMI, H. & YANOSHITA, R. 2008. Exosome-like vesicles with dipeptidyl peptidase IV in human saliva. *Biological and Pharmaceutical Bulletin,* 31**,** 1059-1062.

OGAWA, Y., MIURA, Y., HARAZONO, A., KANAI-AZUMA, M., AKIMOTO, Y., KAWAKAMI, H., YAMAGUCHI, T., TODA, T., ENDO, T. & TSUBUKI, M. 2011. Proteomic analysis of two

types of exosomes in human whole saliva. *Biological and Pharmaceutical Bulletin,* 34**,** 13-23.

OGAWA, Y., TSUJIMOTO, M. & YANOSHITA, R. 2016. Next-generation sequencing of protein-coding and long non-protein-coding RNAs in two types of exosomes derived from human whole saliva. *Biological and Pharmaceutical Bulletin,* 39**,** 1496-1507.

OKSVOLD, M. P., NEURAUTER, A. & PEDERSEN, K. W. 2015. Magnetic Bead-Based Isolation of Exosomes. Springer New York.

ONÓDI, Z., PELYHE, C., TERÉZIA NAGY, C., BRENNER, G. B., ALMÁSI, L., KITTEL, Á., MANČEK-KEBER, M., FERDINANDY, P., BUZÁS, E. I. & GIRICZ, Z. 2018. Isolation of high-purity extracellular vesicles by the combination of iodixanol density gradient ultracentrifugation and bind-elute chromatography from blood plasma. *Frontiers in physiology,* 9**,** 1479.

OSTENFELD, M. S., JEPPESEN, D. K., LAURBERG, J. R., BOYSEN, A. T., BRAMSEN, J. B., PRIMDAL-BENGTSON, B., HENDRIX, A., LAMY, P., DAGNAES-HANSEN, F. & RASMUSSEN, M. H. 2014. Cellular disposal of miR23b by RAB27-dependent exosome release is linked to acquisition of metastatic properties. *Cancer research,* 74**,** 5758-5771.

OSTROUMOV, D., FEKETE-DRIMUSZ, N., SABOROWSKI, M., KÜHNEL, F. & WOLLER, N. 2018. CD4 and CD8 T lymphocyte interplay in controlling tumor growth. *Cellular and molecular life sciences,* 75**,** 689-713.

OTTO, G. P. & NICHOLS, B. J. 2011. The roles of flotillin microdomains–endocytosis and beyond. *Journal of cell science,* 124**,** 3933-3940.

PALANISAMY, V., SHARMA, S., DESHPANDE, A., ZHOU, H., GIMZEWSKI, J. & WONG, D. T. 2010. Nanostructural and transcriptomic analyses of human saliva derived exosomes. *PloS one,* 5**,** e8577.

PAN, B. T. & JOHNSTONE, R. M. 1983. Fate of the transferrin receptor during maturation of sheep reticulocytes in vitro: selective externalization of the receptor. *Cell,* 33**,** 967-78.

PARK, N. J., ZHOU, H., ELASHOFF, D., HENSON, B. S., KASTRATOVIC, D. A., ABEMAYOR, E. & WONG, D. T. 2009. Salivary microRNA: discovery, characterization, and clinical utility for oral cancer detection. *Clinical Cancer Research,* 15**,** 5473-5477.

PAROLINI, I., FEDERICI, C., RAGGI, C., LUGINI, L., PALLESCHI, S., DE MILITO, A., COSCIA, C., IESSI, E., LOGOZZI, M. & MOLINARI, A. 2009. Microenvironmental pH is a key factor for exosome traffic in tumor cells. *Journal of Biological Chemistry,* 284**,** 34211-34222.

PATRO, R., DUGGAL, G., LOVE, M. I., IRIZARRY, R. A. & KINGSFORD, C. 2017. Salmon provides fast and bias-aware quantification of transcript expression. *Nat Methods,* 14**,** 417-419.

PEACOCK, B., RIGBY, A., BRADFORD, J., PINK, R., HUNTER, K., LAMBERT, D. & HUNT, S. 2018. Extracellular vesicle micro RNA cargo is correlated with HPV status in oropharyngeal carcinoma. *Journal of Oral Pathology & Medicine,* 47**,** 954-963.

PELTANOVA, B., RAUDENSKA, M. & MASARIK, M. 2019. Effect of tumor microenvironment on pathogenesis of the head and neck squamous cell carcinoma: a systematic review. *Molecular cancer,* 18**,** 1-24.

PELTIER, H. J. & LATHAM, G. J. 2008. Normalization of microRNA expression levels in quantitative RT-PCR assays: identification of suitable reference RNA targets in normal and cancerous human solid tissues. *Rna,* 14**,** 844-852.

PENG, J., WANG, R., SUN, W., HUANG, M., WANG, R., LI, Y., WANG, P., SUN, G. & XIE, S. 2021. Delivery of miR-320a-3p by gold nanoparticles combined with photothermal therapy for directly targeting Sp1 in lung cancer. Biomaterials Science, 9, 6528-6541.

Peng, Y. and Croce, C.M., 2016. The role of MicroRNAs in human cancer. Signal transduction and targeted therapy, 1(1), pp.1-9.

PERDOMO, S., ROA, G. M., BRENNAN, P., FORMAN, D. & SIERRA, M. S. 2016. Head and neck cancer burden and preventive measures in Central and South America. *Cancer epidemiology,* 44**,** S43-S52.

PEREIRA, E. R., JONES, D., JUNG, K. & PADERA, T. P. The lymph node microenvironment and its role in the progression of metastatic cancer. Seminars in cell & developmental biology, 2015. Elsevier, 98-105.

PERNOT, E., CARDIS, E. & BADIE, C. 2014. Usefulness of saliva samples for biomarker studies in radiation research. *Cancer Epidemiology, Biomarkers & Prevention,* 23**,** 2673-2680.

PETERSON, M. F., OTOC, N., SETHI, J. K., GUPTA, A. & ANTES, T. J. 2015. Integrated systems for exosome investigation. *Methods,* 87**,** 31-45.

PETKEVICH, A. A., ABRAMOV, A. A., POSPELOV, V. I., MALININA, N. A., KUHAREVA, E. I., MAZURCHIK, N. V. & TARASOVA, O. I. 2021. Exosomal and non-exosomal miRNA expression levels in patients with HCV-related cirrhosis and liver cancer. *Oncotarget,* 12**,** 1697-1706.

PETTI, S. 2009. Lifestyle risk factors for oral cancer. *Oral oncology,* 45**,** 340-350.

PIENIMAEKI-ROEMER, A., KUHLMANN, K., BÖTTCHER, A., KONOVALOVA, T., BLACK, A., ORSÓ, E., LIEBISCH, G., AHRENS, M., EISENACHER, M. & MEYER, H. E. 2015. Lipidomic and proteomic characterization of platelet extracellular vesicle subfractions from senescent platelets. *Transfusion,* 55**,** 507-521.

PIETERSE, E. & VAN DER VLAG, J. 2014. Breaking immunological tolerance in systemic lupus erythematosus. *Frontiers in immunology,* 5**,** 164.

PISITKUN, T., SHEN, R.-F. & KNEPPER, M. A. 2004. Identification and proteomic profiling of exosomes in human urine. *Proceedings of the National Academy of Sciences,* 101**,** 13368-13373.

PLATT, F. M., NEISES, G. R., DWEK, R. A. & BUTTERS, T. D. 1994. N-butyldeoxynojirimycin is a novel inhibitor of glycolipid biosynthesis. *Journal of Biological Chemistry,* 269**,** 8362-8365.

PRINCIPE, S., HUI, A. B. Y., BRUCE, J., SINHA, A., LIU, F. F. & KISLINGER, T. 2013. Tumor-derived exosomes and microvesicles in head and neck cancer: Implications for tumor biology and biomarker discovery. *Proteomics,* 13**,** 1608-1623.

PROVENZANO, P. P., ELICEIRI, K. W., CAMPBELL, J. M., INMAN, D. R., WHITE, J. G. & KEELY, P. J. 2006. Collagen reorganization at the tumor-stromal interface facilitates local invasion. *BMC medicine,* 4**,** 1-15.

PUNYANI, S. R. & SATHAWANE, R. S. 2013. Salivary level of interleukin-8 in oral precancer and oral squamous cell carcinoma. *Clinical Oral Investigations,* 17**,** 517-524.

QIN, W., WANG, W., WANG, X., ZHANG, X. & DU, J. 2019. MiR-1290 targets CCNG2 to promote the metastasis of oral squamous cell carcinoma. *Eur. Rev. Med. Pharmacol. Sci,* 23**,** 10332-10342.

QU, Y., LIU, H., LV, X., LIU, Y., WANG, X., ZHANG, M., ZHANG, X., LI, Y., LOU, Q., LI, S. & LI, H. 2017. MicroRNA-16-5p overexpression suppresses proliferation and invasion as well as triggers apoptosis by targeting VEGFA expression in breast carcinoma. *Oncotarget,* 8**,** 72400-72410.

RAK, J. 2013. Extracellular vesicles–biomarkers and effectors of the cellular interactome in cancer. *Frontiers in pharmacology,* 4**,** 21.

RAK, J. & GUHA, A. 2012. Extracellular vesicles–vehicles that spread cancer genes. *Bioessays,* 34**,** 489-497.

RAMIREZ, M. I., AMORIM, M. G., GADELHA, C., MILIC, I., WELSH, J. A., FREITAS, V. M., NAWAZ, M., AKBAR, N., COUCH, Y., MAKIN, L., COOKE, F., VETTORE, A. L., BATISTA, P. X., FREEZOR, R., PEZUK, J. A., ROSA-FERNANDES, L., CARREIRA, A. C. O., DEVITT, A., JACOBS, L., SILVA, I. T., COAKLEY, G., NUNES, D. N., CARTER, D., PALMISANO, G. & DIAS-NETO, E. 2018. Technical challenges of working with extracellular vesicles. *Nanoscale,* 10**,** 881-906.

RANA, S., YUE, S., STADEL, D. & ZÖLLER, M. 2012. Toward tailored exosomes: the exosomal tetraspanin web contributes to target cell selection. *The international journal of biochemistry & cell biology,* 44**,** 1574-1584.

RAO, P. V., REDDY, A. P., LU, X., DASARI, S., KRISHNAPRASAD, A., BIGGS, E., ROBERTS JR, C. T. & NAGALLA, S. R. 2009. Proteomic identification of salivary biomarkers of type-2 diabetes. *Journal of proteome research,* 8**,** 239-245.

RAPOSO, G., NIJMAN, H. W., STOORVOGEL, W., LIEJENDEKKER, R., HARDING, C. V., MELIEF, C. & GEUZE, H. J. 1996a. B lymphocytes secrete antigen-presenting vesicles. *The Journal of experimental medicine,* 183**,** 1161-1172.

RAPOSO, G., NIJMAN, H. W., STOORVOGEL, W., LIEJENDEKKER, R., HARDING, C. V., MELIEF, C. J. & GEUZE, H. J. 1996b. B lymphocytes secrete antigen-presenting vesicles. *Journal of Experimental Medicine,* 183**,** 1161-1172.

RATAJCZAK, J., MIEKUS, K., KUCIA, M., ZHANG, J., RECA, R., DVORAK, P. & RATAJCZAK, M. Z. 2006a. Embryonic stem cell-derived microvesicles reprogram hematopoietic progenitors: evidence for horizontal transfer of mRNA and protein delivery. *Leukemia,* 20**,** 847-56.

RATAJCZAK, J., WYSOCZYNSKI, M., HAYEK, F., JANOWSKA-WIECZOREK, A. & RATAJCZAK, M. 2006b. Membrane-derived microvesicles: important and underappreciated mediators of cell-to-cell communication. *Leukemia,* 20**,** 1487-1495.

REIBEL, J. 2003. Prognosis of oral pre-malignant lesions: significance of clinical, histopathological, and molecular biological characteristics. *Critical Reviews in Oral Biology & Medicine,* 14**,** 47-62.

REITHMAIR, M., LINDEMANN, A., MUSSACK, V. & PFAFFL, M. W. 2022. Isolation and Characterization of Urinary Extracellular Vesicles for MicroRNA Biomarker Signature Development with Reference to MISEV Compliance. Springer US.

REN, W., QIANG, C., GAO, L., LI, S.-M., ZHANG, L.-M., WANG, X.-L., DONG, J.-W., CHEN, C., LIU, C.-Y. & ZHI, K.-Q. 2014. Circulating microRNA-21 (MIR-21) and phosphatase and tensin homolog (PTEN) are promising novel biomarkers for detection of oral squamous cell carcinoma. *Biomarkers,* 19**,** 590-596.

REYES, M., FLORES, T., BETANCUR, D., PEÑA-OYARZÚN, D. & TORRES, V. A. 2020. Wnt/β-catenin signaling in oral carcinogenesis. *International Journal of Molecular Sciences,* 21**,** 4682.

RIAZIFAR, M., PONE, E. J., LÖTVALL, J. & ZHAO, W. 2017. Stem cell extracellular vesicles: extended messages of regeneration. *Annual review of pharmacology and toxicology,* 57**,** 125-154.

RIDDER, K., SEVKO, A., HEIDE, J., DAMS, M., RUPP, A.-K., MACAS, J., STARMANN, J., TJWA, M., PLATE, K. H. & SÜLTMANN, H. 2015. Extracellular vesicle-mediated transfer of functional RNA in the tumor microenvironment. *Oncoimmunology,* 4**,** e1008371.

RIVERA, C. 2015. Essentials of oral cancer. *International journal of clinical and experimental pathology,* 8**,** 11884.

ROHLEDER, N. & NATER, U. M. 2009. Determinants of salivary alpha-amylase in humans and methodological considerations. *Psychoneuroendocrinology,* 34**,** 469-85.

ROMANI, C., SALVIATO, E., PADERNO, A., ZANOTTI, L., RAVAGGI, A., DEGANELLO, A., BERRETTI, G., GUALTIERI, T., MARCHINI, S., D'INCALCI, M., MATTAVELLI, D., PIAZZA, C., BOSSI, P., ROMUALDI, C., NICOLAI, P. & BIGNOTTI, E. 2021. Genome-wide study of salivary miRNAs identifies miR-423-5p as promising diagnostic and prognostic biomarker in oral squamous cell carcinoma. *Theranostics,* 11**,** 2987-2999.

RONG, L., LI, R., LI, S. & LUO, R. 2016. Immunosuppression of breast cancer cells mediated by transforming growth factor-β in exosomes from cancer cells. *Oncology letters,* 11**,** 500-504.

ROSENTHAL, E., MCCRORY, A., TALBERT, M., YOUNG, G., MURPHY-ULLRICH, J. & GLADSON, C. 2004. Elevated expression of TGF-β1 in head and neck cancer–associated fibroblasts. *Molecular Carcinogenesis: Published in cooperation with the University of Texas MD Anderson Cancer Center,* 40**,** 116-121.

ROYLE, S. J. 2006. The cellular functions of clathrin. *Cellular and Molecular Life Sciences CMLS,* 63**,** 1823-1832.

RUIZ-VILLALBA, A., RUIJTER, J. M. & VAN DEN HOFF, M. J. B. 2021. Use and Misuse of Cq in qPCR Data Analysis and Reporting. *Life,* 11**,** 496.

RUSSELL, A. E., SNEIDER, A., WITWER, K. W., BERGESE, P., BHATTACHARYYA, S. N., COCKS, A., COCUCCI, E., ERDBRÜGGER, U., FALCON-PEREZ, J. M. & FREEMAN, D. W. 2019. Biological membranes in EV biogenesis, stability, uptake, and cargo transfer: an ISEV position paper arising from the ISEV membranes and EVs workshop. *Journal of Extracellular Vesicles,* 8**,** 1684862.

RUTTER, B. D. & INNES, R. W. 2017. Extracellular vesicles isolated from the leaf apoplast carry stress-response proteins. *Plant physiology,* 173**,** 728-741.

SAKHA, S., MURAMATSU, T., UEDA, K. & INAZAWA, J. 2016. Exosomal microRNA miR-1246 induces cell motility and invasion through the regulation of DENND2D in oral squamous cell carcinoma. *Scientific Reports,* 6**,** 38750.

SAMAN, S., KIM, W., RAYA, M., VISNICK, Y., MIRO, S., SAMAN, S., JACKSON, B., MCKEE, A. C., ALVAREZ, V. E. & LEE, N. C. 2012. Exosome-associated tau is secreted in tauopathy models and is selectively phosphorylated in cerebrospinal fluid in early Alzheimer disease. *Journal of biological chemistry,* 287**,** 3842-3849.

SAMSONOV, R., BURDAKOV, V., SHTAM, T., RADZHABOVA, Z., VASILYEV, D., TSYRLINA, E., TITOV, S., IVANOV, M., BERSTEIN, L., FILATOV, M., KOLESNIKOV, N., GIL-HENN, H. & MALEK, A. 2016. Plasma exosomal miR-21 and miR-181a differentiates follicular from papillary thyroid cancer. *Tumor Biology,* 37**,** 12011-12021.

SANDHU, S. K., FASSAN, M., VOLINIA, S., LOVAT, F., BALATTI, V., PEKARSKY, Y. & CROCE, C. M. 2013. B-cell malignancies in microRNA Eμ-miR-17∼ 92 transgenic mice. *Proceedings of the National Academy of Sciences,* 110**,** 18208-18213.

SANNIGRAHI, M., SHARMA, R., PANDA, N. & KHULLAR, M. 2018. Role of non-coding RNA s in head and neck squamous cell carcinoma: A narrative review. *Oral Diseases,* 24**,** 1417-1427.

SAPRE, N., HONG, M. K., MACINTYRE, G., LEWIS, H., KOWALCZYK, A., COSTELLO, A. J., CORCORAN, N. M. & HOVENS, C. M. 2014. Curated microRNAs in urine and blood fail to validate as predictive biomarkers for high-risk prostate cancer. *PLoS One,* 9**,** e91729.

SATO, S., VASAIKAR, S., ESKAROS, A., KIM, Y., LEWIS, J. S., ZHANG, B., ZIJLSTRA, A. & WEAVER, A. M. 2019. EPHB2 carried on small extracellular vesicles induces tumor angiogenesis via activation of ephrin reverse signaling. *JCI insight,* 4.

SCANNAPIECO, F. A., TORRES, G. & LEVINE, M. J. 1993. Salivary α-amylase: role in dental plaque and caries formation. *Critical Reviews in Oral Biology & Medicine,* 4**,** 301-307.

SCHAFER, C. A., SCHAFER, J. J., YAKOB, M., LIMA, P., CAMARGO, P. & WONG, D. T. 2014. Saliva diagnostics: utilizing oral fluids to determine health status. *Saliva: Secretion and Functions,* 24**,** 88-98.

SCHEPELER, T., REINERT, J. T., OSTENFELD, M. S., CHRISTENSEN, L. L., SILAHTAROGLU, A. N., DYRSKJØT, L., WIUF, C., SØRENSEN, F. J., KRUHØFFER, M. & LAURBERG, S. 2008. Diagnostic and prognostic microRNAs in stage II colon cancer. *Cancer research,* 68**,** 6416-6424.

Scheinberg, I.H., 1954. Clinical implications of plasma fractionation. Bulletin of the New York Academy of Medicine, 30(10), p.735.

SCHNEIDER, A., VICTORIA, B., LOPEZ, Y. N., SUCHORSKA, W., BARCZAK, W., SOBECKA, A., GOLUSINSKI, W., MASTERNAK, M. M. & GOLUSINSKI, P. 2018. Tissue and serum microRNA profile of oral squamous cell carcinoma patients. *Scientific Reports,* 8.

SCHUH, A. L. & AUDHYA, A. 2014. The ESCRT machinery: From the plasma membrane to endosomes and back again. *Critical Reviews in Biochemistry and Molecular Biology,* 49**,** 242-261.

SERGUIENKO, A., GRAD, I., WENNERSTRØM, A. B., MEZA-ZEPEDA, L. A., THIEDE, B., STRATFORD, E. W., MYKLEBOST, O. & MUNTHE, E. 2015. Metabolic reprogramming of metastatic breast cancer and melanoma by let-7a microRNA. *Oncotarget,* 6**,** 2451.

SHAH, K. M., WEBBER, J., CARZANIGA, R., TAYLOR, D. M., FUSI, L., CLAYTON, A., BROSENS, J. J., HARTSHORNE, G. & CHRISTIAN, M. 2013. Induction of microRNA resistance and secretion in differentiating human endometrial stromal cells. *Journal of molecular cell biology,* 5**,** 67-70.

SHARMA, S., GILLESPIE, B. M., PALANISAMY, V. & GIMZEWSKI, J. K. 2011. Quantitative nanostructural and single-molecule force spectroscopy biomolecular analysis of human-saliva-derived exosomes. *Langmuir,* 27**,** 14394-14400.

SHARMA, S., RASOOL, H. I., PALANISAMY, V., MATHISEN, C., SCHMIDT, M., WONG, D. T. & GIMZEWSKI, J. K. 2010. Structural-mechanical characterization of nanoparticle exosomes in human saliva, using correlative AFM, FESEM, and force spectroscopy. *ACS nano,* 4**,** 1921-1926.

SHEN, H., WENG, X. D., LIU, X. H., YANG, D., WANG, L., GUO, J., WANG, M., WANG, X. & DIAO, C. H. 2018. miR-181a-5p is downregulated and inhibits proliferation and the cell cycle in prostate cancer. *Int J Clin Exp Pathol,* 11**,** 3969-3976.

SHEN, J., HRUBY, G. W., MCKIERNAN, J. M., GURVICH, I., LIPSKY, M. J., BENSON, M. C. & SANTELLA, R. M. 2012. Dysregulation of circulating microRNAs and prediction of aggressive prostate cancer. *The Prostate,* 72**,** 1469-1477.

SHIMODA, M. & KHOKHA, R. 2013. Proteolytic factors in exosomes. *Proteomics,* 13**,** 1624-1636.

SHIN, V., SIU, J., CHEUK, I., NG, E. & KWONG, A. 2015. Circulating cell-free miRNAs as biomarker for triple-negative breast cancer. *British journal of cancer,* 112**,** 1751-1759.

SHTAM, T., SAMSONOV, R., KAMYSHINSKY, R., PANTINA, R., VERLOV, N., VASILIEV, A., KONEVEGA, A. & MALEK, A. Exosomes: Some approaches to cancer diagnosis and therapy. AIP Conference Proceedings, 2017. AIP Publishing LLC, 020066.

SHURTLEFF, M. J., TEMOCHE-DIAZ, M. M., KARFILIS, K. V., RI, S. & SCHEKMAN, R. 2016. Y-box protein 1 is required to sort microRNAs into exosomes in cells and in a cell-free reaction. *elife,* 5**,** e19276.

SIMKIN, M., ABDALLA, M., EL-MOGY, M. & HAJ-AHMAD, Y. 2012. Differences in the quantity of DNA found in the urine and saliva of smokers versus nonsmokers: implications for the timing of epigenetic events. Epigenomics, 4, 343-52.

Simonsen, J.B., 2017. What are we looking at? Extracellular vesicles, lipoproteins, or both?. Circulation research, 121(8), pp.920-922.

SIMONSEN, J. B. 2017. What Are We Looking At? Extracellular Vesicles, Lipoproteins, or Both? Circulation Research, 121, 920-922.

SITAR, S., KEJŽAR, A., PAHOVNIK, D., KOGEJ, K., TUŠEK-ŽNIDARIČ, M., LENASSI, M. & ŽAGAR, E. 2015. Size characterization and quantification of exosomes by asymmetrical-flow field-flow fractionation. *Anal Chem,* 87**,** 9225-33.

SKOGBERG, G., GUDMUNDSDOTTIR, J., VAN DER POST, S., SANDSTRÖM, K., BRUHN, S., BENSON, M., MINCHEVA-NILSSON, L., BARANOV, V., TELEMO, E. & EKWALL, O. 2013. Characterization of human thymic exosomes. *PloS one,* 8**,** e67554.

SLOMIANY, B. L., MURTY, V. L. N. & SLOMIANY, A. 1985. Salivary lipids in health and disease. *Progress in lipid research,* 24 4**,** 311-24.

SMART, E. J., GRAF, G. A., MCNIVEN, M. A., SESSA, W. C., ENGELMAN, J. A., SCHERER, P. E., OKAMOTO, T. & LISANTI, M. P. 1999. Caveolins, liquid-ordered domains, and signal transduction. *Molecular and cellular biology,* 19**,** 7289-7304.

SÓDAR, B. W., KITTEL, Á., PÁLÓCZI, K., VUKMAN, K. V., OSTEIKOETXEA, X., SZABÓ-TAYLOR, K., NÉMETH, A., SPERLÁGH, B., BARANYAI, T., GIRICZ, Z., WIENER, Z., TURIÁK, L., DRAHOS, L., PÁLLINGER, É., VÉKEY, K., FERDINANDY, P., FALUS, A. & BUZÁS, E. I. 2016. Low-density lipoprotein mimics blood plasma-derived exosomes and microvesicles during isolation and detection. *Scientific Reports,* 6**,** 24316.

SOEKMADJI, C., HILL, A. F., WAUBEN, M. H., BUZÁS, E. I., DI VIZIO, D., GARDINER, C., LÖTVALL, J., SAHOO, S. & WITWER, K. W. 2018. Towards mechanisms and standardization in extracellular vesicle and extracellular RNA studies: results of a worldwide survey. *Journal of extracellular vesicles,* 7**,** 1535745.

SOURVINOU, I. S., MARKOU, A. & LIANIDOU, E. S. 2013. Quantification of circulating miRNAs in plasma: effect of preanalytical and analytical parameters on their isolation and stability. *The Journal of Molecular Diagnostics,* 15**,** 827-834.

STAM, J., BARTEL, S., BISCHOFF, R. & WOLTERS, J. C. 2021. Isolation of extracellular vesicles with combined enrichment methods. *Journal of Chromatography B,* 1169**,** 122604.

STATELLO, L., MAUGERI, M., GARRE, E., NAWAZ, M., WAHLGREN, J., PAPADIMITRIOU, A., LUNDQVIST, C., LINDFORS, L., COLLEN, A. & SUNNERHAGEN, P. 2018. Identification of RNA-binding proteins in exosomes capable of interacting with different types of RNA: RBP-facilitated transport of RNAs into exosomes. *PloS one,* 13**,** e0195969.

STRANSKA, R., GYSBRECHTS, L., WOUTERS, J., VERMEERSCH, P., BLOCH, K., DIERICKX, D., ANDREI, G. & SNOECK, R. 2018. Comparison of membrane affinity-based method with size-exclusion chromatography for isolation of exosome-like vesicles from human plasma. *Journal of translational medicine,* 16**,** 1-9.

STREET, J. M., BARRAN, P. E., MACKAY, C. L., WEIDT, S., BALMFORTH, C., WALSH, T. S., CHALMERS, R. T., WEBB, D. J. & DEAR, J. W. 2012. Identification and proteomic profiling of exosomes in human cerebrospinal fluid. *Journal of translational medicine,* 10**,** 1-7.

SUI, Z., ZHANG, Y., TU, S., XIE, J., HUANG, W., PENG, T., DONG, L., YANG, J., OUYANG, Y., LIU, S., LI, L., WANG, Z., PENG, K., FANG, X. & DAI, X. 2021. Evaluation of saliva as an alternative diagnostic specimen source for SARS-CoV-2 detection by RT-dPCR. *J Infect,* 82**,** e38-e40.

SULLIVAN, R., SAEZ, F., GIROUARD, J. & FRENETTE, G. 2005. Role of exosomes in sperm maturation during the transit along the male reproductive tract. *Blood Cells, Molecules, and Diseases,* 35**,** 1-10.

SUMMERER, I., UNGER, K., BRASELMANN, H., SCHUETTRUMPF, L., MAIHOEFER, C., BAUMEISTER, P., KIRCHNER, T., NIYAZI, M., SAGE, E., SPECHT, H. M., MULTHOFF, G., MOERTL, S., BELKA, C. & ZITZELSBERGER, H. 2015. Circulating microRNAs as prognostic therapy biomarkers in head and neck cancer patients. *British Journal of Cancer,* 113**,** 76-82.

SUN, X., MA, X., WANG, J., ZHAO, Y., WANG, Y., BIHL, J. C., CHEN, Y. & JIANG, C. 2017. Glioma stem cells-derived exosomes promote the angiogenic ability of endothelial cells through miR-21/VEGF signal. *Oncotarget,* 8**,** 36137.

SUN, Y., HUO, C., QIAO, Z., SHANG, Z., UZZAMAN, A., LIU, S., JIANG, X., FAN, L.-Y., JI, L. & GUAN, X. 2018. Comparative proteomic analysis of exosomes and microvesicles in human saliva for lung cancer. *Journal of proteome research,* 17**,** 1101-1107.

SUN, Y., XIA, Z., SHANG, Z., SUN, K., NIU, X., QIAN, L., FAN, L.-Y., CAO, C.-X. & XIAO, H. 2016. Facile preparation of salivary extracellular vesicles for cancer proteomics. *Scientific reports,* 6**,** 1-11.

SUNDAR, I. K., LI, D. & RAHMAN, I. 2019. Small RNA-sequence analysis of plasma-derived extracellular vesicle miRNAs in smokers and patients with chronic obstructive pulmonary disease as circulating biomarkers. *Journal of Extracellular Vesicles,* 8**,** 1684816.

SUZUKI, M., RAAB, G., MOSES, M. A., FERNANDEZ, C. A. & KLAGSBRUN, M. 1997. Matrix metalloproteinase-3 releases active heparin-binding EGF-like growth factor by cleavage at a specific juxtamembrane site. *Journal of Biological Chemistry,* 272**,** 31730-31737.

SVENSSON, K. J., CHRISTIANSON, H. C., WITTRUP, A., BOURSEAU-GUILMAIN, E., LINDQVIST, E., SVENSSON, L. M., MÖRGELIN, M. & BELTING, M. 2013. Exosome uptake depends on ERK1/2-heat shock protein 27 signaling and lipid Raft-mediated endocytosis negatively regulated by caveolin-1. *Journal of Biological Chemistry,* 288**,** 17713-17724.

SWANSON, J. A. 2008. Shaping cups into phagosomes and macropinosomes. *Nature reviews Molecular cell biology,* 9**,** 639-649.

SZATANEK, R., BAJ-KRZYWORZEKA, M., ZIMOCH, J., LEKKA, M., SIEDLAR, M. & BARAN, J. 2017. The methods of choice for extracellular vesicles (EVs) characterization. *International journal of molecular sciences,* 18**,** 1153.

SZATANEK, R., BARAN, J., SIEDLAR, M. & BAJ-KRZYWORZEKA, M. 2015. Isolation of extracellular vesicles: Determining the correct approach. *International journal of molecular medicine,* 36**,** 11-17.

SZCZEPANSKI, M. J., SZAJNIK, M., WELSH, A., WHITESIDE, T. L. & BOYIADZIS, M. 2011. Blast-derived microvesicles in sera from patients with acute myeloid leukemia suppress natural killer cell function via membrane-associated transforming growth factor-β1. *Haematologica,* 96**,** 1302.

TAKAHASHI, H., SAKAKURA, K., KAWABATA-IWAKAWA, R., ROKUDAI, S., TOYODA, M., NISHIYAMA, M. & CHIKAMATSU, K. 2015. Immunosuppressive activity of cancer-

associated fibroblasts in head and neck squamous cell carcinoma. *Cancer Immunology, Immunotherapy,* 64**,** 1407-1417.

TAKAHASHI, K., YOKOTA, S.-I., TATSUMI, N., FUKAMI, T., YOKOI, T. & NAKAJIMA, M. 2013. Cigarette smoking substantially alters plasma microRNA profiles in healthy subjects. *Toxicology and applied pharmacology,* 272**,** 154-160.

TALLANT, C., MARRERO, A. & GOMIS-RÜTH, F. X. 2010. Matrix metalloproteinases: fold and function of their catalytic domains. *Biochimica et Biophysica Acta (BBA)-Molecular Cell Research,* 1803**,** 20-28.

TAURO, B. J., GREENING, D. W., MATHIAS, R. A., JI, H., MATHIVANAN, S., SCOTT, A. M. & SIMPSON, R. J. 2012. Comparison of ultracentrifugation, density gradient separation, and immunoaffinity capture methods for isolating human colon cancer cell line LIM1863-derived exosomes. *Methods,* 56**,** 293-304.

TAYLOR, D. & GERCEL-TAYLOR, C. 2005. Tumour-derived exosomes and their role in cancer-associated T-cell signalling defects. *British journal of cancer,* 92**,** 305-311.

TAYLOR, D. D. & GERCEL-TAYLOR, C. 2008. MicroRNA signatures of tumor-derived exosomes as diagnostic biomarkers of ovarian cancer. *Gynecol Oncol,* 110**,** 13-21.

TAYLOR, D. D. & SHAH, S. 2015. Methods of isolating extracellular vesicles impact down-stream analyses of their cargoes. *Methods,* 87**,** 3-10.

TENG, Y., GAO, L., LOVELESS, R., RODRIGO, J. P., STROJAN, P., WILLEMS, S. M., NATHAN, C.-A., MÄKITIE, A. A., SABA, N. F. & FERLITO, A. 2021. The hidden link of exosomes to head and neck cancer. *Cancers,* 13**,** 5802.

TENG, Y., REN, Y., HU, X., MU, J., SAMYKUTTY, A., ZHUANG, X., DENG, Z., KUMAR, A., ZHANG, L. & MERCHANT, M. L. 2017. MVP-mediated exosomal sorting of miR-193a promotes colon cancer progression. *Nature communications,* 8**,** 1-16.

THAKUR, A., PARRA, D. C., MOTALLEBNEJAD, P., BROCCHI, M. & CHEN, H. J. 2022. Exosomes: small vesicles with big roles in cancer, vaccine development, and therapeutics. *Bioactive materials,* 10**,** 281-294.

THAKUR, B. K., ZHANG, H., BECKER, A., MATEI, I., HUANG, Y., COSTA-SILVA, B., ZHENG, Y., HOSHINO, A., BRAZIER, H. & XIANG, J. 2014. Double-stranded DNA in exosomes: a novel biomarker in cancer detection. *Cell research,* 24**,** 766-769.

THEODORAKI, M.-N., YERNENI, S. S., HOFFMANN, T. K., GOODING, W. E. & WHITESIDE, T. L. 2018. Clinical significance of PD-L1+ exosomes in plasma of head and neck cancer patients. *Clinical cancer research,* 24**,** 896-905.

THERY, C., AMIGORENA, S., RAPOSO, G. & CLAYTON, A. 2006. Curr Protoc Cell Biol. *2006; 22: Chapter 3 (Unit 3)*.

THÉRY, C., AMIGORENA, S., RAPOSO, G. & CLAYTON, A. 2006. Isolation and characterization of exosomes from cell culture supernatants and biological fluids. *Current protocols in cell biology,* 30**,** 3.22. 1-3.22. 29.

THÉRY, C., BOUSSAC, M., VÉRON, P., RICCIARDI-CASTAGNOLI, P., RAPOSO, G., GARIN, J. & AMIGORENA, S. 2001. Proteomic analysis of dendritic cell-derived exosomes: a secreted subcellular compartment distinct from apoptotic vesicles. *The Journal of Immunology,* 166**,** 7309-7318.

THÉRY, C., WITWER, K. W., AIKAWA, E., ALCARAZ, M. J., ANDERSON, J. D., ANDRIANTSITOHAINA, R., ANTONIOU, A., ARAB, T., ARCHER, F., ATKIN-SMITH, G. K., AYRE, D. C., BACH, J.-M., BACHURSKI, D., BAHARVAND, H., BALAJ, L., BALDACCHINO, S., BAUER, N. N., BAXTER, A. A., BEBAWY, M., BECKHAM, C., BEDINA ZAVEC, A., BENMOUSSA, A., BERARDI, A. C., BERGESE, P., BIELSKA, E., BLENKIRON, C., BOBIS-

WOZOWICZ, S., BOILARD, E., BOIREAU, W., BONGIOVANNI, A., BORRÀS, F. E., BOSCH, S., BOULANGER, C. M., BREAKEFIELD, X., BREGLIO, A. M., BRENNAN, M. Á., BRIGSTOCK, D. R., BRISSON, A., BROEKMAN, M. L., BROMBERG, J. F., BRYL-GÓRECKA, P., BUCH, S., BUCK, A. H., BURGER, D., BUSATTO, S., BUSCHMANN, D., BUSSOLATI, B., BUZÁS, E. I., BYRD, J. B., CAMUSSI, G., CARTER, D. R., CARUSO, S., CHAMLEY, L. W., CHANG, Y.-T., CHEN, C., CHEN, S., CHENG, L., CHIN, A. R., CLAYTON, A., CLERICI, S. P., COCKS, A., COCUCCI, E., COFFEY, R. J., CORDEIRO-DA-SILVA, A., COUCH, Y., COUMANS, F. A., COYLE, B., CRESCITELLI, R., CRIADO, M. F., D'SOUZA-SCHOREY, C., DAS, S., DATTA CHAUDHURI, A., DE CANDIA, P., DE SANTANA, E. F., DE WEVER, O., DEL PORTILLO, H. A., DEMARET, T., DEVILLE, S., DEVITT, A., DHONDT, B., DI VIZIO, D., DIETERICH, L. C., DOLO, V., DOMINGUEZ RUBIO, A. P., DOMINICI, M., DOURADO, M. R., DRIEDONKS, T. A., DUARTE, F. V., DUNCAN, H. M., EICHENBERGER, R. M., EKSTRÖM, K., EL ANDALOUSSI, S., ELIE-CAILLE, C., ERDBRÜGGER, U., FALCÓN-PÉREZ, J. M., FATIMA, F., FISH, J. E., FLORES-BELLVER, M., FÖRSÖNITS, A., FRELET-BARRAND, A., et al. 2018a. Minimal information for studies of extracellular vesicles 2018 (MISEV2018): a position statement of the International Society for Extracellular Vesicles and update of the MISEV2014 guidelines. *Journal of Extracellular Vesicles,* 7**,** 1535750.

.

THÉRY, C., ZITVOGEL, L. & AMIGORENA, S. 2002. Exosomes: composition, biogenesis and function. *Nature reviews immunology,* 2**,** 569-579.

THOMSEN, L. T. & KJÆR, S. K. 2019. Women with cervical cancer precursor lesions: a high-risk group for human papillomavirus (HPV)-related oropharyngeal cancer? : Taylor & Francis.

TIAN, F., SHEN, Y., CHEN, Z., LI, R. & GE, Q. 2017. No significant difference between plasma miRNAs and plasma-derived exosomal miRNAs from healthy people. *BioMed research international,* 2017.

TONINI, T., ROSSI, F. & CLAUDIO, P. P. 2003. Molecular basis of angiogenesis and cancer. *Oncogene,* 22**,** 6549-6556.

TRAMS, E. G., LAUTER, C. J., SALEM, J. N. & HEINE, U. 1981. Exfoliation of membrane ecto-enzymes in the form of micro-vesicles. *Biochimica et Biophysica Acta (BBA)-Biomembranes,* 645**,** 63-70.

TRELLAKIS, S., BRUDEREK, K., DUMITRU, C. A., GHOLAMAN, H., GU, X., BANKFALVI, A., SCHERAG, A., HÜTTE, J., DOMINAS, N. & LEHNERDT, G. F. 2011. Polymorphonuclear granulocytes in human head and neck cancer: enhanced inflammatory activity, modulation by cancer cells and expansion in advanced disease. *International journal of cancer,* 129**,** 2183-2193.

TŰZESI, Á., KLING, T., WENGER, A., LUNAVAT, T. R., JANG, S. C., RYDENHAG, B., LÖTVALL, J., POLLARD, S. M., DANIELSSON, A. & CARÉN, H. 2017. Pediatric brain tumor cells release exosomes with a miRNA repertoire that differs from exosomes secreted by normal cells. *Oncotarget,* 8**,** 90164.

VALADI, H., EKSTROM, K., BOSSIOS, A., SJOSTRAND, M., LEE, J. & LOTVALL, J. 2007. Glioblastoma microvesicles transport RNA and proteins that promote tumour growth and provide diagnostic biomarkers. *Nat Cell Biol,* 9**,** 654-659.

VALADI, H., EKSTRÖM, K., BOSSIOS, A., SJÖSTRAND, M., LEE, J. J. & LÖTVALL, J. O. 2007b. Exosome-mediated transfer of mRNAs and microRNAs is a novel mechanism of genetic exchange between cells. *Nat Cell Biol,* 9**,** 654-9.

VALLEE, R. B., HERSKOVITS, J. S., AGHAJANIAN, J. G., BURGESS, C. C. & SHPETNER, H. S. 1993. Dynamin, a GTPase involved in the initial stages of endocytosis. *The GTPase Superfamily,* 176**,** 185.

VAN NIEL, G., CHARRIN, S., SIMOES, S., ROMAO, M., ROCHIN, L., SAFTIG, P., MARKS, M. S., RUBINSTEIN, E. & RAPOSO, G. 2011. The tetraspanin CD63 regulates ESCRT-independent and-dependent endosomal sorting during melanogenesis. *Developmental cell,* 21**,** 708-721.

VAN NIEL, G., D'ANGELO, G. & RAPOSO, G. 2018. Shedding light on the cell biology of extracellular vesicles. *Nature Reviews Molecular Cell Biology,* 19**,** 213-228.

VAN STEGEREN, A., ROHLEDER, N., EVERAERD, W. & WOLF, O. T. 2006. Salivary alpha amylase as marker for adrenergic activity during stress: effect of betablockade. *Psychoneuroendocrinology,* 31**,** 137-141.

VAN ZIJL, F., KRUPITZA, G. & MIKULITS, W. 2011. Initial steps of metastasis: cell invasion and endothelial transmigration. *Mutation Research/Reviews in Mutation Research,* 728**,** 23-34.

VICKERS, K. C., PALMISANO, B. T., SHOUCRI, B. M., SHAMBUREK, R. D. & REMALEY, A. T. 2011. MicroRNAs are transported in plasma and delivered to recipient cells by high-density lipoproteins. *Nature cell biology,* 13**,** 423-433.

VICKERS, K. C. & REMALEY, A. T. 2012. Lipid-based carriers of microRNAs and intercellular communication. *Current opinion in lipidology,* 23**,** 91.

VILA-NAVARRO, E., DURAN-SANCHON, S., VILA-CASADESÚS, M., MOREIRA, L., GINÈS, À., CUATRECASAS, M., LOZANO, J. J., BUJANDA, L., CASTELLS, A. & GIRONELLA, M. 2019. Novel Circulating miRNA Signatures for Early Detection of Pancreatic Neoplasia. *Clin Transl Gastroenterol,* 10**,** e00029.

VILLARROYA-BELTRI, C., GUTIÉRREZ-VÁZQUEZ, C., SÁNCHEZ-CABO, F., PÉREZ-HERNÁNDEZ, D., VÁZQUEZ, J., MARTIN-COFRECES, N., MARTINEZ-HERRERA, D. J., PASCUAL-MONTANO, A., MITTELBRUNN, M. & SÁNCHEZ-MADRID, F. 2013. Sumoylated hnRNPA2B1 controls the sorting of miRNAs into exosomes through binding to specific motifs. *Nature communications,* 4**,** 1-10.

VLAEMINCK-GUILLEM, V. 2018. Extracellular Vesicles in Prostate Cancer Carcinogenesis, Diagnosis, and Management. *Front Oncol,* 8**,** 222.

WAGNER, S., WITTEKINDT, C., REUSCHENBACH, M., HENNIG, B., THEVARAJAH, M., WÜRDEMANN, N., PRIGGE, E. S., VON KNEBEL DOEBERITZ, M., DREYER, T. & GATTENLÖHNER, S. 2016. CD 56-positive lymphocyte infiltration in relation to human papillomavirus association and prognostic significance in oropharyngeal squamous cell carcinoma. *International journal of cancer,* 138**,** 2263-2273.

WAHLUND, C. J., EKLUND, A., GRUNEWALD, J. & GABRIELSSON, S. 2017. Pulmonary extracellular vesicles as mediators of local and systemic inflammation. *Frontiers in cell and developmental biology,* 5**,** 39.

WALLER, J. & WARDLE, J. 2008. HPV vaccination in the UK. British Medical Journal Publishing Group.

WANG, E., NORRED, W., BACON, C., RILEY, R. & MERRILL JR, A. H. 1991. Inhibition of sphingolipid biosynthesis by fumonisins. Implications for diseases associated with Fusarium moniliforme. *Journal of Biological Chemistry,* 266**,** 14486-14490.

WANG, H., PENG, R., WANG, J., QIN, Z. & XUE, L. 2018. Circulating microRNAs as potential cancer biomarkers: the advantage and disadvantage. *Clinical Epigenetics,* 10.

WANG, N., FENG, Y., WANG, Q., LIU, S., XIANG, L., SUN, M., ZHANG, X., LIU, G., QU, X. & WEI, F. 2014a. Neutrophils infiltration in the tongue squamous cell carcinoma and its correlation with CEACAM1 expression on tumor cells. *PloS one,* 9**,** e89991.

WANG, N., TAN, H.-Y., FENG, Y.-G., ZHANG, C., CHEN, F. & FENG, Y. 2018b. microRNA-23a in Human Cancer: Its Roles, Mechanisms and Therapeutic Relevance. *Cancers,* 11**,** 7.

WANG, Q., WANG, G., NIU, L., ZHAO, S., LI, J., ZHANG, Z., JIANG, H., ZHANG, Q., WANG, H. & SUN, P. 2021. Exosomal MiR-1290 promotes angiogenesis of hepatocellular carcinoma via targeting SMEK1. *Journal of oncology,* 2021.

WANG, T., LIU, G. & WANG, R. 2014b. The intercellular metabolic interplay between tumor and immune cells. *Frontiers in immunology,* 5**,** 358.

WANG, T., ZHOU, Y., LEI, C., LEI, J. & YANG, Z. 2013. Development of an ingenious method for determination of Dynabeads protein A based on a giant magnetoimpedance sensor. *Sensors and Actuators B: Chemical,* 186**,** 727-733.

WANG, X., ZHANG, X., REN, X.-P., CHEN, J., LIU, H., YANG, J., MEDVEDOVIC, M., HU, Z. & FAN, G.-C. 2010. MicroRNA-494 targeting both proapoptotic and antiapoptotic proteins protects against ischemia/reperfusion-induced cardiac injury. *Circulation,* 122**,** 1308-1318.

WANG, Y., ZHANG, C., ZHANG, P., GUO, G., JIANG, T., ZHAO, X., JIANG, J., HUANG, X., TONG, H. & TIAN, Y. 2018c. Serum exosomal micro RNA s combined with alpha-fetoprotein as diagnostic markers of hepatocellular carcinoma. *Cancer Medicine,* 7**,** 1670-1679.

WANG, Z., LI, F., RUFO, J., CHEN, C., YANG, S., LI, L., ZHANG, J., CHENG, J., KIM, Y. & WU, M. 2020. Acoustofluidic salivary exosome isolation: A liquid biopsy compatible approach for human papillomavirus–associated oropharyngeal cancer detection. *The Journal of Molecular Diagnostics,* 22**,** 50-59.

WEBBER, J. & CLAYTON, A. 2013. How pure are your vesicles? *Journal of extracellular vesicles,* 2**,** 19861.

WEI, R., ZHAO, L., KONG, G., LIU, X., ZHU, S., ZHANG, S. & MIN, L. 2020. Combination of Size-Exclusion Chromatography and Ultracentrifugation Improves the Proteomic Profiling of Plasma-Derived Small Extracellular Vesicles. *Biological Procedures Online,* 22.

WEI, T., CONG, X., WANG, X.-T., XU, X.-J., MIN, S.-N., YE, P., PENG, X., WU, L.-L. & YU, G.-Y. 2017. Interleukin-17A promotes tongue squamous cell carcinoma metastasis through activating miR-23b/versican pathway. *Oncotarget,* 8**,** 6663.

WEN, Y., HAN, J., CHEN, J., DONG, J., XIA, Y., LIU, J., JIANG, Y., DAI, J., LU, J. & JIN, G. 2015a. Plasma mi RNA s as early biomarkers for detecting hepatocellular carcinoma. *International journal of cancer,* 137**,** 1679-1690.

WEN, Y.-C., LEE, W.-J., TAN, P., YANG, S.-F., HSIAO, M., LEE, L.-M. & CHIEN, M.-H. 2015b. By inhibiting snail signaling and miR-23a-3p, osthole suppresses the EMT-mediated metastatic ability in prostate cancer. *Oncotarget,* 6**,** 21120.

WICKMAN, G., JULIAN, L. & OLSON, M. 2012. How apoptotic cells aid in the removal of their own cold dead bodies. *Cell Death & Differentiation,* 19**,** 735-742.

WITWER, K. W., BUZÁS, E. I., BEMIS, L. T., BORA, A., LÄSSER, C., LÖTVALL, J., NOLTE-'T HOEN, E. N., PIPER, M. G., SIVARAMAN, S., SKOG, J., THÉRY, C., WAUBEN, M. H. & HOCHBERG, F. 2013. Standardization of sample collection, isolation and analysis methods in extracellular vesicle research. *J Extracell Vesicles,* 2.

WOLF, P. 1967. The nature and significance of platelet products in human plasma. *British journal of haematology,* 13**,** 269-288.

WOLFERS, J., LOZIER, A., RAPOSO, G., REGNAULT, A., THERY, C., MASURIER, C., FLAMENT, C., POUZIEUX, S., FAURE, F. & TURSZ, T. 2001. Tumor-derived exosomes are a source of shared tumor rejection antigens for CTL cross-priming. *Nature medicine,* 7**,** 297-303.

WONG, D. T. 2015. Salivary extracellular noncoding RNA: emerging biomarkers for molecular diagnostics. *Clinical therapeutics,* 37**,** 540-551.

XAVIER, C. P., CAIRES, H. R., BARBOSA, M. A., BERGANTIM, R., GUIMARÃES, J. E. & VASCONCELOS, M. H. 2020. The role of extracellular vesicles in the hallmarks of cancer and drug resistance. *Cells,* 9**,** 1141.

XIA, S.-S., ZHANG, G.-J., LIU, Z.-L., TIAN, H.-P., HE, Y., MENG, C.-Y., LI, L.-F., WANG, Z.-W. & ZHOU, T. 2017. MicroRNA-22 suppresses the growth, migration and invasion of colorectal cancer cells through a Sp1 negative feedback loop. *Oncotarget,* 8**,** 36266.

XIANG, Y., TIAN, Q., GUAN, L. & NIU, S.-S. 2020. The dual role of miR-186 in cancers: oncomir battling with tumor suppressor miRNA. *Frontiers in Oncology,* 10**,** 233.

XIAO, X., YANG, D., GONG, X., MO, D., PAN, S. & XU, J. 2018. miR-1290 promotes lung adenocarcinoma cell proliferation and invasion by targeting SOCS4. *Oncotarget,* 9**,** 11977-11988.

XIE, C., JI, N., TANG, Z., LI, J. & CHEN, Q. 2019. The role of extracellular vesicles from different origin in the microenvironment of head and neck cancers. *Molecular cancer,* 18**,** 1-15.

XIE, R., WU, S.-N., GAO, C.-C., YANG, X.-Z., WANG, H.-G., ZHANG, J.-L., YAN, W. & MA, T.-H. 2017. Prognostic value of combined and individual expression of microRNA-1290 and its target gene nuclear factor I/X in human esophageal squamous cell carcinoma. *Cancer Biomarkers,* 20**,** 325-331.

XU, D., TAKESHITA, F., HINO, Y., FUKUNAGA, S., KUDO, Y., TAMAKI, A., MATSUNAGA, J., TAKAHASHI, R.-U., TAKATA, T. & SHIMAMOTO, A. 2011. miR-22 represses cancer progression by inducing cellular senescence. *Journal of Cell Biology,* 193**,** 409-424.

XU, Y.-F., HANNAFON, B. N., ZHAO, Y. D., POSTIER, R. G. & DING, W.-Q. 2017. Plasma exosome miR-196a and miR-1246 are potential indicators of localized pancreatic cancer. *Oncotarget,* 8**,** 77028.

YAKOB, M., FUENTES, L., WANG, M. B., ABEMAYOR, E. & WONG, D. T. 2014. Salivary biomarkers for detection of oral squamous cell carcinoma - current state and recent advances. *Curr Oral Health Rep,* 1**,** 133-141.

YAMAKUCHI, M., YAGI, S., ITO, T. & LOWENSTEIN, C. J. 2011. MicroRNA-22 regulates hypoxia signaling in colon cancer cells. *PloS one,* 6**,** e20291.

YÁÑEZ-MÓ, M., SILJANDER, P. R.-M., ANDREU, Z., BEDINA ZAVEC, A., BORRÀS, F. E., BUZAS, E. I., BUZAS, K., CASAL, E., CAPPELLO, F. & CARVALHO, J. 2015. Biological properties of extracellular vesicles and their physiological functions. *Journal of extracellular vesicles,* 4**,** 27066.

YANG, B., FENG, X., LIU, H., TONG, R., WU, J., LI, C., YU, H., CHEN, Y., CHENG, Q., CHEN, J., CAI, X., WU, W., LU, Y., HU, J., LIANG, K., LV, Z., WU, J. & ZHENG, S. 2020. High-metastatic cancer cells derived exosomal miR92a-3p promotes epithelial-mesenchymal transition and metastasis of low-metastatic cancer cells by regulating PTEN/Akt pathway in hepatocellular carcinoma. *Oncogene,* 39**,** 6529-6543.

YANG, C. C., HUNG, P. S., WANG, P. W., LIU, C. J., CHU, T. H., CHENG, H. W. & LIN, S. C. 2011. miR-181 as a putative biomarker for lymph-node metastasis of oral squamous cell carcinoma. *Journal of oral pathology & medicine,* 40**,** 397-404.

YANG, H., FU, H., WANG, B., ZHANG, X., MAO, J., LI, X., WANG, M., SUN, Z., QIAN, H. & XU, W. 2018. Exosomal miR-423-5p targets SUFU to promote cancer growth and metastasis

and serves as a novel marker for gastric cancer. *Molecular Carcinogenesis,* 57**,** 1223-1236.

YANG, H., YU, J., WANG, L., DING, D., ZHANG, L., CHU, C., CHEN, Q., XU, Z., ZOU, Q. & LIU, X. 2014. miR-320a is an independent prognostic biomarker for invasive breast cancer. *Oncology Letters,* 8**,** 1043-1050.

YANG, Q., JIANG, W., ZHUANG, C., GENG, Z., HOU, C., HUANG, D., HU, L. & WANG, X. 2015. microRNA-22 downregulation of galectin-9 influences lymphocyte apoptosis andtumor cell proliferation in liver cancer. *Oncology reports,* 34**,** 1771-1778.

Yi, R., Qin, Y., Macara, I.G. and Cullen, B.R., 2003. Exportin-5 mediates the nuclear export of pre-microRNAs and short hairpin RNAs. Genes & development, 17(24), pp.3011-3016.

YOSHIZAWA, J. M. & WONG, D. T. 2013. Salivary microRNAs and oral cancer detection. *MicroRNA Protocols***,** 313-324.

YU, J., LIN, Y., XIONG, X., LI, K., YAO, Z., DONG, H., JIANG, Z., YU, D., YEUNG, S.-C. J. & ZHANG, H. 2019. Detection of exosomal PD-L1 RNA in saliva of patients with periodontitis. *Frontiers in genetics,* 10**,** 202.

YU, Y., GOOL, E., BERCKMANS, R. J., COUMANS, F. A. W., BARENDRECHT, A. D., MAAS, C., VAN DER WEL, N. N., ALTEVOGT, P., STURK, A. & NIEUWLAND, R. 2018. Extracellular vesicles from human saliva promote hemostasis by delivering coagulant tissue factor to activated platelets. *Journal of Thrombosis and Haemostasis,* 16**,** 1153-1163.

YUAN, F., LI, Y.-M. & WANG, Z. 2021. Preserving extracellular vesicles for biomedical applications: consideration of storage stability before and after isolation. *Drug Delivery,* 28**,** 1501-1509.

YUANA, Y., BÖING, A. N., GROOTEMAAT, A. E., VAN DER POL, E., HAU, C. M., CIZMAR, P., BUHR, E., STURK, A. & NIEUWLAND, R. 2015. Handling and storage of human body fluids for analysis of extracellular vesicles. *Journal of Extracellular Vesicles,* 4**,** 29260.

YUANA, Y., LEVELS, J., GROOTEMAAT, A., STURK, A. & NIEUWLAND, R. 2014. Co-isolation of extracellular vesicles and high-density lipoproteins using density gradient ultracentrifugation. *Journal of extracellular vesicles,* 3**,** 23262.

ZAKOWSKI, J. J. & BRUNS, D. E. 1985. Biochemistry of human alpha amylase isoenzymes. *Crit Rev Clin Lab Sci,* 21**,** 283-322.

ZANELLO, B. & SB, S. J. Brain gene expression signatures from cerebrospinal fluid exosome RNA profiling. NASA Human Research Program Investigators' Workshop, 2014. 12-13.

ZAROVNI, N., CORRADO, A., GUAZZI, P., ZOCCO, D., LARI, E., RADANO, G., MUHHINA, J., FONDELLI, C., GAVRILOVA, J. & CHIESI, A. 2015. Integrated isolation and quantitative analysis of exosome shuttled proteins and nucleic acids using immunocapture approaches. *Methods,* 87**,** 46-58.

ZEKRI, A.-R. N., EL-SISI, E. R., YOUSSEF, A. S. E.-D., KAMEL, M. M., NASSAR, A., AHMED, O. S., EL KASSAS, M., BARAKAT, A. B., ABD EL-MOTALEB, A. I. & BAHNASSY, A. A. 2018. MicroRNA Signatures for circulating CD133-positive cells in hepatocellular carcinoma with HCV infection. *PLOS ONE,* 13**,** e0193709.

ZHANG, K., YUE, Y., WU, S., LIU, W., SHI, J. & ZHANG, Z. 2019a. Rapid Capture and Nondestructive Release of Extracellular Vesicles Using Aptamer-Based Magnetic Isolation. *ACS Sensors,* 4**,** 1245-1251.

ZHANG, W. C., CHIN, T. M., YANG, H., NGA, M. E., LUNNY, D. P., LIM, E. K., SUN, L. L., PANG, Y. H., LEOW, Y. N., MALUSAY, S. R., LIM, P. X., LEE, J. Z., TAN, B. J., SHYH-CHANG, N., LIM, E. H., LIM, W. T., TAN, D. S., TAN, E. H., TAI, B. C., SOO, R. A., TAM, W. L. & LIM, B. 2016.

Tumour-initiating cell-specific miR-1246 and miR-1290 expression converge to promote non-small cell lung cancer progression. *Nat Commun,* 7**,** 11702.

ZHANG, X.-W., LIU, N., CHEN, S., WANG, Y., ZHANG, Z.-X., SUN, Y.-Y., QIU, G.-B. & FU, W.-N. 2015. High microRNA-23a expression in laryngeal squamous cell carcinoma is associated with poor patient prognosis. *Diagnostic Pathology,* 10.

ZHANG, Y., CHEN, C., LIU, Z., GUO, H., LU, W., HU, W. & LIN, Z. 2022. PABPC1-induced stabilization of IFI27 mRNA promotes angiogenesis and malignant progression in esophageal squamous cell carcinoma through exosomal miRNA-21-5p. *Journal of Experimental & Clinical Cancer Research,* 41.

ZHANG, Y., LIU, Y., LIU, H. & TANG, W. H. 2019b. Exosomes: biogenesis, biologic function and clinical potential. *Cell & Bioscience,* 9.

ZHANG, Y., ZHOU, M., BAI, L., HAN, R., LV, K. & WANG, Z. 2018. Extracellular vesicles promote esophageal cancer progression by delivering lncZEB1-AS1 between cells. *Eur Rev Med Pharmacol Sci,* 22**,** 2662-2670.

ZHAO, H., DONG, T., ZHOU, H., WANG, L., HUANG, A., FENG, B., QUAN, Y., JIN, R., ZHANG, W. & SUN, J. 2014. miR-320a suppresses colorectal cancer progression by targeting Rac1. *Carcinogenesis,* 35**,** 886-895.

ZHENG, X., CHEN, F., ZHANG, J., ZHANG, Q. & LIN, J. 2014. Exosome analysis: a promising biomarker system with special attention to saliva. *The Journal of Membrane Biology,* 247**,** 1129-1136.

ZHENG, X., CHEN, F., ZHANG, Q., LIU, Y., YOU, P., SUN, S., LIN, J. & CHEN, N. 2017. Salivary exosomal PSMA7: a promising biomarker of inflammatory bowel disease. *Protein & cell,* 8**,** 686-695.

ZHENG, X., WU, K., LIAO, S., PAN, Y., SUN, Y., CHEN, X., ZHANG, Y., XIA, S., HU, Y. & ZHANG, J. 2018. MicroRNA-transcription factor network analysis reveals miRNAs cooperatively suppress RORA in oral squamous cell carcinoma. *Oncogenesis,* 7.

ZHU, L., JIN, L., JIANG, R., WANG, Q., JIANG, J., MAO, C. & CHEN, D. 2013. Correlations between miRNAs and TGF-β1 in tumor microenvironment of esophageal squamous cell cancer. *Xi bao yu fen zi Mian yi xue za zhi= Chinese Journal of Cellular and Molecular Immunology,* 29**,** 524-528.

ZLOTOGORSKI-HURVITZ, A., DAYAN, D., CHAUSHU, G., KORVALA, J., SALO, T., SORMUNEN, R. & VERED, M. 2015. Human Saliva-Derived Exosomes. *Journal of Histochemistry & Cytochemistry,* 63**,** 181-189.

ZLOTOGORSKI-HURVITZ, A., DAYAN, D., CHAUSHU, G., SALO, T. & VERED, M. 2016. Morphological and molecular features of oral fluid-derived exosomes: oral cancer patients versus healthy individuals. *Journal of cancer research and clinical oncology,* 142**,** 101-110.

ZOMER, A., MAYNARD, C., VERWEIJ, F. J., KAMERMANS, A., SCHÄFER, R., BEERLING, E., SCHIFFELERS, R. M., DE WIT, E., BERENGUER, J. & ELLENBROEK, S. I. J. 2015. In vivo imaging reveals extracellular vesicle-mediated phenocopying of metastatic behavior. *Cell,* 161**,** 1046-1057.

ZOMER, A., STEENBEEK, S. C., MAYNARD, C. & VAN RHEENEN, J. 2016. Studying extracellular vesicle transfer by a Cre-loxP method. *Nature protocols,* 11**,** 87-101.

Squier, C.A. and Kremer, M.J., 2001. Biology of oral mucosa and esophagus. JNCI Monographs, 2001(29), pp.7-15.

ZUO, Q., CAO, L., YU, T., GONG, L., WANG, L., ZHAO, Y., XIAO, B. & ZOU, Q. 2015. MicroRNA-22 inhibits tumor growth and metastasis in gastric cancer by directly targeting MMP14 and Snail. *Cell death & disease,* 6**,** e2000-e2000.